UNIVERSITY OF ALBERTA

DILUTION OF CIRCULAR WALL JET IN CROSSFLOW

BY

JOHN KIPKETER LANGAT

A THESIS

SUBMITTED TO THE FACULTY OF GRADUATE AND

RESEARCH IN PARTIAL FULFILLMENT OF THE

REQUIREMENT FOR THE DEGREE OF

OF

MASTER OF SCIENCE

IN

WATER RESOURCES ENGINEERING

DEPARTMENT OF CIVIL ENGINEERING

EDMONTON, ALBERTA

SPRING, 1994.

ISBN 0-612-11268-3

UNIVERSITY OF ALBERTA

RELEASE FORM

NAME OF AUTHOR: **John Kipketer Langat**

TITLE OF THESIS: **Dilution of Circular Wall Jet in Crossflow**

DEGREE: **Master of Science**

YEAR THIS DEGREE GRANTED: **Spring, 1994.**

John Kipketer Langat

Kabokyek - Kiptugumo
P.O. BOX 25
KIPTUGUMO (KERICHO).

Date 19 Jan 1994

UNIVERSITY OF ALBERTA

FACULTY OF GRADUATE STUDIES AND RESEARCH

The undersigned certify that they have read, and recommended to the Faculty of Graduate Studies and Research for acceptance, a thesis entitled **Dilution of Circular Wall Jet in Crossflow** submitted by John Kipketer Langat in partial fulfillment of the requirements for the degree of Master of Science in Water Resources Engineering.

Dr. N. Rajaratnam
Supervisor

Dr. F. E. Hicks
Co - Supervisor

Dr. D. J. Marsden
External Examiner

Dr. T. Y. Gan
Committee Chairman

Date: 19 Jan 1994

ABSTRACT

Dilution of turbulent circular wall jets discharging perpendicular to crossflow ambients has not received much attention compared to studies on free turbulent jets in crossflows. An effluent diffuser designed as a circular wall jet is an efficient means of enhancing dilution of waste discharges from both industrial and municipal treatment plants under river conditions. The outfall is located at / or near the bed in order to utilize the whole flow depth in mixing and therefore this increases the efficiency of effluent dilution within the mixing zone. The present study considers the dilution characteristics of a circular wall jet in river-like crossflows and its comparison with the free jet discharging perpendicularly from the bed. The location of the jet takes into account the limited depths available for mixing in most shallow rivers.

This thesis presents the results of an experimental study on the dilution produced in circular wall jets discharging perpendicular to a freestream. The deflected wall jets were explored for dilutions up to 100:1 for downstream distance x up to about 200 times the jet nozzle diameter. Dilution characteristics of the jet were studied by first performing a similarity analysis on the 3-dimensional concentration distributions. Non-dimensional concentration profiles were found to be similar both in the vertical and the transverse directions. Minimum dilutions were considered along the axial distance of the jet for the flow regimes defined by the momentum dominated near field, the far filed and the passive plume regions. For practical purposes, a mean equation was developed to describe the minimum dilution in the mixing region. The correlation was found to be of similar magnitude with the results of the free jets. The growth rate of the jet, both in the vertical and the transverse directions was also

investigated. The results indicated that the la[illegible] [illegible] [illegible]th of the deflected jet is about twice that in the vertical direction. Th[illegible] [illegible] characteristic of wall jets takes advantage of the available mixing space since most rivers have widths several times larger than the flow depth, and conse[illegible] increase the effluent dilution.

Effect of the flow depths on the tra[illegible] dilution was also studied. The results indicated significant reduction in tra[illegible] dilution for freestream flow depths less than 10 times the jet nozzle diameter. This problem prevails for effluent discharged into shallow rivers due to early surfacing.

Acknowledgements

The author gratefully acknowledges the efforts provided by Dr. N. Rajaratnam for closely supervising the development of the model and the research work as whole. His keen interests and effort to read and correct the thesis are highly appreciated.

The author would like to express sincere thanks to Dr. Faye E. Hicks for her guidance as an academic advisor and providing supervision on the initial development of the research. Her encouragement and valuable suggestions during the course of the study are specially acknowledged.

Special appreciation also goes to Sheldon Lovell for the construction of the experimental model and the attention provided in the Laboratory when needed. Assistance provided by Dr. A. Mainali during the photographic study and proof - reading of the thesis is also acknowledged. My thanks also goes to my fellow colleagues for their encouragement and support while carrying out this study.

I also like to acknowledge the Canadian International Development Agency for their financial assistance given through the General Training Program of the Republic of Kenya without which my studies at the University of Alberta would not have been possible.

Finally, I wish to dedicate the success of the present study to my wife Florence Langat, and my children Mercy, Getrude and Irene for their patience and encouragement during my absence from home.

TABLE OF CONTENTS

APPENDICES

LIST OF TABLES

APPENDIX

LIST OF FIGURES

APPENDIX

LIST OF PLATES

APPENDIX

NOTATIONS

a	cross - section area of the sample delivery tubes
b	length scale in the velocity distribution for a simple jet
b_c	length scale in the concentration distribution for a simple jet
b_z	length scale on the z - direction
b_*	length scale on the transverse η - direction
C	concentration at a section of the jet
C_o	initial jet concentration at the nozzle
C_m	maximum jet concentration at a section
d	jet nozzle diameter
D	depth of the freestream flow
k	diffusion coefficient ratio
k_1	empirical constant in a simple jet
l_m	momentum length scale [$= M^{1/2} / U$]
M	kinematic momentum flux at the jet nozzle
R	Reynolds number of the jet
r	radial distance to any point from the axis of a simple jet
u	velocity at any point of a simple jet in the axial direction
U	freestream velocity

u_m maximum jet velocity at a section

U_0 initial velocity of the jet at the nozzle

x co - ordinate direction along the freestream

x_* downstream x co - ordinate of the deflected jet where momentum dominated near field ends

$x_\dagger$ downstream x co - ordinate of the deflected jet where momentum dominated far field ends

y co - ordinate direction along the original direction of the jet perpendicular to the freestream

y_c centerline co - ordinate on the y - axis of the deflected jet

z vertical (depth wise) co - ordinate direction above the channel bed

α the ratio of the jet velocity to the ambient freestream velocity

δ elevation of the maximum concentration axis above the bed at a section

υ kinematic viscosity of the fluid

θ angle of the jet deflection from the original orientation

ξ distance along the centerline axis of the deflected jet

ξ_m axial co - ordinate of the deflected jet at the end of the potential core

$\xi_\dagger$ axial co - ordinate of the deflected jet at the end of momentum dominated far field

η transverse co - ordinate direction normal to ξ

ζ vertical co - ordinate direction normal to ξ

ρ density of the jet fluid

1.0 INTRODUCTION

1.1 General

A circular jet discharging at an angle into a moving free stream is of practical interest in the developments associated with waste disposal into rivers, lakes and into the atmosphere. The wastes which result from increased urbanization and industrialization have continuously increased the pollutant loadings of both the hydrosphere and the atmosphere. Examples of waste disposal issuing as a jet at an angle to the moving ambient fluid include the emission of industrial smoke into the wind, treated municipal waste and other industrial wastes into rivers. The aim of these jet discharges is to produce significant mixing in a relatively short distance.

The present study investigates the dilution of a circular wall jet in crossflow. The jet induced turbulence provides the initial mixing and the subsequent dilution of the pollutants and is greatly influenced by the design of the outfall. The interaction which occurs in a jet discharging normal to the streamflow enhances the mixing process and results in high dilutions compared to jets in stagnant or co-flowing ambients. Sufficient knowledge of pollutant concentration distributions within this reach of the river where the outfall is located is important. Outfall design would involve taking into considerations the shallow nature of natural streams and the pollutant control standards imposed to protect against indiscriminatory disposal of toxic effluents into rivers.

The advantages of locating the outfall near or at the stream bed are:

I. most industrial wastes are colored and would be aesthetically objectionable if discharged near the surface of the rivers. Discharges near the bed would utilize the whole depth of flow in the river to diffuse the unpleasant color before surfacing.

II. effluent temperatures are normally slightly higher than that of the receiving waters (about 1° C - 5 ° C difference) due to the biological processes in the retention ponds before release into the river. Effluents therefore tend to float in a stratified manner in the river flow and this could be minimized by locating the jet diffuser near the bed.

A possible disadvantage is the possible erosion of the river bed in the vicinity of the outfall. To minimize the problem, provision of protection works would be necessary, such as constructing a concrete apron or stone pitching the sections that may be affected by the jet. A wall (or bed) jet diffuser similar to the present model and currently in use was designed by N. Rajaratnam and A. Charbannou for the Cariboo Pulp mill in Quesnel, in northern British Columbia which discharges into the Fraser river.

1.2 Turbulent Jet Mixing in Crossflows

Initial concentration of effluents at the outfall may be much higher than the allowable receiving stream concentration. A zone therefore exists where significant dilution occurs in a relatively short distance, normally referred to as the initial dilution or mixing zone. Gowda (1984) described this zone as a limited use zone because the effluent concentrations often exceed the set standards of the receiving stream. Circular turbulent jets discharging the effluent perpendicular to the free stream flow is one of the effective schemes of achieving this significant dilution. In some cases, the effluent is discharged upwards into the free stream from a submerged outfall embedded in the middle of the crossflow (Wright, 1977; Hodgson and Rajaratnam, 1992). To use the limited flow depth in crossflows such as shallow rivers, it is preferable to delay the effluents from surfacing by locating the jet on or near the bed and discharging normal to the freestream as a wall (bed) jet. It is assumed that the ratio of the stream flow depth (D) to the jet diameter (d) is large enough to minimize disturbance of the free surface in the stream by the jet. Therefore, the parameter (D / d) will be considered not important in this analysis of the circular wall jet in crossflows. (It should be mentioned that in our case, the wall jets should be called bed jets but following the general practice in Fluid Mechanics, they are referred to as wall jets, where all boundaries are referred to as walls.)

The work of Hodgson and Rajaratnam (1988) broadly classified deep water and shallow water jets based on the parameter $\alpha d / D$, where α is the ratio of the jet velocity, U_0 to the free stream velocity, U. A photographic study of circular jets discharging into river-like shallow flows showed that the critical value for the parameter $\alpha d / D$ is about 0.34. Larger values of this parameter correspond to shallow water jets and smaller values to deep water jets. In the present work, values of $\alpha d / D$ are as large as 1.2, and the jet showed no surface effects indicating that it behaved as a deep water jet. Use of the same parameter to categorize wall jets is therefore not applicable because the growth towards the surface is only through diffusion and the jet momentum is not in the direction of the freestream depth.

Simple axisymmetric circular turbulent jets discharging into a large quiescent ambient is first considered. Considering the region of developed flow, the dilution along the axis of a simple jet is approximated by the expression (Rajaratnam, 1983):

$$\frac{C_0}{C_m} = k_1 \frac{x}{d} \qquad (1.1)$$

where C_0 and C_m are respectively the concentrations at the jet nozzle of diameter d, and maximum concentration at an axial distance of x downstream of the nozzle and k_1 is an empirical constant determined through experiments. The work of Hodgson and Rajaratnam (1989) found that k_1 is approximately equal to 0.19.

Several studies have been conducted on the mixing of circular jets in crossflows of large extent (Rajaratnam, 1976). One of the more significant studies in this area is the work of Wright (1977). Recently, Hodgson and Rajaratnam studied the dilutions of circular jets in rivers, including shallow flows (Hodgson and Rajaratnam, 1992).

1.3 The Present Investigation

Most of the research work on circular turbulent jets in crossflow have emphasized the momentum characteristics compared to the concentration measurements. The present work emphasizes the practical importance of the jet dilution issuing as a wall jet in crossflows as applied in hydraulics.

The objective of the experimental investigation was to study the main dilution characteristics of circular wall jet in ambient flows normal to the jet discharge and to compare with the existing work for the momentum dominated regimes of the free jet. To understand the problem, general mixing characteristics of turbulent jets in crossflow were first considered, developing from the simple case of the axisymmetric jet. Review of the existing work on the free jet in crossflows formed the basis of studying dilution characteristics of circular wall jet in crossflow. The analysis of the dilution data was based on the flow regimes defined by the momentum dominated near field and far field regions of the jet. The results were then compared with those of the free jet conditions investigated by Wright (1977) and Hodgson and Rajaratnam (1992).

2.0 LITERATURE REVIEW

2.1 General

Circular jets in crossflows have attracted the attention of researchers because of their practical importance in several fields. List (1982) indicated that the earliest work on the subject of jets was by Young (1800) who recognized that the angle of expansion of turbulent jets was not a function of the jet velocity. A simple axisymmetric jet discharging into a stagnant ambient is well understood, but significant differences occur with complex turbulent shear flows when the ambient is changed to a crossflow. The earliest published work on jets in crossflow was carried out by Ruggeri et al, 1949 (see Rajaratnam, 1976) who investigated jet penetration in a wind tunnel. Hodgson (1991) tabulated a comprehensive summary of the previous experimental work on jet discharges in crossflows but none of the 33 references dealt with a wall jet.

To achieve a significant degree of mixing in the immediate vicinity of the outfall, effluent discharges into the environment, especially in rivers, need to be momentum dominated and because of the shallow nature of the rivers the outfalls need to be located near the bed. Such arrangements will maximize the mixing process within the depth of the river and delay the surfacing of the discharges. Dilutions up to 50 : 1 in the initial dilution zone, have been reported when a jet diffuser is used compared to an outfall which relies solely on the river turbulence as in the case of passive plumes (Hodgson, 1991).

To understand the main characteristics of a circular wall jet in crossflow, previous experimental investigations on the well understood free turbulent jets will be reviewed in this chapter. The simple axisymmetric turbulent jet discharging into a stagnant ambient will be described and compared with a wall jet of similar conditions. This will be followed by the description of the basic components of free circular jet discharges in crossflow. The knowledge on the free jet will be used as a basis for understanding the conditions of a wall jet with similar discharges in crossflow.

2.2 Description of Circular Turbulent Jets

The characteristics of the circular jet in crossflow can be better understood by first describing the simple free jet issuing into a stagnant ambient and then moving the ambient as a crossflow. In this section existing experimental observations on simple axisymmetric wall jets will be discussed. This will be later applied when discussing the effects of the wall on dilution of circular jets in crossflow. **Free turbulent jets** discharge into a stagnant ambient with boundaries sufficiently far away, while the **wall jet** discharges tangentially and grows along a wall (Abramovich, 1963). It is useful to note that if the Reynolds number R of the jet, defined as $R = U_0 d / \upsilon$ where υ is the kinematic viscosity of the fluid, is greater than about 1000, the jet becomes turbulent fairly quickly (Fischer et al, 1979).

2.2.1 Simple Axisymmetric Jet

Consider a circular jet of diameter d and discharging with a uniform velocity U_0 into a stagnant ambient. The jet is divided into two distinct regions (Fig. 2.1). The region near the jet nozzle with undiminished discharge velocity U_0 is known as the potential core or flow development region. In the core, the flow is essentially potential with little or no turbulence and extends to about 6 d (Abraham, 1960;

Rajaratnam, 1976). The end of the potential flow occurs when the turbulence generated by the shear at the boundaries spreads to the axis of the jet.

The next zone, known as the fully developed flow region, occurs beyond the end of the potential core. The mean velocity u_m along the centerline decays with the axial distance x . Rajaratnam (1983) found that the velocity and concentration scales decay inversely with the distance along the jet axis and are described by the following equations:

$$\frac{u_m}{U_o} = \frac{6.13}{x/d} \tag{2.1}$$

$$\frac{C_m}{C_o} = \frac{5.34}{x/d} \tag{2.2}$$

where:

U_o is the initial velocity of the jet at the nozzle

u_m is the maximum jet velocity at any section

x is the axial distance from the jet nozzle to that section

d is the diameter of the jet nozzle

C_o is the initial concentration in the jet

C_m is the maximum concentration at the section considered.

The radial distributions of velocity and concentration are also known to be similar. These distributions are well described by the following equations:

$$\frac{u}{u_m} = \exp[-\ln 2(\frac{r}{b})] \tag{2.3}$$

$$\frac{C}{C_m} = \exp[-\ln 2(\frac{r}{b_c})] \tag{2.4}$$

where:

u is the velocity at a point at a section

r is the radial distance to the point from the jet axis

b is the length scale (distance to the point where $u = 1/2\ u_m$)

b_c is the length scale (distance to the point where $C = 1/2\ C_m$) and

C is the concentration at a point.

The variation of the length scale b used in the velocity distribution for the circular turbulent jets has been found to be a linear function of the axial distance x from the nozzle, given by:

$$b = 0.096\ x \qquad (2.5)$$

Similarly, the growth of the concentration length scale b_c was found to be a linear function of the axial distance but with a greater slope and is given as:

$$b_c = 0.096\ k\ x \qquad (2.6)$$

where k is an empirical coefficient.

The work of Rajaratnam (1983) found the diffusion coefficient ratio k to have a constant value of about 1.17 in the whole region of the developed flow.

The work of Sforza and his associates (1966) and that of Rajaratnam and Pani (1974) considered three-dimensional turbulent wall jets. The shape of the nozzles used in the studies included a square, a circle and a rectangle with an aspect ratio close to unity. Experimental observations were carried out in the fully-developed region to find out the velocity distributions and the growth of the jet both in the vertical and the lateral directions.

The results on the three-dimensional wall jet indicated that the center plane velocity distributions in the vertical direction were reasonably similar along the longitudinal distance greater than 10 times the nozzle height (or diameter). The classical wall jet similarity curve (plane turbulent wall jet issuing tangentially to a smooth wall, surrounded by a stagnant ambient of the same fluid of infinite extent) also described well the distributions of the three - dimensional jet. The results of the length scales indicated that both the vertical and the horizontal scales were linear functions of the longitudinal distance downstream of the nozzle. From the length scales, it was found that the lateral scale grows about 4 to 5 times faster than the vertical scale. The wall shear coefficient was also found to increase to a constant value beyond the downstream distance equal to 50 times the square root of the nozzle cross - sectional area. By neglecting the shear on the wall, these authors considered the problem could be analyzed in a manner similar to that of three-dimensional free jets.

2.2.2 Circular Jet in Crossflow: Preliminary discussion

When a moving ambient perpendicular to the jet discharge is introduced to replace the stagnant conditions in the axisymmetric jet, the set is described as a circular jet discharge into a crossflow. Free turbulent jet discharge in an infinite depth of the crossflow preva'' when the walls (or boundaries) are sufficiently far away (Abramovich, 1963) and do not influence the growth of the jet in the momentum dominated region.

The main characteristics of jets in crossflow are defined by considering a circular jet of diameter d discharging with an initial velocity U_o perpendicular to a moving free stream of velocity U (Figure 2.2). The jet would initially penetrate at right angles to the ambient flow but eventually be deformed by the crossflow and deflected from its original course to approximately the ambient flow direction. Rajaratnam and Gangadhariah (1980) indicated the cause of the jet deflection as the result of the pressure field exerted near the jet nozzle by the free stream as well as the entrainment of the ambient fluid. Deflected jets experience three zones of flow, as opposed to two for the simple jet.

The cone-shaped potential core forms the central region of the jet near the nozzle characterized by the shear free flow and undiminished total pressure (Rajaratnam, 1976). Studies by Pratte and Baines (1967), Keffer and Baines (1971) and Rajaratnam and Gangadhariah (1980) have identified the length of the potential core in crossflows to be shorter than that of the simple jet because of the extra shear exerted by the crossflow. Accurate determination of the core length has not been achieved yet. Hodgson (1991) analyzed the measurements from the above mentioned studies and found that this length varies from 1 to 4 times the jet diameter for velocity ratios α greater than 10. Other approximations have considered extrapolating backwards the centerline velocity profile on a log-log plot to the point where $u_m = U_o$. This method was found by Hodgson (1991) to overestimate the length when data from Keffer and Baines (1963) for velocity ratios $\alpha = 4, 6$ and 8 were used. According to Rajaratnam (1976), the end of the potential core is located on the jet centerline for $\alpha > 4$. Platten and Keffer (1971) noted a downwind displacement of the core length by the crossflow for weak jets with velocity ratios $\alpha < 2$.

The zone after the potential core where the jet undergoes major deflection is the second flow region known as the zone of maximum deflection and the jet axis here changes orientation from the original normal direction to almost parallel with the free stream flow . Turbulent mixing causes the outer layers of the jet to lose some of their momentum through entrainment of free stream fluid and become susceptible to the deflection of the crossflow. In this region therefore, the cross-section of the jet is deformed from the original circular to a kidney shape (Abramovich, 1963), which houses two counter-rotating vortices. As the jet continues interacting with the crossflow, it entrains more ambient fluid. This results in a growth in size and strength of the vortex pair and increases the total flow of the jet. Some decay of maximum velocity and hence the concentration in this region occurs along the curvilinear axis of the jet. According to Hodgson (1991) the maximum deflection zone extends to an axial distance (ξ) of about 15 to 20 times the jet diameter.

The third flow region is referred to as the vortex zone and occurs when the cross-section of the jet is almost completely occupied by the vortex pair. Further entraintment increases the size of the vortices and both the jet velocity and direction approach those of the ambient crossflow. Pratte and Baines (1967) and Fearn and Weston (1979) noted in their investigations the presence of the vortices at distances as near as $x = 10\ d$ and as far as $x = 1000\ d$ downstream of the jet nozzle. The strength of the vortices decrease with distance downstream of the jet.

2.2.3 Diffusion of Circular Jets in Crossflow

Several investigations have been carried out examining the structure of the velocity and pressure fields of the jets in crossflow (Sherif and Pletcher, 1989). Initial studies were conducted in air medium and using pitot tubes to measure the total and dynamic pressure heads in the jet. The axis of the jet was then located by the points of maximum pressure (Jordinson, 1956). Similar experiments were carried out by

Gordier (1959) using water instead of air, to measure the distribution of the total pressure in the jet in a water duct. Gordier found that the results were similar to those of the air jet.

The introduction of the Hot - Wire Anemometry (HWA) in the early 1960's and the Laser Doppler Anemometry (LDA) in the mid 1970's improved the understanding of the jet discharges. Both instruments were able to measure the velocity profiles, jet axis trajectory, the turbulence and the vortex structures of the deformed jet.

Rajaratnam and Gangadhariah (1980) studied experimentally the behaviour of circular jet in crossflow for four different discharges of velocity ratios α = 2.73, 4.52, 7.05 and 23, in a water flume. The velocity and piezometric pressure distribution in the full cross-section of the deflected jet were measured using the pitot tube. The results predicted the shape of the deformed jet, the centerline trajectory, the velocity distribution, and the mass and momentum fluxes of the jet discharges.

Photographic investigations were also used in a number of studies to locate the jet axis trajectory and jet boundaries. Gordier (1959) located the jet penetration (outer boundary) and the width from photographs of a deformed jet in a water flume. Pratte and Baines (1967) used photographs to locate the jet axis trajectory, the width and thickness of a jet marked by oil aerosol discharging in an air crossflow. Similar photographic studies were carried out by Crowe and Riesebieter (1967) using smoke, while Margason (1968) used water vapour for the observations. Wright (1977) photographed extensively 60 different deflected jet discharges of dye for the velocity ratio α between 0.8 and 116 for a downstream distance extending to a maximum of x / d = 113. Wright considered both the buoyant and non-buoyant jets in uniform and stratified crossflow and used his photographic trajectory plots to define the distinct flow regimes which occurred in the deflected jet. Wright also defined a momentum length scale $l_m = M^{1/2} / U$ as a criteria for separating the flow regimes.

2.2.4 Dilution of Circular Jets in Crossflow

Investigations of dilution characteristics of circular jets in crossflow are not as numerous as the studies of the diffusion. Studies using temperature and other conservative tracers have added significant knowledge to the understanding of dilution of turbulent jet discharges. The following section summarizes the published experimental studies on dilution of jets in crossflow.

Patrick (1967) investigated both the velocity and concentration distributions of jet discharges in crossflow using nitrous oxide ($NO2$) as a tracer. The experiments were carried out in an air medium for 23 different jet nozzle discharges and velocity ratio α between 8.5 and 54. Sampling was carried out using the pitot tube. The results indicated that the jet centerline dilution was a function of the axial distance (ξ) of the jet. Centerline dilutions of up to 100 : 1 for the downstream distance of $\xi / d = 50$ were reported.

The work of Fan (1967) considered the dilution of buoyant jet discharges in crossflow. The investigation was carried out in a water medium for 10 different discharges of salt solution through a jet orifice. The velocity ratios α were between 4 and 16, and the densimetric Froude number F_o between 10 and 80. Crossflow simulation was done by towing the orifice. Concentration distributions within the flow field were determined using a conductivity meter or probe for downstream distances upto $x / d = 250$. Fan concluded from his results that the enhanced mixing was due to the self-generated turbulence of the jet.

Ramsey and Goldstein (1971) investigated the distribution of temperature for weak air jet discharges in crossflow, and velocity ratios $\alpha = 0.1$, 0.5, 1.0 and 2.0. They used both the hot-wire anemometry and a thermocouple to measure the temperature profiles. Their measurements covered a downstream distance of $x / d = 10$. The results indicated that the weak jets ($\alpha = 0.1$ and 0.5) remained attached to the wall, while the stronger jets ($\alpha = 1$ and 2) were clearly separated from the wall. Similar investigations were carried out by Kamotani and Greber (1972) for high velocity ratios, $\alpha = 3.9$ and 7.7. Their results indicated that the vortex structure was not established for the weaker jet discharge ($\alpha = 3.9$), while the stronger jet discharge ($\alpha = 7.7$) had a developed twin vortex structure typical of jet discharges in crossflow. The decay of the centreline temperature was found to be a function of the axial distance (ξ). Initially the temperature decay was slower for the stronger jet but the dilution was found to be about the same beyond an axial distance of $\xi / d = 70$.

Chu and Goldberg (1974) carried out both the theoretical and experimental investigation on the location and dilution of buoyant jet discharges in crossflow. The experiments were carried out in a water medium for 8 different jet discharges of velocity ratios α between 6.3 and 44. Dyed salt solution was used as a tracer and both the measurements of salinity and the photography were used to interpret the results. Their conclusion indicated that the jet dilution was a function of the downstream distance and described by the two-thirds power law. It will be realized later the two-third power normally describes the dilution of the momentum dominated region of pure jets. The relatively high velocity ratios ($\alpha > 3.5$) used by the authors in most of their tests explains the similarity of their results to those expected for the non-buoyant jets.

Wright (1977) investigated extensively the whole range of buoyant and no-buoyant jets discharging into uniform and stratified crossflows. Wright used dimensional considerations, photographic analysis and dilution measurements using Rhodamine B Extra dye as a tracer. The jet source was towed at a constant velocity discharging into a stagnant ambient in a flume. Concentration measurements were carried out for 20 non-buoyant jet discharges into unstratified crossflows and velocity ratios α between 20 and 35. Relative concentration of samples along the jet trajectory were analyzed using a G.K. Turner Associates Model 111 fluorometer. Dilution analysis were carried out from measurements of the maximum concentrations along the jet centerline. The experimental results agreed with the theoretical formulations and indicated that distinct transitions occur between the various flow regimes of the jet. For the non-buoyant jets discharging into a uniform crossflow, Wright used both the dilution and trajectory plots to define the two slopes of the momentum dominated regions of the jet. The region described by the one-half slope near the jet nozzle was defined as the momentum dominated near field (MDNF) and the next region described by the two-thirds slope as the momentum dominated far field (MDFF). The data also indicated that the concentration centerline was located about 20 % higher than the centerline derived from the photographic analysis.

Hodgson and Rajaratnam (1992) conducted dilution studies in the laboratory with a similar approach to that of Wright (1977) and compared these results with some investigations in rivers. He considered flow velocity ratios α between 1.46 and 10.55, and depth ratios between 15.7 and 41.3. The investigations were meant to simulate more closely the actual field situations for downstream distances in the range $1.1 < \alpha x / d < 990$. The results were well represented by a power law relation.

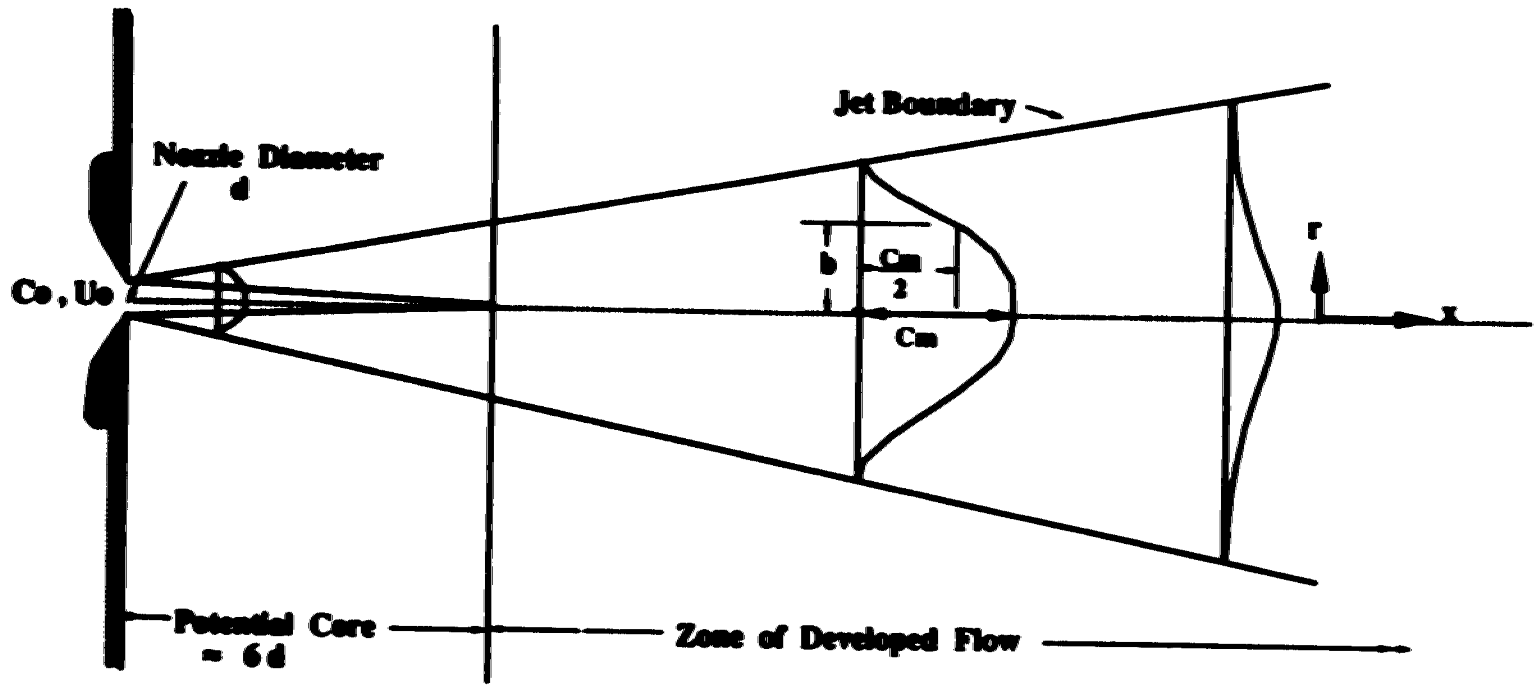

Fig. 2.1 Turbulent Circular Jet Discharge into a Stagnant Ambient

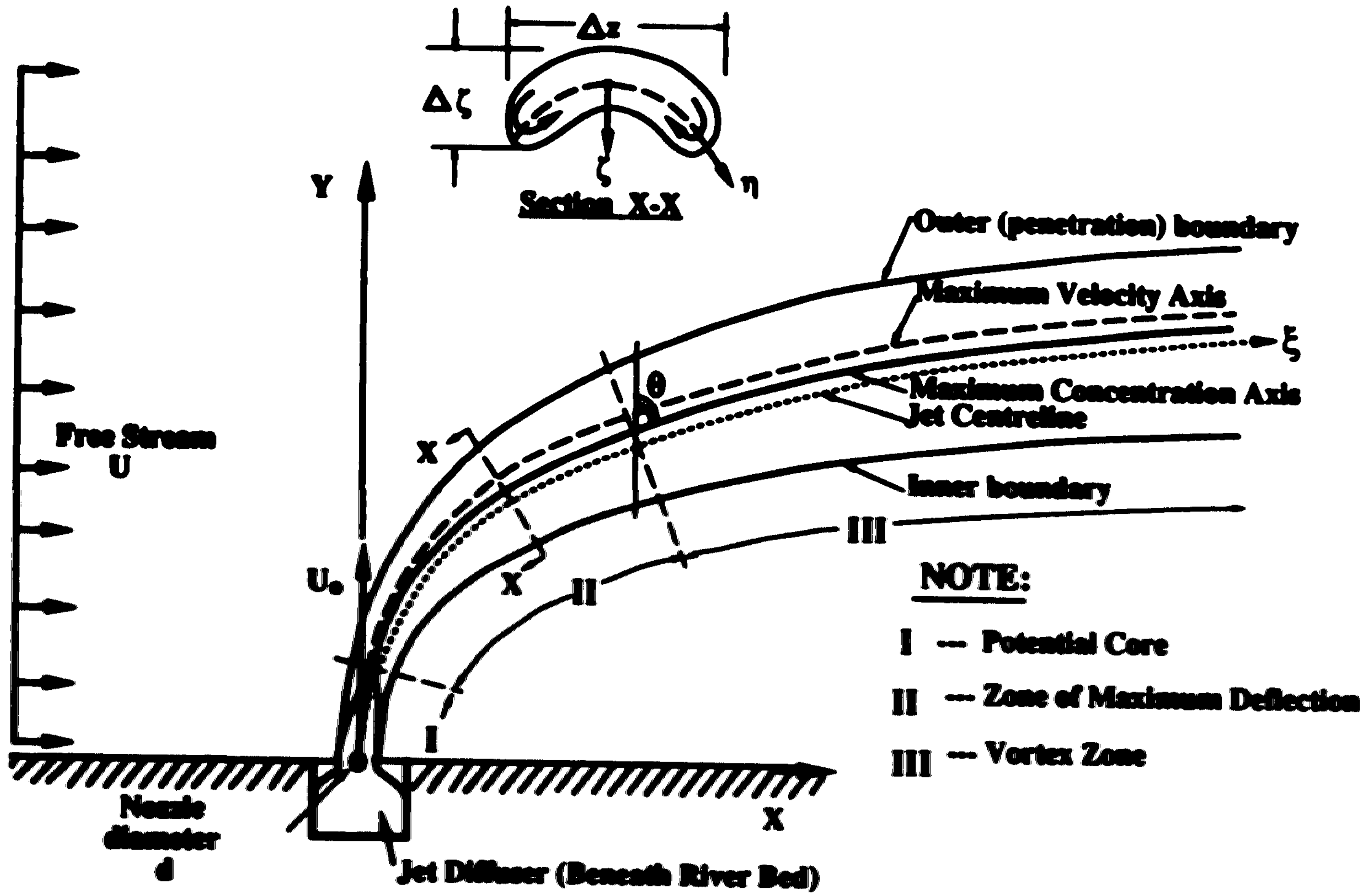

Fig. 2.2. Schematic Sketch of Turbulent Circular Jet Discharge in Crossflow (after Rajaratnam, 1976)

3.0 LABORATORY INVESTIGATIONS

3.1 General

The laboratory study on the dilution of a wall jet in crossflows was carried out to simulate the prototype river conditions by introducing a freestream flow in the channel (here referred to as crossflow) with a flow depth (D) to jet diameter (d) ratio of similar magnitude to the actual field situation. The bed of the channel would not represent the true conditions prevailing in the river but assumed the effect is minimal on the model experimental results. The channel flow was from the laboratory sump water refilled from the regular city water. Temperatures remained constant at the ambient laboratory conditions of about 20 (± 0.5) degrees Celsius throughout the experimental work.

Detailed discussion of the experimental procedure is presented in the following sections under three categories, namely: the experimental arrangement, calibration of the fluorometer and the sampling procedure.

3.2 Experimental Arrangement

3.2.1 The Flume

The experiments were carried out in a rectangular channel 0.91 m wide, 0.77 m deep and 36.5 m long (Plate 3.1) in the University of Alberta's T. Blench Hydraulics Laboratory. The channel is fitted with an adjustable slope mechanism, and the freestream flow was provided by a pump located in the laboratory sump. The discharge was measured using an inline magnetic flow meter with a digital measuring scale (reading to 2 decimal points) and calibrated for 1.0 VC unit to be equivalent to 0.015 m^3/s. The mean velocity in the channel section of the experiment was calculated from the measured discharge in the flume and the section flow area. The average velocity was also measured for 3 locations across the flume at distances of 80 mm, 220 mm and 450 mm (center of the flume) from the side wall using Prandtl-type pitot-static tube and transducers. The velocity profiles shown in Figure 3.1 clearly indicate that the wall effect extends as far as 80 mm into the freestream flow.

3.2.2 Jet Arrangement

Well-designed nozzles of diameters equal to 6.35 mm and 12.7 mm were used to produce the circular wall jets and both were located at a distance of about (22.0 m) downstream of the flume entrance. The nozzles were installed flush with the side wall of the flume with the bottom of the internal diameter at about the same level as the channel bed (Plate 3.2). The jet flows were generated by a 1/3 horsepower Jacuzzi model SP125/B pump fitted with a bypass line and connected to a constant head tank by a nalgene 800 tubing of 25.4 mm (1-inch ID) internal diameter and 3 mm wall thickness. The Rhodamine dye used as a tracer in the present study was mixed in a 900 litres tank connected to the pumping unit near its base, and received both the bypass line flow and the overflow from the head tank. Water used for mixing the dye was pumped from the same sump which provided the freestream flow.

The flow rate through the jet nozzle was measured by a calibrated Fischer rotameter rated in litres per minute (Plate 3.3) and controlled by two gate valves, one on the bypass line and the other on the line connecting to the constant head tank and the jet nozzle. The calibration of the rotameter was also checked by volumetric measurement.

The velocity at the jet nozzle was calculated from the rotameter discharge reading and the jet nozzle diameter. Velocity at the nozzle was maintained constant by the provision of the constant head tank on the flow line with an overflow arrangement.

3.3 Calibration of the Fluorometer

The analysis of the fluid samples was carried out in a Turner model 10 portable fluorometer (Plate 3.4) by manually filling the 35 ml cuvette or a clear test tube, with the sample from each bottle container at a time. The fluorometer output reading is on a double scale from 0 to 10 on the upper scale or 0 to 3.16 on the lower scale and both scales are related to each other by a factor of 3.16. For convenience with the decimal points, the upper scale was used throughout the present work. The fluorometer was calibrated using diluted standards of the Rhodamine dye (original market concentration of 20 % by weight of the dye and specific gravity of 1.19) solution corresponding to its range of 0.01 ppb to 55 ppb in order to derive the relation for interpreting the relative concentrations of the fluorescent dye in the sampled fluid. Standardized dye concentrations were plotted against the fluorometer output scale reading and the calibration indicated that the dye fluorescence is a linear function of the tracer concentration (Figure 3.2). The calibration best fit line ($r^2 = 0.999$) was expressed by the following relation:

$$C\,(\text{ppb}) = \frac{5.56 \,*\, \text{Scale Reading}\,(0-10)}{\text{Multiplier} \,*\, \text{Range}} \tag{3.1}$$

The multiplier was either 1 or 100, while the range of sensitivity was 1, 3.16, 10 or 31.6 and the larger figures indicate low concentration levels of the tracer in the sampled fluid. The multiplier of 1 was constantly used throughout the analysis but the range was varied through all the sensitivities depending on the tracer concentration. The concentrations higher than the maximum reading of the fluorometer could be analyzed by making standard solutions of the dye. The initial concentration (C_0) at the jet nozzle ranged from about 15 ppb to 20 ppb depending on the initial mixing of the dye in the 900 litres tank for the different jet discharges.

Consistency of the fluorometer calibration was checked by taking the readings of the standard solutions before and after the analysis of the samples. It was also necessary to turn on the fluorometer for about 20 minutes before carrying out the analysis of the fluid samples. The fluorometer is capable of measuring the fluorescence intensity of any chemical solution by simply installing the right kind of filter necessary for the particular solution and carrying out similar calibration procedure for the concentrations. The fluorometer could also be equipped with a continuous flow - through sampling procedure when using a single sampling tube.

3.4 Sampling Procedure

3.4.1 Sampling Rake Arrangement

Assessment of the jet dilution in the crossflow was done by carrying out the concentration measurements using Rhodamine WT as a tracer in the jet fluid. Fluid samples were withdrawn by means of a rake comprising a minimum of 7 sampling probes, each of 3.175 mm (1/8-inch OD) and a wall thickness of 0.9 mm, aligned with the ξ-axis (centerline trajectory) of the jet. The ξ-axis at a section was determined from the photographic trajectory plots of the centerline (Appendix III) and by the injection of the food color dye prior to sampling the tracer dye. The angle of the jet deflection from its original perpendicular direction was measured by a protractor, attached to the top of the sampling rake.

The sampling rake shown in Plate 3.5 was made up of L-shaped brass tubes set at a spacing of 30 mm and held in position by a wooden bracket which was kept out of the water surface at all times during the experiments. The spacing between the tubes was adjustable depending on the position of the sampling and the width of the jet. A minimum of 10 mm spacing was used near the jet nozzle and a maximum of 40 mm was used in the region away from the nozzle, where the lateral concentration gradients were small. The probes were set to withdraw the samples at the same level in the transverse η-axis simultaneously, starting from the bed level and the first tube was sampling near the inner boundary of the jet.

The tracer samples were collected for different levels at a spacing of 5 mm in the z-axis until the level which marks the outer boundary of the jet growth in the vertical elevation. To be able to sample across the jet in the η-axis, a second set of sampling was carried out with the last probe sampling the outer boundary (penetration axis) of the jet and the other tubes located between the positions of the first setting. The procedure followed in the first setting is repeated during the second setting for all the levels. It was assumed that steady state flow conditions prevailed both in the jet nozzle and the channel discharges and therefore sampling at any particular location was not time dependent. The samples for the background channel flow were withdrawn concurrently by a similar probe located upstream but near the jet nozzle.

A siphoning system of vinyl nalgene premium tubings of 3.175 mm (1/8-inch ID) internal diameter and 2.0 m long was used to discharge the tracer samples and collect in 60 ml opaque plastic bottles marked with the positions of the sampling probes. The collection bottles were set up and contained in a wooden sample rack (see Plate 3.6) positioned at an appropriate level to create a sampling velocity at the probe nozzle approximately equal to the main channel flow velocity and a continuous free flow in the tubings. All sample bottles were filled within the same amount of time but sufficient duration was allowed to eliminate the adsorption or desorption of the dye onto the delivery tubings. To minimize the loss of the dye fluorescence due to light, the samples were kept in a dark sample box until the concentration analysis of all the samples was completed.

3.4.2 Preliminary Investigations

The preliminary runs were carried out while developing the operational procedures of the experimental arrangements by visual observations of the jet trajectories and measuring the local velocity profiles of the flow in the flume for comparison with the mean value used in the present study. Figure (3.2) gives the profiles for the 3 locations across the flume at the section of the jet nozzle (mean channel flow velocity U = 0.60 m/s) which indicate that the mean velocity used is satisfactory in the region of the flow where the jet would be growing.

The centerline trajectory profiles of the various jet discharges were visually observed with the help of the colored dye and compared with the co-ordinate locations earlier obtained by Diebel and Rajaratnam (1980) for a similar circular wall jet

(Appendix III). Adjustments of the centerline axis were made independently for each jet discharge where necessary during the actual investigations.

In addition to the observations in the flume, the jet discharge was timed to empty the 900 litres tank in order to evaluate the length of the tracer sampling time before refilling the tank. During this process the fluctuation of the dye concentration in the tank was observed to be negligible and assumed constant (as the initial nozzle concentration, C_0) during the actual sampling. It was found that the dye solution in the tank was only enough to carry out sampling for one section of the jet at a time (running for about 3 hours). For every set of sampling it was found that the initial jet nozzle concentration depends on the amount of the dye mixed in the tank and therefore not necessarily constant for the different sections of the jet. To unify a steady state condition of the jet for all the sections investigated, the concentrations were considered with reference to the initial nozzle value (i.e. C / C_0).

3.4.3 Test Series

The present study involved a total of 9 experiments, including five jet discharges (α = 2, 4, 6, 8 and 12), two jet nozzles of diameters (d) 6.35 mm and 12.7 mm, and three flow depth ratios (D / d) of 20, 10 and 5. The summary of the conditions investigated are given in Table 3.1.

Sampling procedure of the tracer concentration began with making standard solutions of the Rhodamine dye (original market concentration is 20 % by weight). A standardized working solution of $1.0 * 10^5$ ppb (parts-per-billion) was made from the original solution and kept in a dark 4 litre bottle for use throughout the experiments. For every experiment, about 20 - 30 ml of the standard solution was withdrawn with the help of a pipette and mixed thoroughly in the 900 litres tank. Tracer mixture in the tank was checked for uniformity by measuring the concentrations at different levels (surface, center and bottom) of the tank. A constant value of the concentration passing through the bypass line of the pumping unit and the overflow line of the constant head tank was used as the initial jet nozzle concentration (C_0) because these flow lines were connected to the nozzle. The nozzle concentration was also checked after every sampling for any fluctuations which might have occurred. Also the temperature of the dye mixture was recorded before and after completing sampling each section of the jet. While the dye mixing was being carried out, a constant discharge was established in the flume.

The movement of the sampling rake perpendicular to the jet axis along the η-axis was restricted because errors could be introduced in the angular shift. The setting therefore was limited to two positions aligned with the centerline axis located by the jet deflection angle (θ) measured from the normal direction to the channel flow. For every setting the parameters noted were; the centerline axis co-ordinates (x, y_c) at the section, the jet deflection angle (θ) and the sampling probe number which locates the centerline of the jet.

The sampling rack containing the bottles for collecting the tracer samples was positioned to determine the discharge velocity of the samples. This was carried out by calculating the discharge velocity (u_s) from the time taken to fill the 60 ml bottles and dividing the discharge by the cross - sectional area (a) of the siphoning delivery tube (i.e. u_s = 60 ml * 1 / time * 1 / a). Repositioning was carried out until the velocity u_s was approximately in the range of the crossflow velocity U and the siphon system was free flowing without the interference of the bubbles in the tubings. This procedure was necessary to avoid the sampling probe acting as a sink in the streamflow or causing obstruction to the tracer discharge. Flushing of the bubbles was carried out whenever they were found.

The jet discharge was allowed to stabilize once all the settings were done before collecting the samples. Sampling was carried out at elevation spacing of 5 mm (z - axis) over the whole jet region in order to minimize the chances of missing the peak concentration (a characteristic maximum) of the jet. The samples were analyzed manually in the fluorometer and the concentration results were corrected for the ambient flow fluorescence which fluctuated between 0.05 - 0.10 ppb, depending on the amount of fresh water fed into the sump.

3.4.4 Error Estimation

The most critical error evaluation was carried out for the concentration measurements using the fluorometer. Significant errors could occur, especially for low values of concentration because the lowest possible reading of the fluorometer scale was 0.05 units when manually operated. The analysis of the standard error introduced by the calibration was carried out using 13 observations of the standard solutions of Rhodamine (diluted to known concentrations with distilled water). The calibration data were compared with the scale reading and the data given in Table 3.2 indicate that the fluorometer scale reading introduces a standard error of 0.01 units (equivalent to 0.002 ppb). This result compared to the lowest recorded reading of 0.5 units of the fluorometer's upper scale gave an error of about 2 % of the tracer concentration. For a 50 : 1 dilution of the tracer, the error introduced in the concentration measurements was less than 1 %. Manual operation of the fluorometer was used and hence resulted in minimal errors compared to those obtained when the automatic mode was in operation. Concentration errors due to desorption, adsorption, the bubbles in the tubing and the mixing process of making the standard solutions were found difficult to quantify, but may add or lower the actual concentration readings.

Other experimental errors were introduced during the measurements of the discharges, the crossflow and jet velocities and the angular measurements of the sampling probe co-ordinates. The error in the jet velocity resulted from the nozzle diameter machined to a precision of 0.025 mm and the rotameter discharge measurements with scale precision of 0.05 L/min. Linear measurements of the flume flow depth and the sampling spacing were carried out using the scale with a precision of 0.5 mm. Table 3.3 gives a summary of the experimental errors estimated for the parameters considered.

Experiment	Jet Diameter d (mm)	D/d	Jet Velocity Uo (m / s)	Channel Velocity U (m / s)	α (Uo/U)	Reynolds No $\frac{U_o d}{\upsilon}$
A100	6.35	20	0.53	0.26	2	3145
A200	6.35	20	2.4	0.59	4	14243
A300	6.35	20	2.6	0.43	6	15430
A400	6.35	20	2.9	0.36	8	17210
A500	6.35	20	3.42	0.285	12	20296
B100	12.7	20	0.86	0.143	6	10207
B200	12.7	10	0.78	0.13	6	9258
B300	12.7	5	1.57	0.26	6	18635
B400	12.7	20	0.86	0.07	12	10207

Table 3.1 Details of Experiments of Turbulent Circular Wall Jet in Crossflow

Standard Solution (ppb) ①	Scale Reading (Upper) ②	Calibration (Equation) ③	Difference (2 - 3) ④
50	8.9	8.962	-0.062
45	8.1	8.064	0.036
40	7.2	7.166	0.034
35	6.3	6.268	0.032
30	5.35	5.370	-0.020
25	4.5	4.472	0.028
20	3.5	3.574	-0.074
15	2.7	2.676	0.024
10	1.8	1.778	0.022
8	1.4	1.419	-0.019
6	1.05	1.060	-0.010
4	0.7	0.700	0.000
2	0.35	0.341	0.009

Note:

Standard Deviation = 0.036 and Standard Error = 0.01

(of the scale reading difference)

Table 3.2 Fluorometer Scale Reading Error Estimation

Measurements	Precision	Error Estimation (± %)
Fluorometer (Upper Scale)	0.05	< 2
Jet Discharge (L/min)	0.05	< 5
Jet Nozzle Diameter (mm)	0.025	< 1
Channel Discharge (L/sec)	0.05	< 5
Flow Depth (mm)	0.5	< 4
Sampling Spacing (mm)	0.5	< 5
Angular Alignment (degree)	0.5	< 5

Table 3.3 Error Estimation

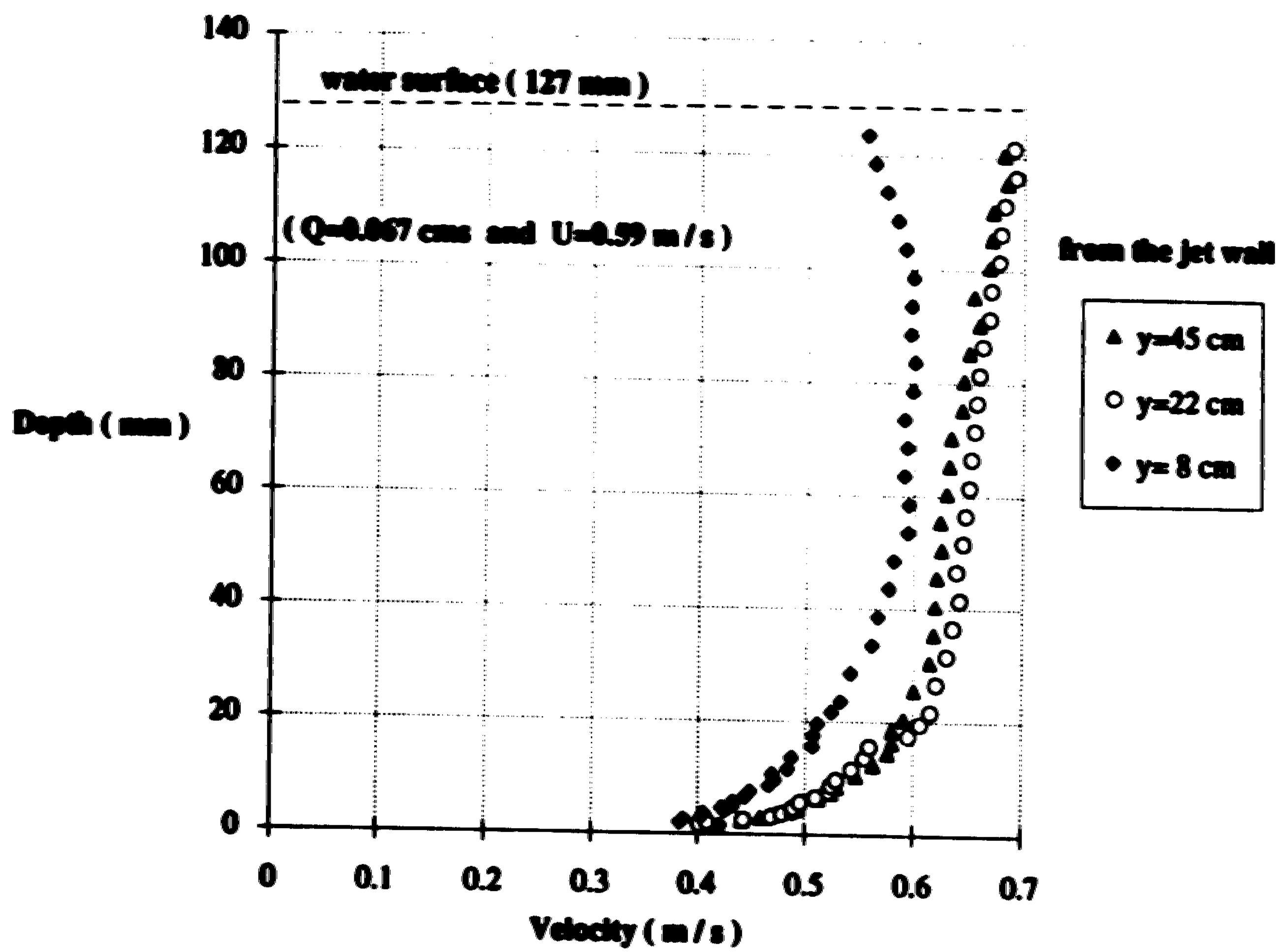

Fig. 3.1 Velocity Profiles across the Flume

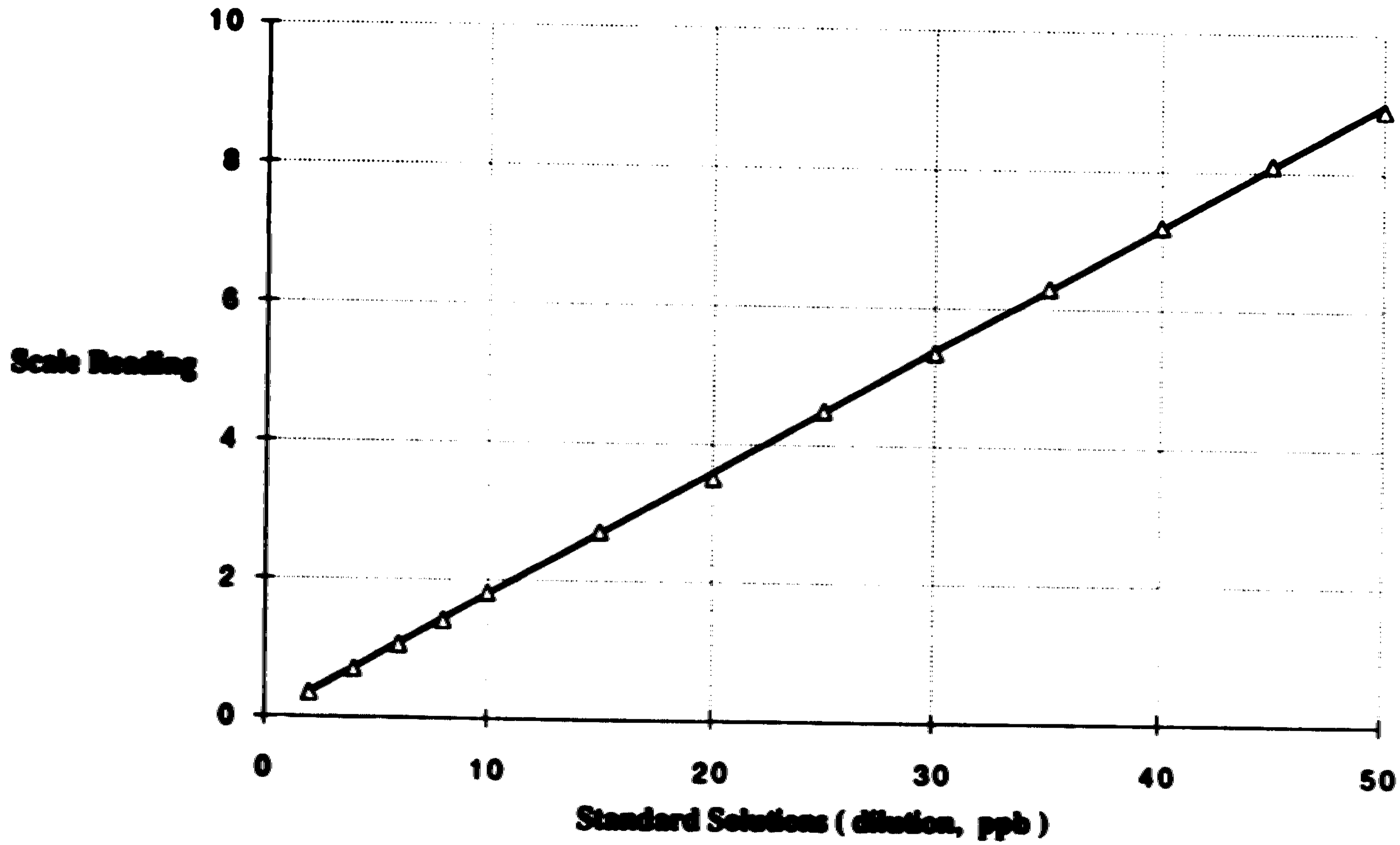

Fig. 3.2 Calibration Curve for the Fluorometer

(a) Side View

(b) Sampling Position

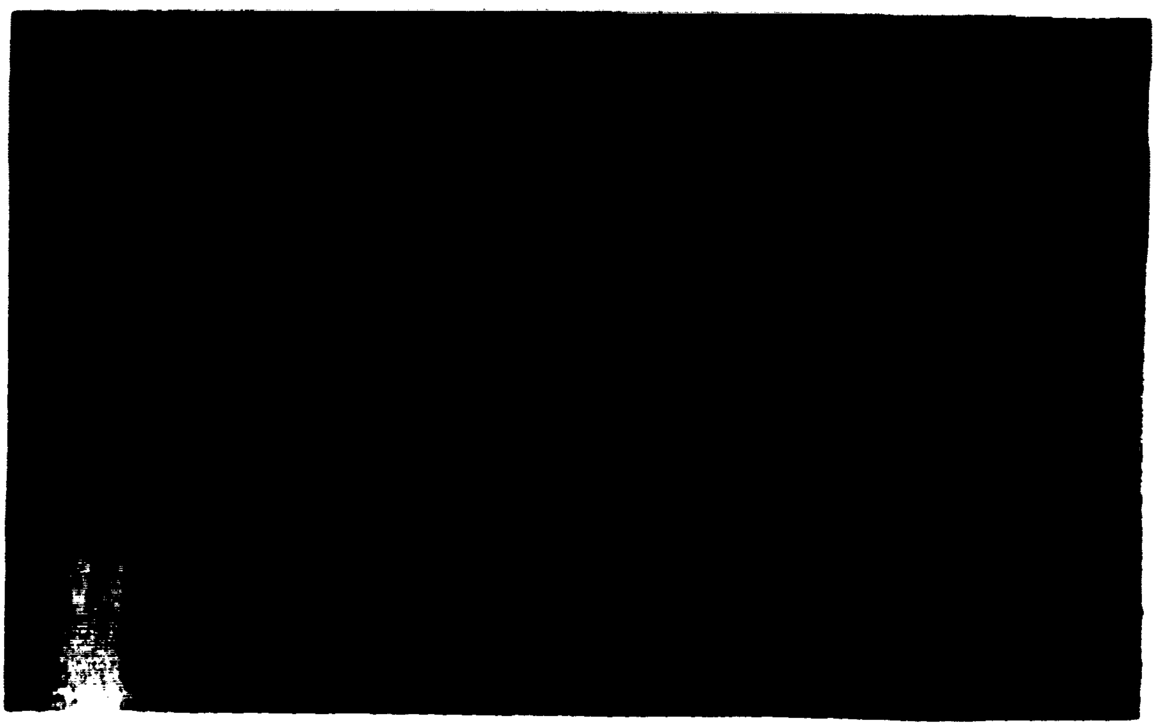

Plate 3.1 Flume Arrangement

(a) Location of the Nozzles

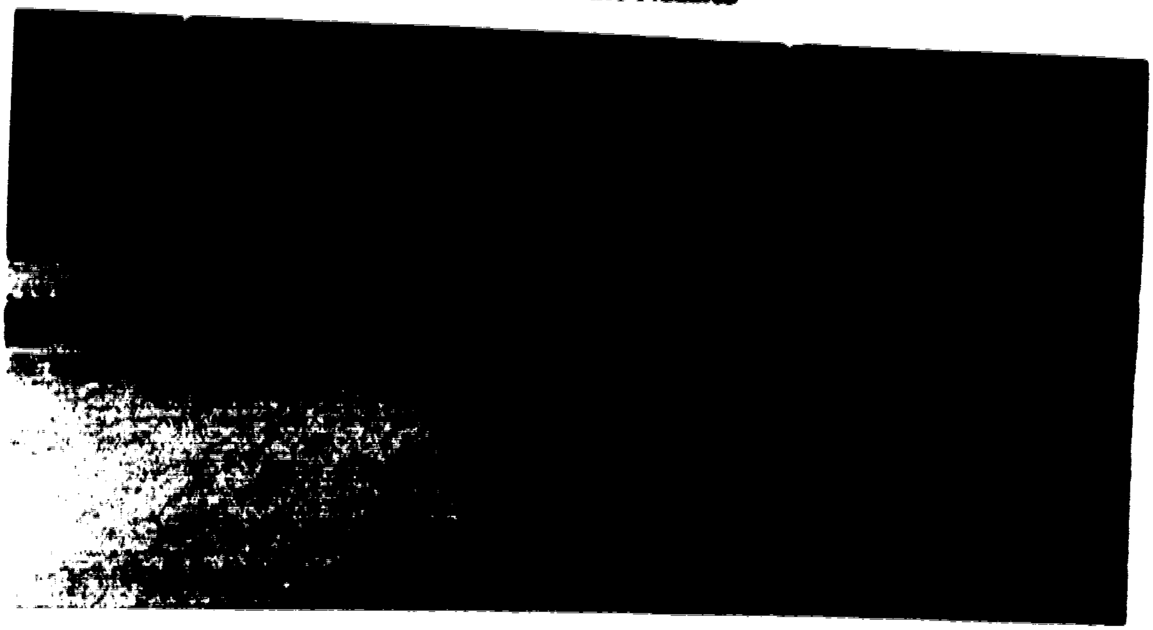

(b) Diffusion of the Jet: $\alpha = 12$, $\frac{D}{d} = 20$ and $d = 6.35$ mm

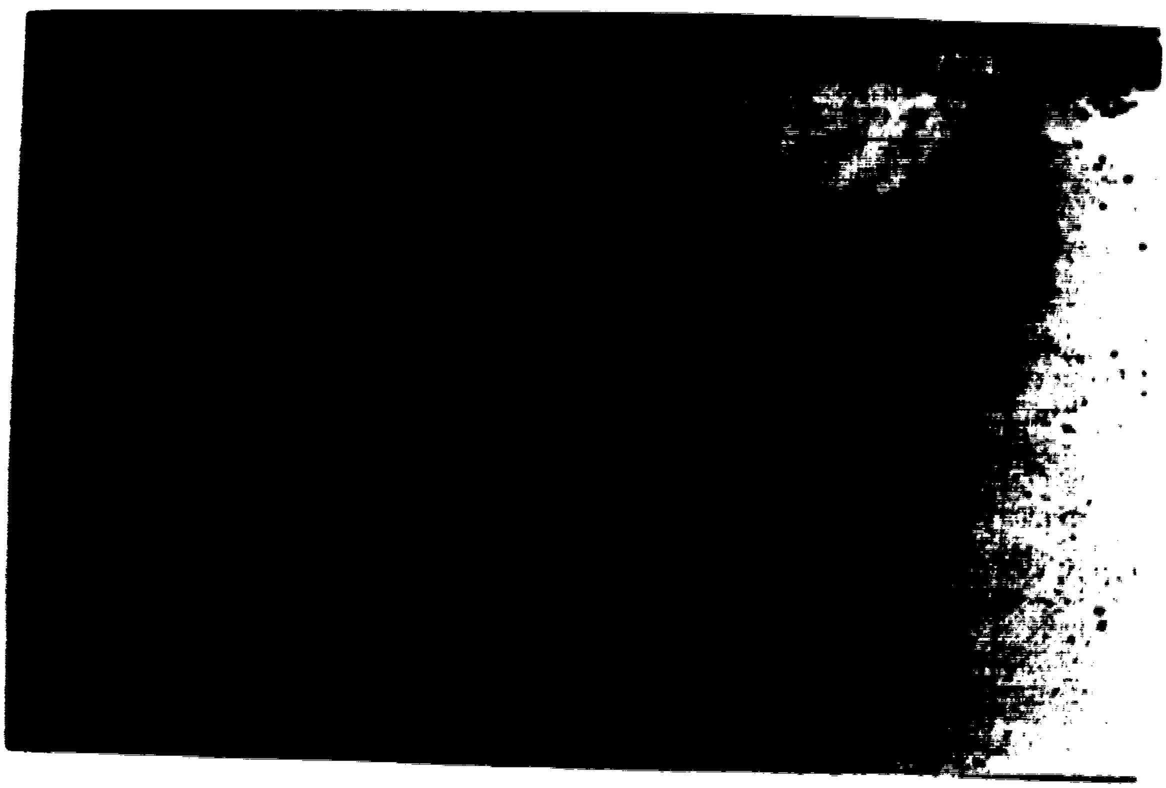

Plate 3.2 Jet Nozzle Arrangement

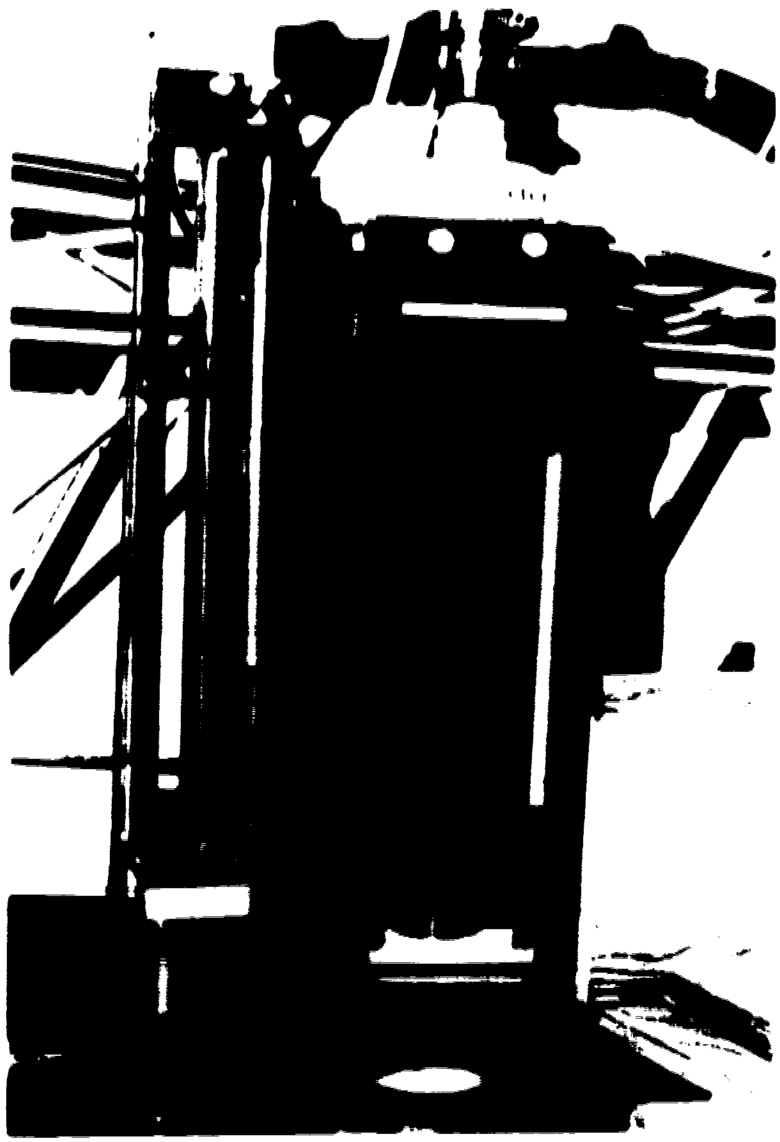

Plate 3.3 Rotameter

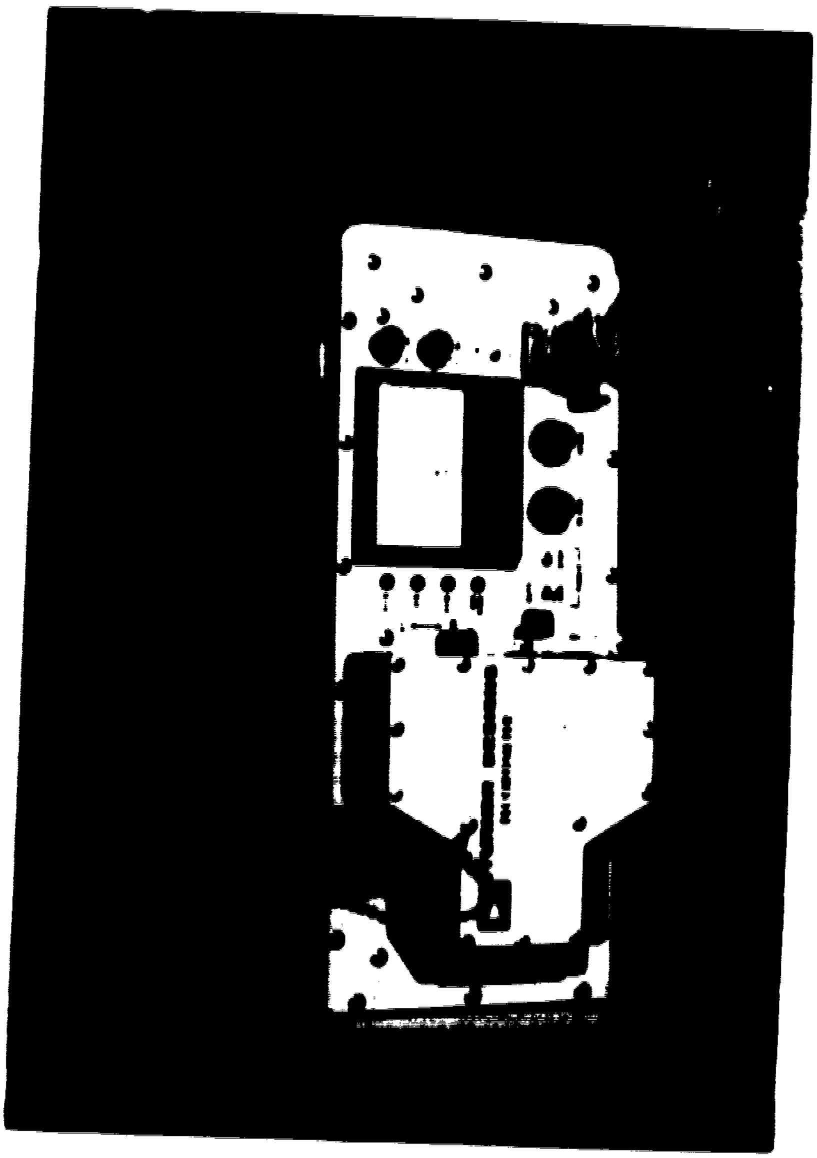

Plate 3.4 Turner Model 10 Fluorometer

(a) Sampling Position in the Flame

(b) Sampling Probes Arrangement

Plate 3.5 Sampling Rake

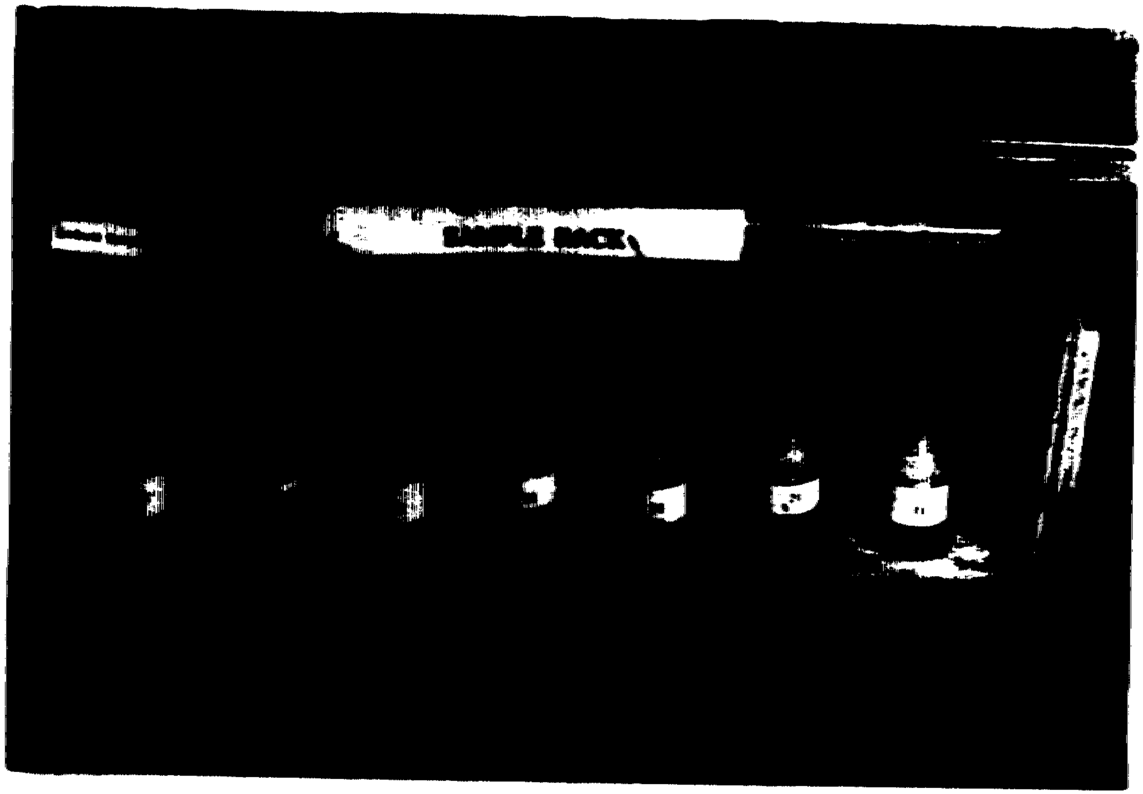

Plate 3.6 Sampling Rack (showing 60 ml bottles and delivery tubes)

4.0 EXPERIMENTAL RESULTS AND ANALYSIS

4.1 General

Interpretation of the concentration results in the following sections follows the objectives of identifying the main characteristics of dilution of circular wall jets in crossflow and comparing with those of the free jets.

The dilution of circular wall jet in crossflow is a complex three-dimensional problem and the present analysis considers the maximum concentration (or minimum dilution) to characterize the dilution problem. Since no published investigations exist on this problem, the present results are compared with those on dilution of the free circular jet (Wright, 1977; and Hodgson and Rajaratnam, 1992). A generalized form of the results is suggested for practical purposes for predicting the minimum dilution (C_0 / C_m) along the non-dimensional distance $\alpha x / d$ for each of the flow regimes earlier defined as the momentum dominated near and far fields, as well as the passive plume region at the end.

The growth of the jet both in the vertical ($z - \xi$ plane) and the transverse ($\eta - \xi$ plane) directions would be assessed from the concentration profiles, by comparing the trends of the length scales along the curvilinear distance (ξ) of the jet. In addition, the effect of changing the jet nozzle diameter (d) and the flow depth ratio (D / d) would be considered.

The boundary limits of the momentum dominated flow regimes identified from the earlier results of Wright (1977) and Rajaratnam and Gangadhariah (1980) would be defined. The results of the present investigation would then be categorized graphically into the momentum dominated near field, the far field and the passive plume regions.

4.2 Boundary Limits of the Momentum Dominated Flow Regimes

The analysis presented in this section defines the momentum dominated flow regimes of the deflected jet in crossflows. Based on existing works, the different mixing regions would be identified first for the free circular jet and then applied to the wall jet in crossflows.

The mixing process experienced by the effluents discharged into a receiving stream, from the review of the existing literature is considered to occur in two momentum dominated regimes; the near field region (MDNF) where $y_c << l_m$ and the far field (MDFF) where $y_c >> l_m$. In the MDNF, the jet is displaced by the crossflow but retains its similarity to jets in a stagnant ambient whereas in the MDFF, the diffusion of the jet is affected by the moving ambient. These two regimes are generally followed by what can be termed the passive plume region (PPR) where the velocity excess in the jet has decayed and the mixing and dilution is due to the turbulence in the ambient. However, the boundary limits of the regions were not clearly defined and now form part of the present analysis. The work of Wright (1977) on the momentum dominated trajectories and that of Rajaratnam and Gangadhariah (1980) on circular jets in crossflow are used in the present investigation to derive the limits of the three regimes.

4.2.1 Momentum Dominated Near Field Regime

The photographic observations of Wright (1977) indicate that the intersection of the 1/2 and the 1/3 slopes on the data plot of y_c / l_m against x / l_m defines the co-ordinates of the separation point between these two regimes. The point is given by $y_c / l_m = 1.5$ and $x / l_m = 1.0$, where l_m is the momentum length scale [$= M^{1/2} / U$] as had earlier been defined. The trajectory relation for the momentum dominated near field flow regime, from dimensional analysis is given by (Wright, 1977):

$$\frac{y_c}{l_m} = C_1 \left(\frac{x}{l_m} \right)^{1/2} \qquad (4.1)$$

where C_1 is the proportionality constant and a function of α.

Let x_* to be the x co-ordinate where MDNF ends. Rewriting the above Equation 4.1 and substituting for y_c / l_m becomes:

$$\frac{x_*}{l_m} = \frac{2.25}{C_1^2} \qquad (4.2)$$

The distance downstream of the freestream flow from the jet nozzle is given in a non-dimensional form as $\alpha x / d$ and, therefore, Equation 4.2 becomes:

$$x_* = \frac{2 \alpha d}{C_1^2} \qquad (4.3)$$

The coefficient C_1 is derived from the experimental data using the general Equation 4.1 and plotted against the velocity ratio α. The data are described by the equation (Hodgson and Rajaratnam, 1988):

$$C_1 = 2.0 - \frac{2.2}{\alpha^{2/3}} \qquad (4.4)$$

Therefore, a plot of $\alpha x_* / d$ against α is given in Fig. 4.1 as the end limit of the MDNF or the lower limit of the MDFF.

4.2.2 Momentum Dominated Far Field Regime

Similar analysis was followed to define the upper limit of the momentum dominated far field region. The centerline trajectory relation derived by Wright (1977) for this region is given by:

$$\frac{y_c}{l_m} = C_2 \left(\frac{x}{l_m} \right)^{1/3} \tag{4.5}$$

The proportionality constant C_2 is again found to be a function of α. The logarithmic plot of the coefficient determined from the experimental data was given by the equation (Hodgson and Rajaratnam, 1988):

$$C_2 = 0.89\, \alpha^{1/6} \tag{4.6}$$

The upper boundary of the MDFF could not be determined from Wright's trajectory plot and therefore a new basis was explored to define the limit. Based on the velocity field of the flow, the end of the MDFF was assumed to occur where the excess velocity in the jet above that of the ambient falls to about 1% of the initial velocity excess given as (U_m - U) = 0.01 (U_o - U). From the work of Rajaratnam and Gangadhariah (1980), (U_m - U) / (U_o - U) = 0.01 occurs approximately when $\xi / \xi_* = 10$ where ξ_* is the length scale in the velocity correlation and defined by the axial distance of the deflected jet from the virtual origin to the end of the potential core. The length scale is a function of α and fitted by the logarithmic function given by:

$$\xi_* / d = 1.5\, \alpha^{0.43} \tag{4.7}$$

Pratte and Baines (1967) plotted the centerline penetration of the deflected jet against the distances along the ξ - axis and the data were described by a straight line with the equation:

$$\frac{y_c}{\alpha d} = 1.63 \left(\frac{\xi}{\alpha d}\right)^{1/3} \qquad (4.8)$$

for all the data points beyond the potential core.

Let $\xi_{\dagger}$ and $x_{\dagger}$ be the axial distance and the downstream longitudinal distance of the deflected jet respectively at the end of the MDFF. Therefore, incorporating the above assumption into Equation 4.8 and combining with Equation 4.5 results in the following relation, for the end limit of the MDFF regime:

$$x_{\dagger} = 5.47 \frac{\xi_{\dagger}}{C_2^3} \qquad (4.9)$$

A plot of $\alpha x_{\dagger} / d$ against α is given in Figure 4.1. The figure indicates the three distinct regions delineated by the Equations 4.3 and 4.9 as the momentum dominated near field regime, momentum dominated far field regime and the passive plume regime which occurs beyond the upper boundary of the far field regime.

4.3 Experimental Results

4.3.1 Parameters Considered

Concentrations across the section of the jet were sampled on a minimum grid of 5 mm by 5 mm near the nozzle to a maximum grid of 10 mm by 10 mm on the wider section of the jet to ensure that the peak concentration point was sampled. The grid system resulted in a minimum of about 80 co-ordinate points near the jet nozzle and a maximum of about 200 co-ordinate points for the fully grown jet, of concentration measurements for one section. An average of 10 sections were investigated for each of the 5 jet discharges covering downstream distances as far as x = 4000 mm (or a maximum of α x /d = 5000).

Two jet nozzles of diameters of 6.35 mm and 12.7 mm were used for the range of velocity ratios α of 2, 4, 6, 8 and 12. The ratio of the freestream flow depth (D) and the jet nozzle diameter (d) was maintained constant at 20 throughout the measurements, except for α = 6 where cases with D / d = 10 and 5 were also investigated.

4.3..2 Presentation of the Results

The concentration data were corrected to eliminate the ambient fluorescence and tabulated in Appendix II. Concentration measurements in all the sections were taken perpendicular to the jet axis. A similar procedure was used by Fan (1967) while Wright (1977) and Hodgson (1991) considered vertical cross-sections (parallel to y-axis) for the free jet. The data for the different transverse (η - ξ plane) levels are presented, with the lowest level fixed at an elevation of 1.5 mm above the bed at the axis of the sampling probe centerline while touching the bed. The schematic sketch given in Figure 4.2 defines the planes considered in the presentation of the results. The unit for the tracer concentration is parts per billion (ppb).

4.4 Analysis

4.4.1 Concentration Profiles

Transverse concentration profiles (η - ξ plane) were plotted for all the sections investigated. Sample plots for the velocity ratio $\alpha = 4$ at locations in the near field (x = 5 mm) and the far field region (x = 100 mm and 285 mm) are given in Fig. 4.3 (a) - (c). Observation of the plots indicates no symmetry between the profiles near the bed and those on the upper half of the jet because of the boundary layer effect. The maximum concentration (C_m) occurs at a distance δ measured from the bed to the elevation of maximum concentration, then decreases to a constant value of the ambient fluorescence. It was also interesting to note the shift of the concentration peak for profiles near the bed, towards the outer part of the jet, and the profiles above the level $z = \delta$ show a shift of their peaks towards the inside boundary of the jet. The shift for profiles near the bed is a result of the low boundary layer velocity which allows greater jet penetration. The maximum concentration is not symmetrically located on the visual centerline of the jet trajectory as observed in axisymmetric jets but occurs generally on the outer half-section of the jet width.

Double peaked concentration profiles appeared for the sections investigated in the maximum deflection zone. The possible explanation could be as a result of the vortex formation which could only be further investigated by plotting the contour profiles. This has not been considered in the present study. Concentration profiles for the locations far downstream indicated complete mixing and little change occurs in the concentration gradient throughout the flow depth where the jet momentum has diminished to ambient flow conditions.

4.4.2 Minimum Dilution

Dilution of the tracer concentration at a section is explored by considering its characteristic minimum value which occurs at the location of maximum concentration in the jet. Minimum dilution is therefore given by the ratio of the initial concentration (C_0) at the jet nozzle to that of the characteristic maximum concentration (C_m). Both the vertical and the transverse planes containing the characteristic value are considered for the similarity test and the growth of the jet half-width (where the instantaneous concentration is one half the maximum value, or $C = 1/2\, C_m$) length scales. The main features of the various flow regimes would be identified by presenting the analysis based on the momentum dominated near field, momentum dominated far field and the passive plume regions.

The vertical (z - ξ plane) concentration profiles were considered by plotting the maximum value of C / C_0 against the elevation z (mm) for all the sections and for each of the five jet discharges as given in Figures 4.4 - 4.8. The results clearly indicate the distributions assume the wall jet shape quickly and the profiles are not symmetrical along the maximum value as expected for the simple jet. This is because the jet growth is restricted near the bed. The plots also indicate that little dilution (less than 2 : 1) occurs near the jet nozzle where the jet penetrates the ambient flow with its undiminished momentum. Most of the tracer accumulated in the lower one-third of the flow depth.

Similarity of the concentration profiles was tested by plotting non-dimensional values of C / C_m against z / b_z (where b_z is the elevation measured from the bed where $C = 1/2\, C_m$), for all the flow discharges. Plots for the different flow regimes are given for each of the five jet discharges in Figures 4.9 - 4.14. The plots indicate reasonably similar concentration distributions on the outer edge of the jet but noticeable scatter exists near the bed due to the boundary layer effects. Considering the data points away from the wall (bed), the concentration distributions for the sections in the momentum dominated near field all collapse into a single curve with minimal scatter. The jet dominates the flow in this region and is least affected by the crossflow ambient, and therefore the mixing processes are similar to those in the simple axisymmetric jet. As similarity trend is also shown by the data in the momentum dominated far field. However, some scatter is displayed by the data points on the outside periphery of the jet. This might be due to the effects of non-uniform velocity distribution of the crossflow.

The distributions for the passive plume region show a lot of scatter over the whole depth of the flow. This indicates that the characteristics of the flow regime are different from those of the momentum dominated regimes. Some trend, however, exists for most of the data points neglecting those near the wall. The jet mixing in the region has grown to the free surface and consequently the dilution is constrained.

Concentration distributions in the transverse (η - ξ plane) direction were investigated by plotting C / C_0 against the lateral distance η measured on both sides from the axis of the maximum concentration as the origin. The plots are given in Figures 4.15 - 4.19 for each of the five jet discharges. The profiles are fairly symmetrical and can be approximated to the Gaussian distribution, especially beyond the maximum deflection zone of the jet when the profiles become more uniform. Concentration profiles for the sections at downstream distance of about $\xi = 50$ d show minimum dilution of about 20 : 1 for each of the jet discharges. The spread of the jet growth to the inner wall occurred faster for the weaker jet discharge of $\alpha = 2$ because of its smaller penetration and susceptibility to deformation by the crossflow ambient compared to the relatively stronger jets of $\alpha = 4, 6, 8$ and 12.

Similarity plots of the transverse concentration profiles were obtained by plotting C / C_m against η / b_* (where the jet half-width, b_* is the transverse distance measured from the axis of the maximum tracer concentration to the position where concentration is one-half the maximum value, or $C = 1/2\ C_m$). The plots for the momentum dominated regime are presented in Figures 4.19 - 4.24 for each of the five jet discharges and the combined distributions given in Figure 4.25. The distributions indicate similarity for the momentum dominated flow regimes. Limited scatter occurs for data points sampled near the inner wall boundary, which is expected because of the uneven distribution of the freestream velocity near the walls (see cross-section velocity distributions, Figure 3.1).

Concentration distributions for the passive plume region were not included because the jet half-width, b_* could not be obtained due to a near uniform concentration profile across the jet flow in the region. This further supports the differences of the passive plume region from those dominated by the jet.

Next we study the decay of the maximum concentration (C_m) along the downstream distance x by considering the minimum dilution ratio (C_0 / C_m). Patrick (1967) expressed the dilution ratio empirically as a function of the curvilinear distance (ξ) of the deflected jet. Wright (1977) used dimensional considerations to define the dilution as proportional to the vertical distance (y_c) of the centerline of the jet. For practical purposes and the convenience of measuring the downstream distance x, Hodgson and Rajaratnam (1992) reduced the dilution expression given by Wright to be a function of $\alpha x / d$. Similar consideration is adopted for the present analysis and the results compared to those of the free jet (Wright, 1977; Hodgson and Rajaratnam, 1992) for the momentum dominated regions.

The power law form of minimum dilution given by Patrick (1967) is reduced with the help of the logarithms into a simple correlation with the downstream distance x . The choice of using the downstream distance x is however limited in the field application where river flow goes through a meandering reach and therefore prior knowledge of the river reach is necessary to ensure sufficient length of the initial dilution zone is available before locating the outfall. In the present investigation plots of the minimum dilution (C_0 / C_m) against the downstream non-dimensional distance ($\alpha x / d$) are given on the double-logarithmic scale for each of the jet discharges investigated in Figures 4.26 - 32 which cover the investigated range of $\alpha x / d$ from 2.0 to 5000. The data indicate a general trend for the characteristic dilution and is fitted by two slopes of 1 / 2 and 2 / 3, respectively. For a free jet in a crossflow, according to Wright (1977), the two flow regimes represent the momentum dominated near field (MDNF) and the momentum dominated far field (MDFF) regions of a circular jet in crossflow. The present consideration of a circular wall jet in crossflow indicates similar slope trends and, therefore, similar flow regimes prevail. The effect of the wall (bed) on the level of dilution would be assessed by comparing the two forms of the jet. The most significant observation of the two slopes is the transition limit. Based on the criteria earlier defined for the limits of the MDNF, MDFF and the PPR regions given in Figure 4.1, the transition for the slopes occur within 2 orders of magnitude ($\alpha x / d < 100$) for the jet discharges with the velocity ratios $\alpha = 2$ and 4 and fairly close to the criteria used. However, the transitions for the stronger jet discharges of velocity ratios $\alpha = 6$, 8 and 12 are shifted more downstream and occur between the distance range of $100 < \alpha x / d < 1000$. This results suggest stronger wall jet flows behave as though the near field regimes are longer than those of the corresponding free jets. The extended length of the near field regime may be due to the underestimated crossflow velocity near the bed which is less than the mean value used. For all the discharges considered, the plots indicate that dilutions less than 2 : 1 are generally non-linear and occur in the vicinity of the outfall ($\alpha x / d < 10$).

The weakest jet, ($\alpha = 2$) shows a more superior dilution as compared to the other jet discharges and also higher than Wright's near field (1/2 slope). Dilutions of between 10 : 1 and 20 : 1, normally recommended within the vicinity of a jet diffuser is achieved by the jet discharge for $\alpha x / d < 100$ and dilution of upto 100 : 1 occurs for $\alpha x / d < 1000$. The model for Hodgson (1991) achieved a maximum dilution of 50 : 1 at a downstream distance of $\alpha x / d = 900$, which extended only through the range for the initial dilution (or mixing) zone.

The jet discharge with velocity ratio $\alpha = 4$ had similar range of dilutions with those of $\alpha = 2$. Dilutions of 10 : 1 upto 20 : 1 were achieved within the downstream distances of $100 < \alpha x / d < 200$. The initial dilution zone requirement of dilution of 50 : 1 was achieved by the jet discharge at a distance of about $\alpha x / d = 700$. The other jet discharges ($\alpha = 6$, 8 and 12) indicated low dilutions ranging generally between 30 : 1 and 35 : 1 within downstream distances $\alpha x / d < 1000$.

Effect of the flow depth ratios (D / d) on the dilution was also investigated by considering $D / d = 10$ and 5 for $\alpha = 6$. The results are given in Figures 4.28 (b) and (c). For $D / d = 10$, the results for the momentum dominated near field compares well with those of Wright's equation and extends to a downstream distance of about $\alpha x / d = 400$ for dilutions of approximately 20 : 1. The same jet discharge and that of $D / d = 20$ fitted similarly well for the near field data for a downstream distance of about $\alpha x / d = 300$ and dilutions of upto about 20 : 1. Further decrease of the flow depth ratio to $D / d = 5$, resulted in significant effects on the dilution because of the surfacing of the jet. The dilutions presented graphically in

Figure 4.28 (c) assumed an almost constant value of about $C_o / C_m = 15$ for downstream distances ($\alpha x / d$) above 100.

The combined results given in Figures 4.31 and 4.32 indicate the lower jet discharge of $\alpha = 2$ compares well with the results of Hodgson (1991) for the near field dilutions but more superior for downstream distances above $\alpha x / d = 100$. This may be explained by the change of the flow regime from the momentum dominated to the passive plume condition which show higher dilutions. Hodgson's results compare well with the data for $\alpha = 4$ above $\alpha x / d = 100$. The higher jet discharges of $\alpha = 6$, 8 and 12 maintained the momentum dominated near field characteristics similar to those of Wright's for distances up to three orders of magnitude ($\alpha x / d = 1000$). The dilutions in the far field regime compare approximately well to those of Hodgson. Therefore, the results in the present investigation suggest that circular wall jet dilutions in the near field regime are represented well by the Wright's (1/2 slope) solution , while for the far field regime are predicted by the results of Hodgson (0.56 slope). However, the use of Wright's far field solution could also be applicable for the wall jet but the coefficient C_4 used and hence the constant in the dilution equation will change and be higher than the given value of 0.223.

For convenience in estimating the dilutions in a practical situation, the results of the present study given in Figure 4.31 are described by a mean equation of the form:

$$C_o / C_m = 0.67 \, (\alpha x / d)^{0.63} \qquad (4.10)$$

The above equation describes fairly well the data points in the momentum dominated near field because all the jet discharges behave similar in the regime. Distinct scatter of the data is shown in the far field because dilutions are more dependent on the strength of the jet discharge. Dilutions of upto 100 : 1 are represented by the correlation.

4.4.3 Length Scale Analysis

The concentration profiles for circular wall jet in crossflow have been shown to be similar both in the vertical, z - ξ plane (depth-wise) and the transverse, η - ξ planes. The following analysis considers the variation of the respective characteristic length scales along the curvilinear (ξ) distance. The jet nozzle diameter d is used as a length scale to make the results non-dimensional.

4.4.3.1 Vertical Scale, b_z

The vertical length scale b_z is measured from the bed ($z = 0$) to the point where the concentration is one-half of the maximum value at the section ($C = 1/2\, C_m$). Figure 4.33 graphically shows the variation of b_z / d along the axial distance, ξ / d (measured along the trajectory of maximum concentrations) for the five jet discharges. The results indicate that the momentum dominated near field flow regime ($\xi / d < 30$) is fitted by a unifying length scale described by the following relation:

$$\frac{b_z}{d} = 1.0 + 0.3\,(\xi / d) \qquad (4.11)$$

The variation of the scale in the momentum dominated far field appears to be a function of the flow velocity ratio α. The weakest growth is shown by the jet discharge of velocity ratio $\alpha = 2$, while for $\alpha = 4$ and 6, b_z grows at rates higher than that of $\alpha = 2$. Jet discharges of velocity ratios $\alpha = 8$ and 12, grow at rates higher than those of the weaker jets. However, all the jet flows grow with similar slopes and are described by the following relations:

$$\frac{b_z}{d} = 3.0 + 0.02\,(\,\xi / d\,) \qquad (\alpha = 2) \qquad (4.12)$$

$$\frac{b_z}{d} = 6.0 + 0.03\,(\,\xi / d\,) \qquad (\alpha = 4 \text{ and } 6) \qquad (4.13)$$

$$\frac{b_z}{d} = 10.0 + 0.03\,(\,\xi / d\,) \qquad (\alpha = 8 \text{ and } 12) \qquad (4.14)$$

The dependence of α of the scale in the momentum dominated far field region is shown by plotting ξ / ξ_m against $b_z / \alpha\, d$ (where ξ_m is the axial distance where $x = \alpha\, d$) and given in Figures 4.34 (a) and (b). For velocity ratios α greater than 4, the plot indicate the dimensionless distance ξ_m / d is a linear function of α.

The variation of the vertical scale, b_z indicates that the wall jet grows at about 10 times faster in the momentum dominated near field compared to the momentum dominated far field regime.

4.4.3.2 Transverse Scale, b_ϕ

Transverse characteristic length b_ϕ at a section is defined as the distance measured from the jet axis (defined by maximum tracer concentration) to the location where the instantaneous concentration is one - half the maximum value on either sides of the axis. The outer scale is conventionally considered positive and the inner scale negative. The transverse growth characteristics of the wall jet are derived graphically by plotting ξ / d against the absolute sum of the scale $(+b_\phi + | -b_\phi |) / d$ and given in Figure 4.35. The results for all the five jet discharges fall into two distinct flow regimes. For the first region defined by the momentum dominated near field, the variation is described by the linear relation:

$$\frac{(+b_* + |-b_*|)}{d} = 0.53 \frac{\xi}{d} \qquad (4.15)$$

For the second flow region known as the momentum dominated far field, the corresponding relation is:

$$\frac{(+b_* + |-b_*|)}{d} = 7.5 + 0.075 \frac{\xi}{d} \qquad (4.16)$$

Unique trends were observed when the transverse length scales for the growth on the outside (positive) and the inside (negative) regions of the deflected jet were considered separately. The results given in Figure 4.36 (a) and (b) indicate that the transition between the momentum dominated near field and far field regions for the outside scale does not occur gradually whereas for the inner scale, there is a smooth transition.

Comparing these results to those obtained for the vertical scale easily, we can conclude that for circular wall jets in crossflow, the transverse growth is about two times that of the corresponding growth in the vertical (depth - wise) direction. These results support the fact that the wall (bed) restricts the vertical growth of the jet but favors the horizontal transverse growth and it is an advantage for dilution in shallow rivers where normally the widths are several times more than the flow depth.

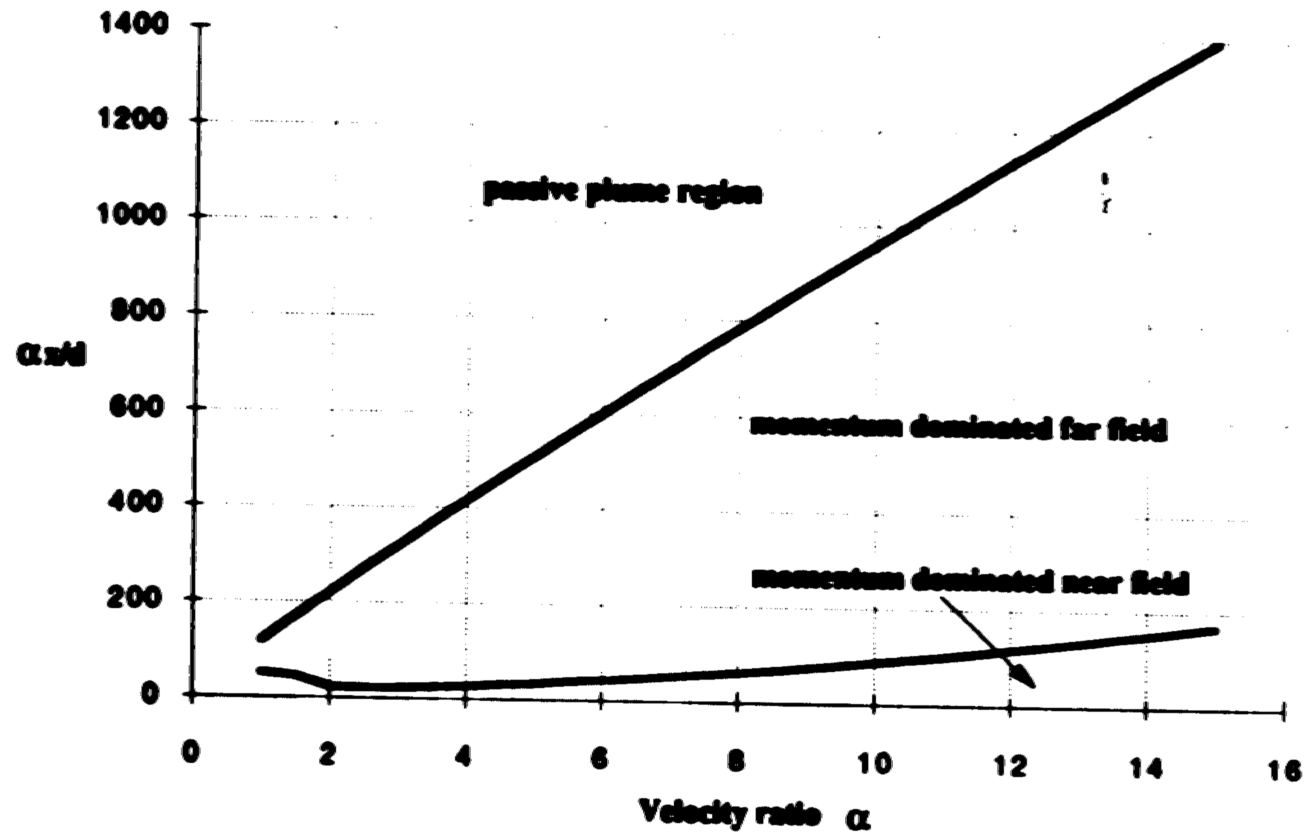

Fig. 4.1 Boundary Limits for the Momentum Diminated Regions

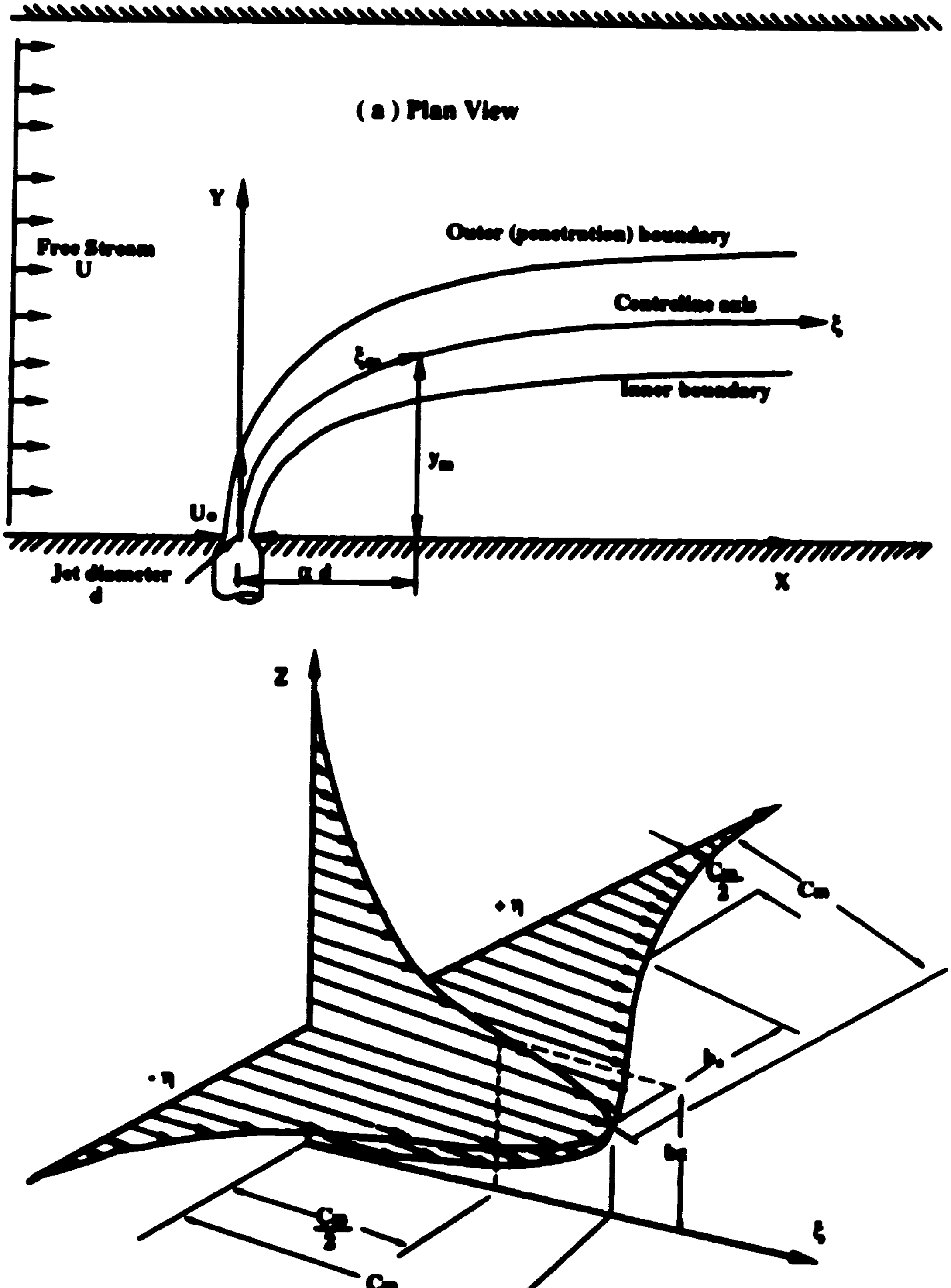

(b) Three-Dimensional Concentration Profiles of a Wall Jet

Fig. 4.2 Definition Sketches of a Circular Wall Jet in Crossflow

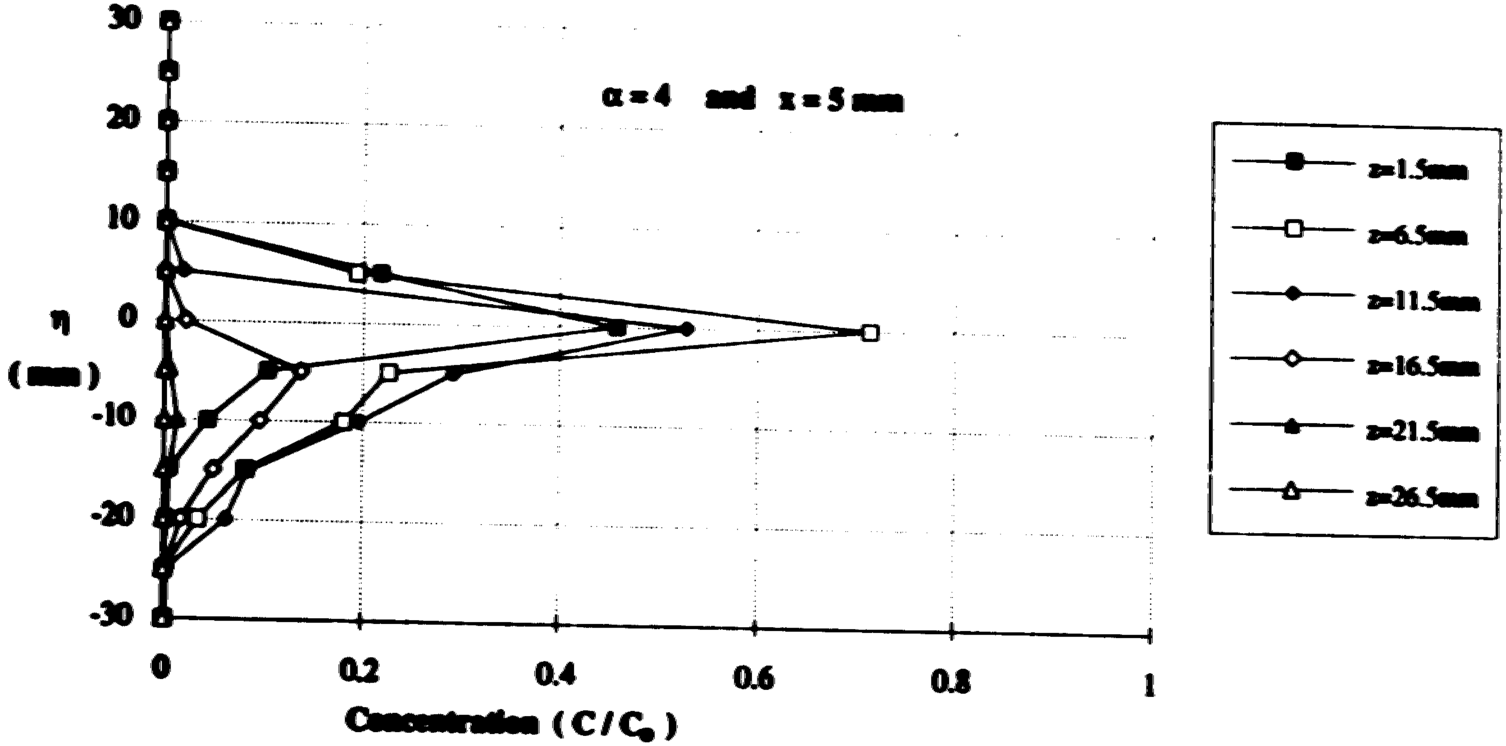

Fig. 4.3 (a) Transverse Concentration Profiles

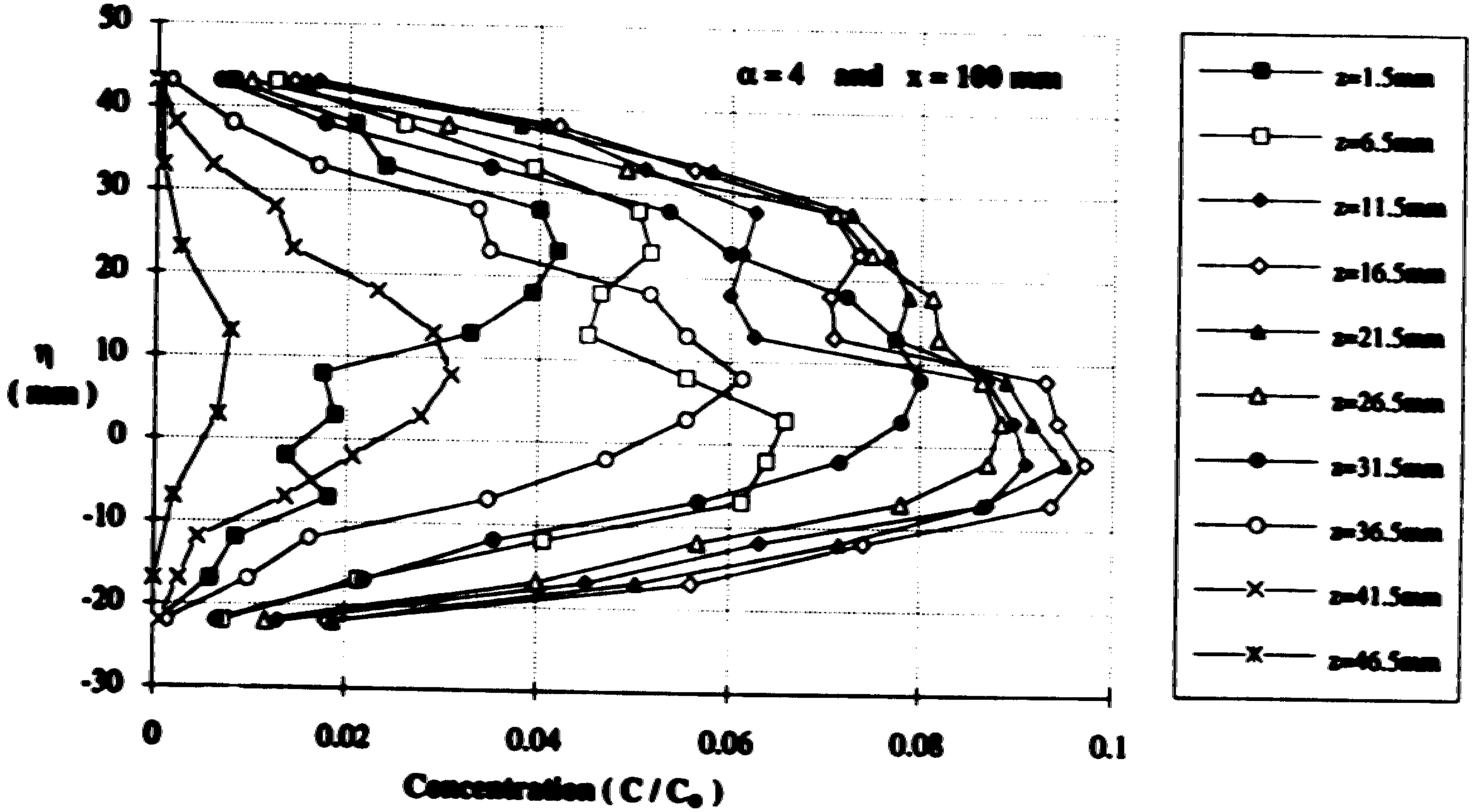

Fig. 4.3 (b) Transverse Concentration Profiles

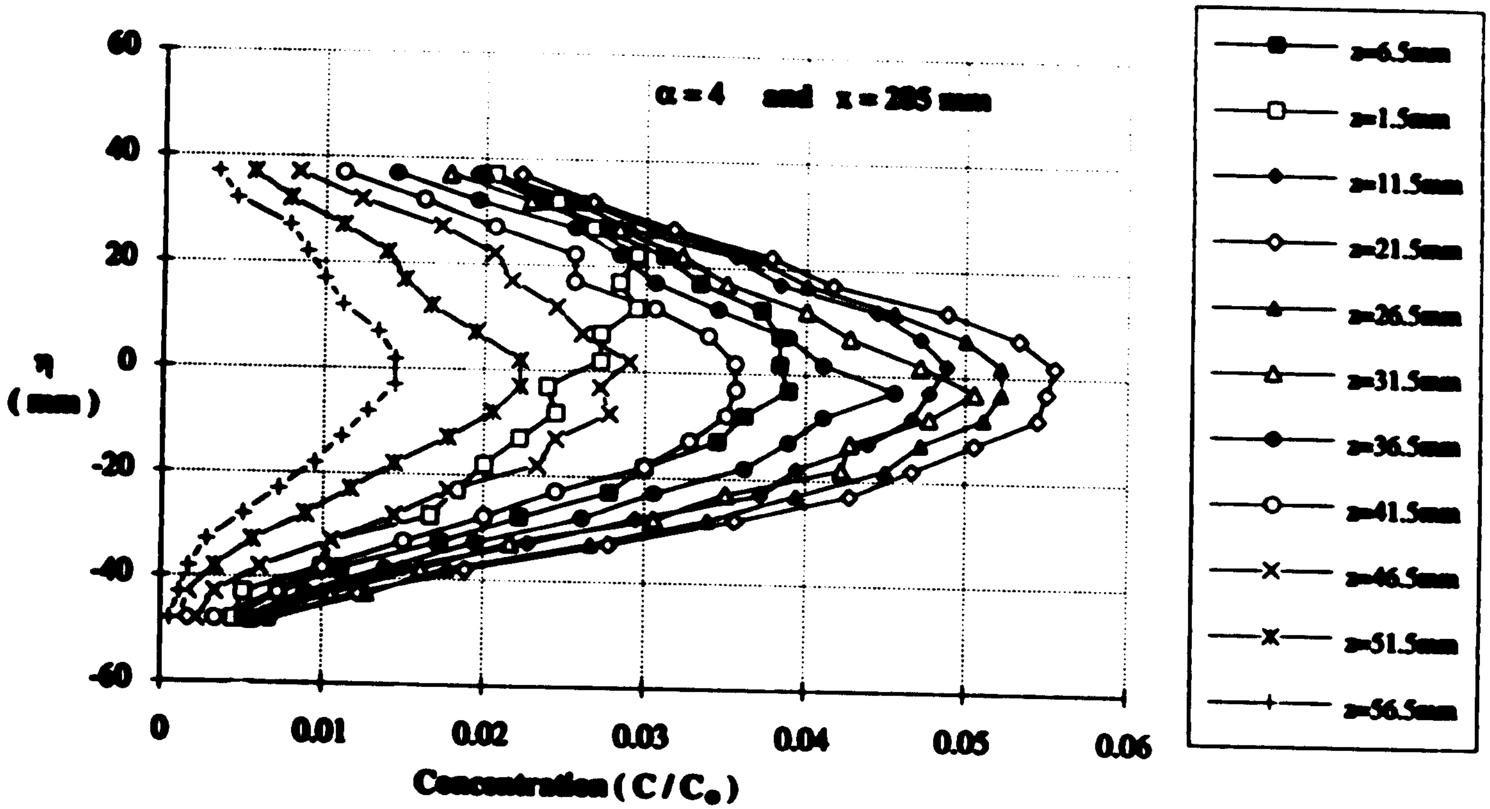

Fig. 4.3 (c) Transverse Concentration Profiles

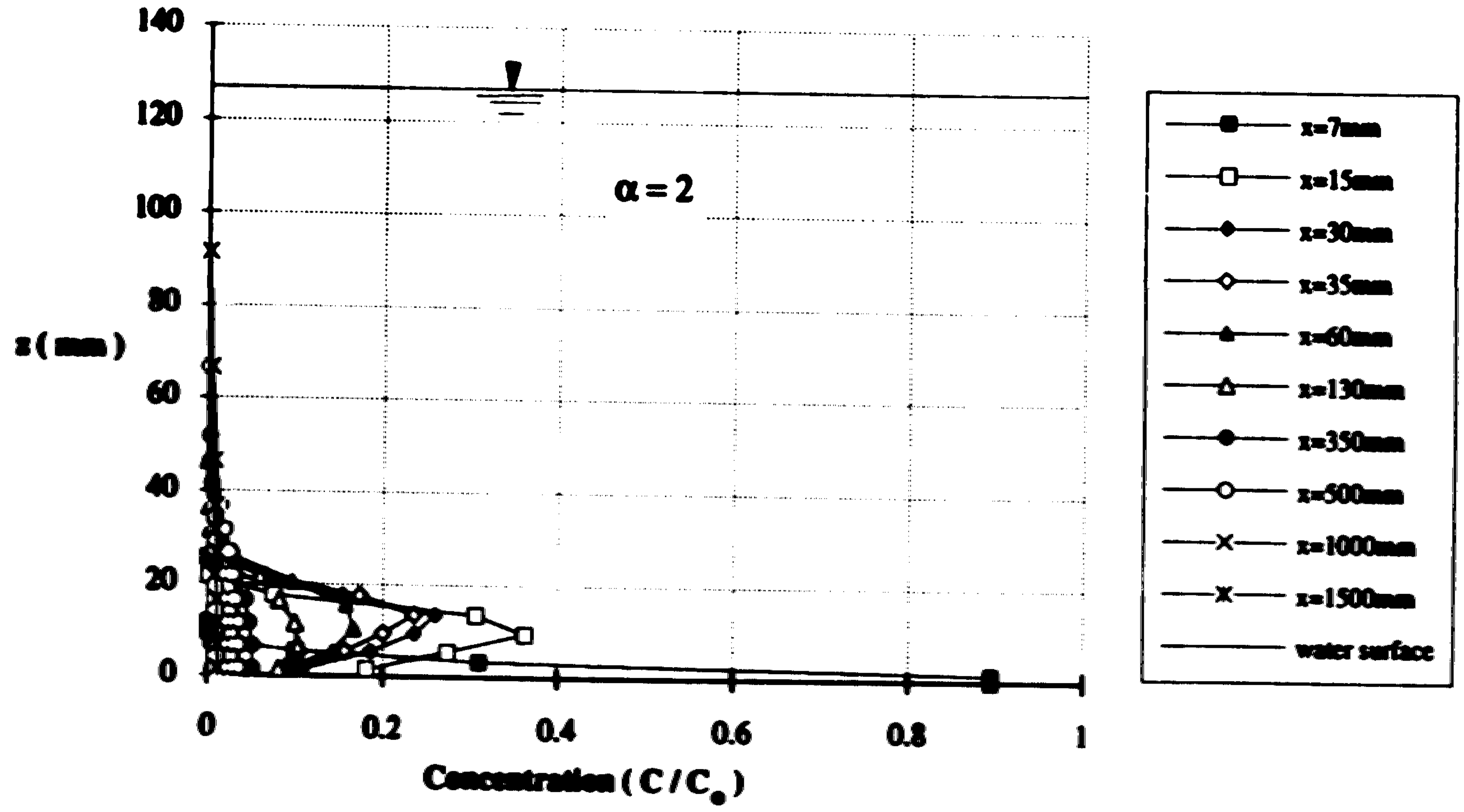

Fig. 4.4 Concentration Profiles along the Centreline of the Jet

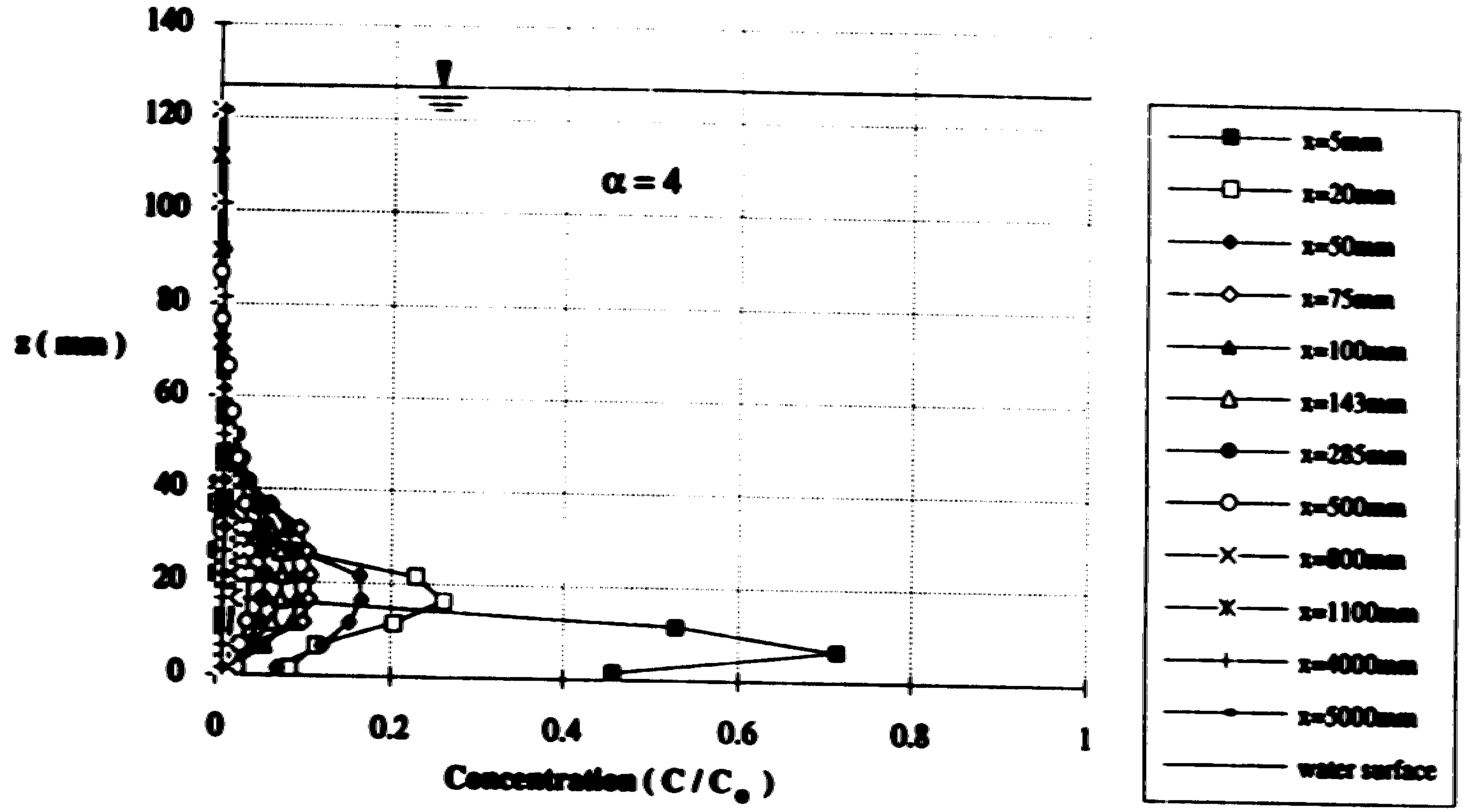

Fig. 4.5 Concentration Profiles along the Centreline of the Jet

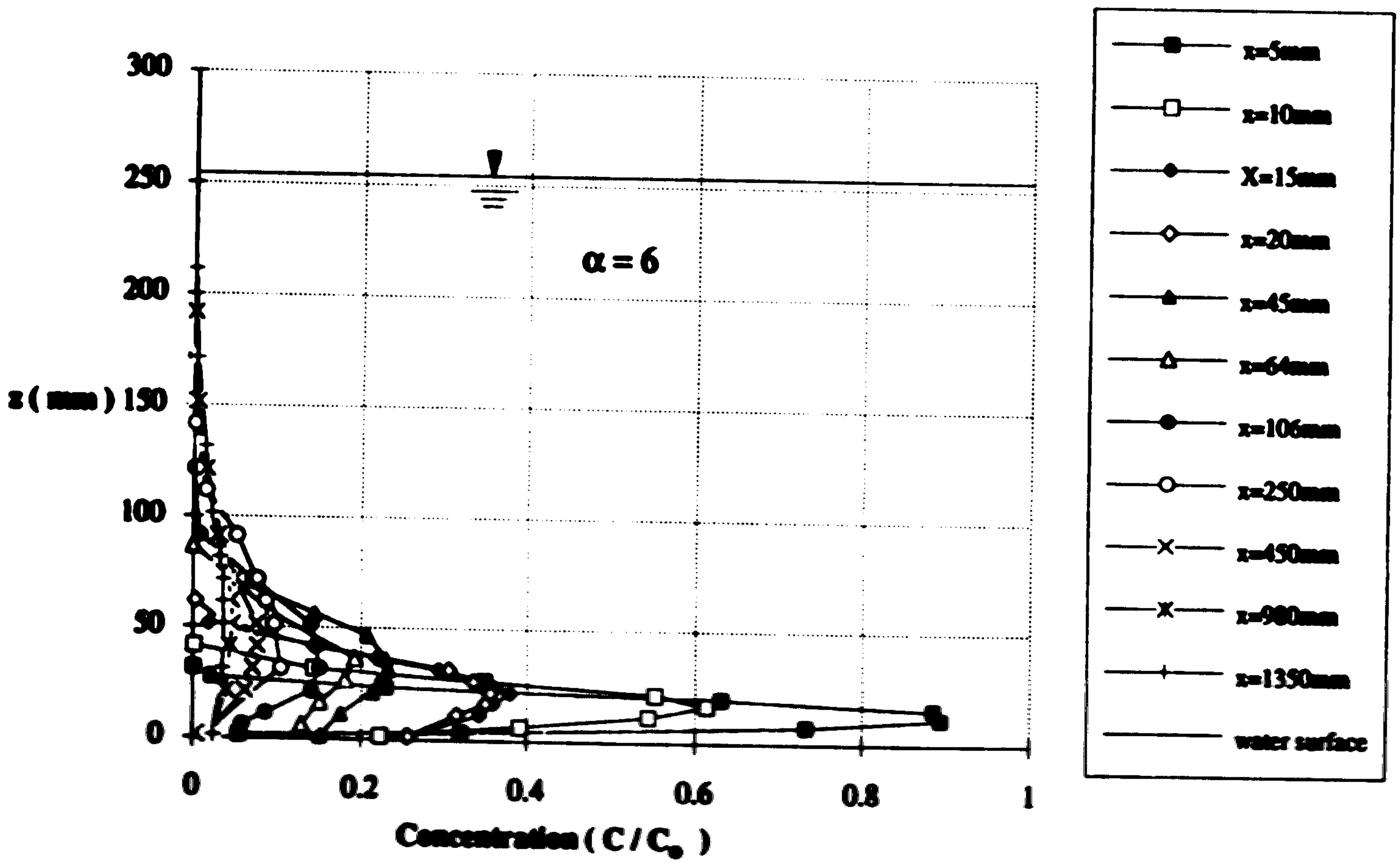

Fig. 4.6 Concentration Profiles along the Centreline of the Jet

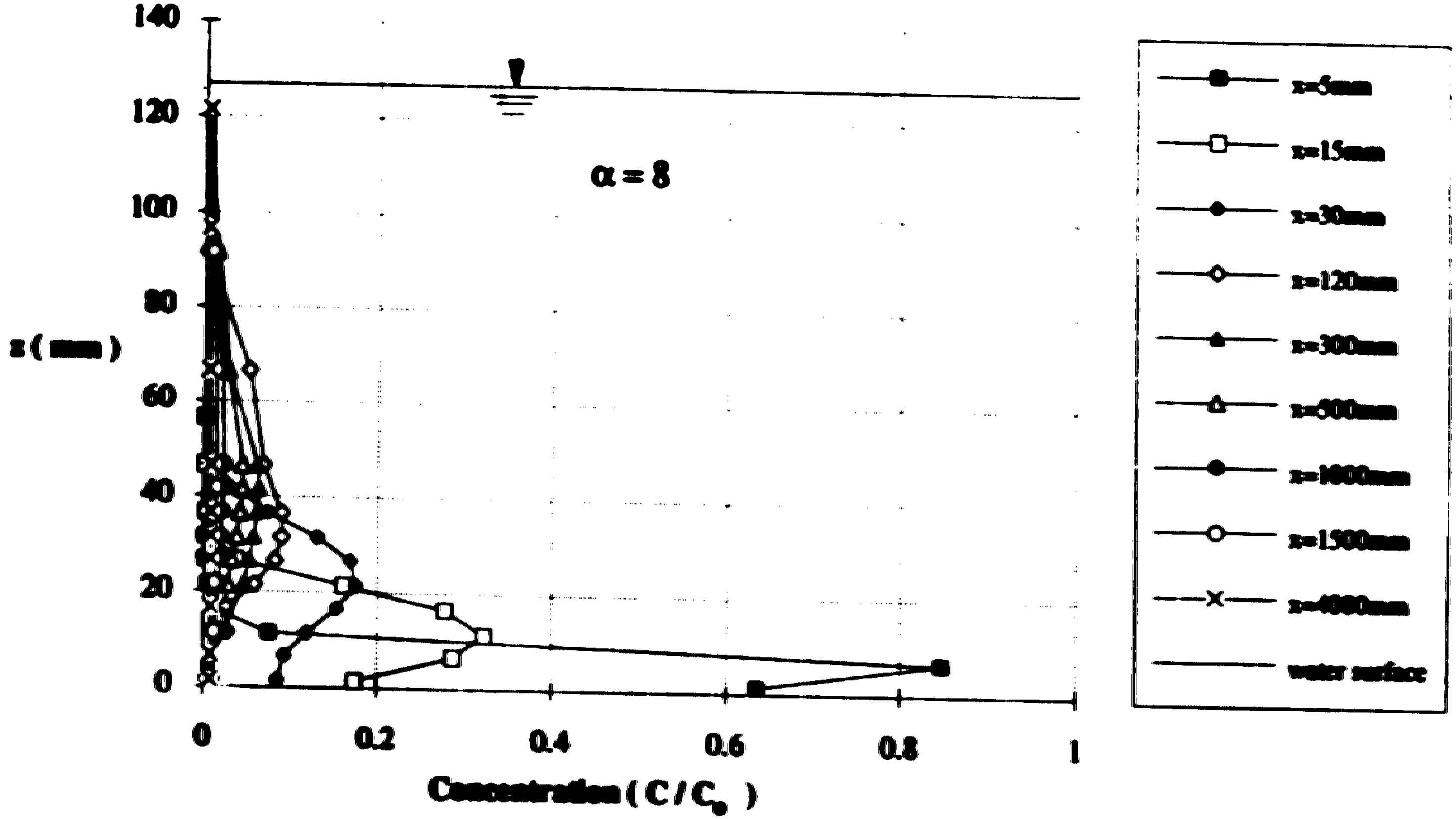

Fig. 4.7 Concentration Profiles along the Centreline of the Jet

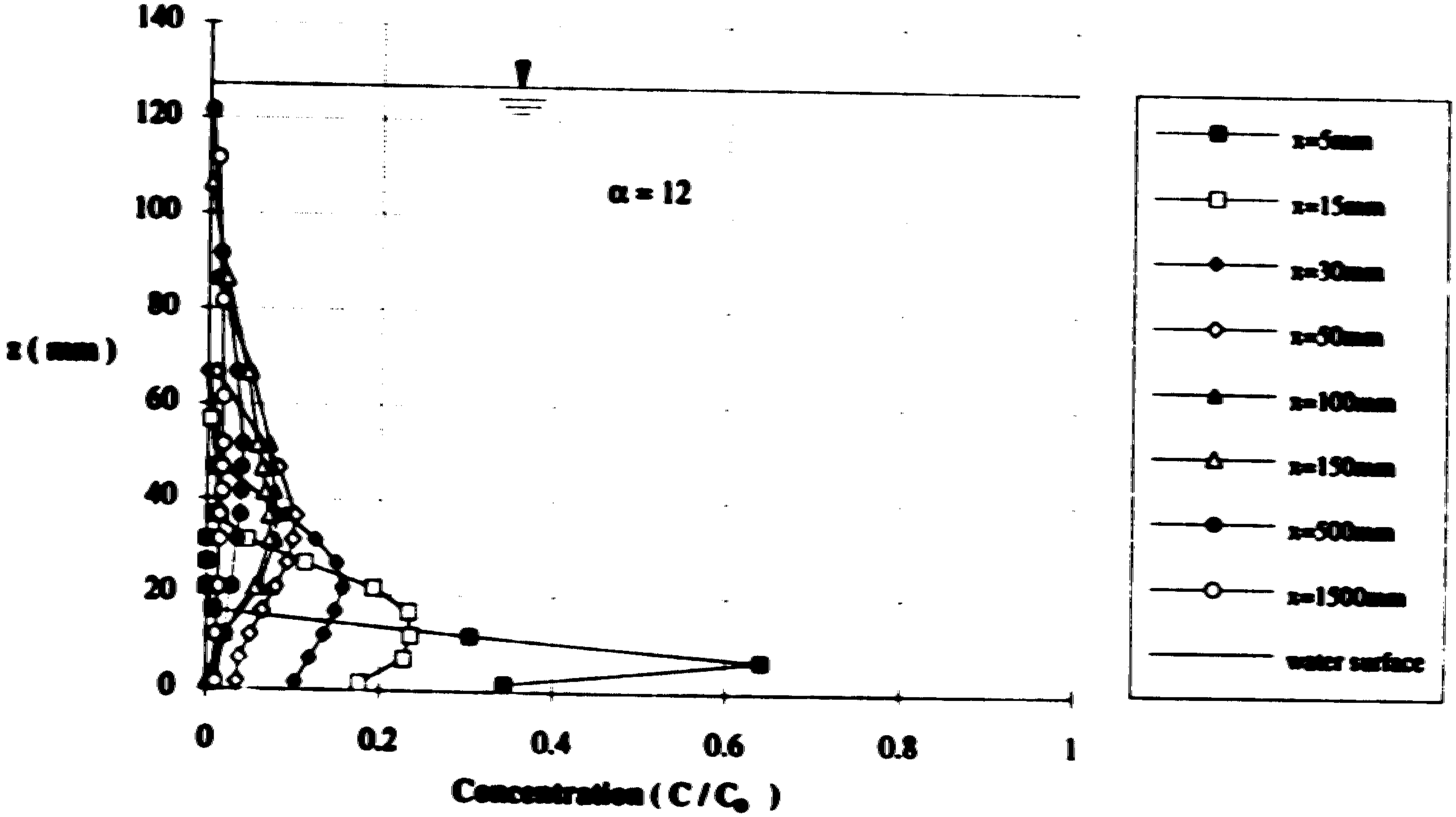

Fig. 4.8 Concentration Profiles along the Centreline of the Jet

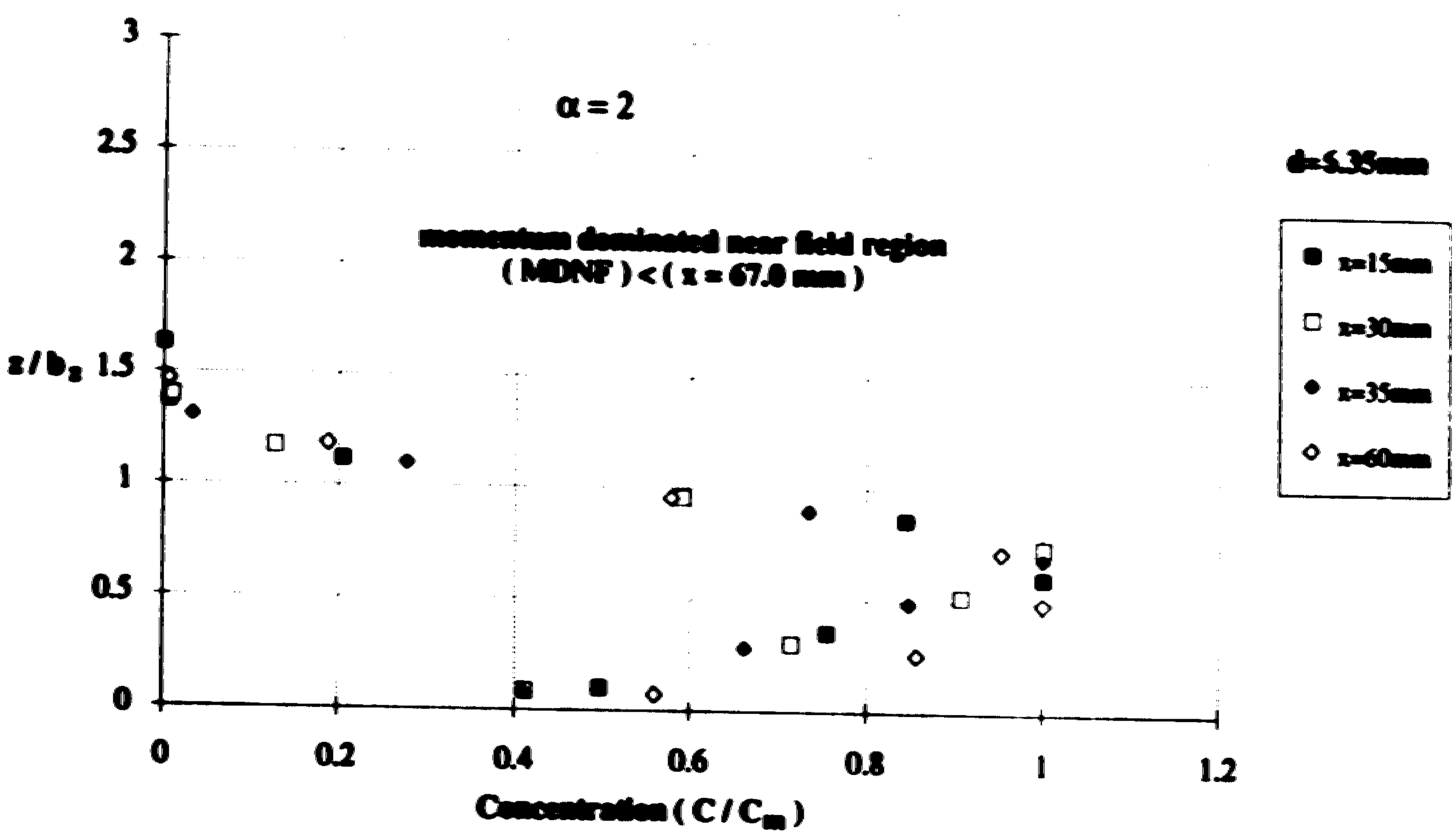

Fig. 4.9 (a) Non - dimensional Profiles of Concentration Distribution in the Vertical Direction

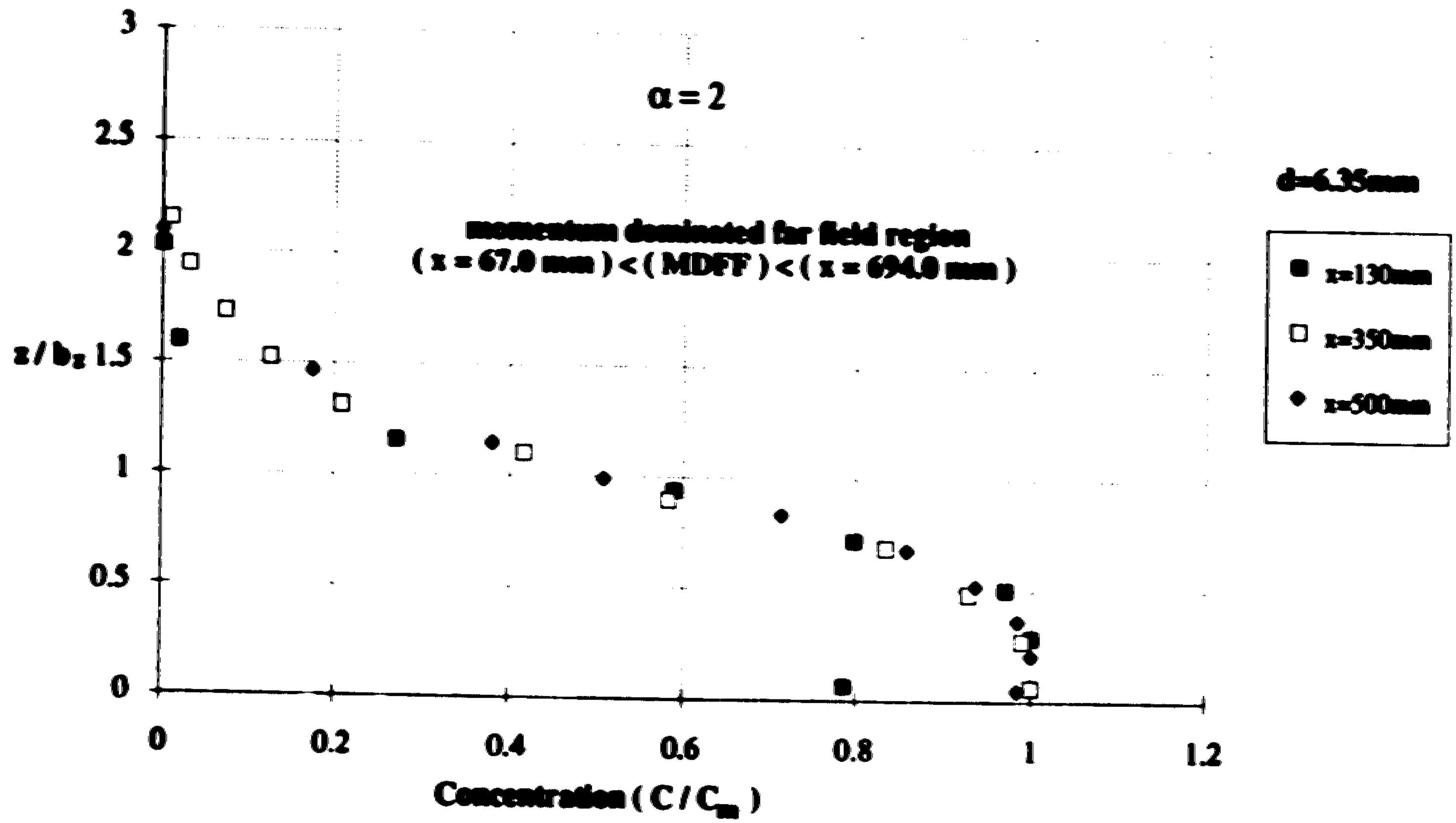

Fig. 4.9 (b) Non - Dimensional Profiles of Concentration Distribution in the Vertical Direction

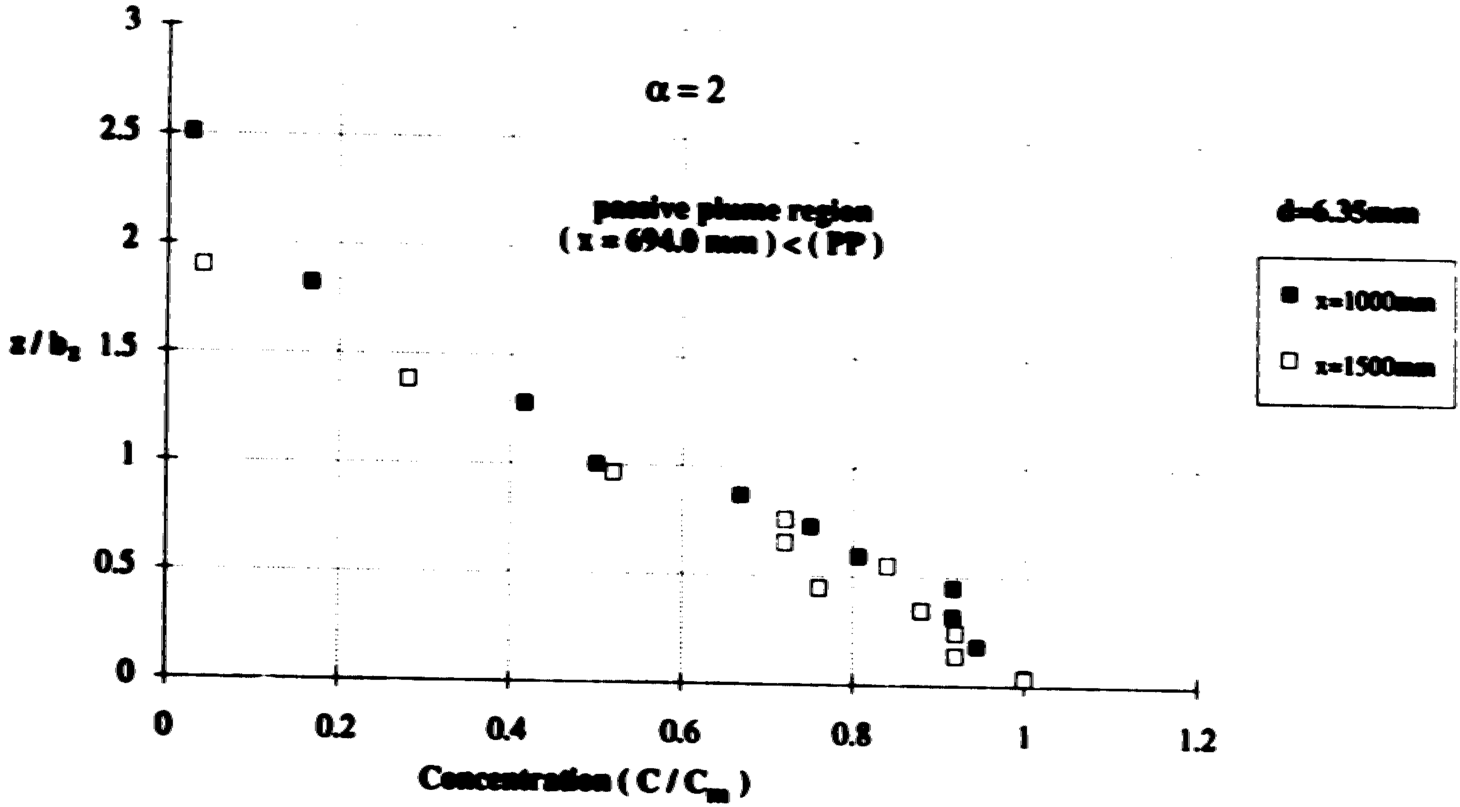

Fig. 4.9 (c) Non - Dimensional Profiles of Concentration Distributio in the Vertical Direction

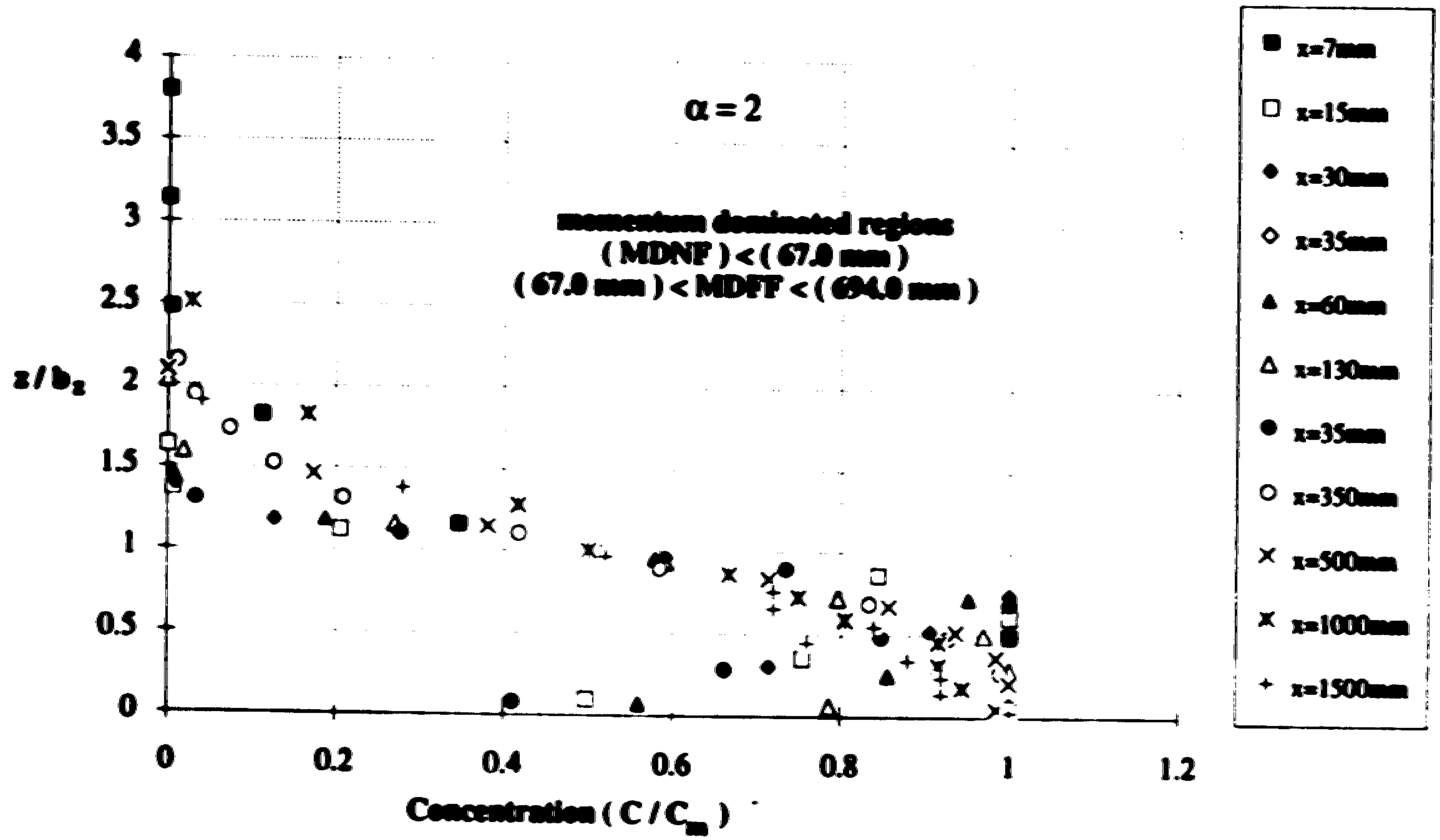

Fig. 4.9 (d) Non - Dimensional Profiles of Concentration Distribution in the V..tical Direction

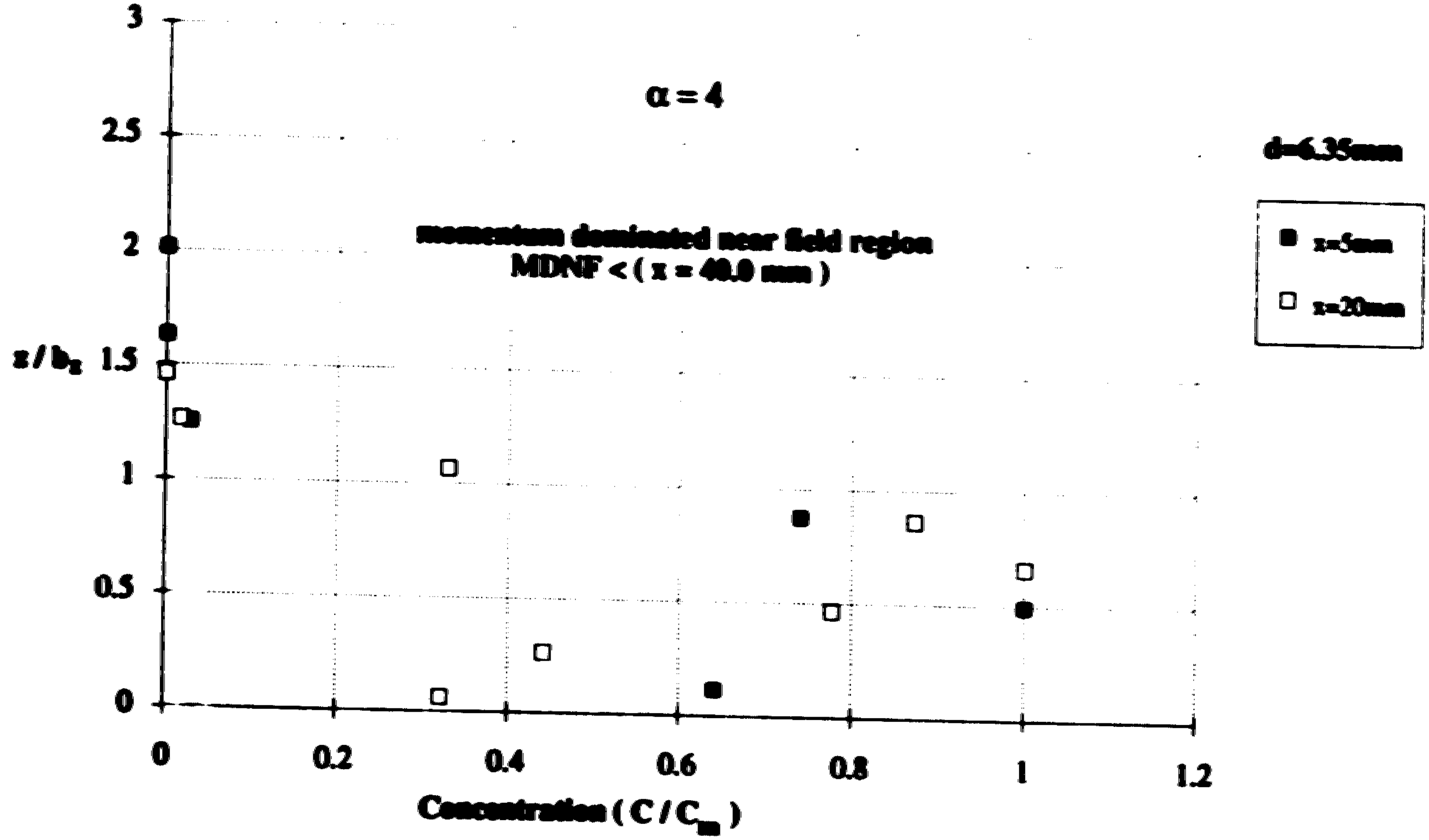

Fig. 4.10 (a) Non - Dimensional Profiles of Concentration Distribution in the Vertical Direction

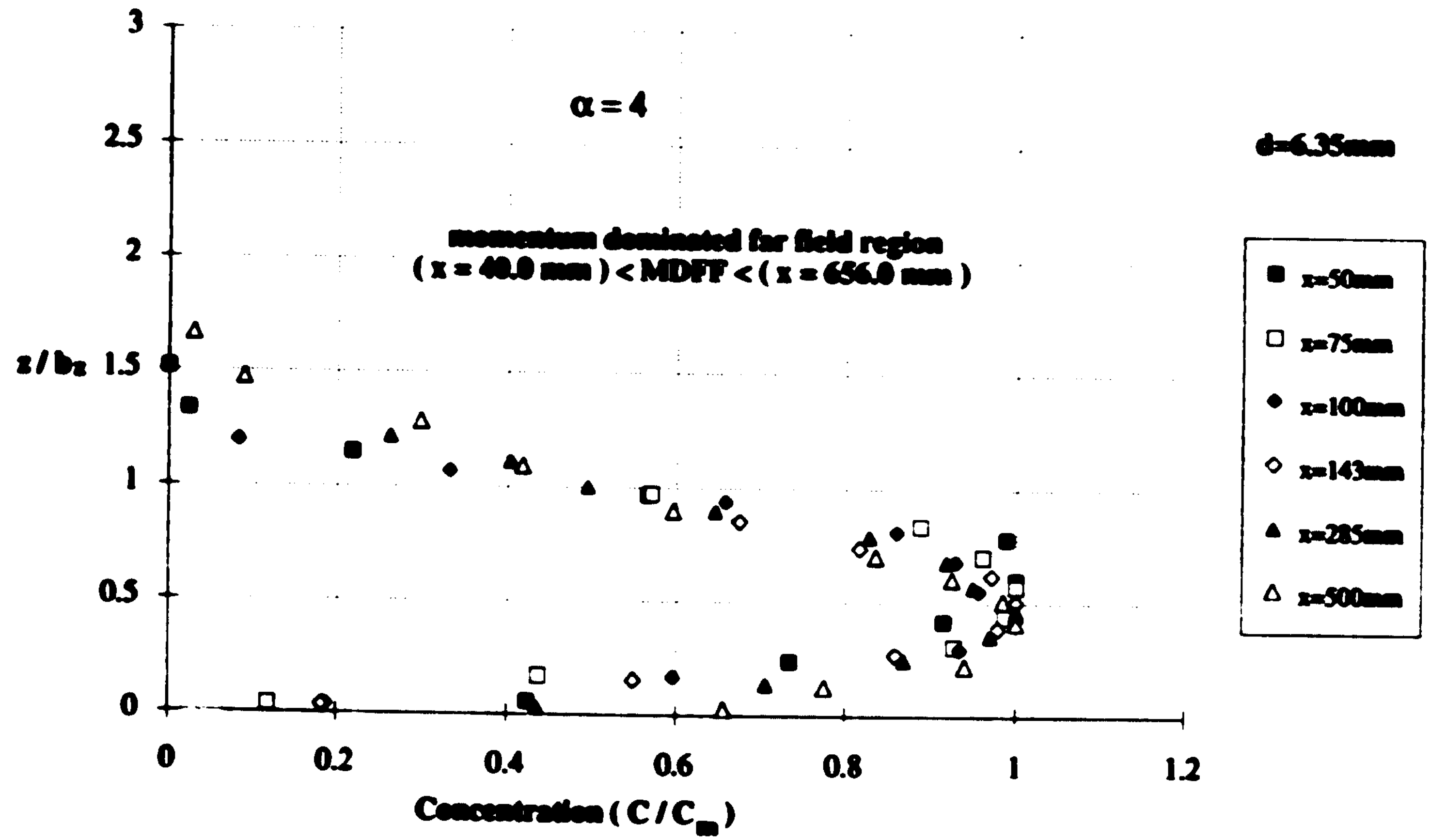

Fig. 4.10 (b) Non - Dimensional Profiles of Concentration Distribution in the Vertical Direction

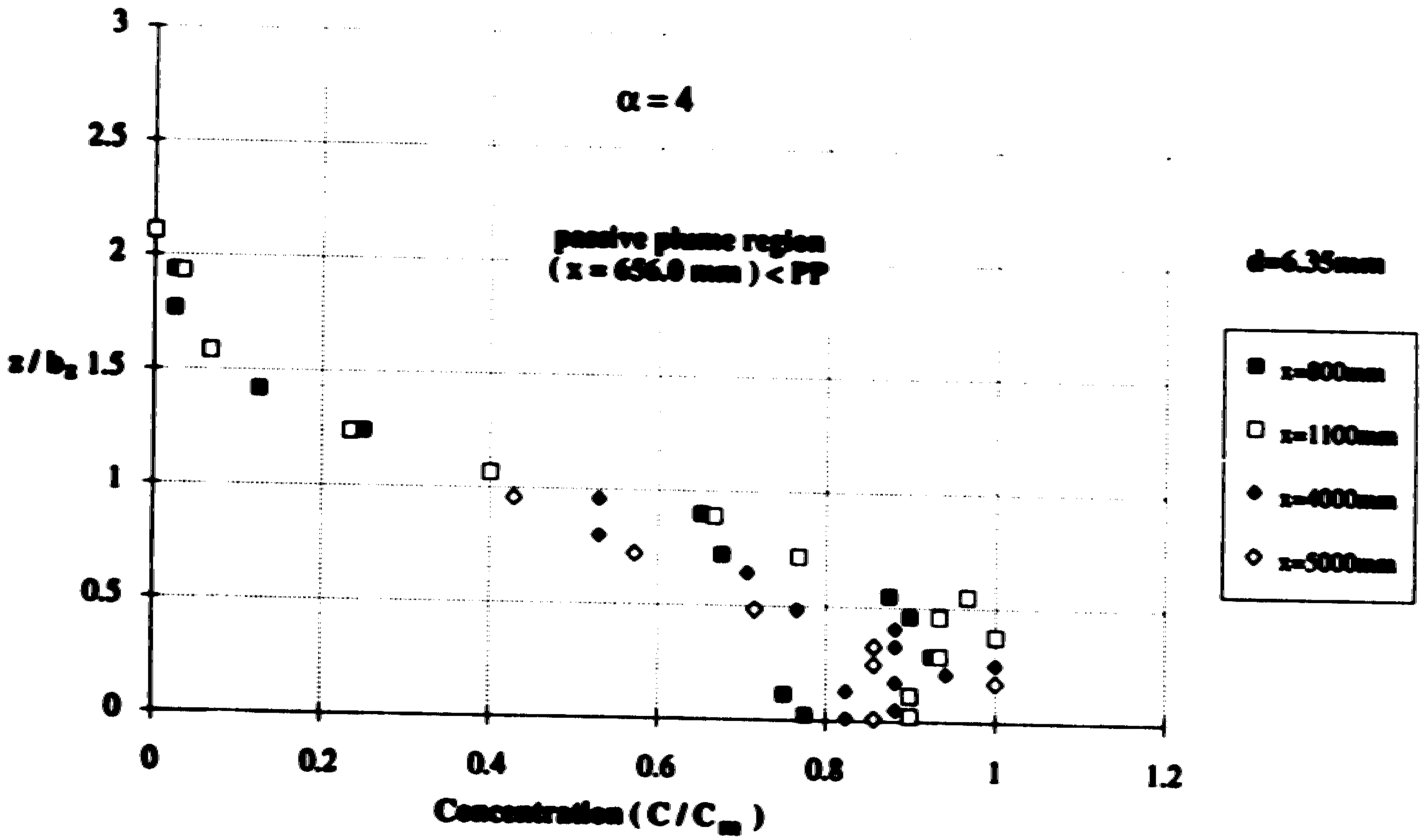

Fig. 4.10 (c) Non - Dimensional Profiles of Concentration Distribution in the Vertical Direction

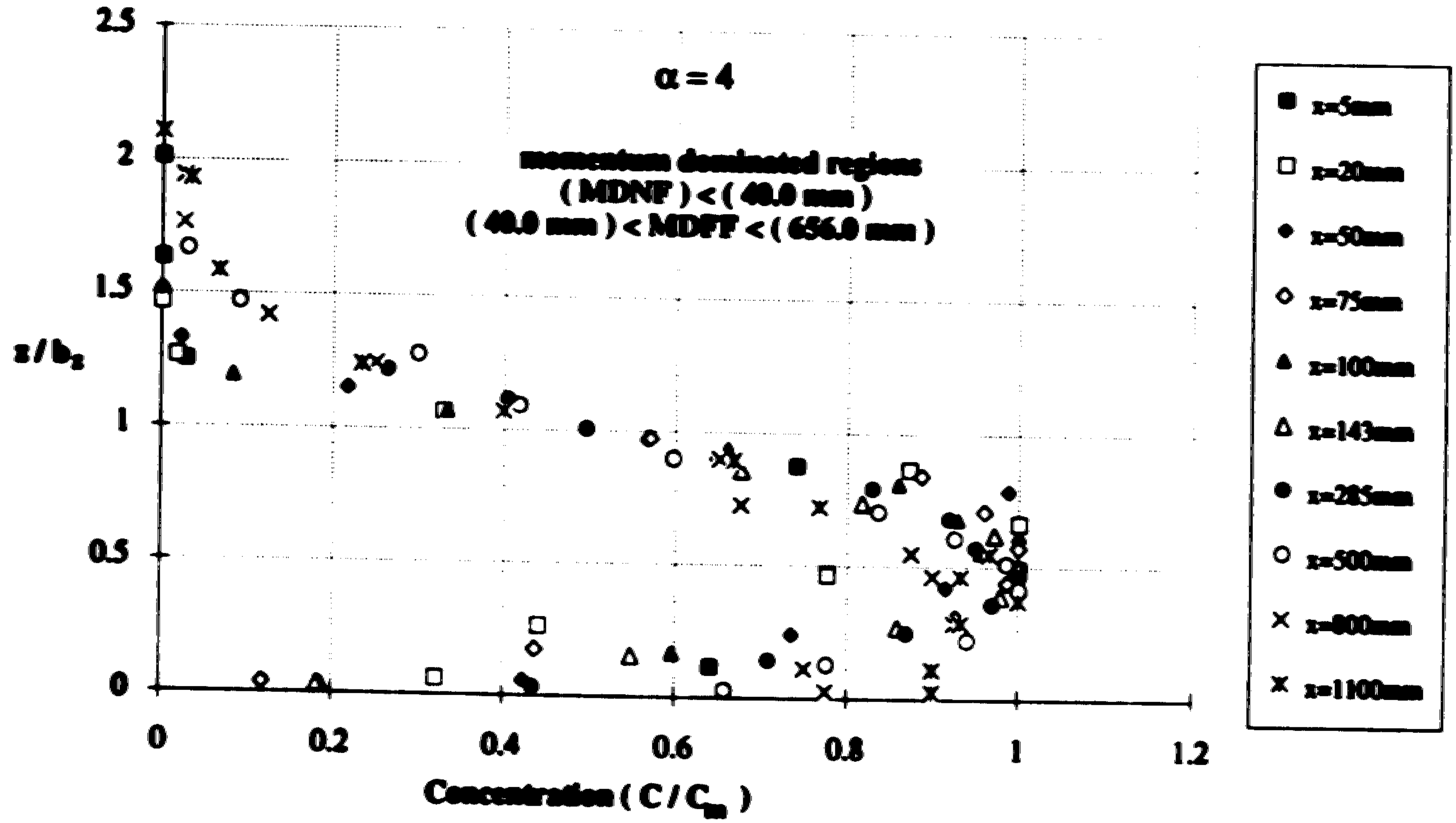

Fig. 4.10 (d) Non - Dimensional Profiles of Concentration Distribution in the Vertical Direction

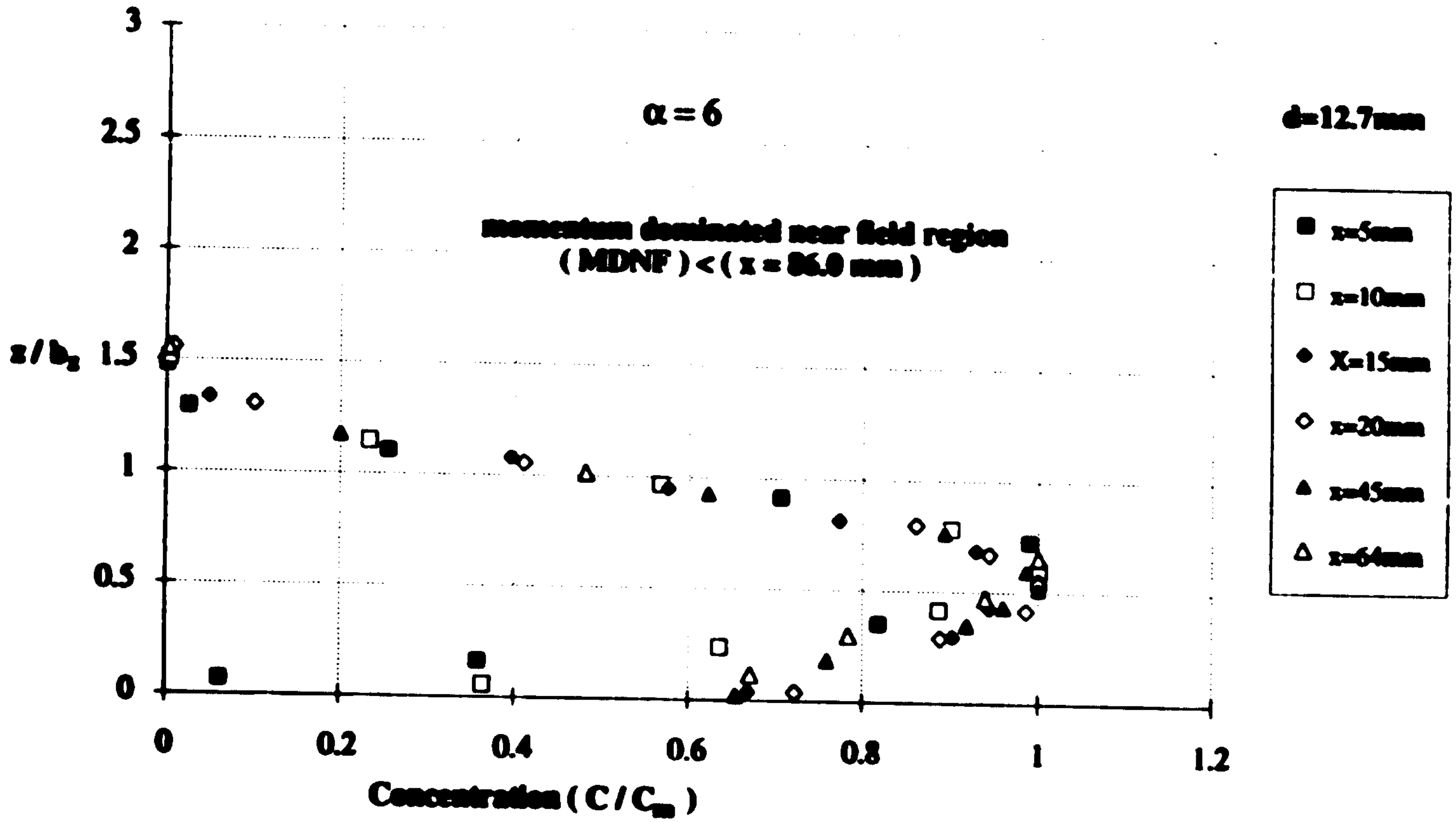

Fig. 4.11 (a) Non - Dimensional Profiles of Concentration Distribution in the Vertical Direction

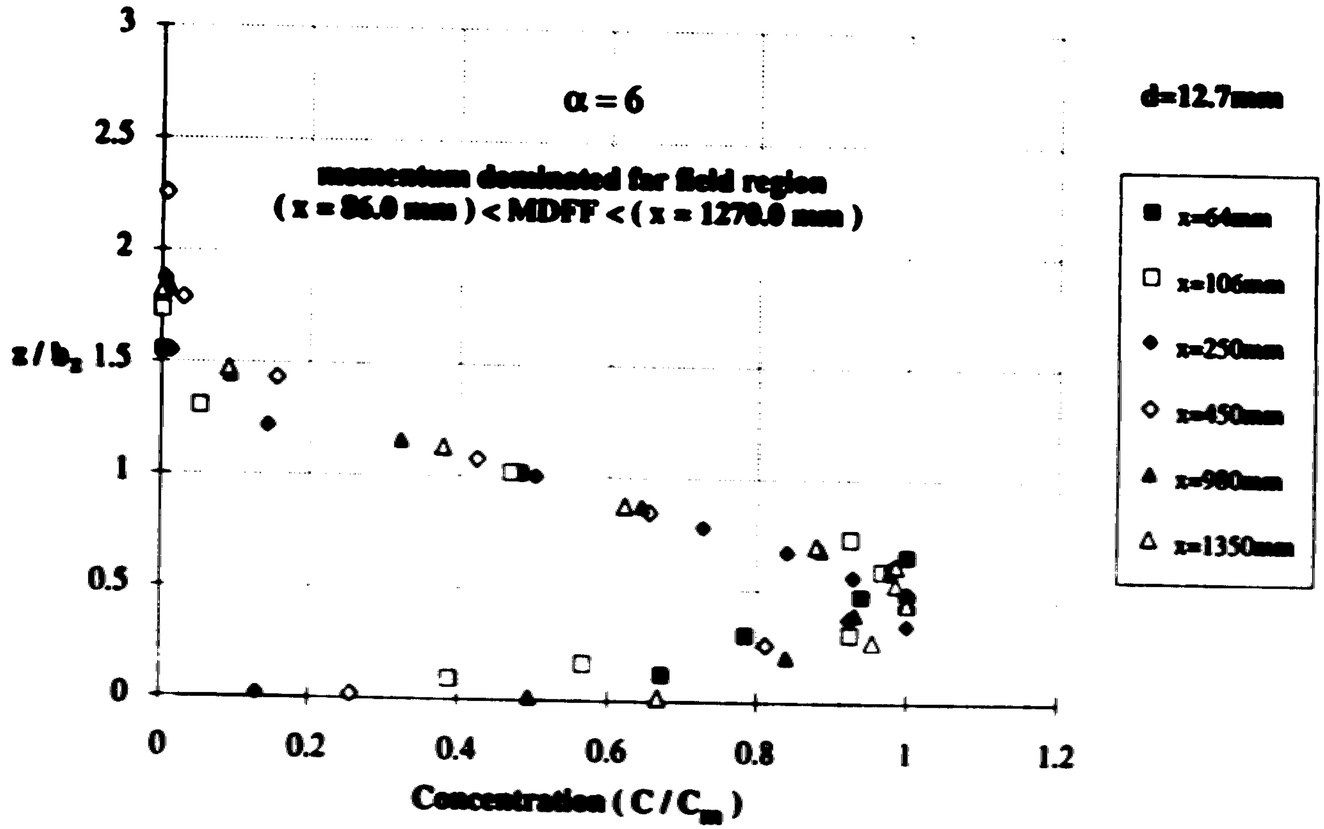

Fig. 4.11 (b) Non - Dimensional Profiles of Concentration Distribution in the Vertical Direction

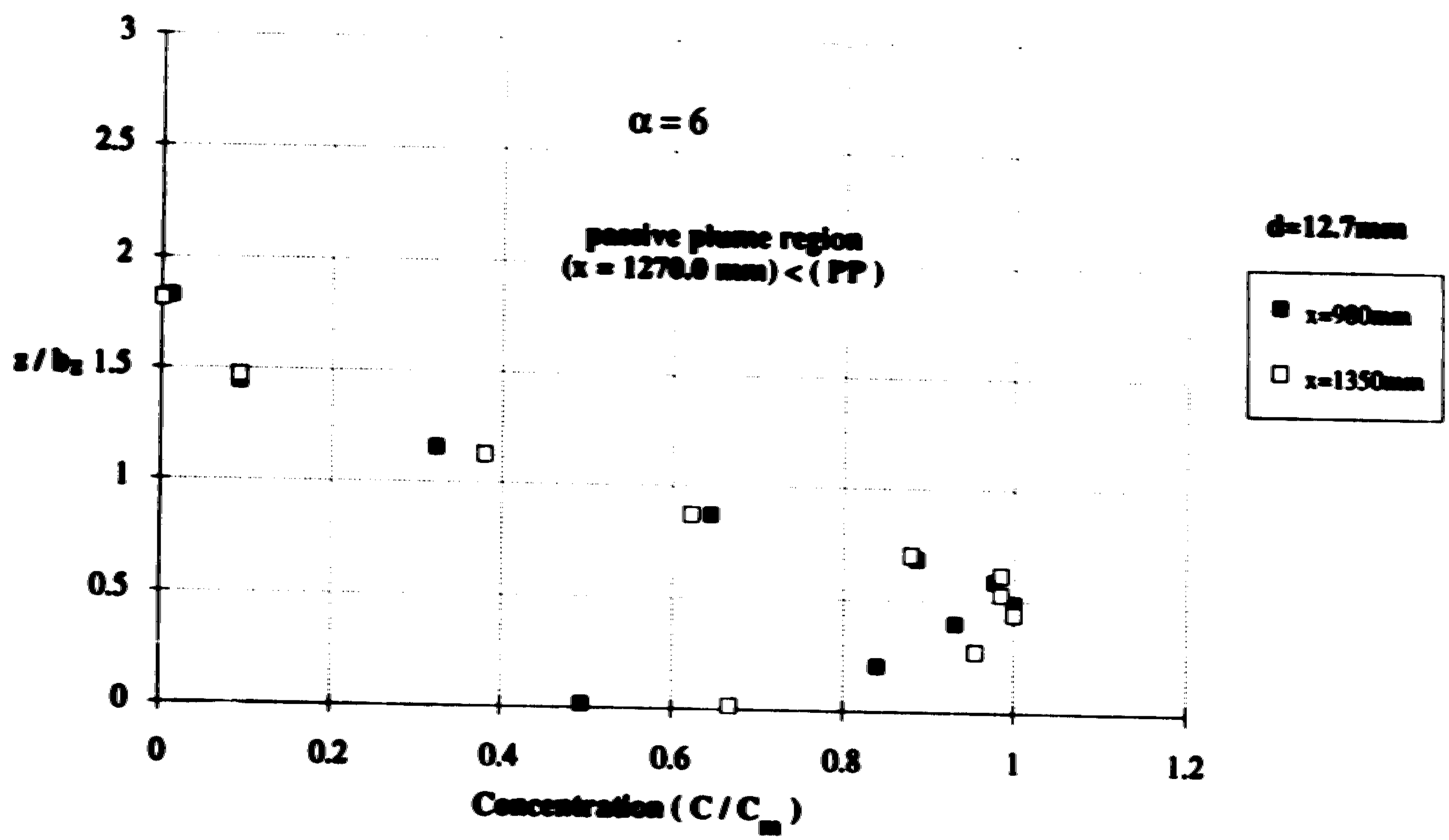

Fig. 4.11 (c) Non - Dimensional Profiles of Concentration Distribution in the Vertical Direction

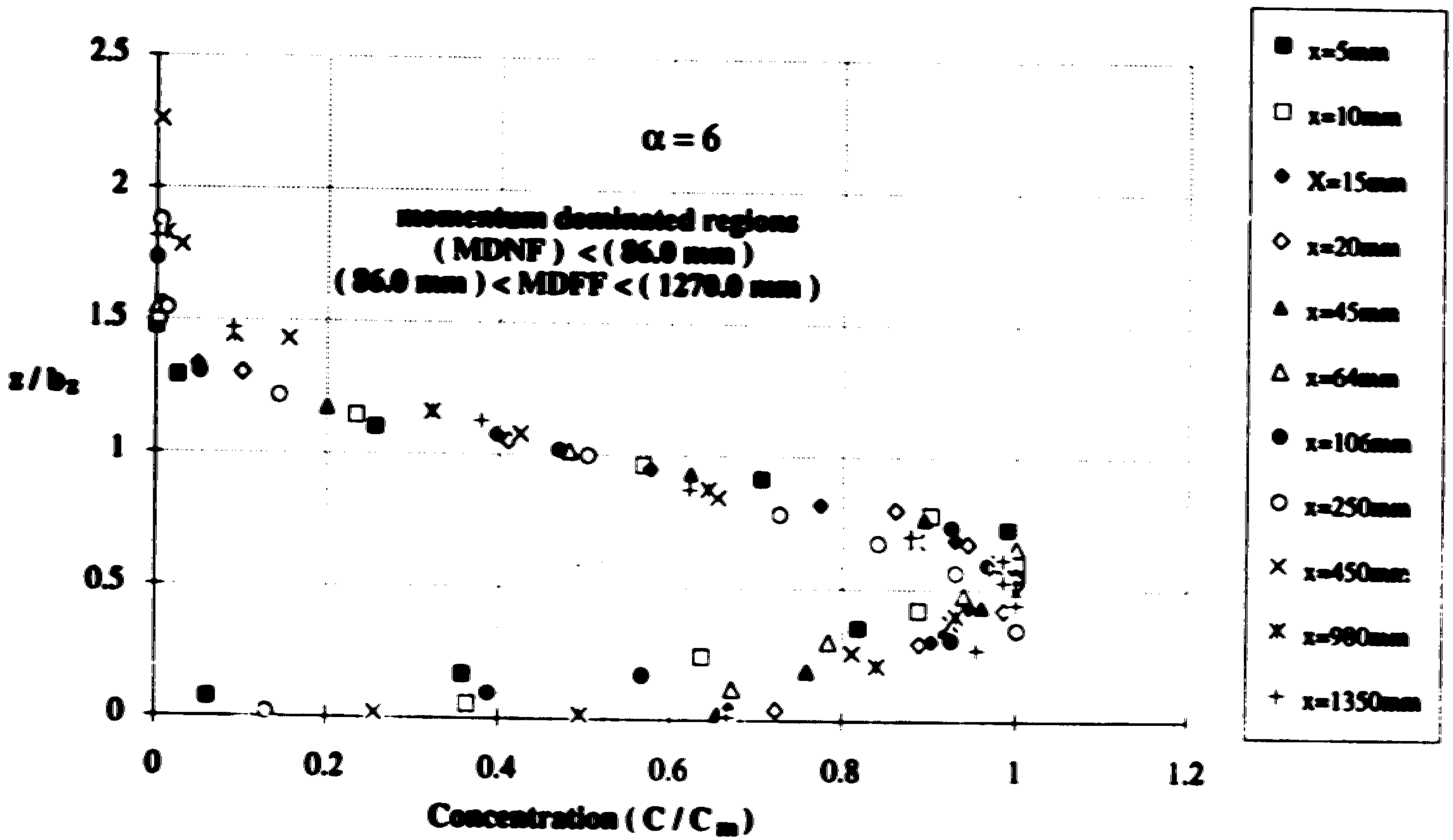

Fig. 4.11 (d) Non - Dimensional Profiles of Concentration Distribution in the Vertical Direction

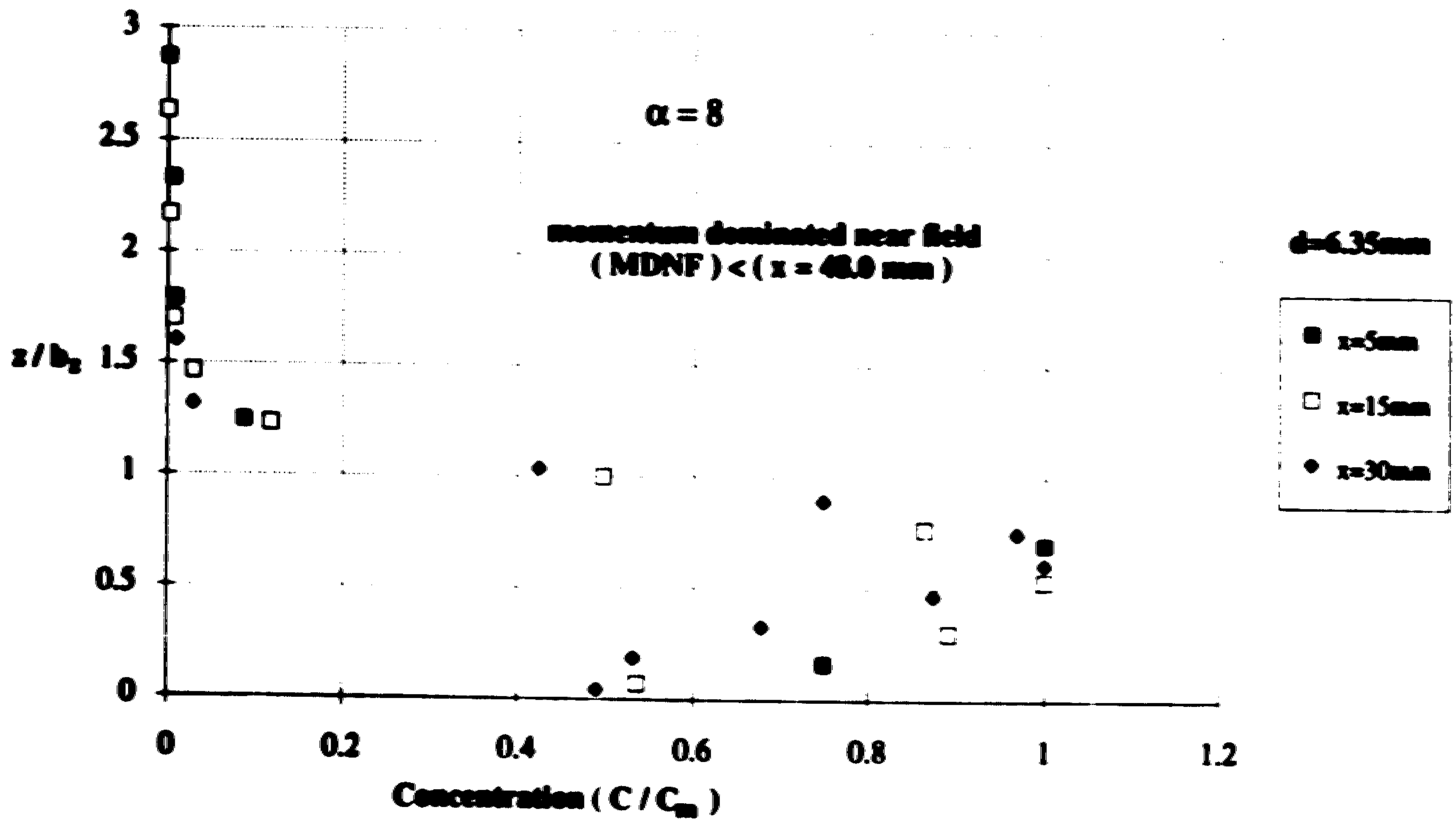

Fig. 4.12 (a) Non - Dimensional Profiles of Concentration Distribution in the Vertical Direction

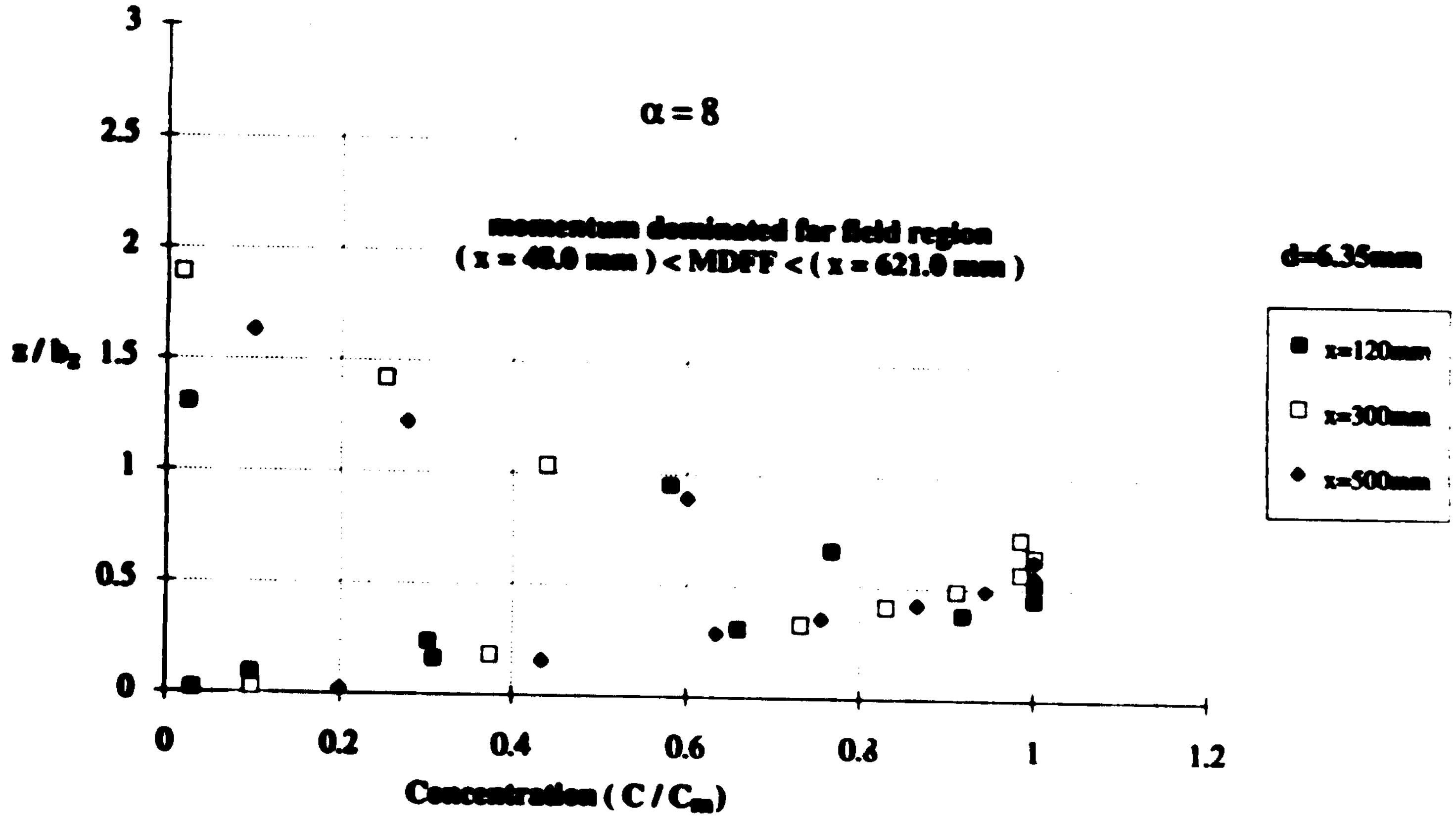

Fig. 4.12 (b) Non - Dimensional Profiles of Concentration Distribution in the Vertical Direction

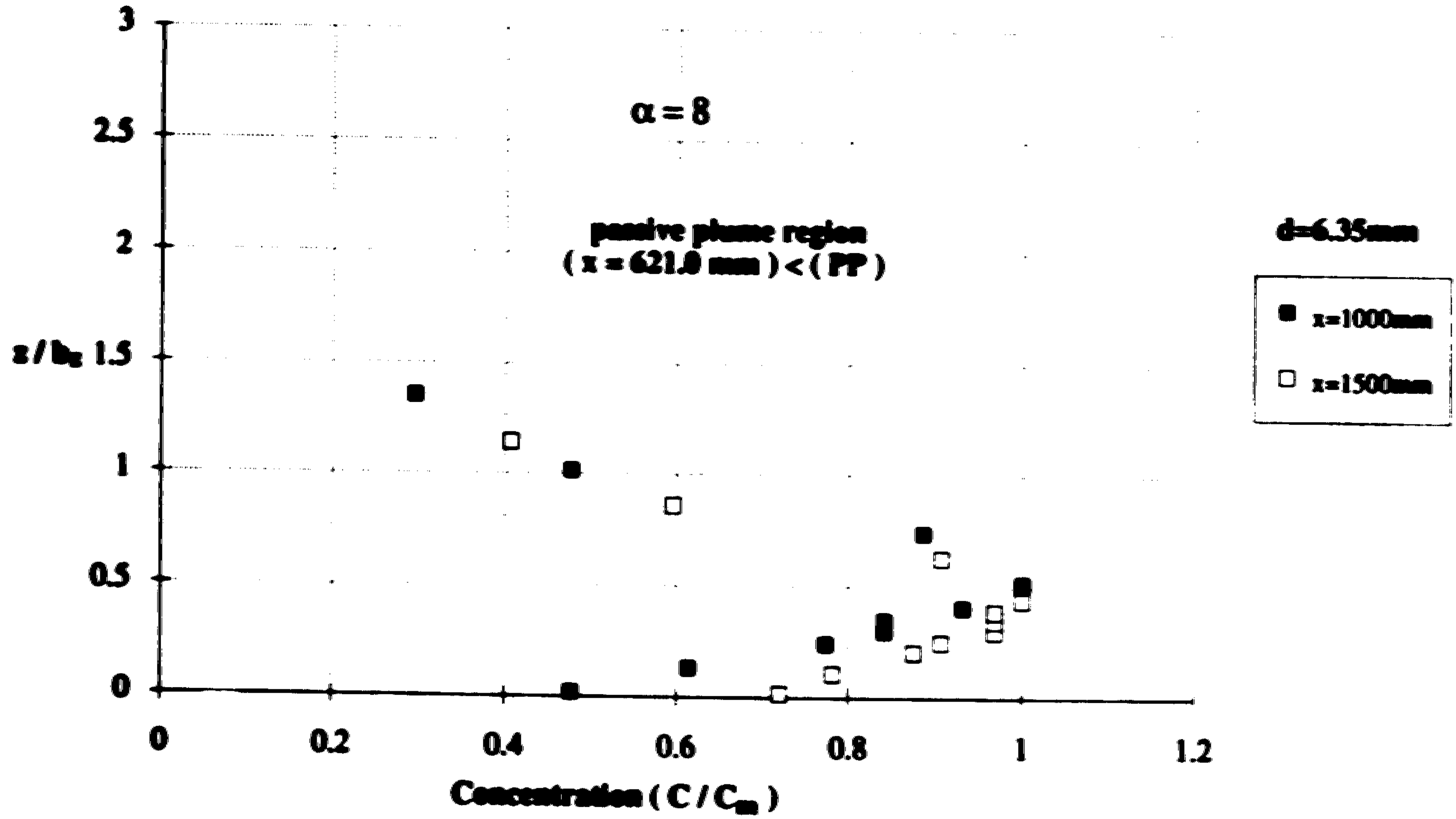

Fig. 4.12 (c) Non - Dimensional Profiles of Concentration Distribution in the Vertical Direction

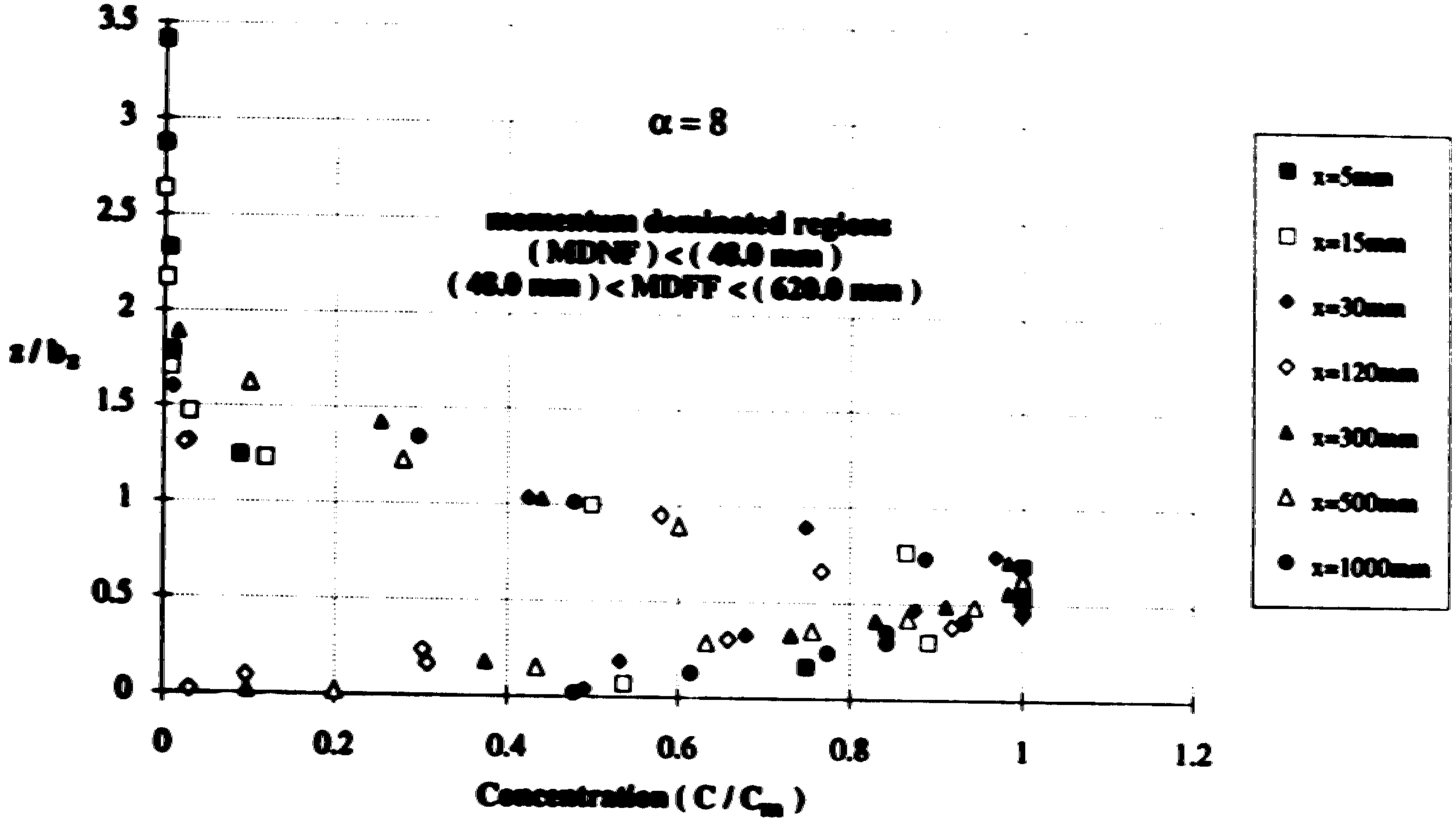

Fig. 4.12 (d) Non - Dimensional Profiles of the Concentration Distribution in the Vertical Direction

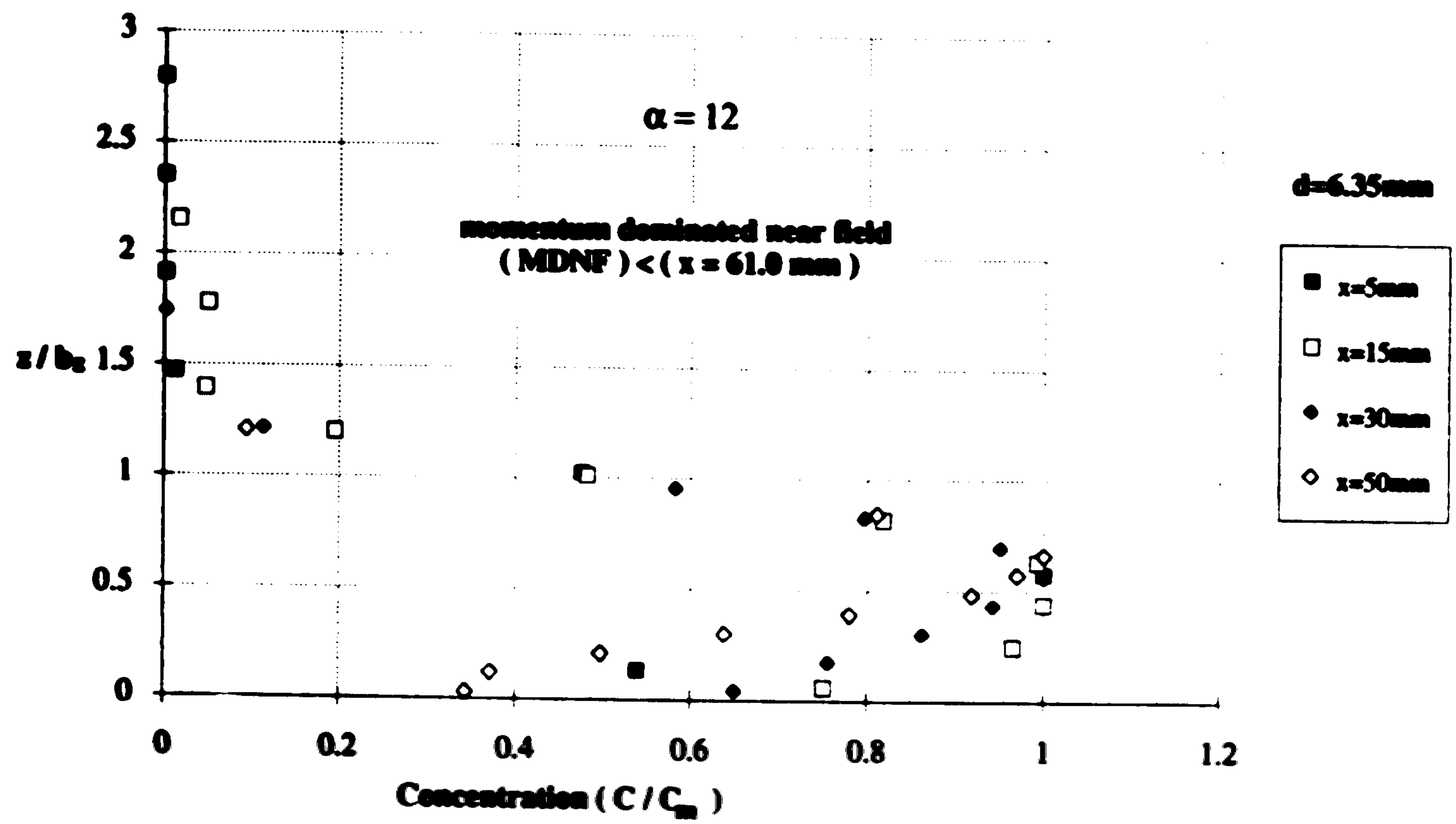

Fig. 4.13 (a) Non - Dimensional Profiles of Concentration Distribution in the Vertical Direction

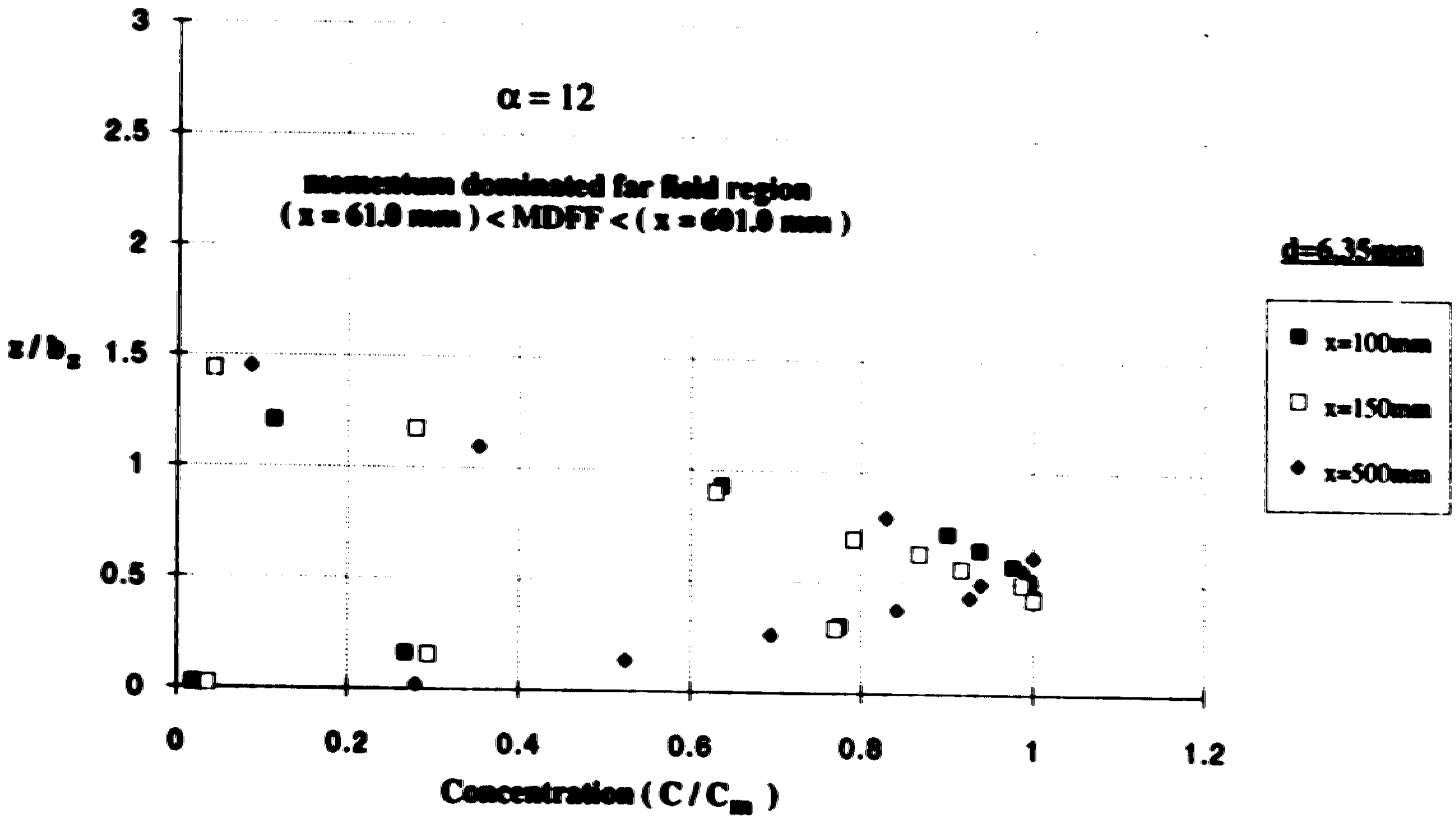

Fig. 4.13 (b) Non - Dimensional Profiles of the Concentration Distribution in the Vertical Direction

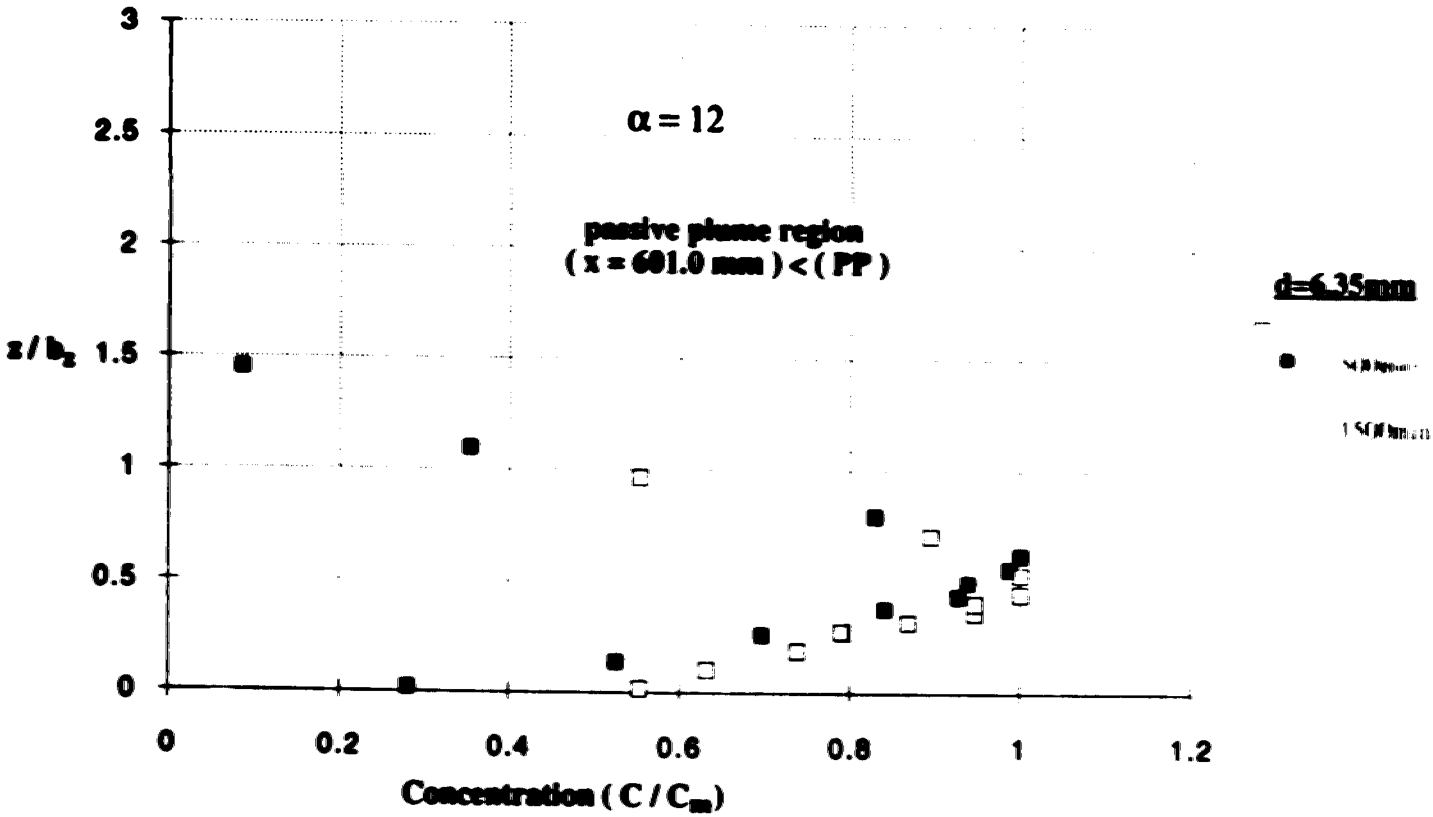

Fig. 4.13 (c) Non - Dimensional Profiles of Concentration Distribution in the Vertical Direction

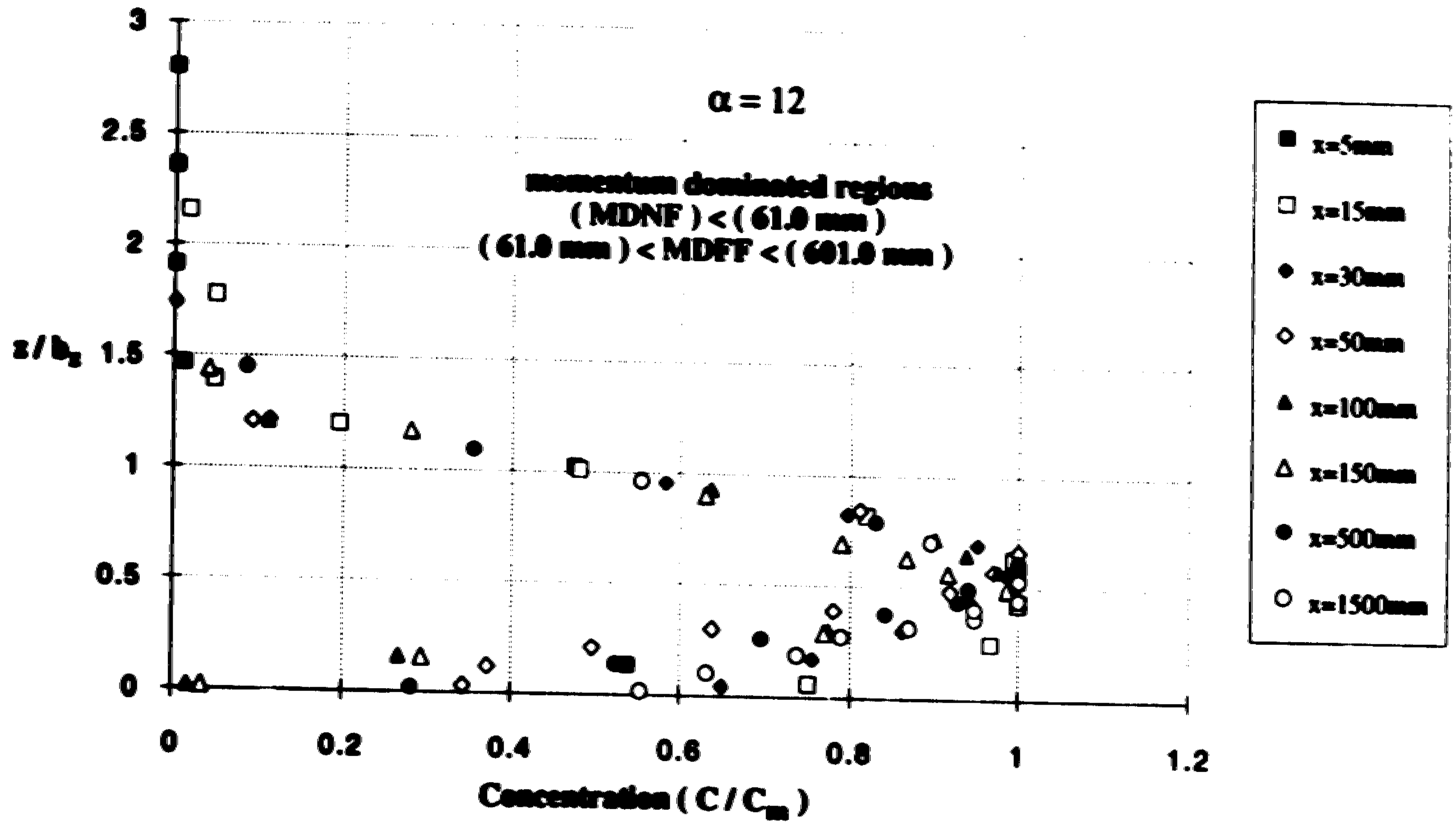

Fig. 4.13 (d) Non - Dimensional Profiles of Concentration Distribution in the Vertical Direction

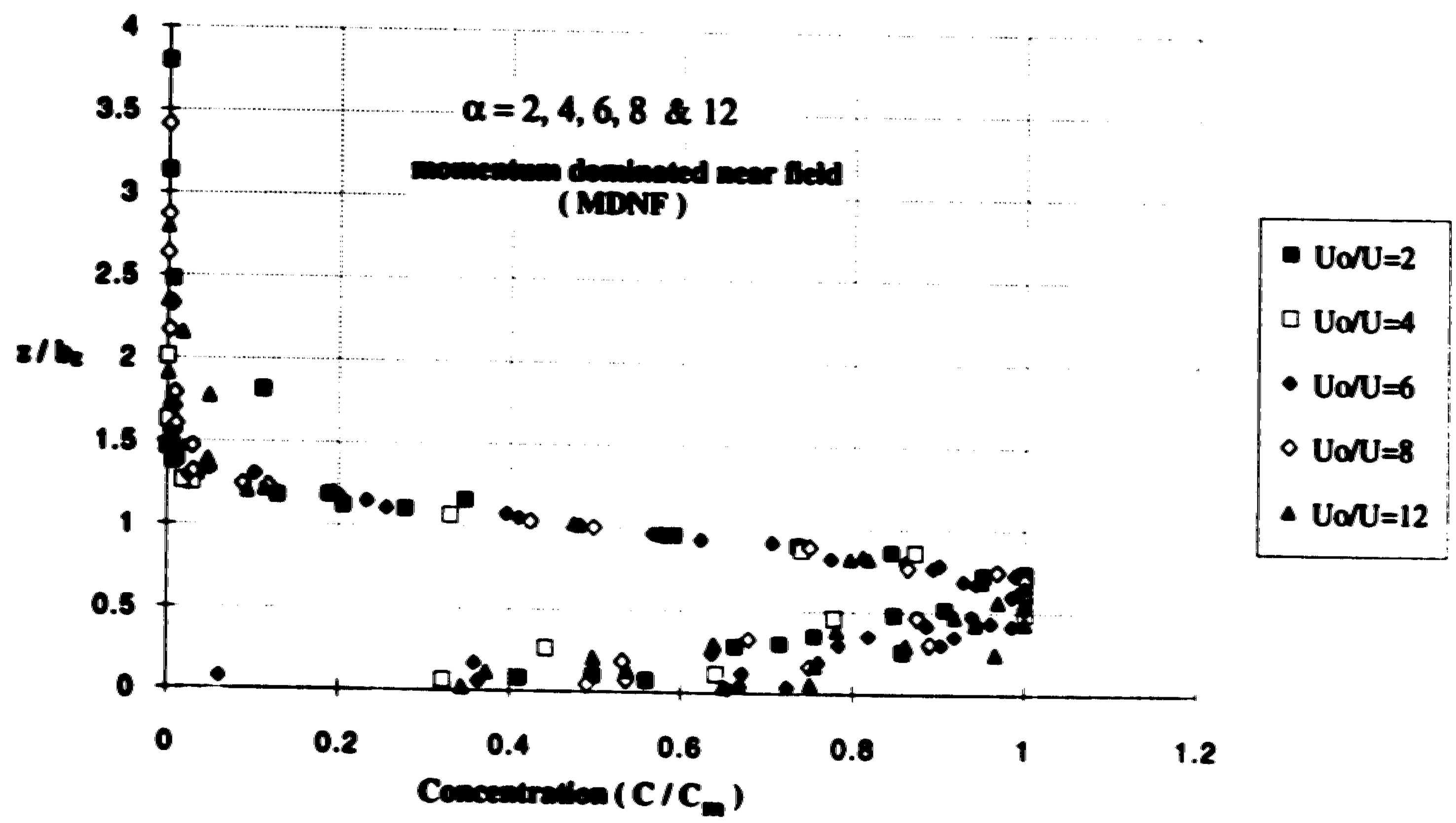

Fig. 4.14 (a) Similarity Profiles of Concentration Distribution in the Vertical Direction

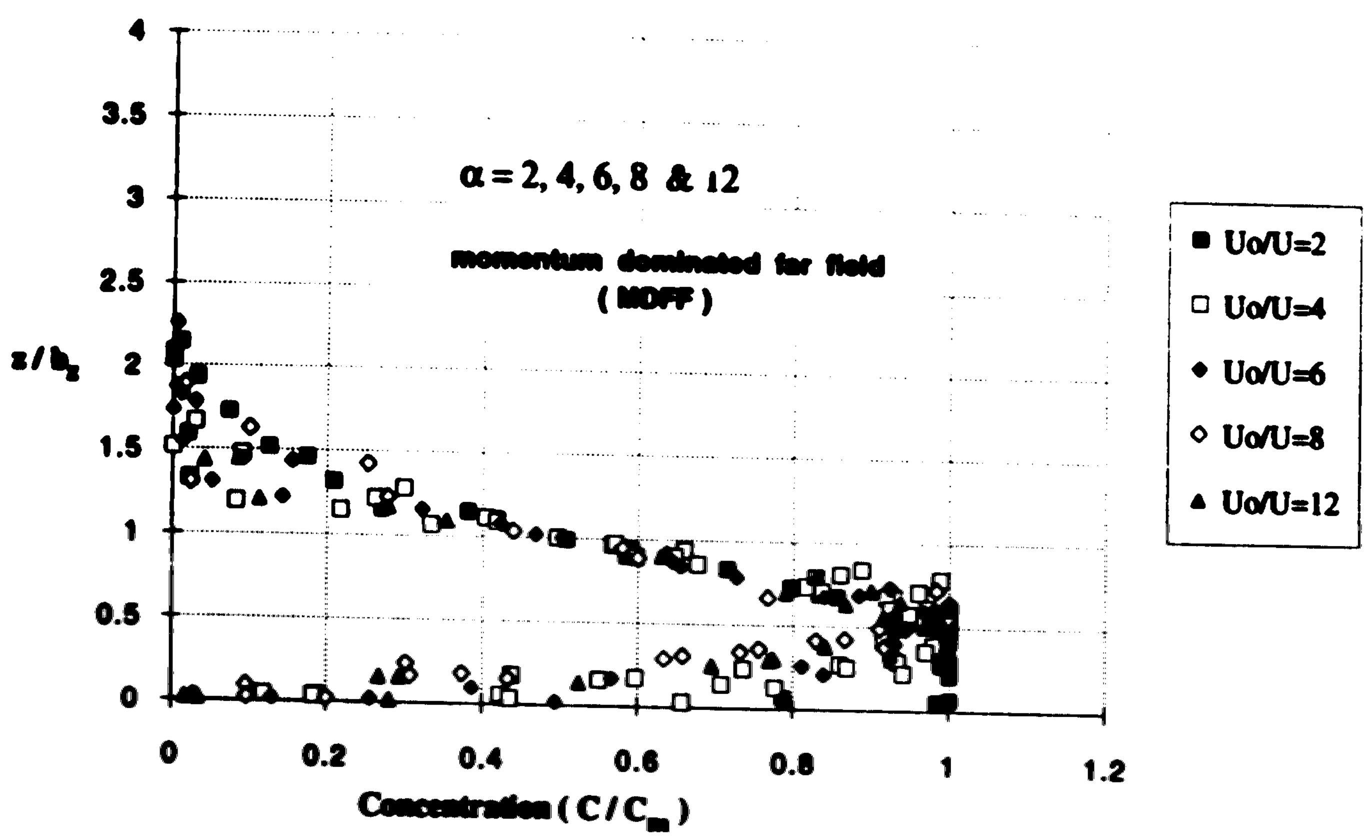

Fig. 4.14 (b) Similarity Profiles of Concentration Distribution in the Vertical Direction

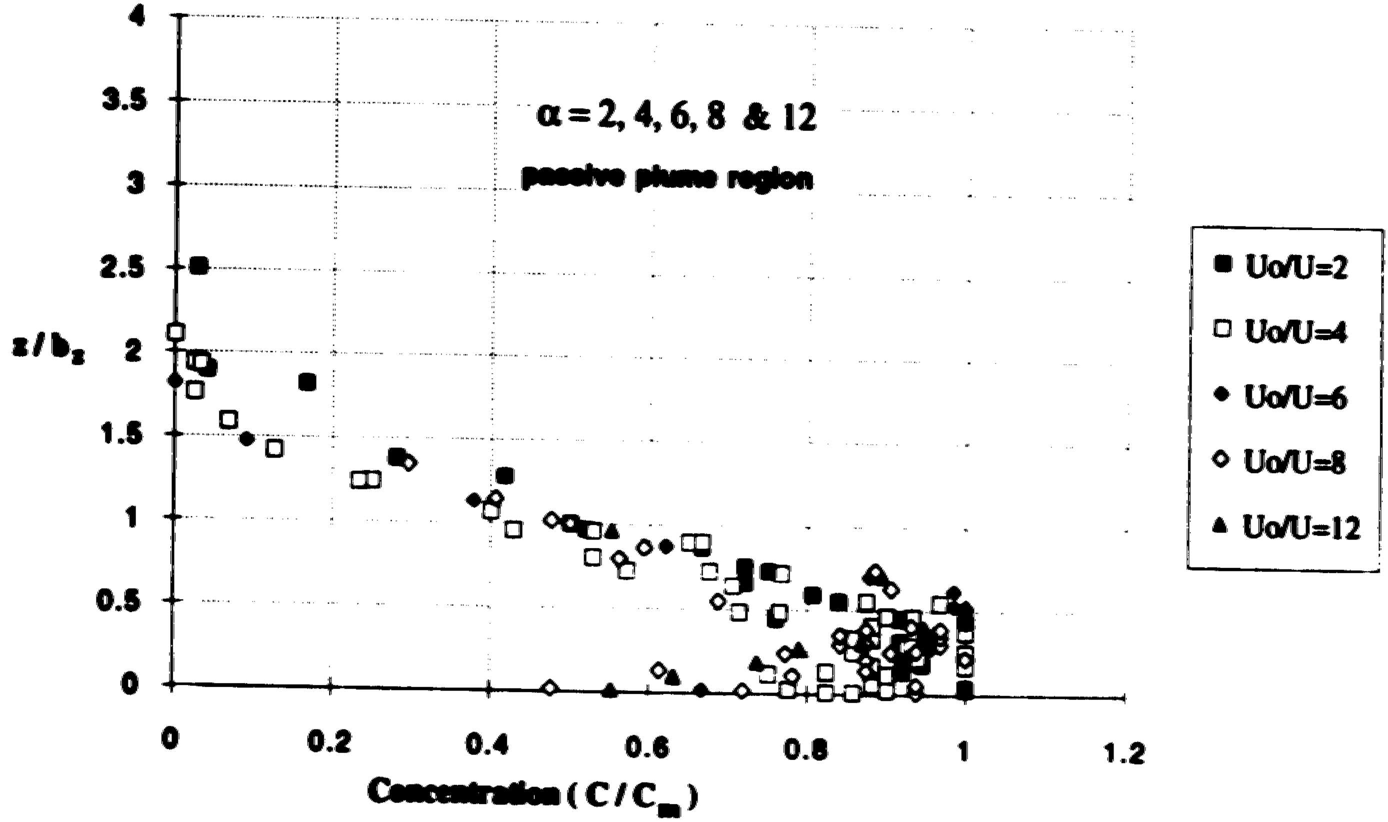

Fig. 4.14 (c) Similarity Profiles of Concentration Distribution in the Vertical Direction

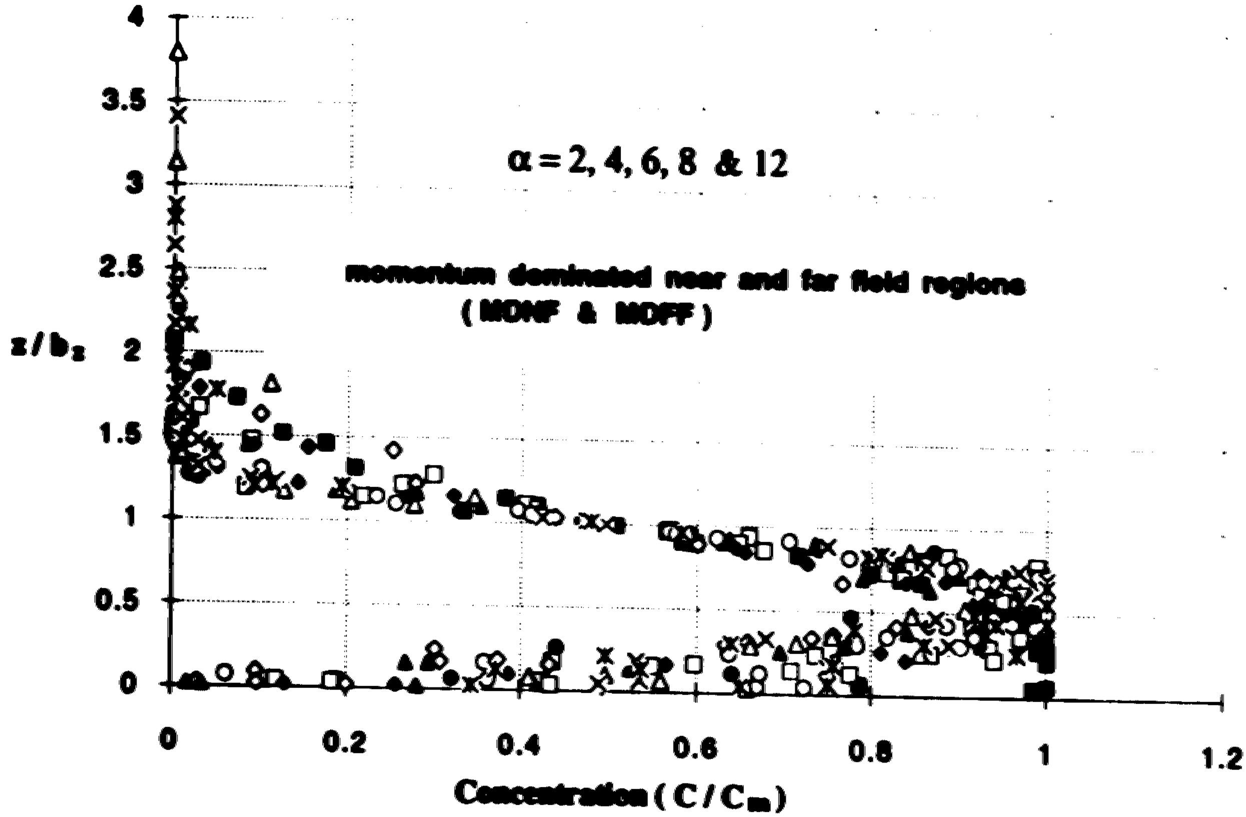

Fig. 4.14 (d) Similarity Profiles of Concentration Distribution in the Vertical Direction

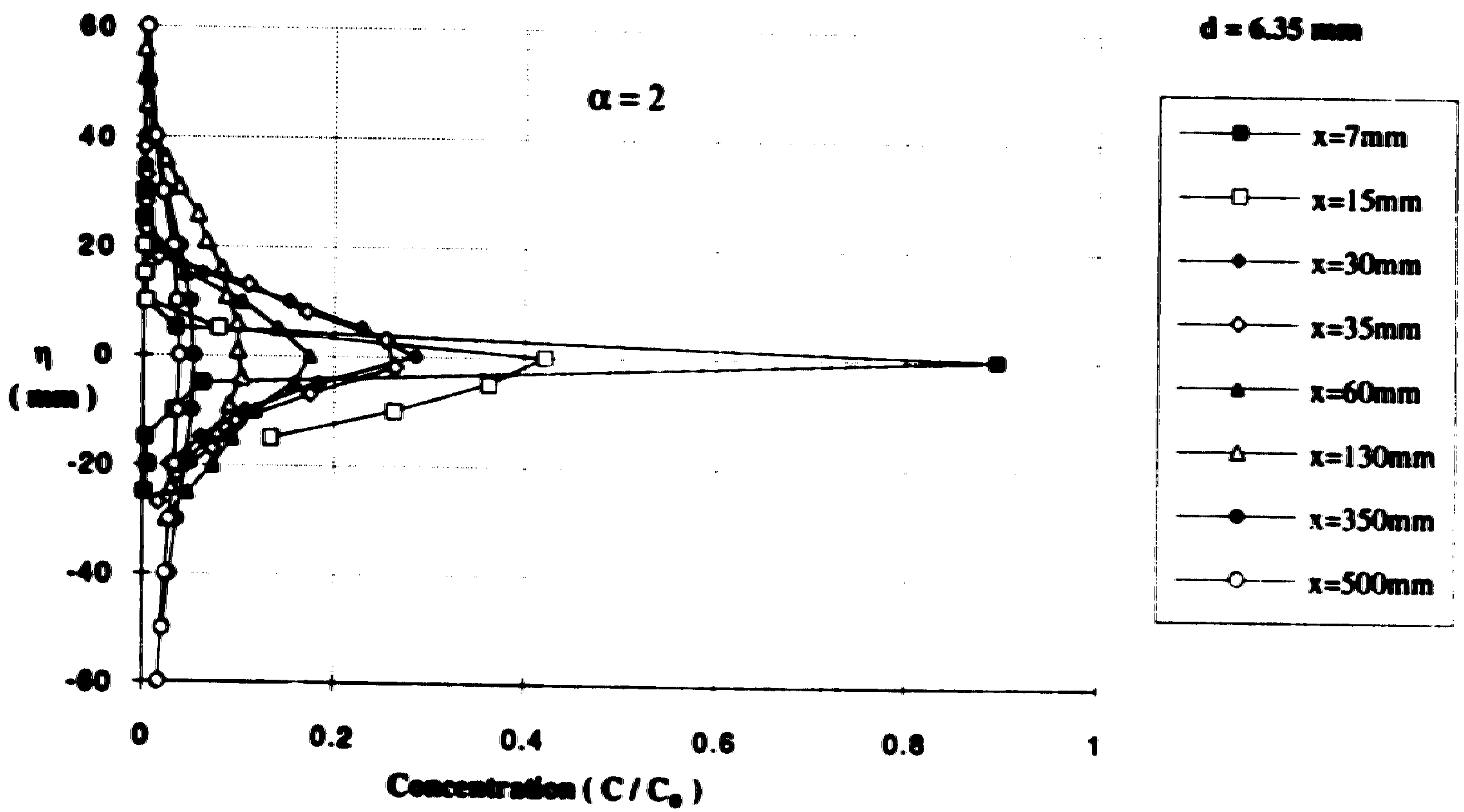

Fig. 4.15 Transverse Concentration Profiles Perpendicular to the Jet Axis

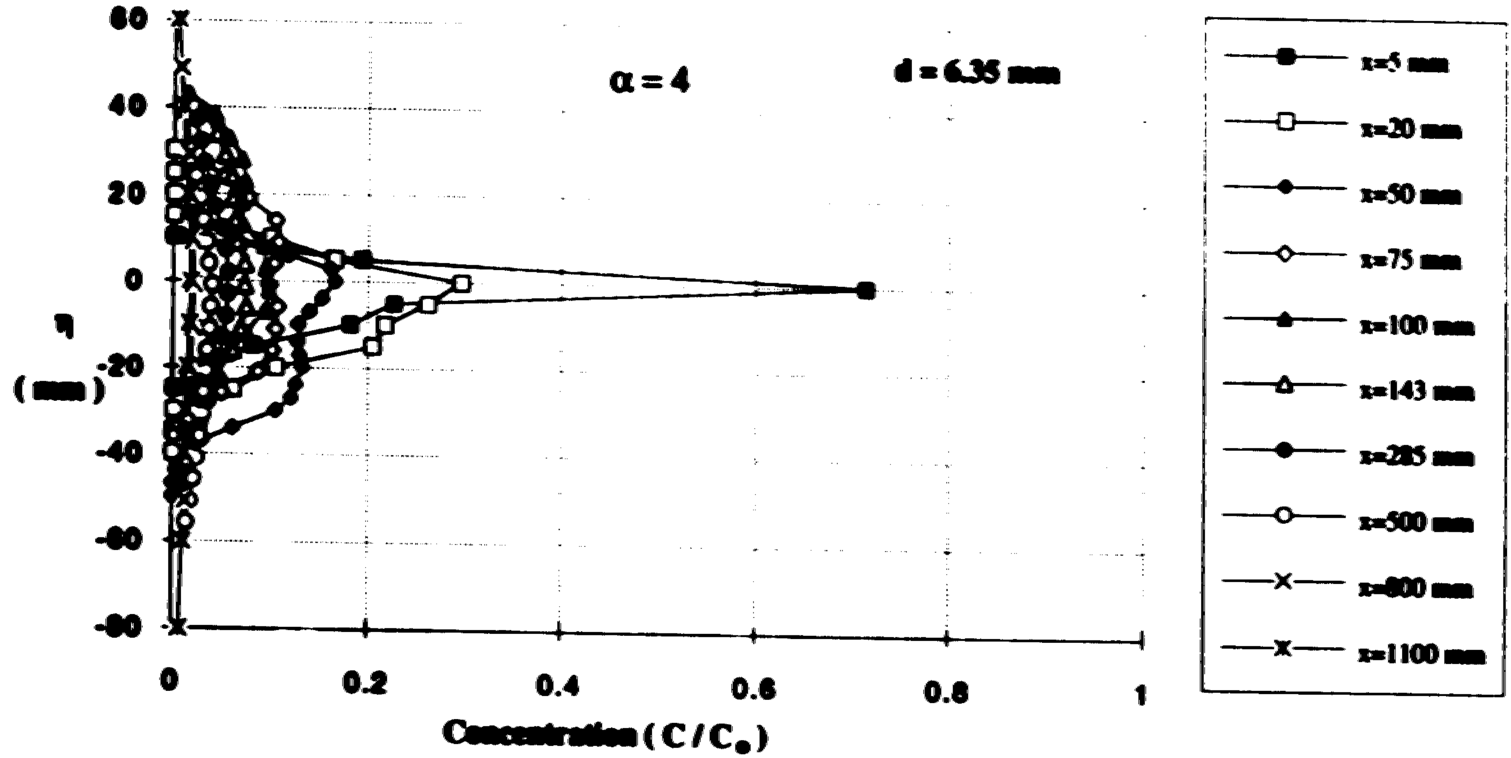

Fig. 4.16 Transverse Concentration Profiles Perpendicular to the Jet Axis

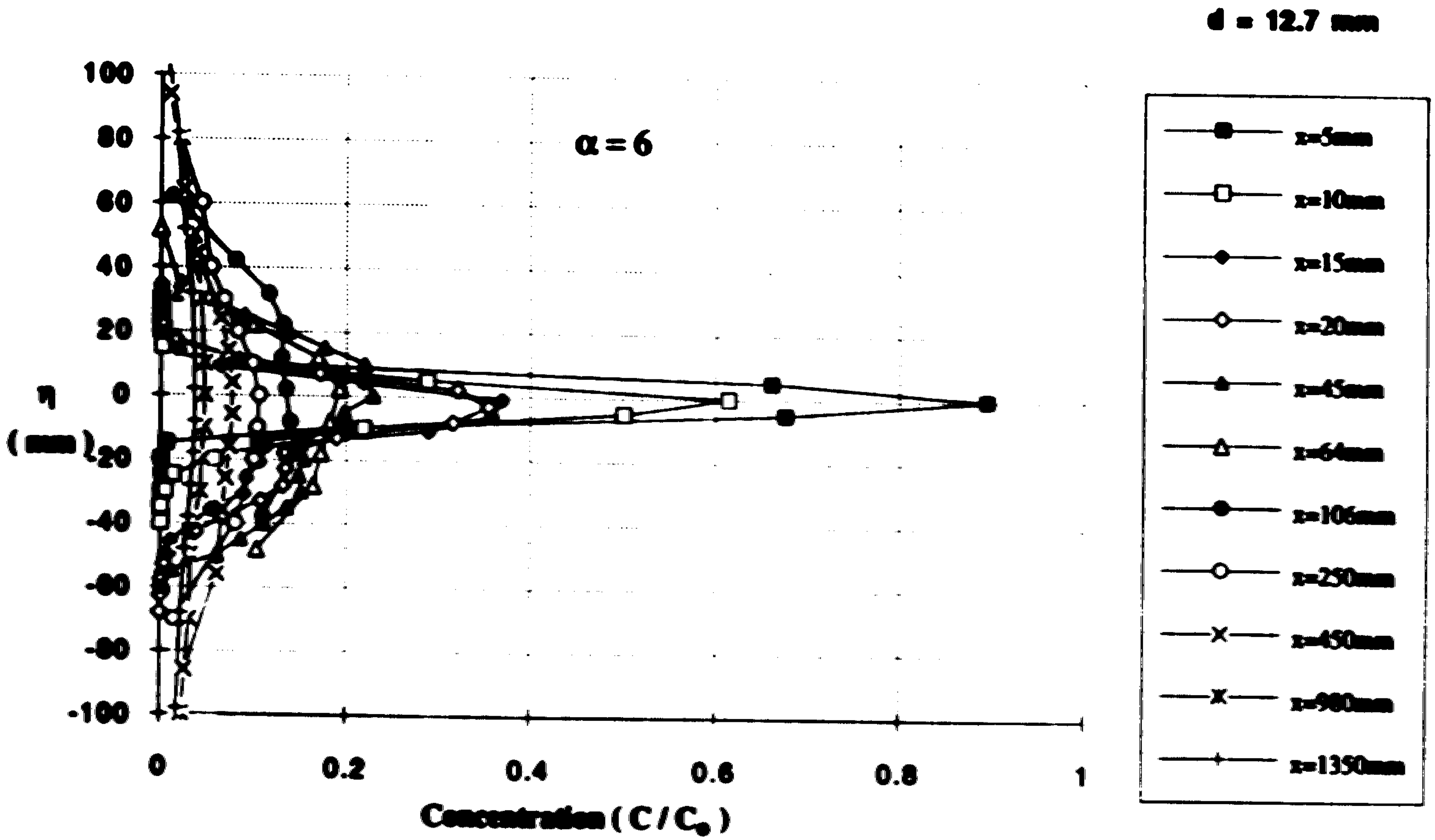

Fig. 4.17 Transverse Concentration Profiles Perpendicular to the Jet Axis

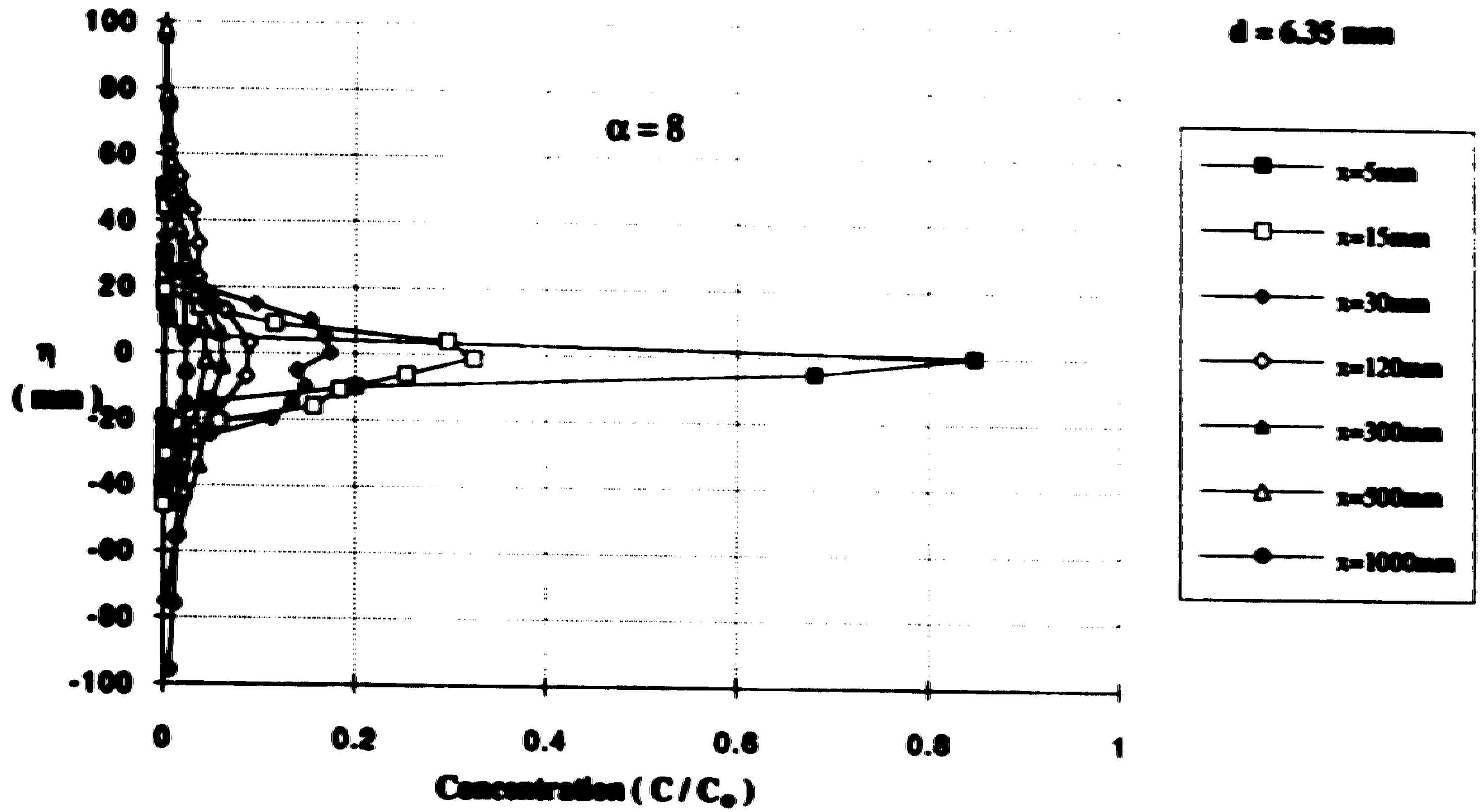

Fig. 4.18 Transverse Concentration Profiles Perpendicular to the Jet Axis

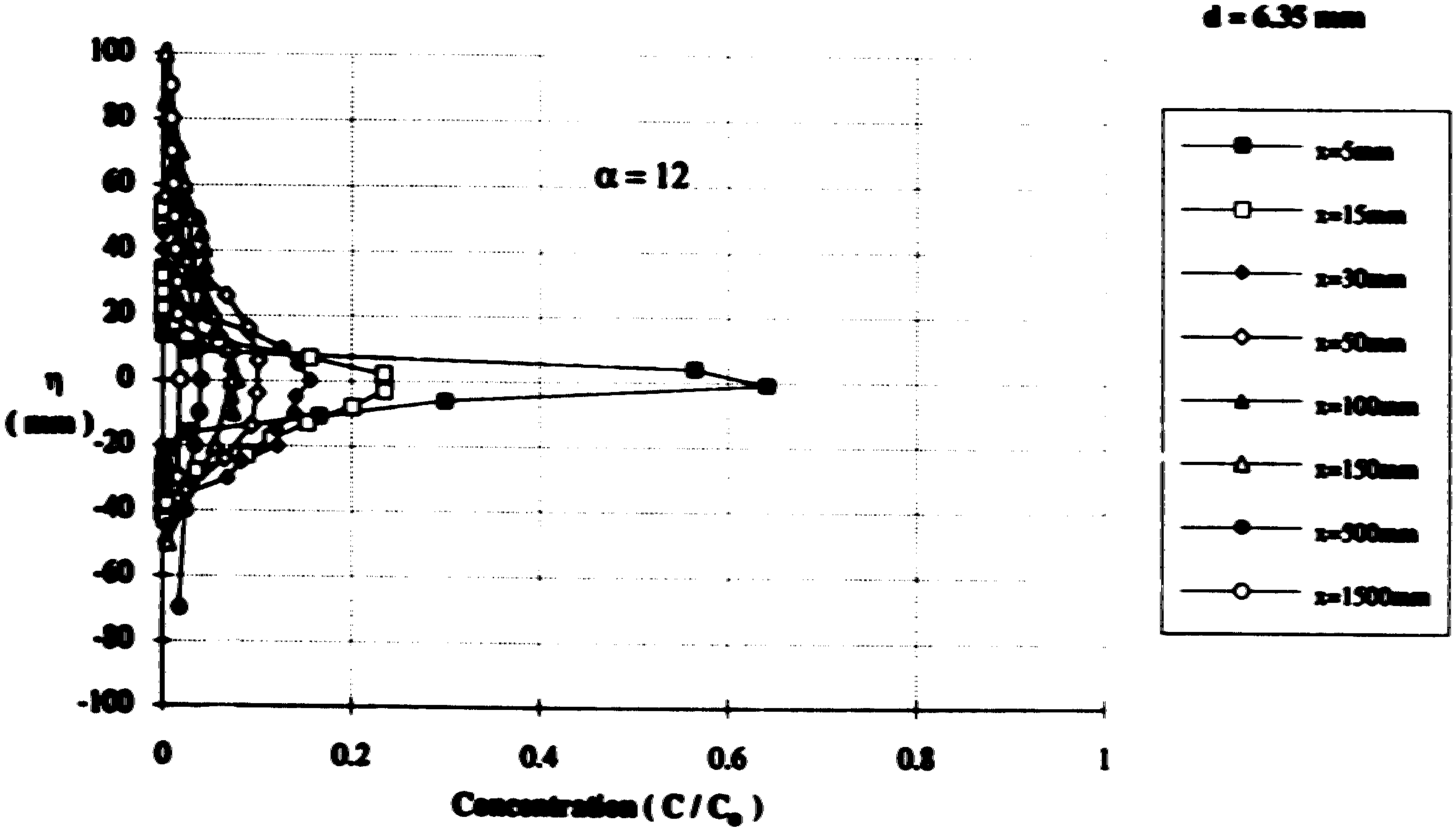

Fig. 4.19 Transverse Concentration Profiles Perpendicular to the Jet Axis

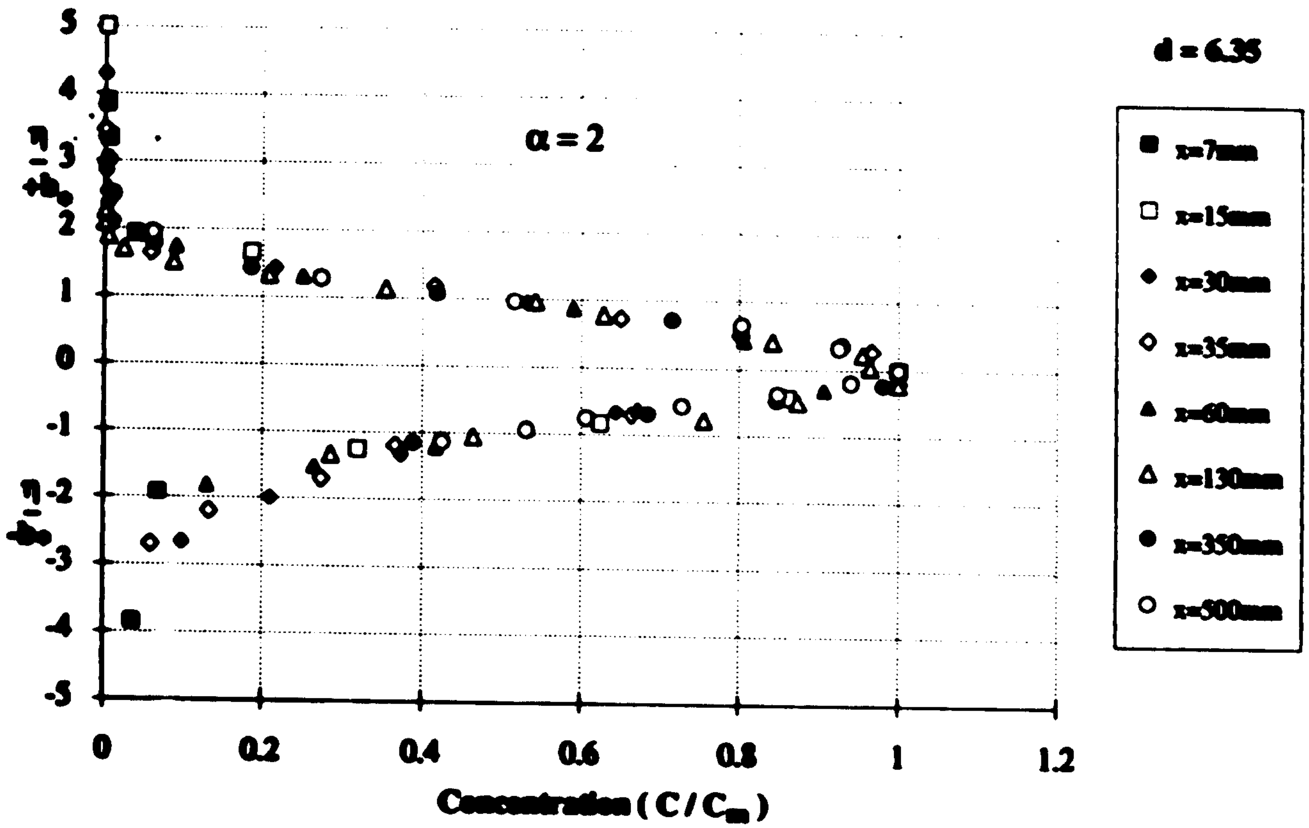

Fig. 4.20 Non - Dimensional Profiles of Concentration Distribution in the Transverse Direction

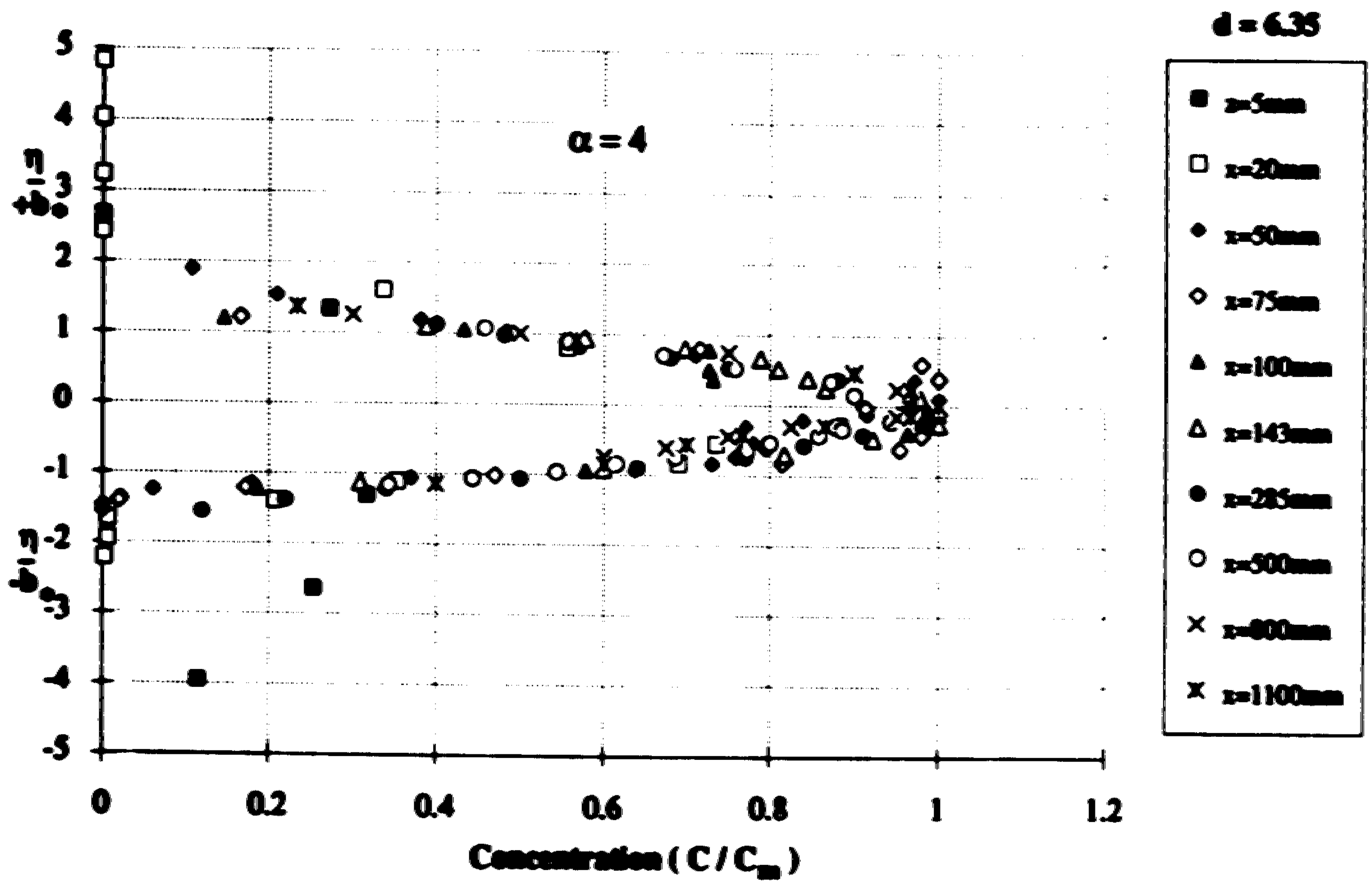

Fig. 4.21 Non - Dimensional Profiles of Concentration Distribution in the Transverse Direction

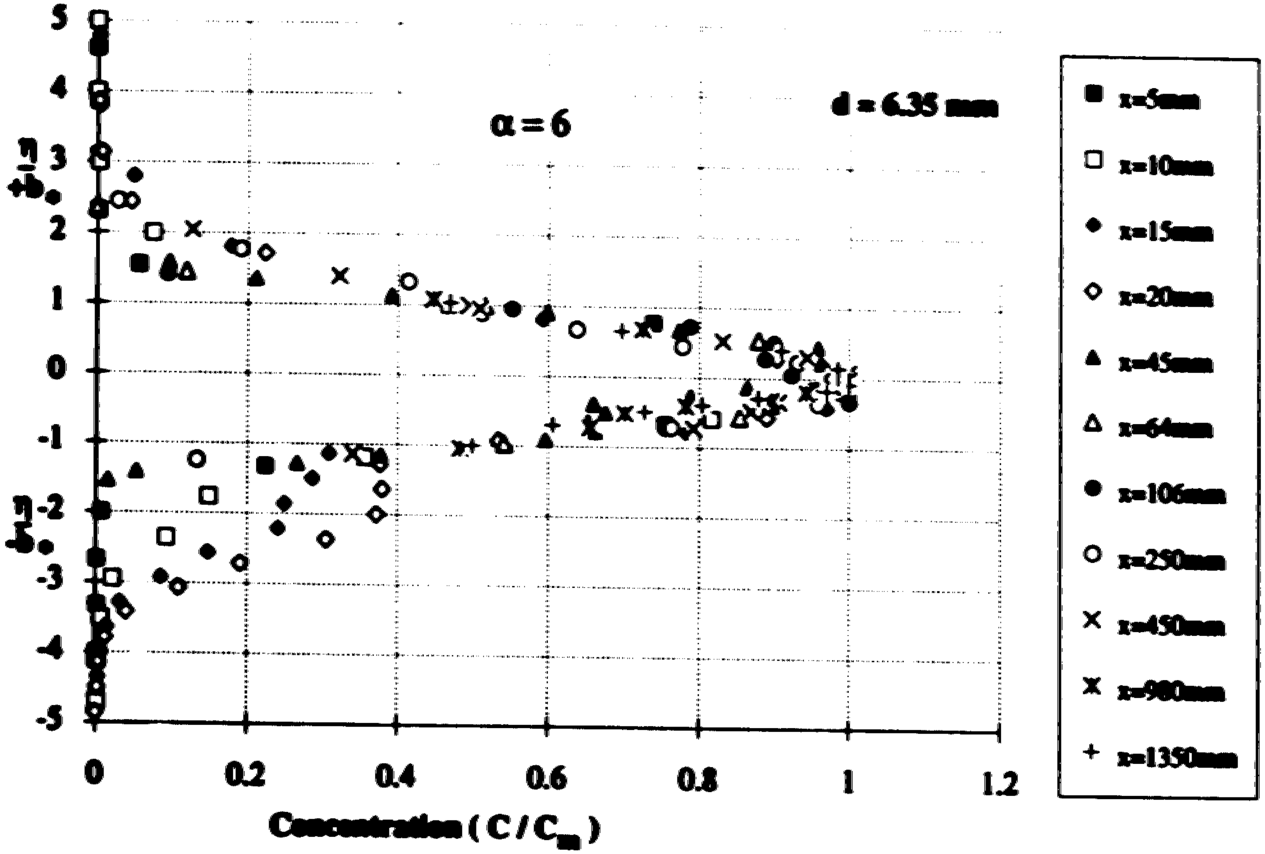

Fig. 4.22 Non - Dimensional Profiles of Concentration Distribution in the Transverse Direction

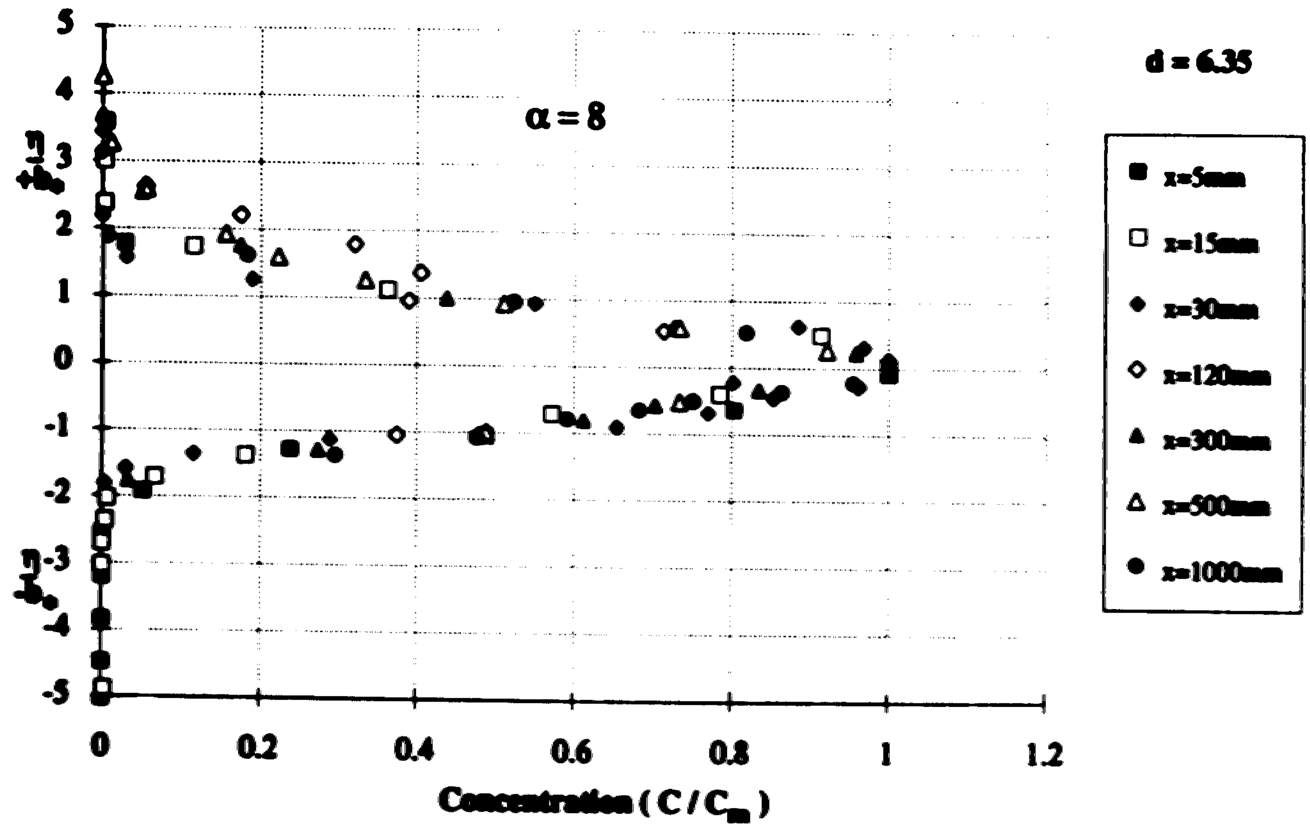

Fig. 4.23 Non - Dimensional Profiles of Concentration Distribution in the Transverse Direction

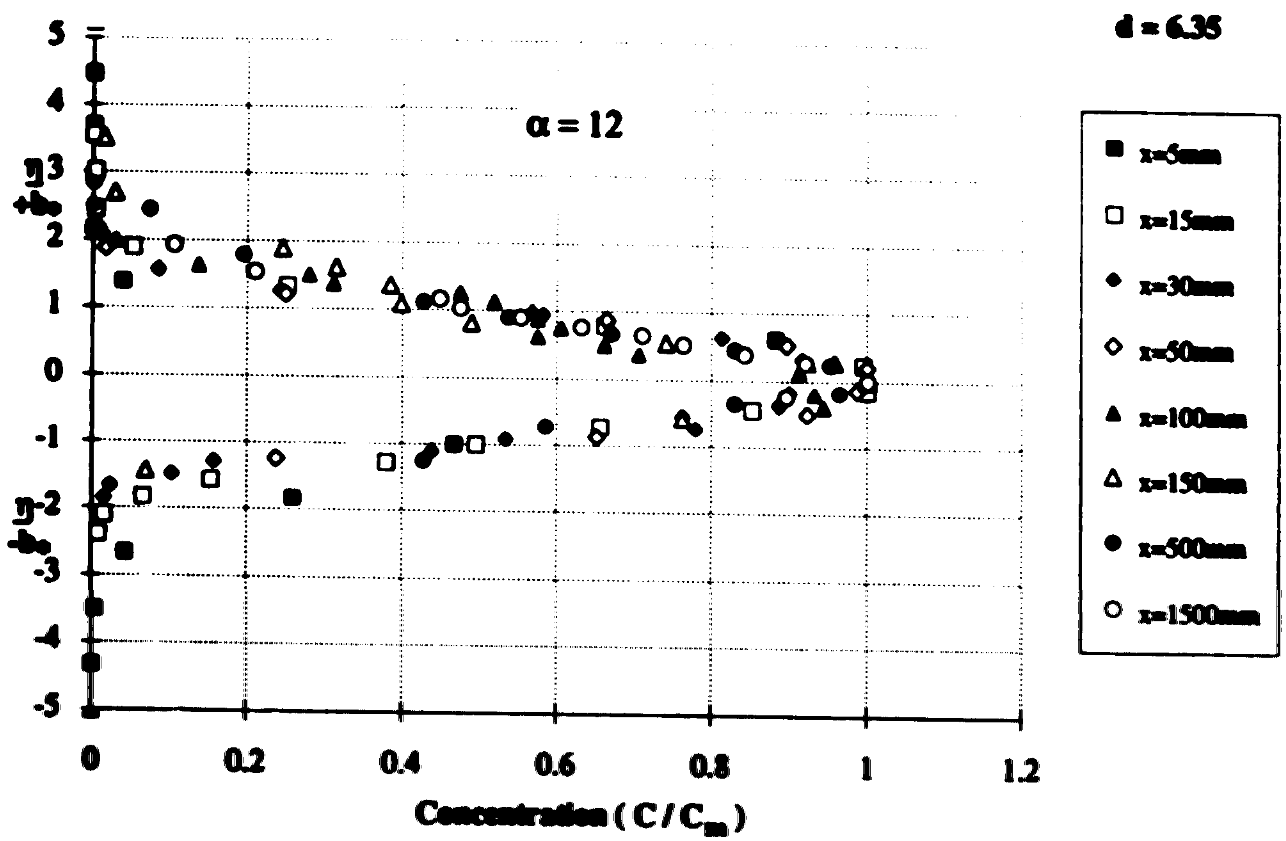

Fig. 4.24 Non - Dimensional Profiles of Concentration Distribution in the Transverse Direction

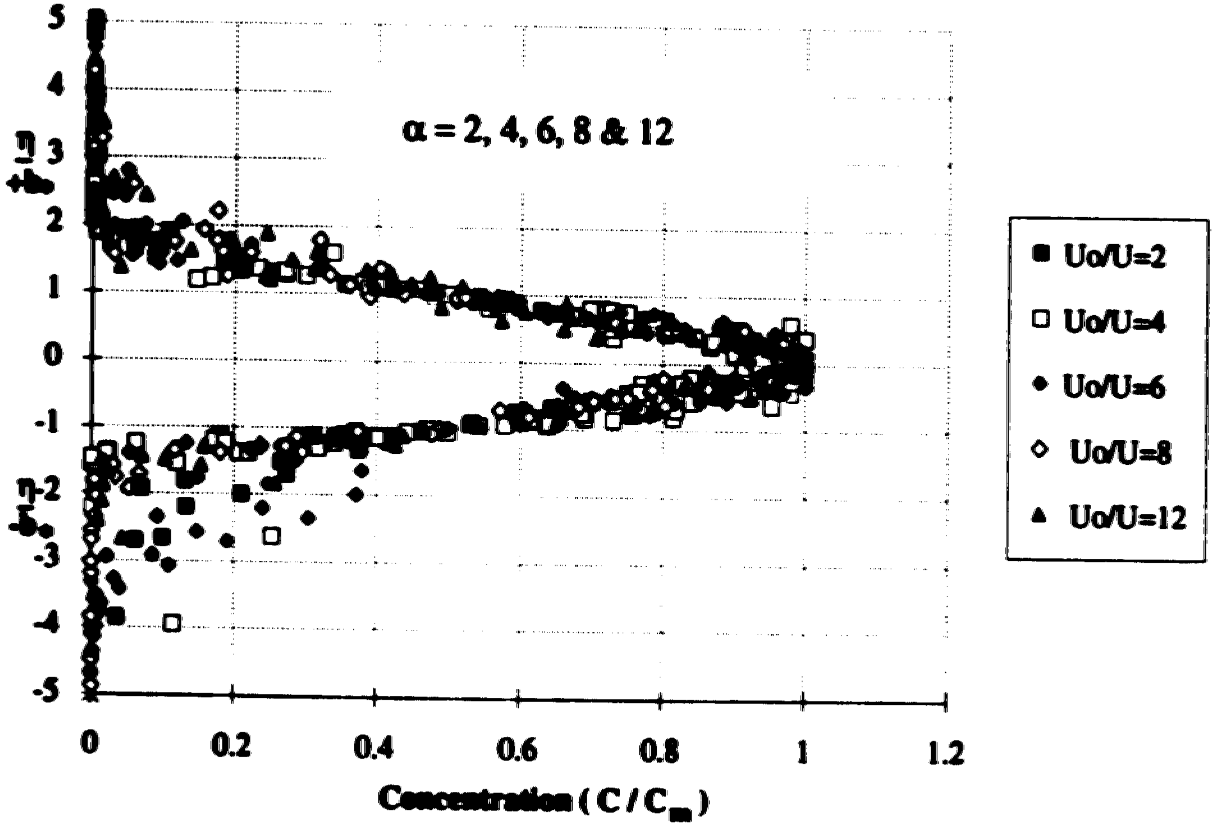

Fig. 4.25 Similarity Profiles of Concentration Distribution in the Transverse Direction

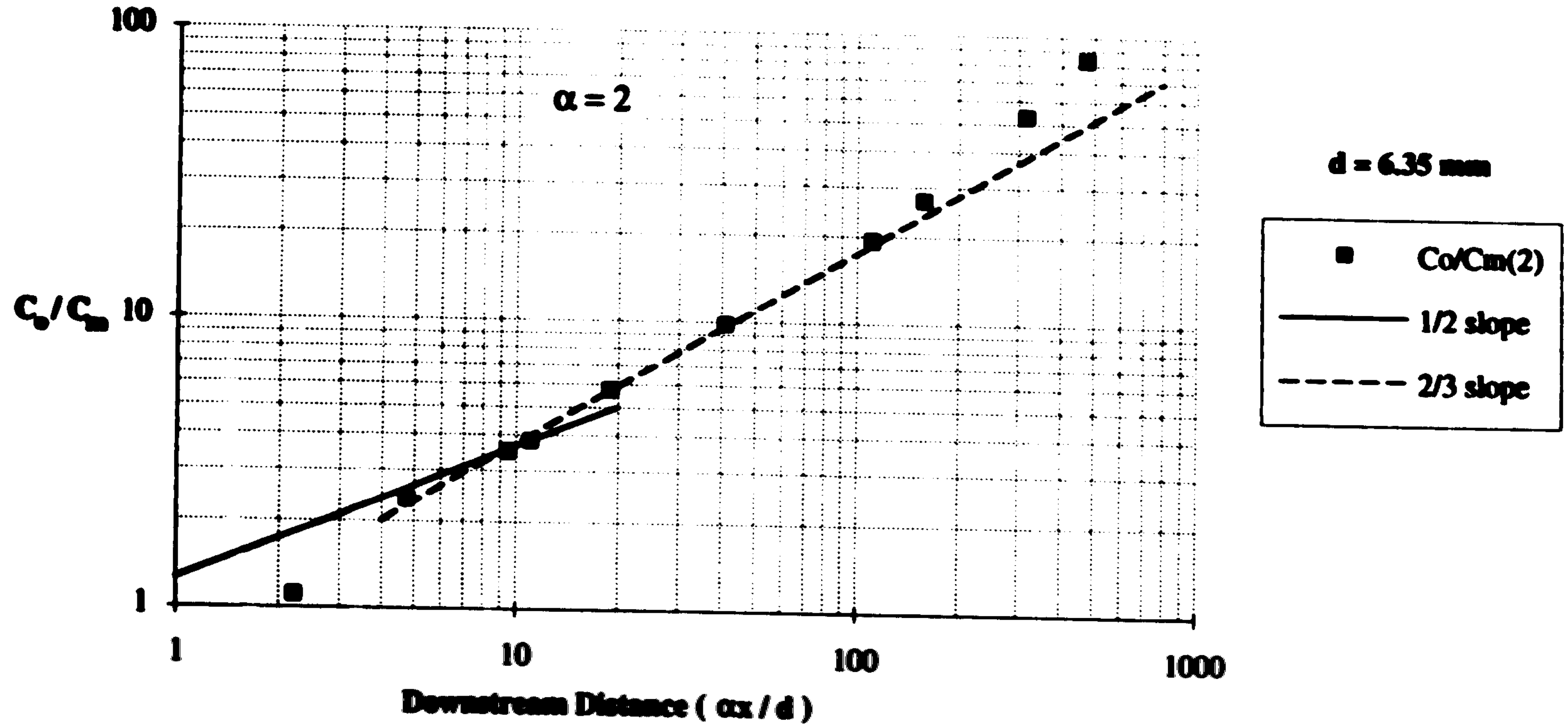

Fig. 4.26 Characteristic Minimum Dilution of the Deflected Jet

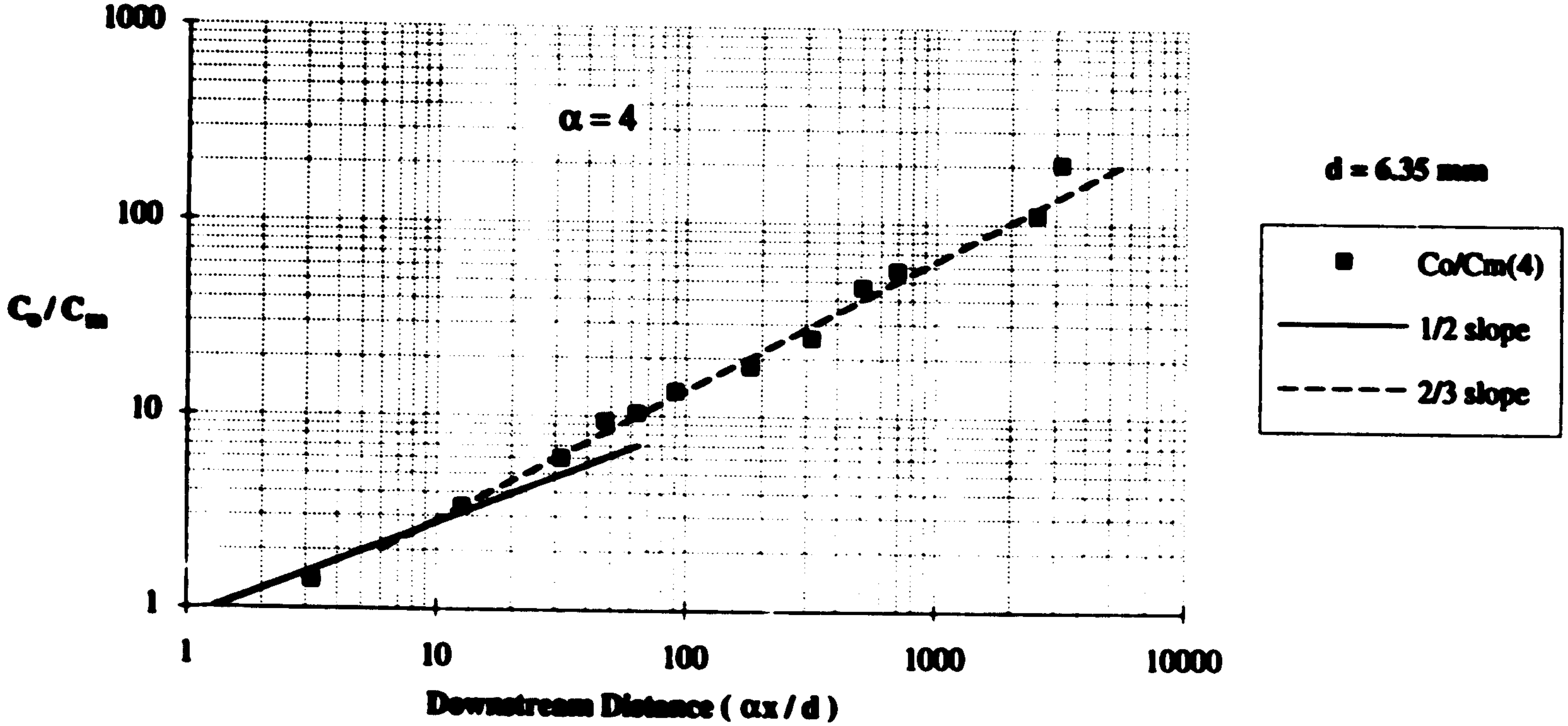

Fig. 4.27 Characteristic Minimum Dilution of the Deflected jet

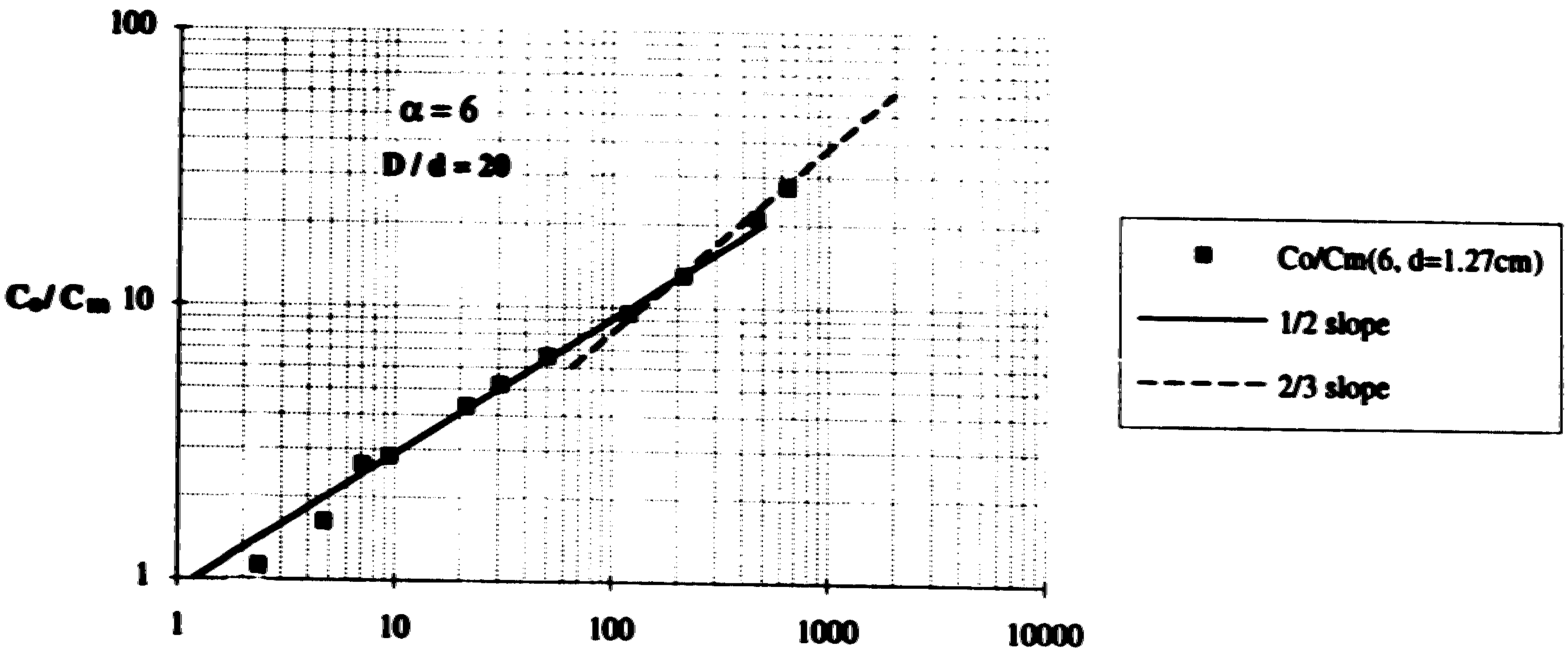

Fig. 4.28 (a) Characteristic Minimum Dilution of the Deflected Jet

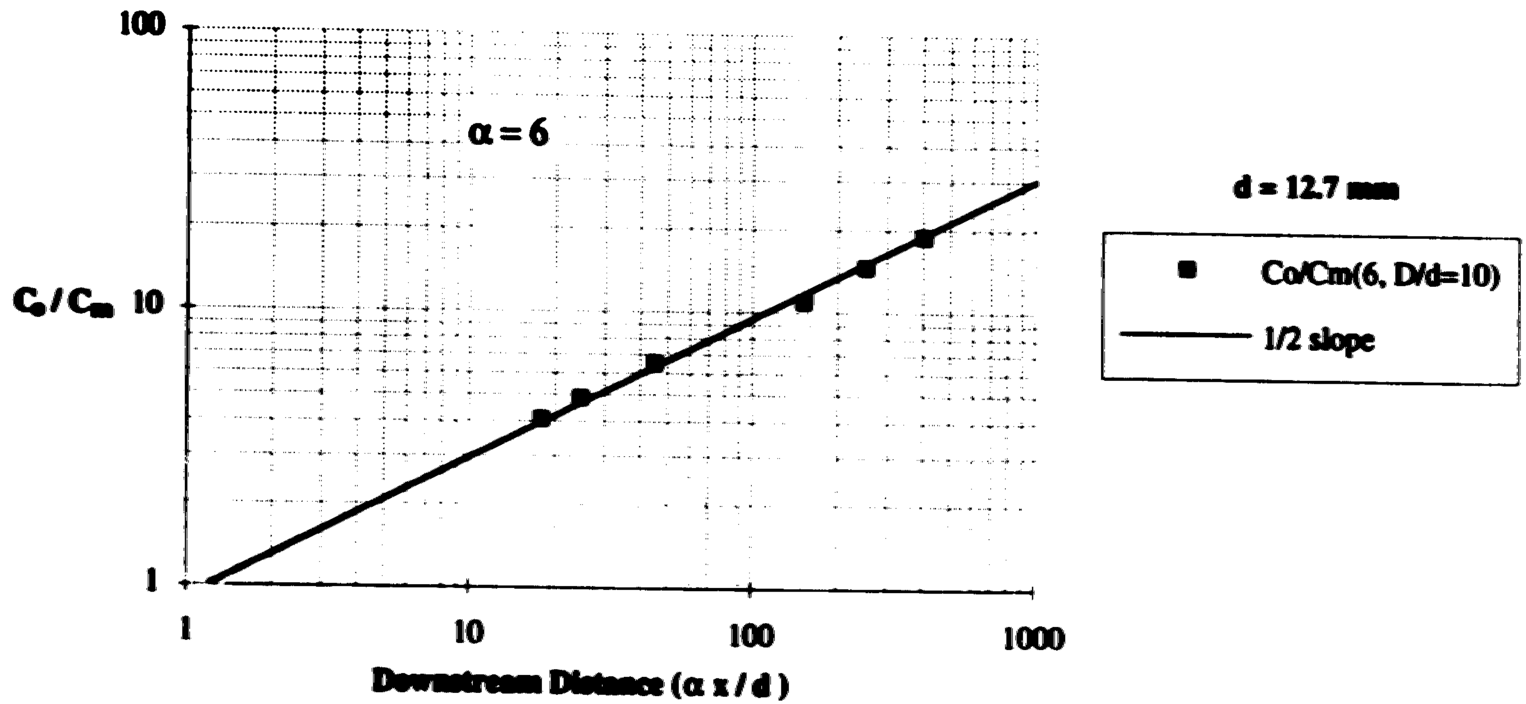

Fig. 4.28 (b) Characteristic Minimum Dilution of the Deflected Jet

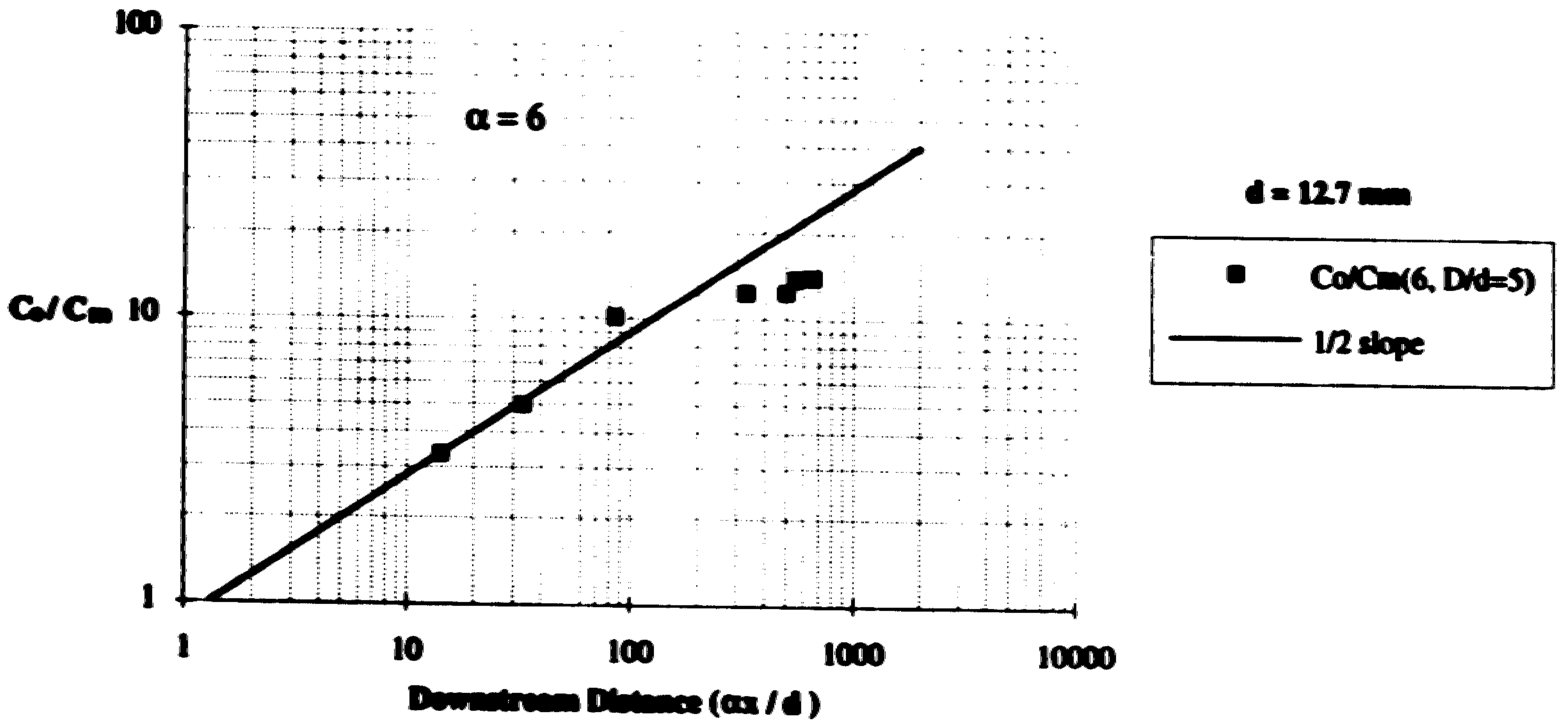

Fig. 4.28 (c) Characteristic Minimum Dilution of the Deflected Jet

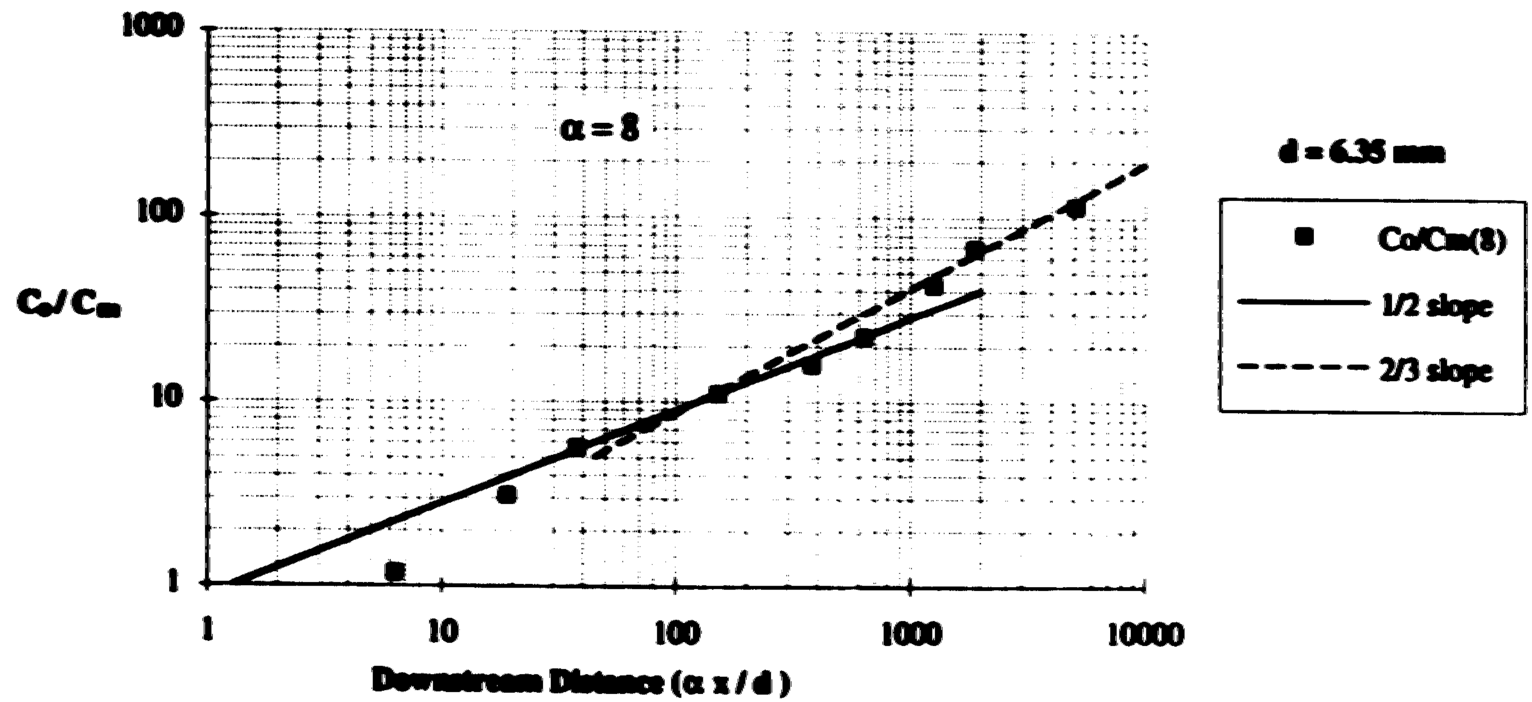

Fig. 4.29 Characteristic Minimum Dilution of the Deflected Jet

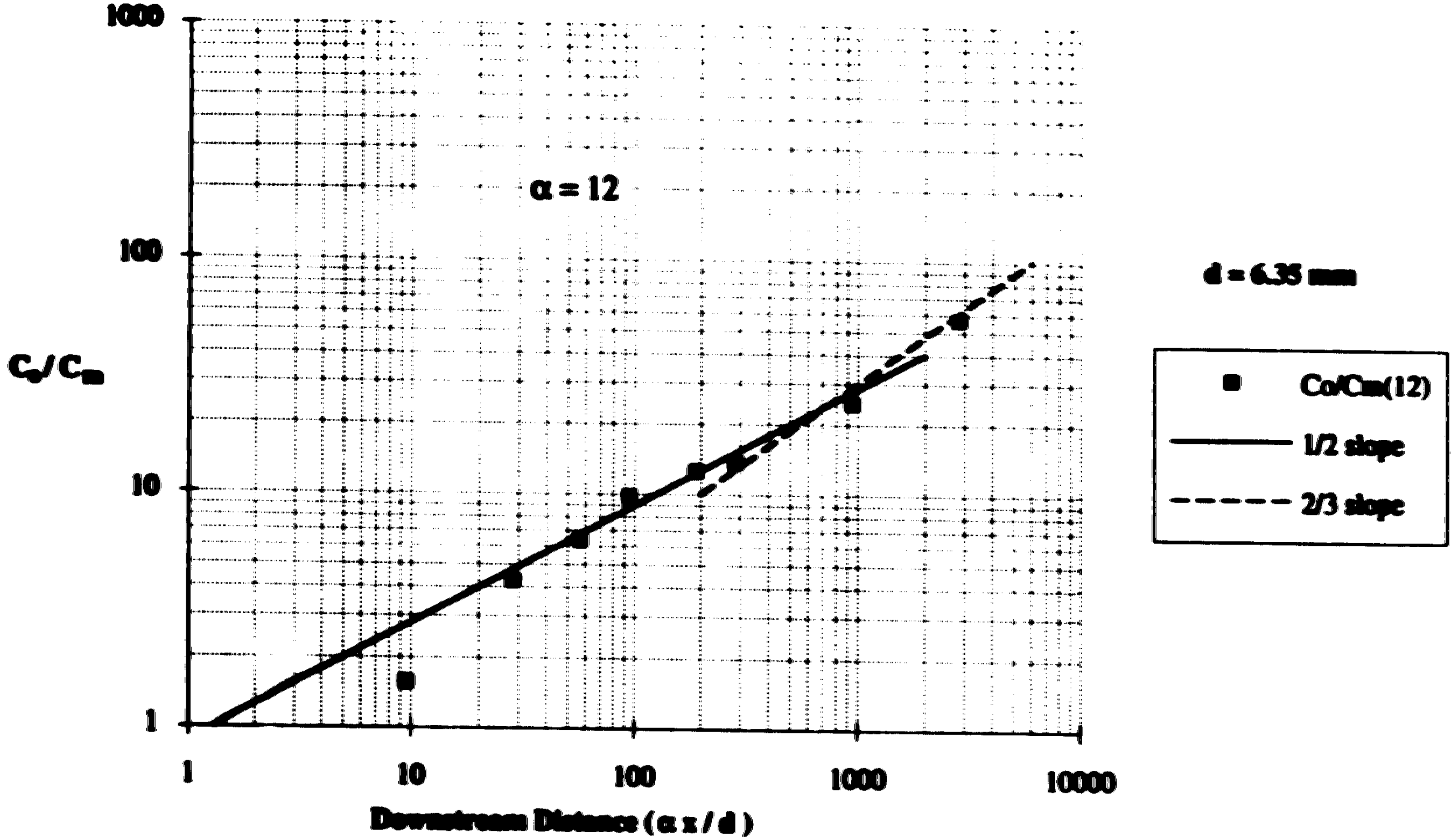

Fig. 4.30 (a) Characteristic Minimum Dilution of the Deflected Jet

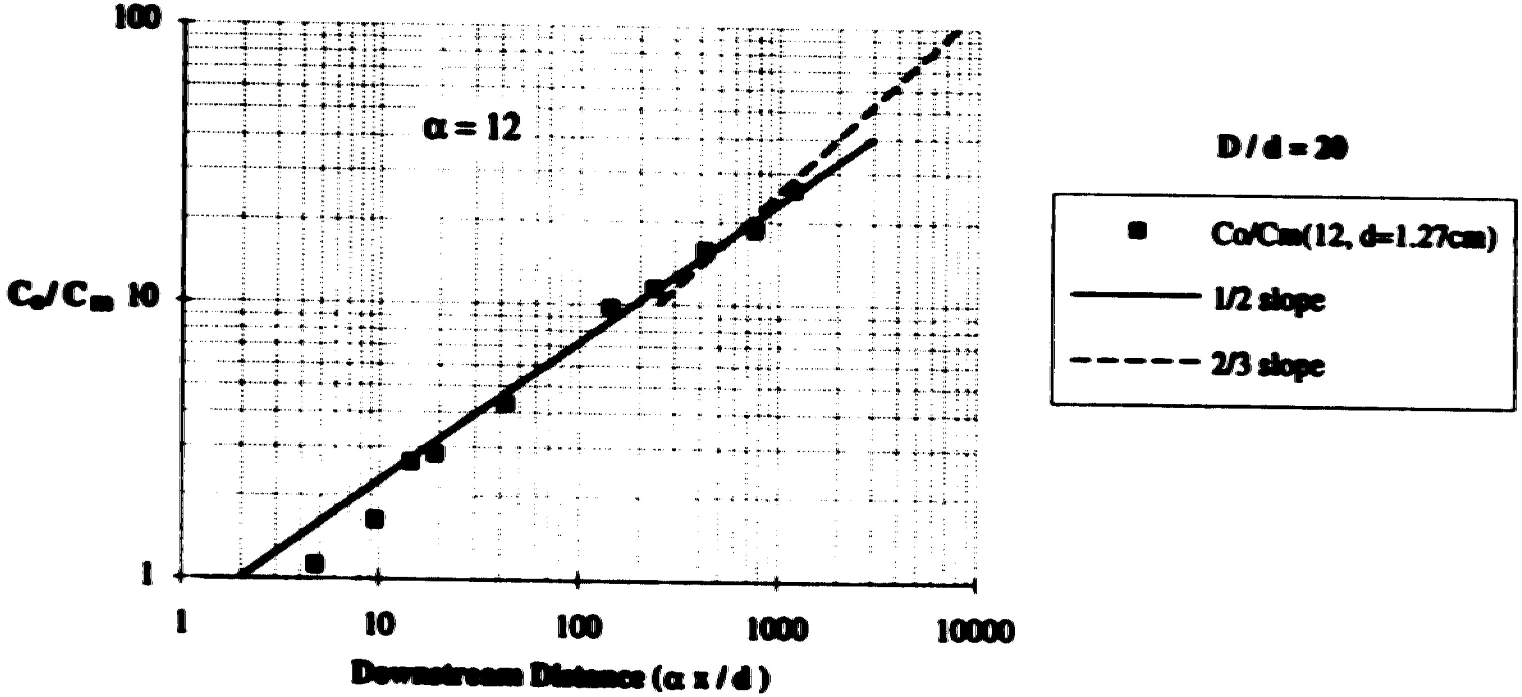

Fig. 4.30 (b) Characteristic Minimum Dilution of the Deflected Jet

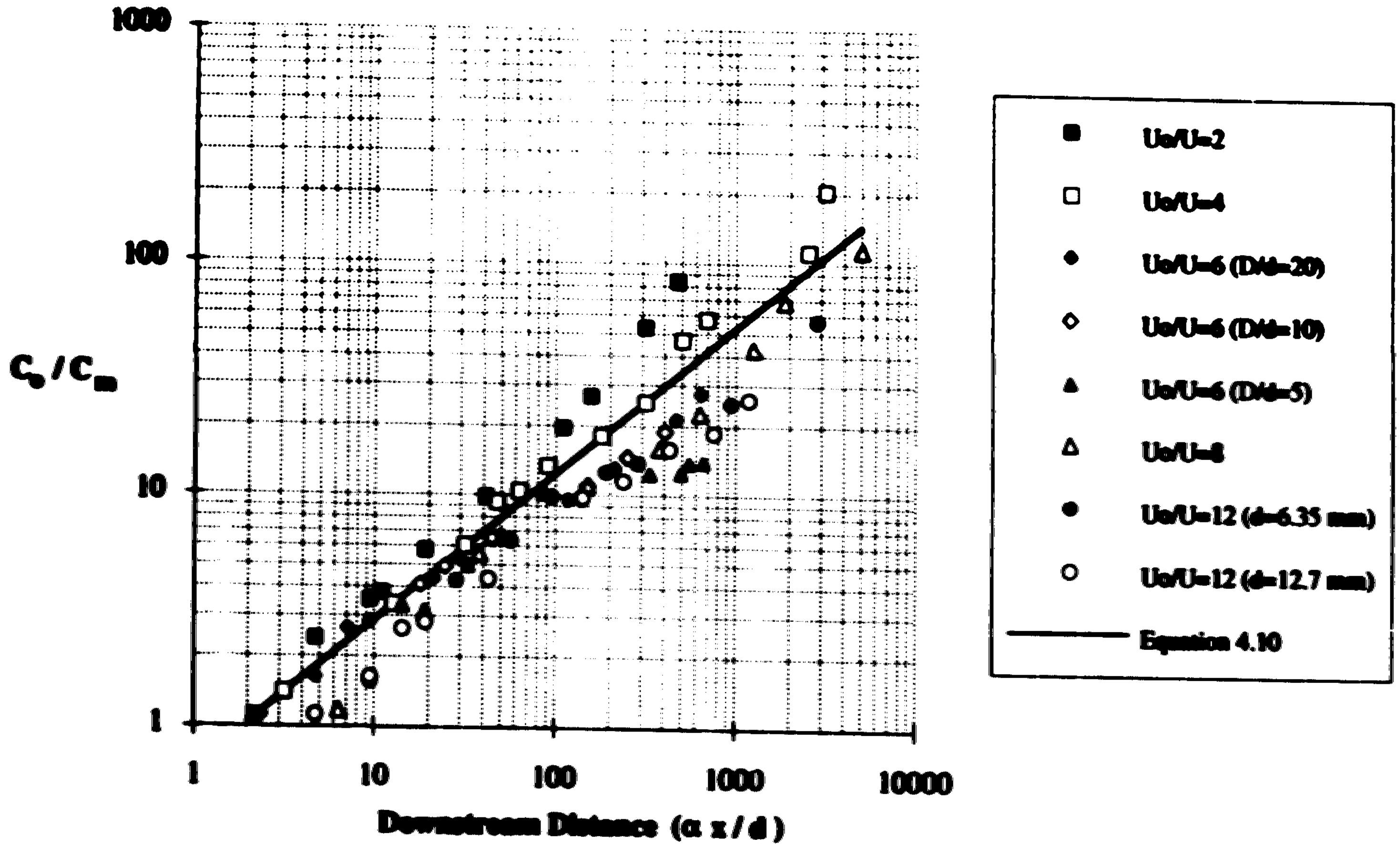

Fig. 4.31 Generalized Minimum Dilution of the Deflected Wall Jet

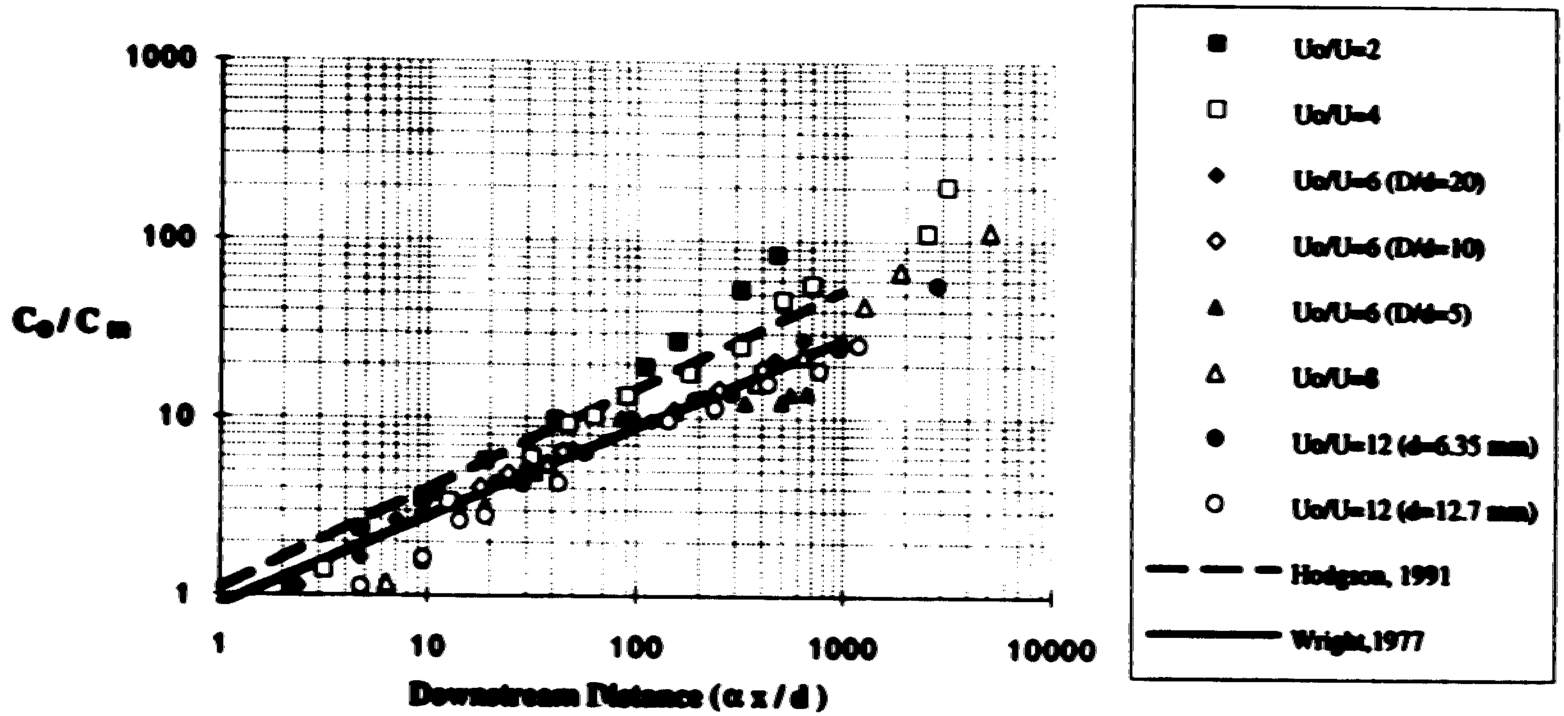

Fig.4.32 Comparison of Free and Wall Jet Minimum Dilutions

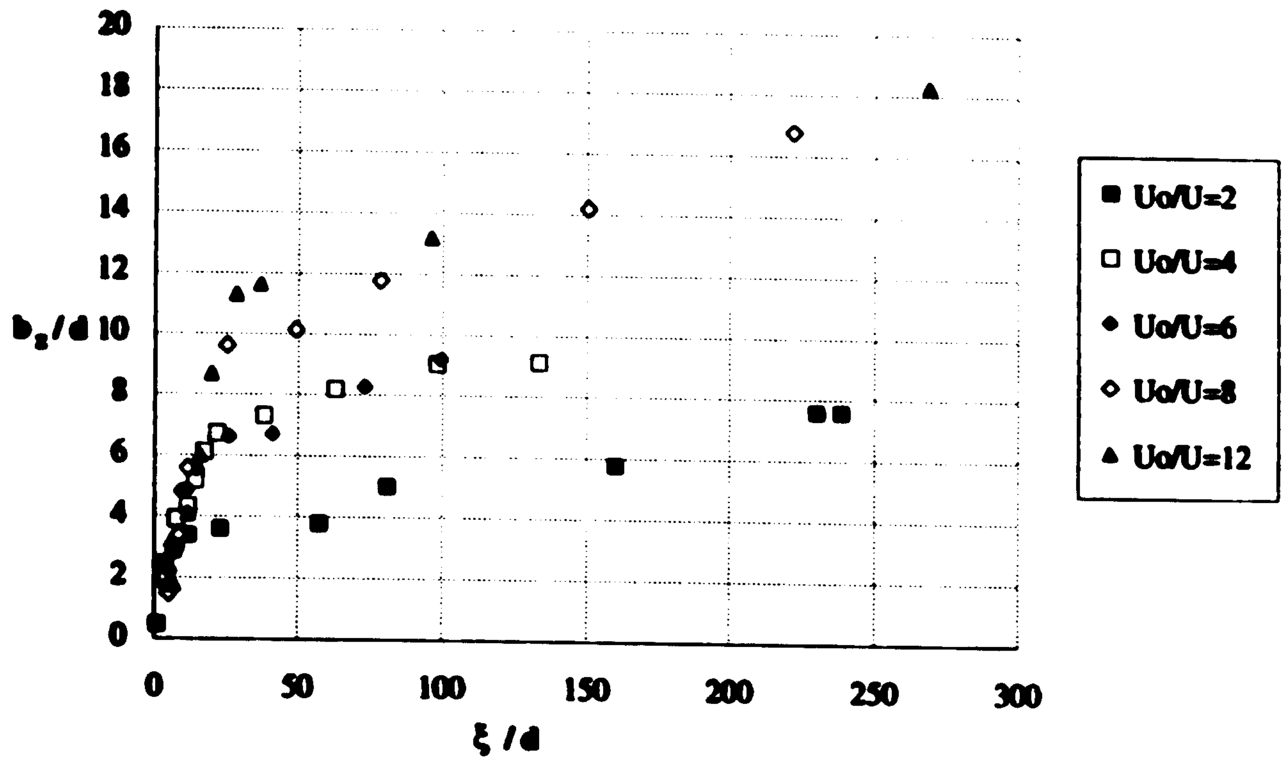

Fig. 4.33 Generalized Scales for the Vertical Concentration Profiles of the Deflected Jet

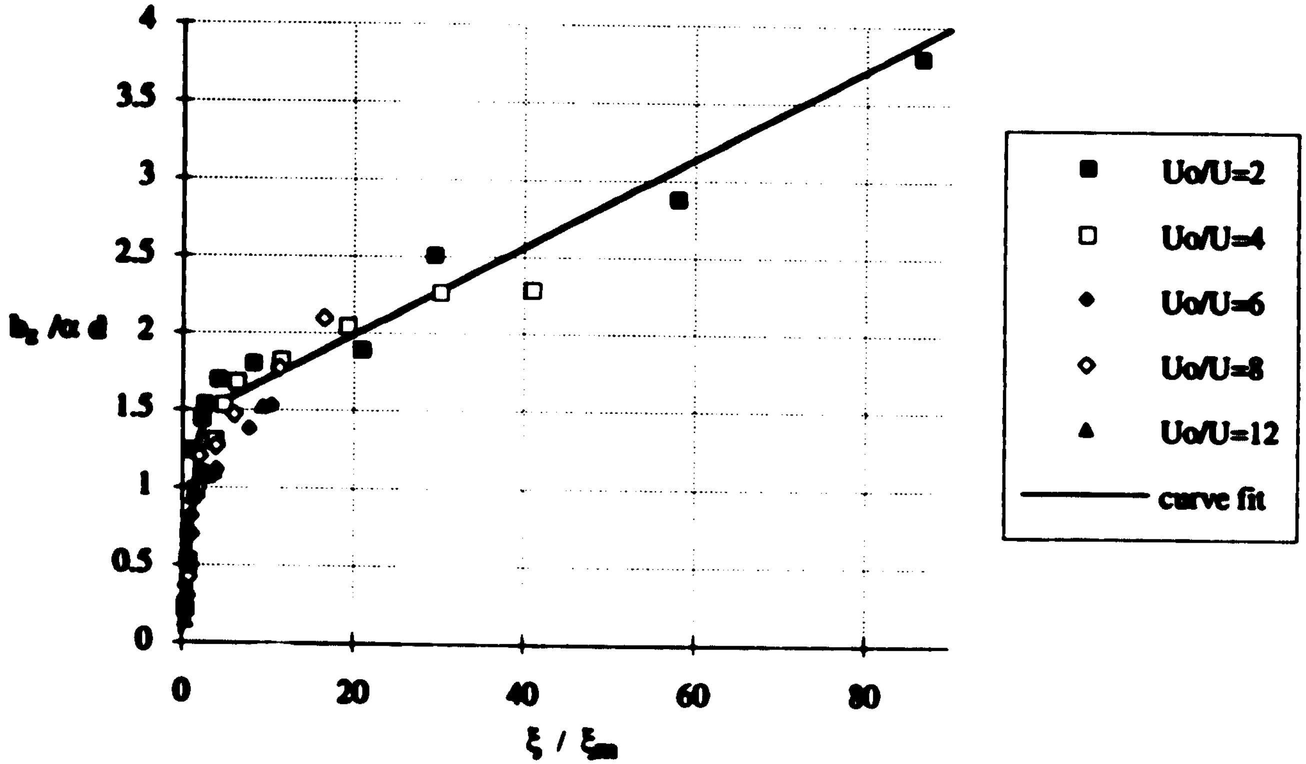

Fig. 4.34 (a) Generalized Scale for the Vertical Concentration Distribution of the Deflected Jet

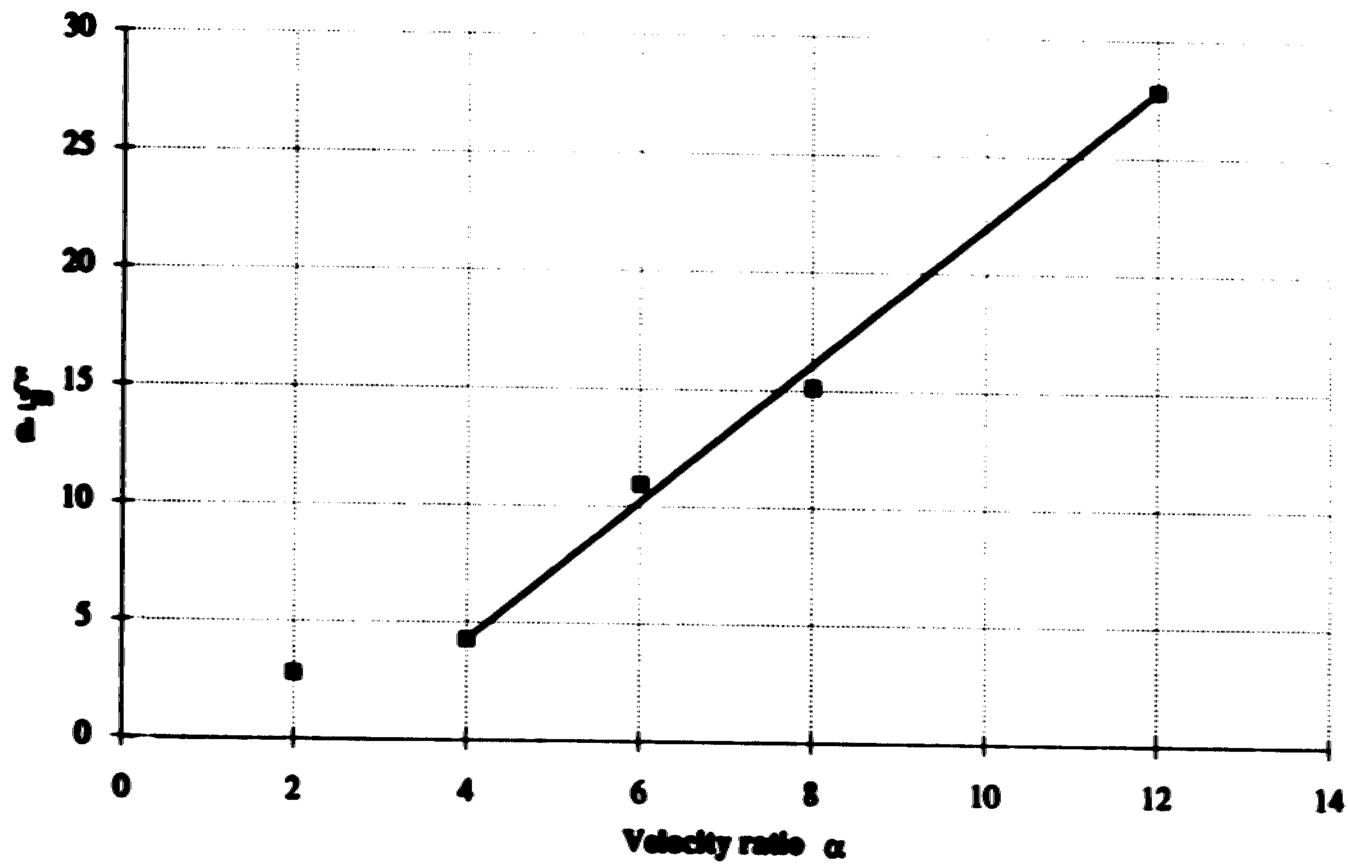

Fig.4.34 (b) Relationship of the Scale

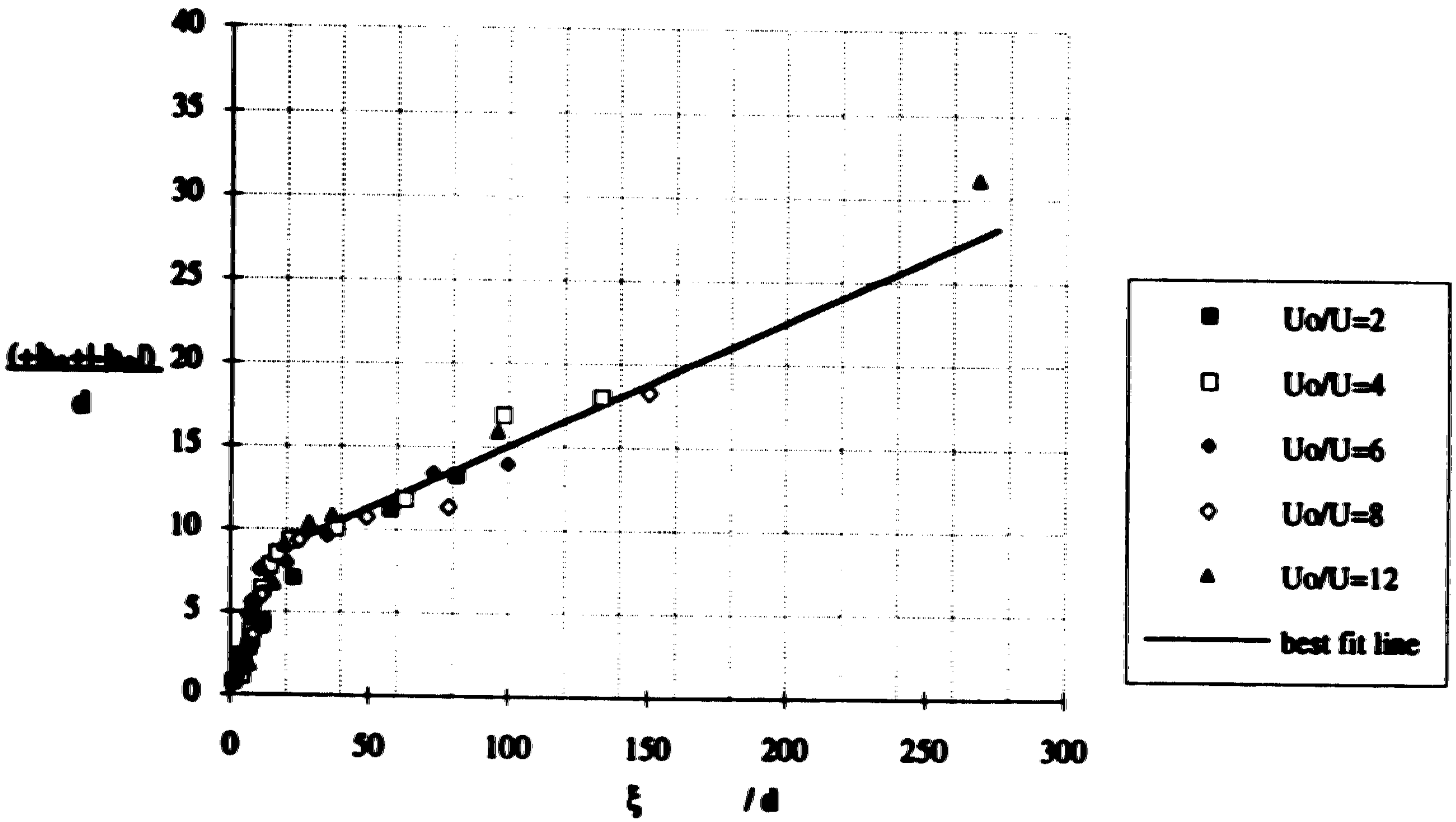

Fig. 4.35 Generalized Scales for the Transverse Concentration Profiles of the Deflected Jet

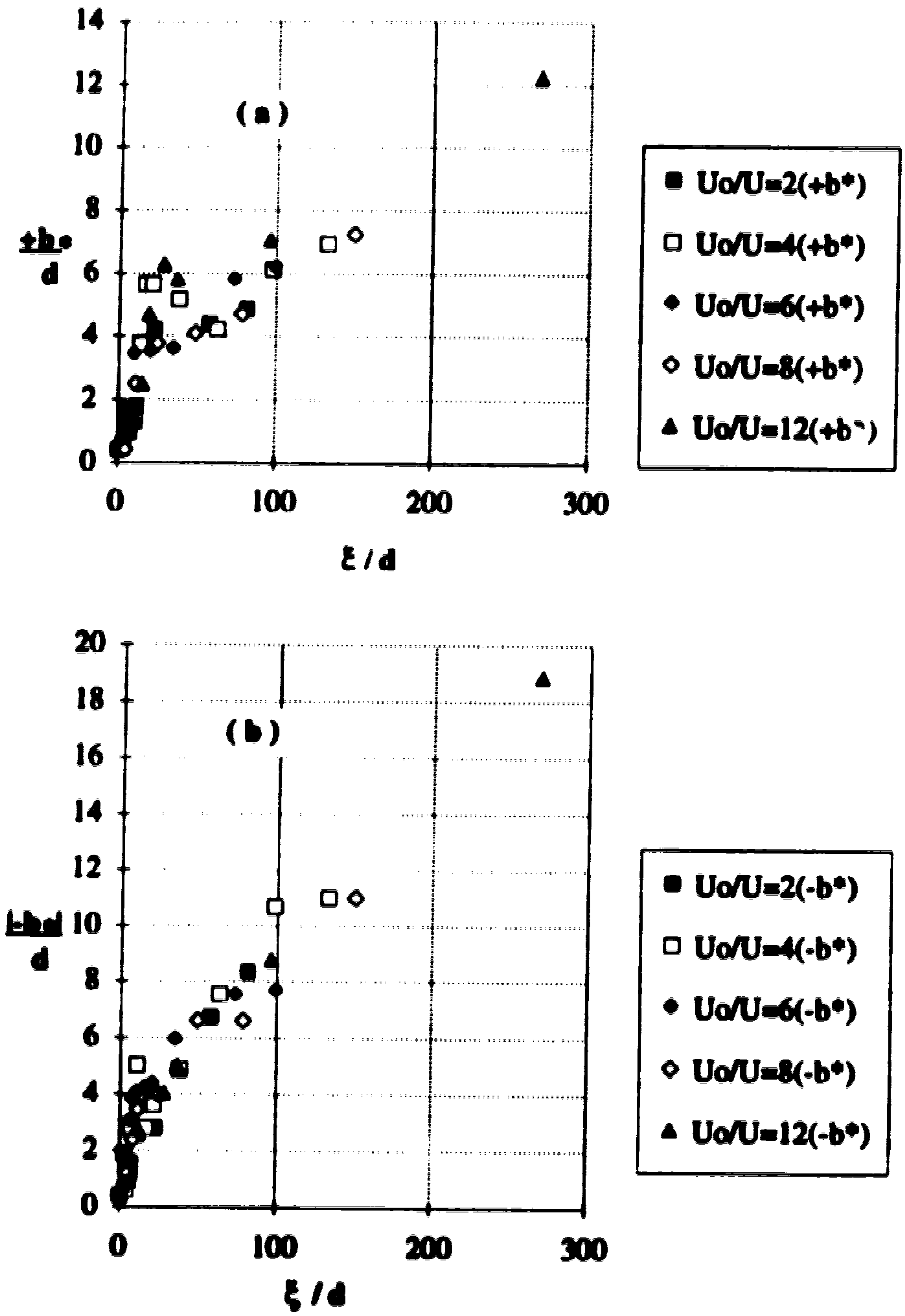

Fig. 4.36 Generalized Positive and Negative Transverse Scales

5.0 CONCLUSIONS AND RECOMMENDATIONS

5.1 Conclusions

The objective of the present study was to investigate the dilution characteristics of circular wall jets in crossflows. These include the similarity analysis of the concentration profiles both in the vertical and transverse directions, minimum dilution and the growth of the jet half - width. The maximum concentrations (C_m) was used as a characteristic scale parameter. It is of practical importance to have knowledge of the maximum value of tracer concentration at any section of the jet because it is useful in assessing the extend of pollutant dilutions released into the environment.

The conclusions presented below are applicable for the region where the jet generated turbulence dominates the ambient flow conditions. The characteristics in the region where the jet strength has decayed to the ambient flow turbulence and referred to in the text as a passive plume condition, was not considered in detail but could be investigated under a separate study.

5.1.1 Interpretation of the Experimental Results

The similarity profiles of concentration distributions both in the vertical (z - ξ plane) and the transverse (η - ξ plane) are presented in Figures 4.14 and 4.25. The plots indicate that normalized concentration distributions for a circular wall jet in crossflow are preserved from section to section. This behavior is assumed to hold true under the boundary conditions of zero jet velocity at the wall where some scatter on the dilution data were observed, and the upper boundary of the free mixing region is marked by the jet decay to the ambient flow velocity (U). The dimensionless plots of both the momentum dominated near field and the far field regimes showed no observable distinction because the jet momentum dominates the mixing and hence controls the dilution in the regions. The concentration distributions in the passive plume region were not similar to those of the momentum dominated region.

The wall effect was shown by the scatter of dilution data for all the jet discharges. The generalized distributions in the vertical direction indicated that the boundary layer thickness δ could be derived approximately by the elevation $z = 0.5\ b_Z$. Transverse concentration distributions were approximately symmetrical along the jet axis and could be described by the Gaussian distribution.

The minimum dilution (C_o / C_m) plots along the downstream distance $\alpha\ x / d$ indicated a general trend of increase in tracer dilution shown by the data slope transition from 1/2 to 2/3. The trends imply that the dilution along the axis of the jet are governed by the inter - dependent cross - sections with similar rates, or constant slope. Beyond the momentum dominated region, the stream turbulence influences mixing. The passive plume flow regime is shown by the data with steeper slope than the 2/3 of the momentum dominated far field. This feature was clearly distinct for the weaker jet with the velocity ratio $\alpha = 2$ beyond the downstream distance $\alpha\ x / d = 100$.

The results have shown that dilutions of 50 : 1 were achieved by all the jet discharges within the momentum dominated far field regime. Dilutions in the range of 3 : 1 to 20 : 1 were attained in the momentum dominated near field depending on the strength of the jet discharge. These results indicate that the momentum dominated far field is a very important region in achieving significant dilutions within the initial dilution zone in river discharges.

The dilution data were correlated by a unifying equation which describes the whole region dominated by the jet. The relation (Equation 4.10) is sufficient for practical purposes in estimating tracer dilution in rivers.

The length scale analysis for both the vertical and the transverse directions indicated that the jet grows faster in the momentum dominated near field than in the far field regime. The result is attributed to the dominance of the jet strength in the MDNF; while in the MDFF, the growth behavior is similar to that of a jet in a co - flowing stream. It was also found that the jet growth was about twice in the transverse direction compared to that in the vertical direction.

The transition between the momentum dominated near and the far fields occurred approximately at $x / \alpha d = 1$ for $\alpha = 2$ and 4. The stronger jets with velocity ratios greater than 4 had their transitions at distances ($x / \alpha d$) > 2.

The effect of the freestream flow depth was also considered and found that significant reduction in the tracer dilution occurred for depths less than 10 times the jet nozzle diameter. This result indicates the restriction which occurs in the vertical mixing in shallow rivers.

5.1.2 Comparison with Previous Studies

Dilution of circular wall jet in crossflows has not been studied previously. The present results therefore, are compared with the investigations of Wright (1977) and Hodgson and Rajaratnam (1992) on circular free jets in crossflows.

The results plotted in Figure 4.32 show that the dilution characteristics of the wall jet discharges are fitted well by the results of Wright (1977) for the MDNF and those of Hodgson and Rajaratnam (1992) approximates the MDFF. When each of the jet discharges was considered separately, the dilution of the wall jet in the MDFF were fitted well by a 2 / 3 - slope of the power law equation but with a higher constant coefficient than that given for the Wright's equation.

The transition from the MDNF to the MDFF, based on the trajectory plots of Wright, occurs approximately where $l_m = x$, and therefore reduces $\alpha\ x / d$ to approximately α^2. For α varying between 2 and 12, corresponds to α^2 in the range of 4 to 144. This criteria was only met by the wall jet discharges of $\alpha = 2$ and 4 For α greater than 4, the transition values were greater than the α^2 values. Higher values may have been caused by the smaller resistance of low velocity of the crossflow near the bed.

5.2 Recommendations

The present investigation considered only the dilution characteristics of circular wall jet in crossflow. To complete the study of the jet requires an integration of all the other related hydraulic aspects. Some of the important characteristics recommended for further study include:

I. detailed study of the concentration contours across the section of the jet. The study would identify the differences in the vortex structure of both the wall and free jets in crossflow.

II. measurements of the bed shear as an indicator of the extent of the jet erosion of the river bed.

III. detailed photographic study of the jet growth to compare with the known conditions of the free jet in crossflow.

IV. dilution study of buoyant jet discharges for comparison with the non-buoyant cases.

V. to carry out the dilution study under the prototype river conditions similar to the investigations of Hodgson and Rajaratnam (1992).

VI. to study the turbulence characteristics of the wall jet in crossflow.

References

Abraham, G., " Jet Diffusion in Liquid of Greater Density " ASCE Journal of the Hydraulics Division, Vol.86, June, pp 1-13, 1960.

Abramovich, G. N., 1963, " The Theory of Turbulent Jets ", M.I.T. Press Publication, Cambridge, Massachusetts, 671 p, 1963.

Chan, D. T. L., J. T. Lin and J. F. Kennedy, " Entrainment and Drag Forces on Deflected Jets ", ASCE Journal of the Hydraulics Division, Vol.102, May, pp 615-635, 1976.

Chu, V. H. and M.B. Goldberg, " Buoyant Forced - Plumes in Crossflow ", ASCE Journal of the Hydraulics Division, Vol. 100, September, pp 1203-1213, 1974.

Chu, V. H., " L. N. Fan's Data on Buoyant Jets in Crossflow ", Technical Note. ASCE Journal of the Hydraulics Division, Vol. 105, May, pp 612-617, 1979.

Diebel, M., and N. Rajaratnam, " Diffusion of Circular Wall Jets in Crossflows " (unpublished)., University of Alberta. Edmonton, Alberta., 1980.

Fischer, H. B., E. J. List, R. C. Y. Koh, J. Imberger and N. H. Brooks, " Mixing in Inland and Coastal waters ", Academic Press, San Diego, California, 483 p, 1979.

Gowda, T. P. H., " Critical Point Methods for Mixing Zones in Rivers " ASCE Journal of Environmental Engineering, Vol.110, No. 1, pp 244-262, 1984.

Hodgson, J. E. and N. Rajaratnam, " The Location of Circular Jet Discharges in Crossflows of Finite Depth ", Technical Report WRE 88 - 5, Department of Civil Engineering, University of Alberta, Edmonton, Alberta, 1988.

Hodgson, J. E. and N. Rajaratnam, " The Dilution of Circular Jet Discharges in Crossflows ", Technical Report WRE 88 - 8, Department of Civil Engineering, University of Alberta, Edmonton, Alberta, 1988.

Hodgson, J. E., " Turbulent Jet Discharges in Rivers ", Ph.D. Thesis, Department of Civil Engineering, University of Alberta, Edmonton, Alberta, 1991.

Hodgson, J. E. and N. Rajaratnam, " An Experimental Study of Jet Dilution in Crossflows ", Canadian Journal of Civil Engineering, Vol. 19, No. 5, pp 733-743, 1992.

Kamotani, Y. and I. Greber, " Experiments on a Turbulent Jet in a Crossflow " AIAA Journal, Vol. 10, No. 11, November, pp 1425-1429, 1972.

Keffer, J. F. and W. D. Baines, " The Round Turbulent Jet in a Crosswind ", Journal of Fluid Mechanics, Vol. 15, pp 481-496, 1963.

Kotsovinos, N. E., " Dilution in a Vertical Round Buoyant Jet " ASCE Journal of the Hydraulics Division, Vol.104, May, pp 795-798, 1978.

McCorquodale, J. A., S. P. Zhou, Z. Jhong, A. Moawad, E - M. Yuen and

N. Rajaratnam, " Near Field Modelling in the Connecting Channels of the Great Lakes " The Industrial Research Institute of the University of Windsor, July, 96 p, 1992.

Patrick, M. A., " Experimental Investigations of the Mixing and Penetration of a Round Turbulent Jet Injected Perpendicular into a Transverse Stream " Transactions, Institute of Chemical Engineers, Vol. 45, pp T16-T31, 1967.

Platten, J. L. and J. F. Keffer, " Deflected Turbulent Jet Flows " ASME Journal of Applied Mechanics, pp 756-758, 1971.

Pratte, B. D. and W. D. Baines, " Profiles of Round Turbulent Jet in a Crossflow " ASCE Journal of the Hydraulics Division, Vol.92, November, pp 53-64, 1967.

Rajaratnam, N. and B. S. Pani, " Three - Dimensional Turbulent Wall Jets " ASCE Journal of the Hydraulics Division, Vol.100, January, pp 69-83, 1974.

Rajaratnam, N., " Turbulent Jets " Elsevier Scientific Publishing Company, Amsterdam, 304 p, 1976.

Rajaratnam, N., " Theory of Turbulent Jets " A Chapter in Handbook of Fluids in Motion, N. P. Cheremisinoff and R. Gupta (Editors), Ann Arbor Science, pp 251-278, 1983.

Rajaratnam, N. and T. Gangadhariah, " Circular Jets in Crossflow " Technical Report, Department of Civil engineering, University of Alberta, Edmonton, Alberta., 1980

Rajaratnam, N. and T. Gangadhariah, " Axis of a Circular Jet in Crossflow " Water, Air and Soil Pollution, Vol. 15, pp 317-321, 1981.

Rajaratnam, N. and T. Gangadhariah, " Scales for Circular Jets in Crossflow " Technical Note., ASCE Journal of the Hydraulics Division, Vol.107, April, pp 497-500, 1981.

Rajaratnam, N. and T. Gangadhariah, " Entrainment by Circular Jets in Crossflow " Journal of Wind engineering and Industrial Aerodynamics, Vol. 9, pp 251-255, 1982.

Rajaratnam, N. and T. Gangadhariah, " Vortex Structure of Circular Jets in Crossflow " Journal of Wind engineering and Industrial Aerodynamics, Vol. 12, pp 155-164, 1983.

Ramsey, J. W. and R. J. Goldstein, " Interactions of a Heated Jet with a Deflecting Stream " ASME Journal of Heat Transfer, Vol. 94, pp 365-372, 1971.

Rodi, W., (Editor) " Turbulent Buoyant Jets and Plumes " The Science and Applications of Heat and Mass Transfer, Pergamon Press, pp 1-68, 1982.

Schlichting, H., " Boundary - Layer Theory " McGraw - Hill Book Company, New York, 817 p, 1979.

Sherif, S. A. and R. H. Pletcher, " Measurements of the Flow and Turbulence Characteristics of Round Jets in Crossflow " Journal of Fluids Engineering, Vol. 111, pp 165-171, 1989.

Steffler, P. M., " Deflection of Jets by Weak Crossflows " M.Sc. Thesis, University of Alberta, Edmonton, Alberta., 1980.

Wright, S. J., " Effects of Ambient Crossflows and Density Stratification on the Characteristic Behavior of Round Turbulent Buoyant Jets " Report No. KH - R - 36. W. M. Keck Laboratory of Hydraulics and Water Resources, California Institute of Technology, Pasadena, California., May, 254 p, 1977.

Wright, S. J., " Mean Behavior of Buoyant Jets in a Crossflow " ASCE Journal of the Hydraulics Division, Vol.103, May, pp 499-513, 1977.

Yotsukura, N. and W. Sayre, " Transverse Mixing in Natural Channels " Water Resources Research, Vol. 12, No. 4, pp 695-704, 1976.

APPENDIX I

Photographic Representation of the Circular Wall Jet Diffusion in Crossflow

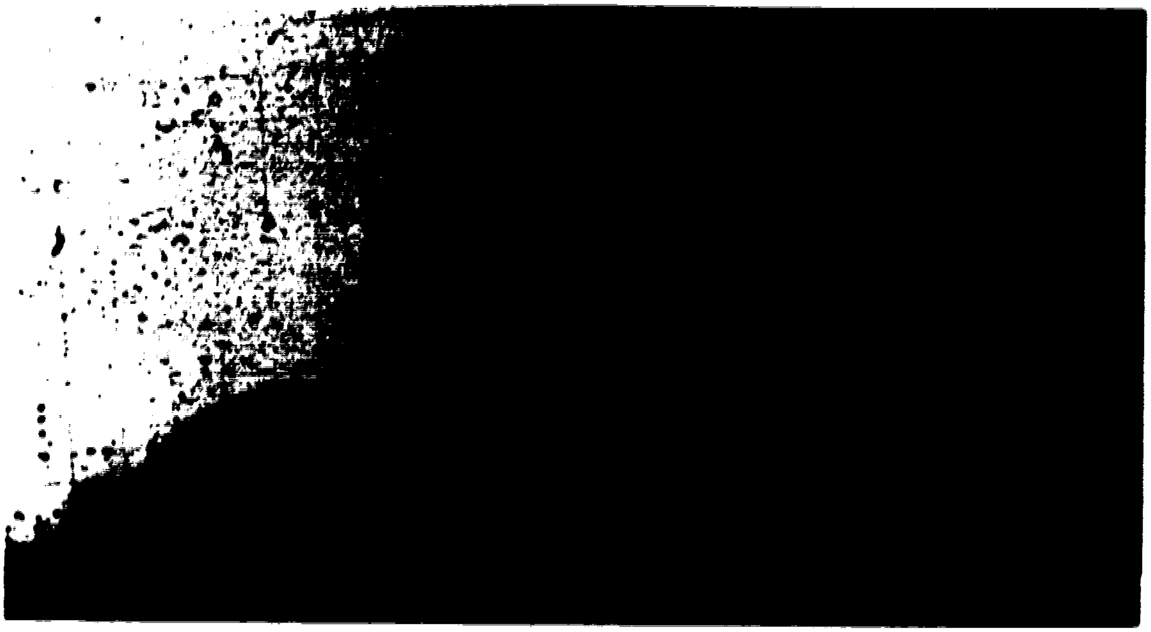

Plate I (a) Experiment No. A100: Velocity Ratio $(U_0/U) = 2$
D = 127 mm, d = 6.35 mm

Plate I (b) Experiment No. A200: Velocity Ratio $(U_0/U) = 4$
D = 127 mm, d = 6.35 mm

Plate I (c) Experiment No. A300: Velocity Ratio $(U_o/U) = 6$
$D = 127$ mm, $d = 6.35$ mm

Plate I (d) Experiment No. B100: Velocity Ratio $(U_o/U) = 6$
$D = 254$ mm, $d = 12.7$ mm

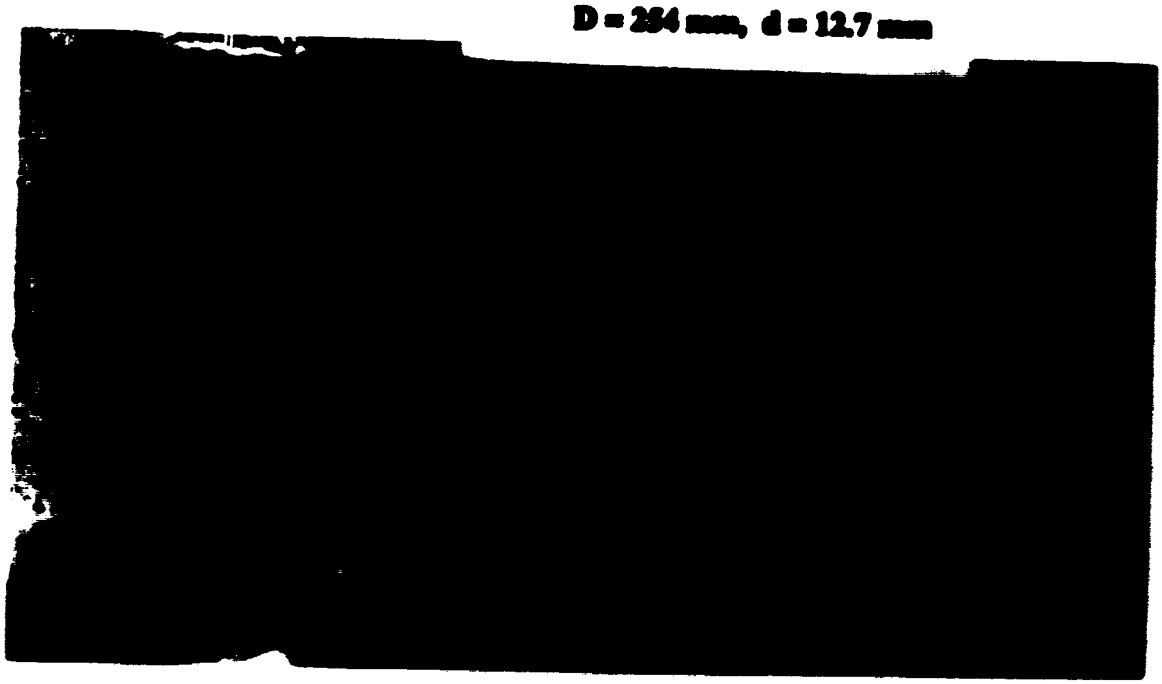

Plate I (e) Experiment No. A400: Velocity Ratio $(U_0/U) = 8$

$D = 127$ mm, $d = 6.35$ mm

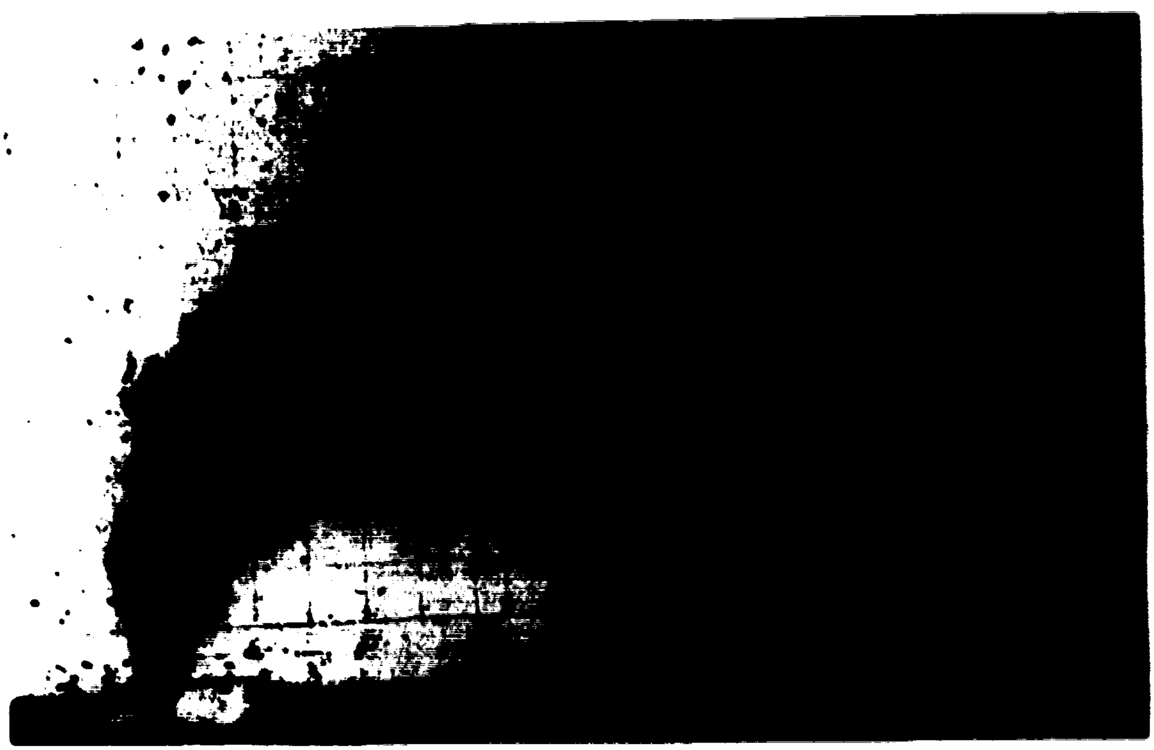

Plate I (f) Experiment No. A500: Velocity Ratio $(U_0/U) = 12$

$D = 127$ mm, $d = 6.35$ mm

APPENDIX II

Experimental Dilution Data

Uo/U = 2 D/d = 20, d = 6.35 mm (Concentration readings have been corrected for the ambient value)

Note: Transverse measurements are referenced from the inner boundary of the deflected jet

Experiment No. A101 x = 7 mm, y = 5 mm Ambient Concentration = 0.062 ppb Jet Nozzle Concentration = 13.9 ppb

z = 1.5 mm		z = 3.5 mm		z = 5.5 mm		z = 7.5 mm		z = 9.5 mm		z = 11.5 mm	
η (mm)	C (ppb)	η (mm)	C (ppb)	η (mm)	C (ppb)	η (mm)	C (ppb)	η (mm)	C (ppb)	η (mm)	C (ppb)
0.0	0.009	0.0	0.009	0.0	0.026	0.0	0.053	0.0	0.053	0.0	0.018
5.0	0.053	5.0	0.026	5.0	0.035	5.0	0.053	5.0	0.026	5.0	0.009
10.0	0.035	10.0	0.044	10.0	0.062	10.0	0.062	10.0	0.044	10.0	0.018
15.0	0.440	15.0	0.106	15.0	0.088	15.0	0.062	15.0	0.026	15.0	0.009
20.0	0.853	20.0	0.299	20.0	0.079	20.0	0.062	20.0	0.018	20.0	0.009
25.0	12.431	25.0	4.383	25.0	1.384	25.0	0.062	25.0	0.009	25.0	0.009
30.0	0.466	30.0	0.035	30.0	0.026	30.0	0.018	30.0	0.018	30.0	0.009
35.0	0.026	35.0	0.018	35.0	0.018	35.0	0.018	35.0	0.009	35.0	0.009
40.0	0.035	40.0	0.026	40.0	0.018	40.0	0.009	40.0	0.000	40.0	0.000
45.0	0.026	45.0	0.018	45.0	0.009	45.0	0.000	45.0	0.000	45.0	0.000

Experiment No. A102: x=15 mm Ambient Con. = 0.062 ppb, Jet Nozzle Con. = 16.363 ppb.

z = 1.5 mm		z = 6.5 mm		z = 9.5 mm		z = 13.5 mm		z = 17.5 mm		z = 21.5 mm		z = 25.5 mm	
η (mm)	C (ppb)	η (mm)	C (ppb)	η (mm)	C (ppb)	η (mm)	C (ppb)	η (mm)	C (ppb)	η (mm)	C (ppb)	η (mm)	C (ppb)
0.0	0.343	0.0	1.384	0.0	2.190	0.0	0.939	0.0	0.097	0.0	0.000	0.0	0.000
5.0	1.217	5.0	3.497	5.0	4.294	5.0	3.210	5.0	0.792	5.0	0.018	5.0	0.000
10.0	2.941	10.0	4.470	10.0	5.921	10.0	4.998	10.0	1.214	10.0	0.035	10.0	0.000
15.0	6.088	15.0	6.537	15.0	6.088	15.0	4.628	15.0	0.924	15.0	0.018	15.0	0.000
20.0	4.498	20.0	2.162	20.0	1.273	20.0	0.578	20.0	0.044	20.0	0.009	20.0	0.000
25.0	1.006	25.0	0.123	25.0	0.035	25.0	0.026	25.0	0.000	25.0	0.000	25.0	0.000
30.0	0.176	30.0	0.026	30.0	0.009	30.0	0.000	30.0	0.000	30.0	0.000	30.0	0.000
35.0	0.053	35.0	0.009	35.0	0.000	35.0	0.000	35.0	0.000	35.0	0.000	35.0	0.000
40.0	0.009	40.0	0.009	40.0	0.000	40.0	0.000	40.0	0.000	40.0	0.000	40.0	0.000
45.0	0.000	45.0	0.000	45.0	0.000	45.0	0.000	45.0	0.000	45.0	0.000	45.0	0.000
50.0	0.000	50.0	0.000	50.0	0.000	50.0	0.000	50.0	0.000	50.0	0.000	50.0	0.000
55.0	0.000	55.0	0.000	55.0	0.000	55.0	0.000	55.0	0.000	55.0	0.000	55.0	0.000
60.0	0.000	60.0	0.000	60.0	0.000	60.0	0.000	60.0	0.000	60.0	0.000	60.0	0.000
65.0	0.000	65.0	0.000	65.0	0.000	65.0	0.000	65.0	0.000	65.0	0.000	65.0	0.000

Velocity Ratio (Uo / U) = 2 D / d = 20, d = 6.35 mm (Concentration readings have been corrected for the ambient value)

Note: Transverse measurements are referenced from the inner boundary of the deflected jet

Experiment No. A103: x =30 mm Ambient Conc. = 0.106 ppb, Jet Nozzle Conc. = 17.236 ppb

z = 1.5 mm η (mm)	C (ppb)	z = 5.5 mm η (mm)	C (ppb)	z = 9.5 mm η (mm)	C (ppb)	z = 13.5 mm η (mm)	C (ppb)	z = 17.5 mm η (mm)	C (ppb)	z = 21.5 mm η (mm)	C (ppb)	z = 25.5 mm η (mm)	C (ppb)
0.0	0.404	0.0	1.340	0.0	2.285	0.0	1.646	0.0	0.545	0.0	0.853	0.0	0.009
5.0	1.034	5.0	2.591	5.0	3.731	5.0	3.425	5.0	1.785	5.0	0.343	5.0	0.018
10.0	1.840	10.0	3.283	10.0	4.064	10.0	4.481	10.0	2.647	10.0	0.572	10.0	0.044
15.0	3.175	15.0	3.314	15.0	4.259	15.0	4.315	15.0	2.535	15.0	0.519	15.0	0.026
20.0	4.926	20.0	4.064	20.0	3.453	20.0	2.647	20.0	0.895	20.0	0.132	20.0	0.009
25.0	3.953	25.0	2.309	25.0	1.062	25.0	0.867	25.0	0.211	25.0	0.026	25.0	0.009
30.0	2.619	30.0	0.867	30.0	0.167	30.0	0.062	30.0	0.009	30.0	0.009	30.0	0.000
35.0	1.062	35.0	0.282	35.0	0.009	35.0	0.009	35.0	0.009	35.0	0.000	35.0	0.000
40.0	0.229	40.0	0.026	40.0	0.009	40.0	0.009	40.0	0.009	40.0	0.000	40.0	0.000
45.0	0.018	45.0	0.009	45.0	0.009	45.0	0.009	45.0	0.009	45.0	0.000	45.0	0.000
50.0	0.009	50.0	0.009	50.0	0.009	50.0	0.009	50.0	0.009	50.0	0.000	50.0	0.000
55.0	0.000	55.0	0.009	55.0	0.000	55.0	0.000	55.0	0.000	55.0	0.000	55.0	0.000
60.0	0.000	60.0	0.009	60.0	0.000	60.0	0.000	60.0	0.000	60.0	0.000	60.0	0.000
65.0	0.000	65.0	0.000	65.0	0.000	65.0	0.000	65.0	0.000	65.0	0.000	65.0	0.000

Experiment No. A104: x =35 mm Ambient Conc. = 0.079 ppb, Jet Nozzle Conc. = 17.792 ppb

z = 1.5 mm η (mm)	C (ppb)	z = 5.5 mm η (mm)	C (ppb)	z = 9.5 mm η (mm)	C (ppb)	z = 13.5 mm η (mm)	C (ppb)	z = 17.5 mm η (mm)	C (ppb)	z = 21.5 mm η (mm)	C (ppb)	z = 25.5 mm η (mm)	C (ppb)
0.0	0.382	0.0	0.457	0.0	0.651	0.0	0.413	0.0	0.132	0.0	0.026	0.0	0.000
5.0	0.425	5.0	1.364	5.0	2.247	5.0	2.853	5.0	1.891	5.0	0.229	5.0	0.026
10.0	1.283	10.0	2.840	10.0	3.665	10.0	3.721	10.0	2.497	10.0	0.809	10.0	0.088
15.0	1.719	15.0	2.775	15.0	3.554	15.0	4.193	15.0	3.081	15.0	1.161	15.0	0.141
20.0	3.118	20.0	3.396	20.0	3.832	20.0	3.832	20.0	2.470	20.0	0.677	20.0	0.070
25.0	4.094	25.0	3.443	25.0	3.304	25.0	2.775	25.0	1.274	25.0	0.299	25.0	0.026
30.0	4.536	30.0	2.173	30.0	0.885	30.0	0.551	30.0	0.211	30.0	0.053	30.0	0.000
35.0	3.853	35.0	1.441	35.0	0.334	35.0	0.062	35.0	0.018	35.0	0.009	35.0	0.000
40.0	1.950	40.0	0.699	40.0	0.062	40.0	0.009	40.0	0.009	40.0	0.009	40.0	0.000
45.0	0.273	45.0	0.070	45.0	0.009	45.0	0.000	45.0	0.000	45.0	0.000	45.0	0.000
50.0	0.044	50.0	0.026	50.0	0.018	50.0	0.000	50.0	0.000	50.0	0.000	50.0	0.000
55.0	0.018	55.0	0.009	55.0	0.000	55.0	0.000	55.0	0.000	55.0	0.000	55.0	0.000
60.0	0.026	60.0	0.018	60.0	0.000	60.0	0.000	60.0	0.000	60.0	0.000	60.0	0.000
65.0	0.000	65.0	0.000	65.0	0.000	65.0	0.000	65.0	0.000	65.0	0.000	65.0	0.000

Velocity Ratio (Uo / U) = 2 D / d = 20, d = 6.35 mm (Concentration readings have been corrected for the ambient value)

Note: Transverse measurements are referenced from the inner boundary of the deflected jet

Experiment No. A105: x = 40 mm Ambient Conc. = 0.062 ppb, Jet Nozzle Conc. = 17.307 ppb

z = 1.5 mm η (mm)	C (ppb)	z = 5.5 mm η (mm)	C (ppb)	z = 10.5 mm η (mm)	C (ppb)	z = 15.5 mm η (mm)	C (ppb)	z = 20.5 mm η (mm)	C (ppb)	z = 21.5 mm η (mm)	C (ppb)	z = 31.5 mm η (mm)	C (ppb)
0.0	0.396	0.0	0.757	0.0	1.245	0.0	0.939	0.0	0.352	0.0	0.044	0.0	0.000
5.0	0.800	5.0	1.081	5.0	2.209	5.0	1.876	5.0	0.836	5.0	0.176	5.0	0.009
10.0	1.273	10.0	2.607	10.0	2.996	10.0	2.913	10.0	1.662	10.0	0.396	10.0	0.018
15.0	1.625	15.0	2.487	15.0	2.904	15.0	2.765	15.0	1.681	15.0	0.545	15.0	0.018
20.0	2.051	20.0	2.440	20.0	2.718	20.0	2.635	20.0	1.273	20.0	0.361	20.0	0.018
25.0	2.765	25.0	2.710	25.0	2.654	25.0	2.098	25.0	1.014	25.0	0.194	25.0	0.009
30.0	3.052	30.0	2.301	30.0	1.523	30.0	0.939	30.0	0.229	30.0	0.070	30.0	0.000
35.0	2.459	35.0	1.598	35.0	1.069	35.0	0.405	35.0	0.114	35.0	0.009	35.0	0.000
40.0	1.801	40.0	0.856	40.0	0.229	40.0	0.044	40.0	0.018	40.0	0.000	40.0	0.000
45.0	0.764	45.0	0.352	45.0	0.123	45.0	0.000	45.0	0.000	45.0	0.000	45.0	0.000
50.0	0.273	50.0	0.079	50.0	0.018	50.0	0.009	50.0	0.000	50.0	0.000	50.0	0.000
55.0	0.018	55.0	0.000	55.0	0.000	55.0	0.000	55.0	0.000	55.0	0.000	55.0	0.000
60.0	0.000	60.0	0.000	60.0	0.000	60.0	0.000	60.0	0.000	60.0	0.000	60.0	0.000
65.0	0.000	65.0	0.000	65.0	0.000	65.0	0.000	65.0	0.000	65.0	0.000	65.0	0.000

Experiment No. A106: x = 130 mm Ambient Conc. = 0.070 ppb, Jet Nozzle Conc. = 17.792 ppb

z = 1.5 mm η (mm)	C (ppb)	z = 6.5 mm η (mm)	C (ppb)	z = 11.5 mm η (mm)	C (ppb)	z = 16.5 mm η (mm)	C (ppb)	z = 21.5 mm η (mm)	C (ppb)	z = 26.5 mm η (mm)	C (ppb)	z = 36.5 mm η (mm)	C (ppb)	z = 46.5 mm η (mm)	C (ppb)
0.0	0.413	0.0	0.519	0.0	0.633	0.0	0.493	0.0	0.282	0.0	0.123	0.0	0.000	0.0	0.000
5.0	0.600	5.0	0.845	5.0	1.029	5.0	0.915	5.0	0.589	5.0	0.282	5.0	0.035	5.0	0.000
10.0	0.900	10.0	1.375	10.0	1.570	10.0	1.339	10.0	0.827	10.0	0.422	10.0	0.035	10.0	0.000
15.0	1.170	15.0	1.500	15.0	1.672	15.0	1.450	15.0	1.073	15.0	0.580	15.0	0.062	15.0	0.000
20.0	1.431	20.0	1.820	20.0	1.764	20.0	1.505	20.0	1.073	20.0	0.493	20.0	0.035	20.0	0.000
25.0	1.306	25.0	1.756	25.0	1.728	25.0	1.450	25.0	1.056	25.0	0.501	25.0	0.035	25.0	0.000
30.0	1.406	30.0	1.737	30.0	1.570	30.0	1.311	30.0	0.871	30.0	0.369	30.0	0.018	30.0	0.000
35.0	1.500	35.0	1.533	35.0	1.366	35.0	1.000	35.0	0.704	35.0	0.273	35.0	0.000	35.0	0.000
40.0	1.700	40.0	1.459	40.0	1.042	40.0	0.699	40.0	0.387	40.0	0.132	40.0	0.009	40.0	0.000
45.0	1.422	45.0	1.144	45.0	0.810	45.0	0.477	45.0	0.211	45.0	0.070	45.0	0.000	45.0	0.000
50.0	1.282	50.0	0.906	50.0	0.501	50.0	0.264	50.0	0.114	50.0	0.026	50.0	0.000	50.0	0.000
55.0	0.644	55.0	0.644	55.0	0.352	55.0	0.185	55.0	0.018	55.0	0.009	55.0	0.000	55.0	0.000
60.0	0.483	60.0	0.378	60.0	0.176	60.0	0.035	60.0	0.018	60.0	0.000	60.0	0.000	60.0	0.000
65.0	0.000	65.0	0.158	65.0	0.062	65.0	0.035	65.0	0.000	65.0	0.000	65.0	0.000	65.0	0.000
70.0	0.044	70.0	0.044	70.0	0.026	70.0	0.000	70.0	0.000	70.0	0.000	70.0	0.000	70.0	0.000
75.0	0.000	75.0	0.009	75.0	0.009	75.0	0.000	75.0	0.000	75.0	0.000	75.0	0.000	75.0	0.000
80.0	0.000	80.0	0.000	80.0	0.000	80.0	0.000	80.0	0.000	80.0	0.000	80.0	0.000	80.0	0.000
85.0	0.000	85.0	0.000	85.0	0.000	85.0	0.000	85.0	0.000	85.0	0.000	85.0	0.000	85.0	0.000

Velocity Ratio (Uo / U) = 2 D / d = 20, d = 6.35 mm (Concentration readings have been corrected for the ambient value)

Note: Transverse measurements are referenced from the inner boundary of the deflected jet

Experiment No. A107: x = 350 mm Ambient Conc. = 0.062 ppb, Jet Nozzle Conc. = 16.68 ppb

z = 1.5 mm η (mm)	C (ppb)	z = 6.5 mm η (mm)	C (ppb)	z = 11.5 mm η (mm)	C (ppb)	z = 16.5 mm η (mm)	C (ppb)	z = 21.5 mm η (mm)	C (ppb)	z = 26.5 mm η (mm)	C (ppb)	z = 31.5 mm η (mm)	C (ppb)	z = 36.5 mm η (mm)	C (ppb)	z = 41.5 mm η (mm)	C (ppb)	z = 46.5 mm η (mm)	C (ppb)
0.0	0.334	0.0	0.255	0.0	0.211	0.0	0.176	0.0	0.141	0.0	0.106	0.0	0.062	0.0	0.044	0.0	0.026	0.0	0.018
10.0	0.457	10.0	0.396	10.0	0.352	10.0	0.299	10.0	0.246	10.0	0.176	10.0	0.088	10.0	0.053	10.0	0.044	10.0	0.018
20.0	0.581	20.0	0.554	20.0	0.475	20.0	0.431	20.0	0.334	20.0	0.229	20.0	0.123	20.0	0.070	20.0	0.053	20.0	0.018
30.0	0.730	30.0	0.721	30.0	0.642	30.0	0.509	30.0	0.449	30.0	0.317	30.0	0.185	30.0	0.114	30.0	0.062	30.0	0.026
40.0	0.845	40.0	0.836	40.0	0.783	40.0	0.704	40.0	0.493	40.0	0.352	40.0	0.176	40.0	0.106	40.0	0.062	40.0	0.026
50.0	0.862	50.0	0.862	50.0	0.774	50.0	0.651	50.0	0.484	50.0	0.308	50.0	0.202	50.0	0.097	50.0	0.053	50.0	0.018
60.0	0.801	60.0	0.721	60.0	0.633	60.0	0.440	60.0	0.326	60.0	0.211	60.0	0.132	60.0	0.062	60.0	0.035	60.0	0.009
70.0	0.686	70.0	0.484	70.0	0.413	70.0	0.413	70.0	0.185	70.0	0.097	70.0	0.070	70.0	0.026	70.0	0.009	70.0	0.000
80.0	0.361	80.0	0.290	80.0	0.246	80.0	0.123	80.0	0.088	80.0	0.053	80.0	0.044	80.0	0.018	80.0	0.000	80.0	0.000
90.0	0.158	90.0	0.132	90.0	0.114	90.0	0.053	90.0	0.035	90.0	0.026	90.0	0.009	90.0	0.009	90.0	0.000	90.0	0.000
100.0	0.088	100.0	0.053	100.0	0.035	100.0	0.018	100.0	0.009	100.0	0.009	100.0	0.000	100.0	0.000	100.0	0.000	100.0	0.000
120.0	0.000	120.0	0.009	120.0	0.000	120.0	0.000	120.0	0.000	120.0	0.000	120.0	0.000	120.0	0.000	120.0	0.000	120.0	0.000

Experiment No. A108: x = 500 mm Ambient Conc. = 0.062 ppb, Jet Nozzle Conc. = 15.568 ppb

z = 1.5 mm η (mm)	C (ppb)	z = 6.5 mm η (mm)	C (ppb)	z = 11.5 mm η (mm)	C (ppb)	z = 16.5 mm η (mm)	C (ppb)	z = 21.5 mm η (mm)	C (ppb)	z = 26.5 mm η (mm)	C (ppb)	z = 31.5 mm η (mm)	C (ppb)	z = 36.5 mm η (mm)	C (ppb)	z = 46.5 mm η (mm)	C (ppb)	z = 66.5 mm η (mm)	C (ppb)
0.0	0.246	0.0	0.211	0.0	0.211	0.0	0.167	0.0	0.123	0.0	0.106	0.0	0.070	0.0	0.053	0.0	0.026	0.0	0.000
10.0	0.308	10.0	0.255	10.0	0.264	10.0	0.220	10.0	0.176	10.0	0.158	10.0	0.106	10.0	0.079	10.0	0.044	10.0	0.000
20.0	0.352	20.0	0.334	20.0	0.334	20.0	0.290	20.0	0.246	20.0	0.211	20.0	0.158	20.0	0.106	20.0	0.053	20.0	0.000
30.0	0.422	30.0	0.413	30.0	0.422	30.0	0.387	30.0	0.352	30.0	0.308	30.0	0.220	30.0	0.167	30.0	0.070	30.0	0.000
40.0	0.493	40.0	0.493	40.0	0.493	40.0	0.440	40.0	0.422	40.0	0.361	40.0	0.273	40.0	0.194	40.0	0.088	40.0	0.000
50.0	0.545	50.0	0.554	50.0	0.545	50.0	0.519	50.0	0.475	50.0	0.396	50.0	0.282	50.0	0.211	50.0	0.097	50.0	0.000
60.0	0.581	60.0	0.572	60.0	0.528	60.0	0.493	60.0	0.413	60.0	0.352	60.0	0.255	60.0	0.167	60.0	0.070	60.0	0.000
70.0	0.537	70.0	0.484	70.0	0.440	70.0	0.485	70.0	0.308	70.0	0.273	70.0	0.202	70.0	0.106	70.0	0.035	70.0	0.000
80.0	0.466	80.0	0.369	80.0	0.343	80.0	0.290	80.0	0.238	80.0	0.185	80.0	0.132	80.0	0.070	80.0	0.026	80.0	0.000
90.0	0.299	90.0	0.220	90.0	0.220	90.0	0.167	90.0	0.132	90.0	0.106	90.0	0.062	90.0	0.035	90.0	0.009	90.0	0.000
100.0	0.158	100.0	0.132	100.0	0.132	100.0	0.097	100.0	0.062	100.0	0.053	100.0	0.035	100.0	0.009	100.0	0.000	100.0	0.000
120.0	0.035	120.0	0.026	120.0	0.026	120.0	0.018	120.0	0.009	120.0	0.009	120.0	0.000	120.0	0.000	120.0	0.000	120.0	0.000

Velocity Ratio (Uo / U) = 2 D / d = 20, d = 6.35 mm (Concentration readings have been corrected for the ambient value)

Note: Transverse measurements are referenced from the inner boundary of the deflected jet

Experiment No. A109: x = 1000 mm Ambient Conc. = 0.070 ppb, Jet Nozzle Conc. = 16.08 ppb

z = 1.5 mm		z = 6.5 mm		z = 11.5 mm		z = 16.5 mm		z = 21.5 mm		z = 26.5 mm		z = 31.5 mm		z = 36.5 mm		z = 46.5 mm		z = 66.5 mm	
η (mm)	C (ppb)	η (mm)	C (ppb)	η (mm)	C (ppb)	η (mm)	C (ppb)	η (mm)	C (ppb)	η (mm)	C (ppb)	η (mm)	C (ppb)	η (mm)	C (ppb)	η (mm)	C (ppb)	η (mm)	C (ppb)
0.0	0.202	0.0	0.202	0.0	0.185	0.0	0.158	0.0	0.158	0.0	0.158	0.0	0.141	0.0	0.114	0.0	0.097	0.0	0.044
10.0	0.220	10.0	0.220	10.0	0.211	10.0	0.194	10.0	0.176	10.0	0.176	10.0	0.167	10.0	0.141	10.0	0.114	10.0	0.044
20.0	0.238	20.0	0.238	20.0	0.229	20.0	0.211	20.0	0.194	20.0	0.202	20.0	0.185	20.0	0.158	20.0	0.132	20.0	0.053
30.0	0.273	30.0	0.264	30.0	0.255	30.0	0.238	30.0	0.229	30.0	0.229	30.0	0.211	30.0	0.167	30.0	0.141	30.0	0.053
40.0	0.308	40.0	0.290	40.0	0.282	40.0	0.273	40.0	0.246	40.0	0.238	40.0	0.211	40.0	0.176	40.0	0.158	40.0	0.053
50.0	0.317	50.0	0.299	50.0	0.290	50.0	0.290	50.0	0.255	50.0	0.238	50.0	0.211	50.0	0.158	50.0	0.132	50.0	0.053
60.0	0.317	60.0	0.290	60.0	0.290	60.0	0.282	60.0	0.246	60.0	0.220	60.0	0.194	60.0	0.141	60.0	0.106	60.0	0.044
70.0	0.290	70.0	0.255	70.0	0.255	70.0	0.255	70.0	0.220	70.0	0.194	70.0	0.167	70.0	0.123	70.0	0.088	70.0	0.035
80.0	0.255	80.0	0.238	80.0	0.238	80.0	0.202	80.0	0.185	80.0	0.158	80.0	0.123	80.0	0.106	80.0	0.062	80.0	0.026
90.0	0.202	90.0	0.202	90.0	0.185	90.0	0.150	90.0	0.132	90.0	0.106	90.0	0.088	90.0	0.079	90.0	0.044	90.0	0.018
100.0	0.141	100.0	0.150	100.0	0.132	100.0	0.106	100.0	0.097	100.0	0.070	100.0	0.062	100.0	0.053	100.0	0.026	100.0	0.009
120.0	0.062	120.0	0.070	120.0	0.053	120.0	0.053	120.0	0.044	120.0	0.035	120.0	0.035	120.0	0.026	120.0	0.009	120.0	0.000

Experiment No. A110: x = 1500 mm Ambient Conc. = 0.053 ppb, Jet Nozzle Conc. = 18.348 ppb

z = 1.5 mm		z = 6.5 mm		z = 11.5 mm		z = 16.5 mm		z = 21.5 mm		z = 26.5 mm		z = 31.5 mm		z = 36.5 mm		z = 46.5 mm		z = 66.5 mm	
η (mm)	C (ppb)	η (mm)	C (ppb)	η (mm)	C (ppb)	η (mm)	C (ppb)	η (mm)	C (ppb)	η (mm)	C (ppb)	η (mm)	C (ppb)	η (mm)	C (ppb)	η (mm)	C (ppb)	η (mm)	C (ppb)
0.0	0.141	0.0	0.123	0.0	0.141	0.0	0.123	0.0	0.114	0.0	0.114	0.0	0.097	0.0	0.097	0.0	0.079	0.0	0.053
10.0	0.150	10.0	0.132	10.0	0.150	10.0	0.132	10.0	0.123	10.0	0.123	10.0	0.106	10.0	0.097	10.0	0.088	10.0	0.053
20.0	0.158	20.0	0.141	20.0	0.158	20.0	0.141	20.0	0.132	20.0	0.132	20.0	0.114	20.0	0.106	20.0	0.097	20.0	0.062
30.0	0.176	30.0	0.167	30.0	0.167	30.0	0.167	30.0	0.141	30.0	0.141	30.0	0.132	30.0	0.114	30.0	0.106	30.0	0.062
40.0	0.194	40.0	0.176	40.0	0.185	40.0	0.176	40.0	0.150	40.0	0.158	40.0	0.141	40.0	0.132	40.0	0.114	40.0	0.062
50.0	0.202	50.0	0.194	50.0	0.194	50.0	0.185	50.0	0.158	50.0	0.167	50.0	0.158	50.0	0.150	50.0	0.114	50.0	0.062
60.0	0.211	60.0	0.202	60.0	0.202	60.0	0.194	60.0	0.167	60.0	0.176	60.0	0.158	60.0	0.158	60.0	0.114	60.0	0.062
70.0	0.220	70.0	0.202	70.0	0.202	70.0	0.194	70.0	0.167	70.0	0.185	70.0	0.158	70.0	0.158	70.0	0.114	70.0	0.062
80.0	0.211	80.0	0.202	80.0	0.202	80.0	0.194	80.0	0.167	80.0	0.167	80.0	0.158	80.0	0.141	80.0	0.097	80.0	0.062
90.0	0.211	90.0	0.194	90.0	0.194	90.0	0.185	90.0	0.158	90.0	0.150	90.0	0.150	90.0	0.132	90.0	0.088	90.0	0.053
100.0	0.194	100.0	0.185	100.0	0.167	100.0	0.150	100.0	0.150	100.0	0.141	100.0	0.123	100.0	0.114	100.0	0.079	100.0	0.044
120.0	0.123	120.0	0.141	120.0	0.123	120.0	0.114	120.0	0.123	120.0	0.097	120.0	0.097	120.0	0.079	120.0	0.053	120.0	0.018

Velocity Ratio (Uo / U) = 4 D / d = 20, d = 6.35 mm (Concentration readings have been corrected for the ambient value)

Note: Transverse measurements are referenced from the inner boundary of the deflected jet

Experiment No. A201: x = 5 mm, y = 20 mm, Ambient Conc. = 0.114 ppb, Jet Nozzle Conc. = 16.124 ppb

z = 1.5 mm η (mm)	C (ppb)	z = 6.5 mm η (mm)	C (ppb)	z = 11.5 mm η (mm)	C (ppb)	z = 16.5 mm η (mm)	C (ppb)	z = 21.5 mm η (mm)	C (ppb)	z = 26.5 mm η (mm)	C (ppb)
0.0	0.000	0.0	0.000	0.0	0.000	0.0	0.000	0.0	0.000	0.0	0.000
5.0	0.000	5.0	0.000	5.0	0.000	5.0	0.000	5.0	0.000	5.0	0.000
10.0	0.000	10.0	0.000	10.0	0.044	10.0	0.009	10.0	0.000	10.0	0.000
15.0	0.000	15.0	0.000	15.0	0.053	15.0	0.053	15.0	0.000	15.0	0.000
20.0	0.035	20.0	0.554	20.0	1.083	20.0	0.282	20.0	0.053	20.0	0.000
25.0	0.097	25.0	1.314	25.0	1.369	25.0	0.801	25.0	0.097	25.0	0.000
30.0	0.704	30.0	2.916	30.0	3.166	30.0	1.545	30.0	0.211	30.0	0.000
35.0	1.056	35.0	3.640	35.0	4.707	35.0	2.288	35.0	0.097	35.0	0.000
40.0	7.363	40.0	11.498	40.0	8.507	40.0	0.334	40.0	0.000	40.0	0.000
45.0	3.519	45.0	3.121	45.0	0.290	45.0	0.000	45.0	0.000	45.0	0.000
50.0	0.000	50.0	0.000	50.0	0.000	50.0	0.000	50.0	0.000	50.0	0.000
55.0	0.000	55.0	0.000	55.0	0.000	55.0	0.000	55.0	0.000	55.0	0.000
60.0	0.000	60.0	0.000	60.0	0.000	60.0	0.000	60.0	0.000	60.0	0.000

Experiment No. A202: x = 20 mm, y = 40 mm, Ambient Conc. = 0.114 ppb, Jet Nozzle Conc. = 16.124 ppb

z = 1.5 mm η (mm)	C (ppb)	z = 6.5 mm η (mm)	C (ppb)	z = 11.5 mm η (mm)	C (ppb)	z = 16.5 mm η (mm)	C (ppb)	z = 21.5 mm η (mm)	C (ppb)	z = 26.5 mm η (mm)	C (ppb)	z = 31.5 mm η (mm)	C (ppb)	z = 36.5 mm η (mm)	C (ppb)
0.0	0.000	0.0	0.000	0.0	0.009	0.0	0.000	0.0	0.000	0.0	0.000	0.0	0.000	0.0	0.000
5.0	0.000	5.0	0.000	5.0	0.000	5.0	0.026	5.0	0.000	5.0	0.000	5.0	0.000	5.0	0.000
10.0	0.000	10.0	0.000	10.0	0.035	10.0	0.085	10.0	0.000	10.0	0.000	10.0	0.000	10.0	0.000
15.0	0.000	15.0	0.370	15.0	1.188	15.0	1.021	15.0	0.299	15.0	0.035	15.0	0.000	15.0	0.000
20.0	0.079	20.0	1.240	20.0	2.246	20.0	1.745	20.0	0.986	20.0	0.167	20.0	0.018	20.0	0.000
25.0	0.317	25.0	2.840	25.0	3.554	25.0	3.415	25.0	2.442	25.0	0.695	25.0	0.035	25.0	0.000
30.0	0.238	30.0	2.691	30.0	3.552	30.0	3.636	30.0	3.099	30.0	1.240	30.0	0.097	30.0	0.000
35.0	1.309	35.0	1.922	35.0	3.387	35.0	4.360	35.0	3.884	35.0	1.434	35.0	0.079	35.0	0.000
40.0	1.029	40.0	3.525	40.0	4.776	40.0	4.942	40.0	3.377	40.0	0.572	40.0	0.018	40.0	0.000
45.0	1.223	45.0	2.951	45.0	3.748	45.0	2.748	45.0	0.996	45.0	0.053	45.0	0.009	45.0	0.000
50.0	0.625	50.0	1.304	50.0	2.023	50.0	1.662	50.0	0.361	50.0	0.018	50.0	0.000	50.0	0.000
55.0	0.009	55.0	0.000	55.0	0.000	55.0	0.000	55.0	0.000	55.0	0.000	55.0	0.000	55.0	0.000
60.0	0.000	60.0	0.000	60.0	0.000	60.0	0.000	60.0	0.000	60.0	0.000	60.0	0.000	60.0	0.000
65.0	0.000	65.0	0.000	65.0	0.000	65.0	0.000	65.0	0.000	65.0	0.000	65.0	0.000	65.0	0.000
70.0	0.000	70.0	0.000	70.0	0.000	70.0	0.000	70.0	0.000	70.0	0.000	70.0	0.000	70.0	0.000

Velocity Ratio (U0 / U) = 4 D / d = 28, d = 6.35 mm (Concentration readings have been corrected for the ambient value)

Note: Transverse measurements are referenced from the inner boundary of the deflected jet

Experiment No. A2[illegible]: x = 50 mm, y = 54 mm, Ambient Conc. = 0.167 ppb, Jet Nozzle Conc. = 13.9 ppb

z = 1.5 mm η (mm)	C (ppb)	z = 4.5 mm η (mm)	C (ppb)	z = 11.5 mm η (mm)	C (ppb)	z = 16.5 mm η (mm)	C (ppb)	z = 21.5 mm η (mm)	C (ppb)	z = 26.5 mm η (mm)	C (ppb)	z = 31.5 mm η (mm)	C (ppb)	z = 36.5 mm η (mm)	C (ppb)	z = 41.5 mm η (mm)	C (ppb)
0.0	[illegible]	0.0	[illegible]	0.0	[illegible]	0.0	[illegible]	0.0	[illegible]	0.0	[illegible]	0.0	[illegible]	0.0	[illegible]	0.0	[illegible]
3.0	0.000	3.0	0.000	3.0	0.000	3.0	0.000	3.0	0.000	3.0	0.026	3.0	0.000	3.0	0.000	3.0	0.000
6.0	0.000	6.0	0.035	6.0	0.053	6.0	0.053	6.0	0.070	6.0	0.018	6.0	0.000	6.0	0.009	6.0	0.000
10.0	0.000	10.0	0.079	10.0	0.150	10.0	0.141	10.0	0.185	10.0	0.018	10.0	0.000	10.0	0.009	10.0	0.000
13.0	0.035	13.0	0.202	13.0	0.361	13.0	0.413	13.0	0.273	13.0	0.044	13.0	0.079	13.0	0.009	13.0	0.000
16.0	0.000	16.0	0.589	16.0	0.853	16.0	0.853	16.0	0.801	16.0	0.343	16.0	0.114	16.0	0.018	16.0	0.000
20.0	0.114	20.0	1.144	20.0	1.501	20.0	1.473	20.0	1.556	20.0	0.730	20.0	0.167	20.0	0.026	20.0	0.000
23.0	0.202	23.0	1.240	23.0	1.741	23.0	1.605	23.0	1.435	23.0	1.129	23.0	0.361	23.0	0.026	23.0	0.000
26.0	0.238	26.0	1.390	26.0	1.666	26.0	1.750	26.0	1.611	26.0	1.284	26.0	0.501	26.0	0.070	26.0	0.000
30.0	0.308	30.0	1.640	30.0	1.890	30.0	1.834	30.0	1.862	30.0	1.473	30.0	0.677	30.0	0.132	30.0	0.000
33.0	0.405	33.0	1.380	33.0	1.741	33.0	1.796	33.0	1.796	33.0	1.491	33.0	0.651	33.0	0.097	33.0	0.000
36.0	0.607	36.0	1.284	36.0	1.611	36.0	1.777	36.0	1.805	36.0	1.540	36.0	0.609	36.0	0.106	36.0	0.000
40.0	0.933	40.0	1.240	40.0	1.473	40.0	1.779	40.0	1.807	40.0	1.612	40.0	0.695	40.0	0.123	40.0	0.000
43.0	1.021	43.0	1.221	43.0	1.546	43.0	1.935	43.0	1.935	43.0	1.657	43.0	0.581	43.0	0.079	43.0	0.000
46.0	0.977	46.0	1.416	46.0	1.777	46.0	2.111	46.0	2.083	46.0	1.504	46.0	0.545	46.0	0.070	46.0	0.000
50.0	0.977	50.0	1.605	50.0	2.112	50.0	2.307	50.0	2.279	50.0	1.306	50.0	0.501	50.0	0.053	50.0	0.000
53.0	0.994	53.0	1.555	53.0	2.102	53.0	2.241	53.0	1.685	53.0	1.129	53.0	0.255	53.0	0.026	53.0	0.000
56.0	0.805	56.0	1.214	56.0	1.611	56.0	1.638	56.0	1.385	56.0	0.704	56.0	0.150	56.0	0.018	56.0	0.000
60.0	0.273	60.0	0.774	60.0	0.905	60.0	0.880	60.0	0.757	60.0	0.114	60.0	0.018	60.0	0.000	60.0	0.000
63.0	0.238	63.0	0.431	63.0	0.704	63.0	0.404	63.0	0.158	63.0	0.053	63.0	0.000	63.0	0.000	63.0	0.000
66.0	0.167	66.0	0.211	66.0	0.449	66.0	0.246	66.0	0.000	66.0	0.000	66.0	0.000	66.0	0.000	66.0	0.000

Experiment No. A2[illegible]: x = 75 mm, y = 60 mm, Ambient Conc. = 0.220 ppb, Jet Nozzle Conc. = 12.404 ppb

z = 1.5 mm η (mm)	C (ppb)	z = 4.5 mm η (mm)	C (ppb)	z = 11.5 mm η (mm)	C (ppb)	z = 16.5 mm η (mm)	C (ppb)	z = 21.5 mm η (mm)	C (ppb)	z = 26.5 mm η (mm)	C (ppb)	z = 31.5 mm η (mm)	C (ppb)	z = 36.5 mm η (mm)	C (ppb)
0.0	[illegible]	0.0	[illegible]	0.0	[illegible]	0.0	[illegible]	0.0	[illegible]	0.0	[illegible]	0.0	[illegible]	0.0	[illegible]
5.0	0.000	5.0	0.053	5.0	0.141	5.0	0.273	5.0	0.229	5.0	0.088	5.0	0.044	5.0	0.018
10.0	0.035	10.0	0.202	10.0	0.537	10.0	0.677	10.0	0.625	10.0	0.413	10.0	0.202	10.0	0.018
15.0	0.062	15.0	0.405	15.0	0.968	15.0	1.126	15.0	1.082	15.0	0.880	15.0	0.475	15.0	0.185
20.0	0.106	20.0	0.580	20.0	1.126	20.0	1.295	20.0	1.267	20.0	1.108	20.0	0.801	20.0	0.387
25.0	0.158	25.0	0.721	25.0	1.232	25.0	1.299	25.0	1.302	25.0	1.232	25.0	1.029	25.0	0.598
30.0	0.220	30.0	0.686	30.0	1.179	30.0	1.311	30.0	1.320	30.0	1.276	30.0	1.117	30.0	0.730
35.0	0.361	35.0	0.581	35.0	0.985	35.0	1.117	35.0	1.214	35.0	1.249	35.0	1.179	35.0	0.757
40.0	0.655	40.0	0.695	40.0	0.924	40.0	1.082	40.0	1.276	40.0	1.276	40.0	1.064	40.0	0.607
45.0	0.757	45.0	0.845	45.0	1.058	45.0	1.204	45.0	1.328	45.0	1.267	45.0	0.968	45.0	0.493
50.0	0.685	50.0	0.941	50.0	1.188	50.0	1.298	50.0	1.302	50.0	1.091	50.0	0.730	50.0	0.290
55.0	0.581	55.0	0.774	55.0	1.021	55.0	1.085	55.0	0.950	55.0	0.845	55.0	0.466	55.0	0.141
60.0	0.413	60.0	0.598	60.0	0.730	60.0	0.792	60.0	0.642	60.0	0.396	60.0	0.202	60.0	0.053
65.0	0.220	65.0	0.255	65.0	0.343	65.0	0.238	65.0	0.220	65.0	0.202	65.0	0.062	65.0	0.026

Velocity Ratio (Uo / U) = 4 D / d = 20, d = 6.35 mm (Concentration readings have been corrected for the ambient value)

Note: Transverse measurements are referenced from the inner boundary of the deflected jet

Experiment No. A305: x = 100 mm, y = 64 mm, Ambient Conc. = 0.167 ppb, Jet Nozzle Conc. = 13.636 ppb

z = 1.5 mm		z = 6.5 mm		z = 11.5 mm		z = 16.5 mm		z = 21.5 mm		z = 26.5 mm		z = 31.5 mm		z = 36.5 mm		z = 41.5 mm		z = 46.5 mm	
η (mm)	C (ppb)	η (mm)	C (ppb)	η (mm)	C (ppb)	η (mm)	C (ppb)	η (mm)	C (ppb)	η (mm)	C (ppb)	η (mm)	C (ppb)	η (mm)	C (ppb)	η (mm)	C (ppb)	η (mm)	C (ppb)
0.0	0.000	0.0	0.097	0.0	0.176	0.0	0.246	0.0	0.255	0.0	0.158	0.0	0.088	0.0	0.018	0.0	0.009	5.0	0.000
5.0	0.079	5.0	0.290	5.0	0.616	5.0	0.765	5.0	0.686	5.0	0.545	5.0	0.299	5.0	0.132	5.0	0.035	15.0	0.026
10.0	0.114	10.0	0.554	10.0	0.862	10.0	1.012	10.0	0.977	10.0	0.774	10.0	0.484	10.0	0.220	10.0	0.062	25.0	0.088
15.0	0.246	15.0	0.836	15.0	1.188	15.0	1.276	15.0	1.179	15.0	1.064	15.0	0.774	15.0	0.475	15.0	0.185	35.0	0.106
20.0	0.185	20.0	0.871	20.0	1.240	20.0	1.324	20.0	1.296	20.0	1.188	20.0	0.977	20.0	0.642	20.0	0.282	45.0	0.035
25.0	0.255	25.0	0.897	25.0	1.223	25.0	1.284	25.0	1.249	25.0	1.205	25.0	1.064	25.0	0.757	25.0	0.378	55.0	0.009
30.0	0.238	30.0	0.757	30.0	1.185	30.0	1.268	30.0	1.213	30.0	1.179	30.0	1.091	30.0	0.836	30.0	0.422	65.0	0.009
35.0	0.449	35.0	0.616	35.0	0.853	35.0	0.968	35.0	1.056	35.0	1.117	35.0	1.056	35.0	0.757	35.0	0.396		
40.0	0.537	40.0	0.633	40.0	0.818	40.0	0.962	40.0	1.074	40.0	1.108	40.0	0.985	40.0	0.704	40.0	0.317		
45.0	0.572	45.0	0.704	45.0	0.836	45.0	1.083	45.0	1.047	45.0	1.021	45.0	0.818	45.0	0.475	45.0	0.194		
50.0	0.545	50.0	0.686	50.0	0.853	50.0	0.962	50.0	0.990	50.0	0.968	50.0	0.730	50.0	0.457	50.0	0.167		
55.0	0.326	55.0	0.537	55.0	0.686	55.0	0.765	55.0	0.792	55.0	0.669	55.0	0.475	55.0	0.229	55.0	0.079		
60.0	0.282	60.0	0.352	60.0	0.554	60.0	0.573	60.0	0.518	60.0	0.413	60.0	0.238	60.0	0.106	60.0	0.026		
65.0	0.106	65.0	0.167	65.0	0.229	65.0	0.194	65.0	0.211	65.0	0.132	65.0	0.088	65.0	0.018	65.0	0.000		

Experiment No. A306: x = 143 mm, y = 70 mm, Ambient Conc. = 0.264 ppb, Jet Nozzle Conc. = 16.68 ppb

z = 1.5 mm		z = 6.5 mm		z = 11.5 mm		z = 16.5 mm		z = 21.5 mm		z = 26.5 mm		z = 31.5 mm		z = 36.5 mm	
η (mm)	C (ppb)	η (mm)	C (ppb)	η (mm)	C (ppb)	η (mm)	C (ppb)	η (mm)	C (ppb)	η (mm)	C (ppb)	η (mm)	C (ppb)	η (mm)	C (ppb)
0.0	0.035	0.0	0.141	0.0	0.273	0.0	0.387	0.0	0.387	0.0	0.378	0.0	0.282	0.0	0.132
5.0	0.097	5.0	0.290	5.0	0.581	5.0	0.730	5.0	0.748	5.0	0.625	5.0	0.475	5.0	0.317
10.0	0.150	10.0	0.493	10.0	0.827	10.0	0.994	10.0	1.021	10.0	0.950	10.0	0.677	10.0	0.493
15.0	0.220	15.0	0.651	15.0	1.029	15.0	1.152	15.0	1.152	15.0	1.082	15.0	0.924	15.0	0.721
20.0	0.229	20.0	0.686	20.0	1.073	20.0	1.223	20.0	1.249	20.0	1.214	20.0	1.021	20.0	0.845
25.0	0.273	25.0	0.704	25.0	1.073	25.0	1.223	25.0	1.223	25.0	1.188	25.0	1.100	25.0	0.915
30.0	0.308	30.0	0.704	30.0	1.038	30.0	1.188	30.0	1.223	30.0	1.179	30.0	1.091	30.0	0.941
35.0	0.413	35.0	0.633	35.0	0.915	35.0	1.064	35.0	1.082	35.0	1.100	35.0	1.073	35.0	0.915
40.0	0.528	40.0	0.686	40.0	0.897	40.0	1.083	40.0	1.056	40.0	1.073	40.0	1.083	40.0	0.836
45.0	0.677	45.0	0.739	45.0	0.818	45.0	0.959	45.0	1.012	45.0	1.056	45.0	0.941	45.0	0.704
50.0	0.695	50.0	0.792	50.0	0.880	50.0	0.950	50.0	0.985	50.0	0.941	50.0	0.774	50.0	0.589
55.0	0.633	55.0	0.739	55.0	0.818	55.0	0.880	55.0	0.871	55.0	0.827	55.0	0.616	55.0	0.378
60.0	0.528	60.0	0.633	60.0	0.739	60.0	0.774	60.0	0.721	60.0	0.616	60.0	0.422	60.0	0.264
65.0	0.361	65.0	0.457	65.0	0.581	65.0	0.545	65.0	0.484	65.0	0.413	65.0	0.264	65.0	0.123

Velocity Ratio (U_0/U) = 4 b/d = 28, d = 6.35 mm (Concentration readings have been corrected for the ambient value)

Note: Transverse measurements are referenced from the inner boundary of the deflected jet

Experiment No. A[illegible]: x = [illegible] mm, y = [illegible] mm, Ambient Conc. = [illegible] ppb, Jet Nozzle Conc. = 13.835 ppb

z = 1.5 mm η (mm)	C (ppb)	z = 6.5 mm η (mm)	C (ppb)	z = 11.5 mm η (mm)	C (ppb)	z = 16.5 mm η (mm)	C (ppb)	z = 21.5 mm η (mm)	C (ppb)	z = 26.5 mm η (mm)	C (ppb)	z = 31.5 mm η (mm)	C (ppb)	z = 36.5 mm η (mm)	C (ppb)	z = 41.5 mm η (mm)	C (ppb)	z = 46.5 mm η (mm)	C (ppb)	z = 51.5 mm η (mm)	C (ppb)	z = 56.5 mm η (mm)	C (ppb)
0.0	[illegible]	0.0	[illegible]	0.0	[illegible]	0.0	[illegible]	0.0	[illegible]	0.0	[illegible]	0.0	[illegible]	0.0	0.079	0.0	0.053	0.0	[illegible]	0.0	[illegible]	0.0	[illegible]
5.0	0.079	5.0	0.114	5.0	0.158	5.0	0.194	5.0	0.194	5.0	0.282	5.0	0.167	5.0	0.141	5.0	0.114	5.0	0.053	5.0	0.026	5.0	0.018
10.0	0.150	10.0	0.176	10.0	0.238	10.0	0.273	10.0	0.299	10.0	0.282	10.0	0.255	10.0	0.220	10.0	0.158	10.0	0.097	10.0	0.053	10.0	0.026
15.0	0.167	15.0	0.273	15.0	0.361	15.0	0.413	15.0	0.449	15.0	0.422	15.0	0.343	15.0	0.308	15.0	0.238	15.0	0.167	15.0	0.088	15.0	0.044
20.0	0.264	20.0	0.352	20.0	0.466	20.0	0.537	20.0	0.563	20.0	0.537	20.0	0.484	20.0	0.413	20.0	0.317	20.0	0.229	20.0	0.141	20.0	0.079
25.0	0.290	25.0	0.449	25.0	0.590	25.0	0.660	25.0	0.677	25.0	0.625	25.0	0.554	25.0	0.484	25.0	0.387	25.0	0.282	25.0	0.185	25.0	0.114
30.0	0.317	30.0	0.475	30.0	0.625	30.0	0.713	30.0	0.739	30.0	0.713	30.0	0.669	30.0	0.572	30.0	0.475	30.0	0.308	30.0	0.229	30.0	0.150
35.0	0.352	35.0	0.545	35.0	0.695	35.0	0.800	35.0	0.801	35.0	0.748	35.0	0.677	35.0	0.646	35.0	0.519	35.0	0.387	35.0	0.282	35.0	0.176
40.0	0.387	40.0	0.572	40.0	0.739	40.0	0.818	40.0	0.862	40.0	0.809	40.0	0.757	40.0	0.651	40.0	0.554	40.0	0.440	40.0	0.326	40.0	0.202
45.0	0.378	45.0	0.616	45.0	0.757	45.0	0.845	45.0	0.871	45.0	0.827	45.0	0.801	45.0	0.721	45.0	0.563	45.0	0.431	45.0	0.352	45.0	0.229
50.0	0.431	50.0	0.607	50.0	0.774	50.0	0.845	50.0	0.880	50.0	0.827	50.0	0.748	50.0	0.651	50.0	0.563	50.0	0.459	50.0	0.352	50.0	0.229
55.0	0.431	55.0	0.607	55.0	0.748	55.0	0.836	55.0	0.845	55.0	0.792	55.0	0.677	55.0	0.616	55.0	0.537	55.0	0.413	55.0	0.308	55.0	0.211
60.0	0.466	60.0	0.590	60.0	0.704	60.0	0.757	60.0	0.774	60.0	0.721	60.0	0.633	60.0	0.545	60.0	0.484	60.0	0.387	60.0	0.264	60.0	0.176
65.0	0.449	65.0	0.528	65.0	0.607	65.0	0.660	65.0	0.660	65.0	0.633	65.0	0.554	65.0	0.484	65.0	0.405	65.0	0.343	65.0	0.238	65.0	0.158
70.0	0.466	70.0	0.493	70.0	0.563	70.0	0.572	70.0	0.598	70.0	0.581	70.0	0.510	70.0	0.449	70.0	0.405	70.0	0.326	70.0	0.220	70.0	0.141
75.0	0.422	75.0	0.431	75.0	0.457	75.0	0.510	75.0	0.501	75.0	0.484	75.0	0.449	75.0	0.405	75.0	0.326	75.0	0.273	75.0	0.176	75.0	0.123
80.0	0.387	80.0	0.387	80.0	0.405	80.0	0.405	80.0	0.422	80.0	0.413	80.0	0.361	80.0	0.308	80.0	0.255	80.0	0.194	80.0	0.123	80.0	0.070
85.0	0.396	85.0	0.317	85.0	0.387	85.0	0.334	85.0	0.352	85.0	0.317	85.0	0.282	85.0	0.229	85.0	0.176	85.0	0.132	85.0	0.088	85.0	0.053

Experiment No. A[illegible]: x = [illegible] mm, y = [illegible] mm, Ambient Conc. = 0.114 ppb, Jet Nozzle Conc. = 13.588 ppb

z = 1.5 mm η (mm)	C (ppb)	z = 6.5 mm η (mm)	C (ppb)	z = 11.5 mm η (mm)	C (ppb)	z = 21.5 mm η (mm)	C (ppb)	z = 26.5 mm η (mm)	C (ppb)	z = 31.5 mm η (mm)	C (ppb)	z = 36.5 mm η (mm)	C (ppb)	z = 41.5 mm η (mm)	C (ppb)	z = 56.5 mm η (mm)	C (ppb)	z = 66.5 mm η (mm)	C (ppb)	z = 76.5 mm η (mm)	C (ppb)	z = 86.5 mm η (mm)	C (ppb)
0.0	0.132	0.0	[illegible]	0.0	[illegible]	0.0	[illegible]	0.0	0.211	0.0	[illegible]	0.0	0.167	0.0	0.123	0.0	0.070	0.0	[illegible]	0.0	[illegible]	0.0	[illegible]
5.0	0.150	5.0	0.194	5.0	0.238	5.0	0.264	5.0	0.273	5.0	0.238	5.0	0.238	5.0	0.150	5.0	0.106	5.0	0.053	5.0	0.026	5.0	0.009
10.0	0.194	10.0	0.238	10.0	0.308	10.0	0.326	10.0	0.334	10.0	0.326	10.0	0.299	10.0	0.211	10.0	0.141	10.0	0.062	10.0	0.026	10.0	0.009
15.0	0.229	15.0	0.282	15.0	0.352	15.0	0.370	15.0	0.378	15.0	0.352	15.0	0.334	15.0	0.255	15.0	0.158	15.0	0.106	15.0	0.044	15.0	0.009
20.0	0.255	20.0	0.326	20.0	0.405	20.0	0.413	20.0	0.422	20.0	0.396	20.0	0.308	20.0	0.273	20.0	0.176	20.0	0.114	20.0	0.044	20.0	0.018
25.0	0.290	25.0	0.361	25.0	0.440	25.0	0.466	25.0	0.475	25.0	0.440	25.0	0.405	25.0	0.308	25.0	0.202	25.0	0.123	25.0	0.044	25.0	0.018
30.0	0.290	30.0	0.387	30.0	0.466	30.0	0.484	30.0	0.493	30.0	0.457	30.0	0.440	30.0	0.334	30.0	0.220	30.0	0.150	30.0	0.053	30.0	0.018
35.0	0.308	35.0	0.422	35.0	0.510	35.0	0.537	35.0	0.528	35.0	0.493	35.0	0.440	35.0	0.343	35.0	0.238	35.0	0.167	35.0	0.053	35.0	0.018
40.0	0.361	40.0	0.501	40.0	0.537	40.0	0.554	40.0	0.545	40.0	0.519	40.0	0.475	40.0	0.343	40.0	0.238	40.0	0.150	40.0	0.062	40.0	0.018
45.0	0.387	45.0	0.457	45.0	0.554	45.0	0.590	45.0	0.581	45.0	0.545	45.0	0.493	45.0	0.352	45.0	0.246	45.0	0.176	45.0	0.053	45.0	0.018
50.0	0.387	50.0	0.466	50.0	0.572	50.0	0.590	50.0	0.590	50.0	0.545	50.0	0.484	50.0	0.343	50.0	0.238	50.0	0.150	50.0	0.062	50.0	0.018
55.0	0.422	55.0	0.484	55.0	0.581	55.0	0.616	55.0	0.616	55.0	0.537	55.0	0.475	55.0	0.326	55.0	0.229	55.0	0.141	55.0	0.053	55.0	0.018
60.0	0.422	60.0	0.466	60.0	0.572	60.0	0.572	60.0	0.554	60.0	0.493	60.0	0.440	60.0	0.299	60.0	0.194	60.0	0.123	60.0	0.053	60.0	0.009
65.0	0.431	65.0	0.484	65.0	0.537	65.0	0.554	65.0	0.537	65.0	0.449	65.0	0.396	65.0	0.282	65.0	0.194	65.0	0.106	65.0	0.044	65.0	0.009
70.0	0.431	70.0	0.457	70.0	0.493	70.0	0.493	70.0	0.466	70.0	0.413	70.0	0.352	70.0	0.246	70.0	0.158	70.0	0.088	70.0	0.035	70.0	0.009
75.0	0.387	75.0	0.422	75.0	0.431	75.0	0.422	75.0	0.413	75.0	0.343	75.0	0.317	75.0	0.211	75.0	0.150	75.0	0.070	75.0	0.044	75.0	0.009
80.0	0.361	80.0	0.387	80.0	0.387	80.0	0.390	80.0	0.343	80.0	0.299	80.0	0.246	80.0	0.176	80.0	0.106	80.0	0.053	80.0	0.018	80.0	0.009
85.0	0.308	85.0	0.317	85.0	0.317	85.0	0.299	85.0	0.282	85.0	0.238	85.0	0.211	85.0	0.150	85.0	0.088	85.0	0.035	85.0	0.018	85.0	0.009

Velocity Ratio (Uo / U) = 4   D / d = 20, d = 6.35 mm   (Concentration readings have been corrected for the ambient value)

Note: Transverse measurements are referenced from the inner boundary of the deflected jet

Experiment No. A209: x = 880 mm, y = 95 mm, Ambient Conc. = 0.044 ppb, Jet Nozzle Conc. = 16.402 ppb

z = 1.5 mm		z = 6.5 mm		z = 16.5 mm		z = 21.5 mm		z = 26.5 mm		z = 31.5 mm		z = 41.5 mm		z = 51.5 mm		z = 61.5 mm		z = 71.5 mm		z = 81.5 mm	
η (mm)	C (ppb)	η (mm)	C (ppb)	η (mm)	C (ppb)	η (mm)	C (ppb)	η (mm)	C (ppb)	η (mm)	C (ppb)	η (mm)	C (ppb)	η (mm)	C (ppb)	η (mm)	C (ppb)	η (mm)	C (ppb)	η (mm)	C (ppb)
0.0	0.282	0.0	0.220	0.0	0.229	0.0	0.211	0.0	0.220	0.0	0.158	0.0	0.132	0.0	0.114	0.0	0.070	0.0	0.053	0.0	0.026
10.0	0.238	10.0	0.255	10.0	0.273	10.0	0.255	10.0	0.264	10.0	0.194	10.0	0.167	10.0	0.150	10.0	0.088	10.0	0.062	10.0	0.035
20.0	0.264	20.0	0.299	20.0	0.308	20.0	0.299	20.0	0.308	20.0	0.220	20.0	0.194	20.0	0.167	20.0	0.106	20.0	0.070	20.0	0.044
25.0	0.211	25.0	0.220	25.0	0.238	25.0	0.264	25.0	0.246	25.0	0.238	25.0	0.211	25.0	0.211	25.0	0.141	25.0	0.088	30.0	0.044
30.0	0.299	30.0	0.317	30.0	0.343	30.0	0.334	30.0	0.343	30.0	0.246	30.0	0.211	30.0	0.185	30.0	0.123	30.0	0.088	40.0	0.044
35.0	0.238	35.0	0.246	35.0	0.264	35.0	0.290	35.0	0.299	35.0	0.255	35.0	0.220	35.0	0.220	35.0	0.158	35.0	0.088	50.0	0.044
40.0	0.326	40.0	0.361	40.0	0.378	40.0	0.378	40.0	0.387	40.0	0.273	40.0	0.246	40.0	0.185	40.0	0.114	40.0	0.088	60.0	0.035
45.0	0.255	45.0	0.255	45.0	0.290	45.0	0.334	45.0	0.308	45.0	0.290	45.0	0.229	45.0	0.220	45.0	0.141	45.0	0.088	70.0	0.026
50.0	0.352	50.0	0.370	50.0	0.413	50.0	0.422	50.0	0.422	50.0	0.308	50.0	0.255	50.0	0.202	50.0	0.123	50.0	0.088	80.0	0.018
55.0	0.273	55.0	0.264	55.0	0.326	55.0	0.352	55.0	0.317	55.0	0.308	55.0	0.238	55.0	0.229	55.0	0.141	55.0	0.088	z = 101.5 mm	
60.0	0.370	60.0	0.396	60.0	0.431	60.0	0.431	60.0	0.422	60.0	0.308	60.0	0.238	60.0	0.176	60.0	0.106	60.0	0.070	0.0	0.009
65.0	0.290	65.0	0.282	65.0	0.317	65.0	0.334	65.0	0.308	65.0	0.299	65.0	0.211	65.0	0.194	65.0	0.123	65.0	0.070	10.0	0.009
70.0	0.396	70.0	0.413	70.0	0.431	70.0	0.422	70.0	0.413	70.0	0.290	70.0	0.220	70.0	0.158	70.0	0.088	70.0	0.053	20.0	0.009
75.0	0.299	75.0	0.282	75.0	0.290	75.0	0.317	75.0	0.282	75.0	0.255	75.0	0.176	75.0	0.167	75.0	0.088	75.0	0.053	30.0	0.009
80.0	0.396	80.0	0.396	80.0	0.387	80.0	0.308	80.0	0.273	80.0	0.238	80.0	0.176	80.0	0.132	80.0	0.070	80.0	0.035	40.0	0.009
85.0	0.264	85.0	0.255	85.0	0.246	85.0	0.264	85.0	0.220	85.0	0.202	85.0	0.132	85.0	0.114	85.0	0.062	85.0	0.035	50.0	0.009
95.0	0.282	95.0	0.194	95.0	0.167	95.0	0.176	95.0	0.141	95.0	0.123	95.0	0.088	95.0	0.079	95.0	0.035	95.0	0.018	60.0	0.009
105.0	0.123	105.0	0.123	105.0	0.097	105.0	0.106	105.0	0.097	105.0	0.070	105.0	0.044	105.0	0.044	105.0	0.018	105.0	0.009	70.0	0.009

Experiment No. A210: x = 110 mm, y = 100.2 mm, Ambient Conc. = 0.114 ppb, Jet Nozzle Conc. = 15.812 ppb

z = 1.5 mm		z = 6.5 mm		z = 16.5 mm		z = 21.5 mm		z = 26.5 mm		z = 31.5 mm		z = 41.5 mm		z = 51.5 mm		z = 61.5 mm		z = 71.5 mm		z = 91.5 mm	
η (mm)	C (ppb)	η (mm)	C (ppb)	η (mm)	C (ppb)	η (mm)	C (ppb)	η (mm)	C (ppb)	η (mm)	C (ppb)	η (mm)	C (ppb)	η (mm)	C (ppb)	η (mm)	C (ppb)	η (mm)	C (ppb)	η (mm)	C (ppb)
0.0	0.106	0.0	0.114	0.0	0.106	0.0	0.106	0.0	0.106	0.0	0.097	0.0	0.088	0.0	0.053	0.0	0.070	0.0	0.035	0.0	0.009
20.0	0.150	20.0	0.150	20.0	0.158	20.0	0.158	20.0	0.158	20.0	0.158	20.0	0.132	20.0	0.114	20.0	0.088	20.0	0.044	20.0	0.018
40.0	0.176	40.0	0.185	40.0	0.194	40.0	0.185	40.0	0.194	40.0	0.176	40.0	0.158	40.0	0.141	40.0	0.114	40.0	0.062	40.0	0.018
50.0	0.194	50.0	0.194	50.0	0.211	50.0	0.202	50.0	0.211	50.0	0.202	50.0	0.167	50.0	0.158	50.0	0.123	50.0	0.070	50.0	0.018
60.0	0.202	60.0	0.202	60.0	0.238	60.0	0.229	60.0	0.211	60.0	0.211	60.0	0.176	60.0	0.167	60.0	0.114	60.0	0.070	60.0	0.026
70.0	0.220	70.0	0.220	70.0	0.246	70.0	0.255	70.0	0.246	70.0	0.255	70.0	0.185	70.0	0.185	70.0	0.123	70.0	0.070	70.0	0.026
80.0	0.238	80.0	0.238	80.0	0.246	80.0	0.264	80.0	0.246	80.0	0.255	80.0	0.202	80.0	0.176	80.0	0.106	80.0	0.062	80.0	0.018
90.0	0.238	90.0	0.246	90.0	0.255	90.0	0.255	90.0	0.255	90.0	0.264	90.0	0.194	90.0	0.167	90.0	0.097	90.0	0.053	90.0	0.018
100.0	0.238	100.0	0.238	100.0	0.246	100.0	0.238	100.0	0.246	100.0	0.229	100.0	0.176	100.0	0.150	100.0	0.097	100.0	0.053	100.0	0.018
120.0	0.167	120.0	0.176	120.0	0.150	120.0	0.150	120.0	0.158	120.0	0.150	120.0	0.106	120.0	0.079	120.0	0.053	120.0	0.026	120.0	0.009
140.0	0.062	140.0	0.062	140.0	0.053	140.0	0.062	140.0	0.079	140.0	0.053	140.0	0.053	140.0	0.035	140.0	0.009	140.0	0.009	140.0	0.000

Velocity Ratio (Uo / U) = 4 D / d = 20, d = 6.35 mm (Concentration readings have been corrected for the ambient value)

Note: Transverse measurements are referenced from the inner boundary of the deflected jet

Experiment No. A211: x = 4000 mm, y = 120 mm, Ambient Conc. = 0.150 ppb, Jet Nozzle Conc. = 16.68 ppb

z = 1.5 mm		z = 6.5 mm		z = 16.5 mm		z = 21.5 mm		z = 26.5 mm		z = 31.5 mm	
η (mm)	C (ppb)	η (mm)	C (ppb)	η (mm)	C (ppb)	η (mm)	C (ppb)	η (mm)	C (ppb)	η (mm)	C (ppb)
0.0	0.106	0.0	0.114	0.0	0.106	0.0	0.114	0.0	0.123	0.0	0.132
20.0	0.106	20.0	0.114	20.0	0.106	20.0	0.123	20.0	0.132	20.0	0.141
40.0	0.114	40.0	0.123	40.0	0.114	40.0	0.132	40.0	0.132	40.0	0.141
50.0	0.114	50.0	0.123	50.0	0.114	50.0	0.141	50.0	0.141	50.0	0.141
60.0	0.114	60.0	0.123	60.0	0.114	60.0	0.141	60.0	0.141	60.0	0.141
70.0	0.114	70.0	0.132	70.0	0.114	70.0	0.141	70.0	0.141	70.0	0.150
80.0	0.123	80.0	0.132	80.0	0.123	80.0	0.132	80.0	0.141	80.0	0.150
90.0	0.123	90.0	0.132	90.0	0.123	90.0	0.132	90.0	0.141	90.0	0.150
100.0	0.123	100.0	0.132	100.0	0.123	100.0	0.132	100.0	0.150	100.0	0.150
120.0	0.114	120.0	0.114	120.0	0.114	120.0	0.123	120.0	0.132	120.0	0.141
140.0	0.097	140.0	0.106	140.0	0.097	140.0	0.106	140.0	0.123	140.0	0.132
180.0	0.062	180.0	0.062	180.0	0.062	180.0	0.070	180.0	0.079	180.0	0.088

z = 41.5 mm		z = 51.5 mm		z = 61.5 mm		z = 81.5 mm		z = 101.5 mm		z = 121.5 mm	
η (mm)	C (ppb)	η (mm)	C (ppb)	η (mm)	C (ppb)	η (mm)	C (ppb)	η (mm)	C (ppb)	η (mm)	C (ppb)
0.0	0.114	0.0	0.114	0.0	0.123	0.0	0.097	0.0	0.088	0.0	0.079
20.0	0.123	20.0	0.123	20.0	0.123	20.0	0.097	20.0	0.079	20.0	0.079
40.0	0.123	40.0	0.123	40.0	0.123	40.0	0.106	40.0	0.079	40.0	0.079
50.0	0.123	50.0	0.123	50.0	0.123	50.0	0.106	50.0	0.079	50.0	0.079
60.0	0.123	60.0	0.123	60.0	0.123	60.0	0.097	60.0	0.079	60.0	0.079
70.0	0.123	70.0	0.132	70.0	0.114	70.0	0.106	70.0	0.079	70.0	0.088
80.0	0.132	80.0	0.132	80.0	0.114	80.0	0.106	80.0	0.079	80.0	0.079
90.0	0.132	90.0	0.132	90.0	0.114	90.0	0.097	90.0	0.079	90.0	0.079
100.0	0.132	100.0	0.132	100.0	0.114	100.0	0.097	100.0	0.079	100.0	0.079
120.0	0.123	120.0	0.114	120.0	0.114	120.0	0.097	120.0	0.079	120.0	0.079
140.0	0.106	140.0	0.106	140.0	0.106	140.0	0.088	140.0	0.070	140.0	0.070
180.0	0.070	180.0	0.079	180.0	0.088	180.0	0.070	180.0	0.053	180.0	0.053

Experiment No. A212: x = 5000 mm, y = 123 mm, Ambient Conc. = 0.114 ppb, Jet Nozzle Conc. = 12.31 ppb

z = 1.5 mm		z = 21.5 mm		z = 31.5 mm		z = 41.5 mm		z = 61.5 mm		z = 91.5 mm		z = 121.5 mm	
η (mm)	C (ppb)	η (mm)	C (ppb)	η (mm)	C (ppb)	η (mm)	C (ppb)	η (mm)	C (ppb)	η (mm)	C (ppb)	η (mm)	C (ppb)
0.0	0.053	0.0	0.062	0.0	0.053	0.0	0.053	0.0	0.053	0.0	0.035	0.0	0.035
20.0	0.053	20.0	0.062	20.0	0.053	20.0	0.053	20.0	0.053	20.0	0.035	20.0	0.035
40.0	0.053	40.0	0.062	40.0	0.053	40.0	0.053	40.0	0.053	40.0	0.035	40.0	0.035
50.0	0.053	50.0	0.062	50.0	0.053	50.0	0.053	50.0	0.053	50.0	0.035	50.0	0.035
60.0	0.053	60.0	0.062	60.0	0.053	60.0	0.053	60.0	0.044	60.0	0.035	60.0	0.026
70.0	0.053	70.0	0.062	70.0	0.053	70.0	0.053	70.0	0.044	70.0	0.035	70.0	0.026
80.0	0.053	80.0	0.062	80.0	0.044	80.0	0.044	80.0	0.044	80.0	0.026	80.0	0.018
90.0	0.044	90.0	0.053	90.0	0.044	90.0	0.044	90.0	0.044	90.0	0.026	90.0	0.018
100.0	0.044	100.0	0.044	100.0	0.044	100.0	0.044	100.0	0.044	100.0	0.026	100.0	0.018
120.0	0.035	120.0	0.035	120.0	0.035	120.0	0.035	120.0	0.035	120.0	0.026	120.0	0.018
140.0	0.018	140.0	0.026	140.0	0.026	140.0	0.026	140.0	0.026	140.0	0.018	140.0	0.018

Velocity Ratio (Uo / U) = 6 D / d = 20, d = 6.35 mm (Concentration readings have been corrected for the ambient value)

Note: Transverse measurements are referenced from the inner boundary of the deflected jet

Experiment No. A301: x = 10 mm, y = 40 mm Ambient Concentration = 0.185 ppb, jet Nozzle Concentration = 14.423 ppb

z = 1.5 mm		z = 6.5 mm		z = 11.5 mm		z = 16.5 mm		z = 21.5 mm		z = 26.5 mm		z = 31.5 mm		z = 36.5 mm		z = 41.5 mm	
η (mm)	C (ppb)	η (mm)	C (ppb)	η (mm)	C (ppb)	η (mm)	C (ppb)	η (mm)	C (ppb)	η (mm)	C (ppb)	η (mm)	C (ppb)	η (mm)	C (ppb)	η (mm)	C (ppb)
0.0	0.000	0.0	0.000	0.0	0.000	0.0	0.000	0.0	0.000	0.0	0.000	0.0	0.000	0.0	0.000	0.0	0.000
5.0	0.000	5.0	0.000	5.0	0.035	5.0	0.026	5.0	0.009	5.0	0.000	5.0	0.000	5.0	0.000	5.0	0.000
10.0	0.009	10.0	0.079	10.0	0.273	10.0	0.273	10.0	0.079	10.0	0.009	10.0	0.009	10.0	0.000	10.0	0.000
15.0	0.044	15.0	0.739	15.0	1.530	15.0	1.126	15.0	0.326	15.0	0.035	15.0	0.000	15.0	0.009	15.0	0.000
20.0	0.141	20.0	1.650	20.0	2.540	20.0	2.262	20.0	0.809	20.0	0.000	20.0	0.009	20.0	0.009	20.0	0.000
25.0	0.370	25.0	2.225	25.0	2.781	25.0	3.022	25.0	1.382	25.0	0.132	25.0	0.009	25.0	0.009	25.0	0.000
30.0	0.740	30.0	2.957	30.0	3.735	30.0	4.263	30.0	1.872	30.0	0.150	30.0	0.009	30.0	0.009	30.0	0.000
35.0	0.705	35.0	5.709	35.0	6.844	35.0	5.340	35.0	1.466	35.0	0.035	35.0	0.009	35.0	0.009	35.0	0.000
40.0	0.097	40.0	3.596	40.0	4.541	40.0	1.567	40.0	0.070	40.0	0.000	40.0	0.009	40.0	0.000	40.0	0.000
45.0	0.018	45.0	0.062	45.0	0.070	45.0	0.018	45.0	0.000	45.0	0.000	45.0	0.000	45.0	0.000	45.0	0.000
50.0	0.000	50.0	0.000	50.0	0.000	50.0	0.000	50.0	0.000	50.0	0.000	50.0	0.000	50.0	0.000	50.0	0.000
55.0	0.000	55.0	0.000	55.0	0.009	55.0	0.000	55.0	0.000	55.0	0.000	55.0	0.000	55.0	0.000	55.0	0.000
60.0	0.000	60.0	0.000	60.0	0.000	60.0	0.000	60.0	0.000	60.0	0.000	60.0	0.000	60.0	0.000	60.0	0.000

Experiment No. A302: x = 40 mm, y = 67.5 mm Ambient Concentration = 0.229 ppb, jet Nozzle Concentration = 17.236 ppb

z = 1.5 mm		z = 6.5 mm		z = 11.5 mm		z = 16.5 mm		z = 21.5 mm		z = 26.5 mm		z = 31.5 mm		z = 36.5 mm		z = 41.5 mm		z = 46.5 mm	
η (mm)	C (ppb)	η (mm)	C (ppb)	η (mm)	C (ppb)	η (mm)	C (ppb)	η (mm)	C (ppb)	η (mm)	C (ppb)	η (mm)	C (ppb)	η (mm)	C (ppb)	η (mm)	C (ppb)	η (mm)	C (ppb)
0.0	0.097	0.0	0.933	0.0	1.820	0.0	2.265	0.0	2.106	0.0	1.606	0.0	1.082	0.0	0.387	0.0	0.079	0.0	0.000
5.0	0.190	5.0	1.372	5.0	2.311	5.0	2.450	5.0	2.339	5.0	2.144	5.0	1.500	5.0	0.897	5.0	0.264	5.0	0.035
10.0	0.282	10.0	1.495	10.0	2.412	10.0	2.460	10.0	2.301	10.0	2.245	10.0	1.745	10.0	0.915	10.0	0.255	15.0	0.062
15.0	0.572	15.0	0.915	15.0	1.449	15.0	1.672	15.0	2.117	15.0	2.311	15.0	1.950	15.0	1.082	15.0	0.352	25.0	0.044
20.0	0.950	20.0	0.911	20.0	1.320	20.0	1.773	20.0	2.301	20.0	2.460	20.0	2.106	20.0	1.196	20.0	0.370	35.0	0.009
25.0	0.897	25.0	1.179	25.0	1.500	25.0	2.172	25.0	2.561	25.0	2.450	25.0	1.922	25.0	1.029	25.0	0.282	45.0	0.000
30.0	0.774	30.0	1.272	30.0	1.804	30.0	2.384	30.0	2.662	30.0	2.496	30.0	1.717	30.0	0.809	30.0	0.246	55.0	0.000
35.0	0.431	35.0	0.853	35.0	1.505	35.0	1.922	35.0	2.085	35.0	1.561	35.0	1.032	35.0	0.396	35.0	0.062	65.0	0.000
40.0	0.273	40.0	0.744	40.0	1.384	40.0	1.495	40.0	1.439	40.0	1.106	40.0	0.405	40.0	0.123	40.0	0.026		
45.0	0.070	45.0	0.190	45.0	0.365	45.0	0.405	45.0	0.365	45.0	0.246	45.0	0.114	45.0	0.018	45.0	0.000		
50.0	0.035	50.0	0.062	50.0	0.150	50.0	0.167	50.0	0.167	50.0	0.000	50.0	0.026	50.0	0.009	50.0	0.009		
55.0	0.000	55.0	0.000	55.0	0.000	55.0	0.000	55.0	0.000	55.0	0.000	55.0	0.000	55.0	0.000	55.0	0.000		
60.0	0.000	60.0	0.000	60.0	0.000	60.0	0.000	60.0	0.000	60.0	0.000	60.0	0.000	60.0	0.000	60.0	0.000		

Velocity Ratio (U0/U) = 6 D/d = 20, d = 12.7 mm

(Concentration readings have been corrected for the ambient value)

Note: Transverse measurements are referenced from the inner boundary of the deflected jet

Experiment No. [illegible]: x = 5 mm, y = 25 mm, Ambient Conc. = 0.018 ppb, Jet Nozzle Conc. = 18.348 ppb

z = 1.5 mm η (mm)	C (ppb)	z = 3.5 mm η (mm)	C (ppb)	z = 7.5 mm η (mm)	C (ppb)	z = 11.5 mm η (mm)	C (ppb)	z = 15.5 mm η (mm)	C (ppb)	z = 19.5 mm η (mm)	C (ppb)	z = 23.5 mm η (mm)	C (ppb)	z = 27.5 mm η (mm)	C (ppb)	z = 30.5 mm η (mm)	C (ppb)
0.0	0.000	0.0	0.000	0.0	0.009	0.0	0.009	0.0	0.000	0.0	0.000	0.0	0.000	0.0	0.000	5.0	0.000
10.0	0.000	5.0	0.000	5.0	0.009	5.0	0.009	5.0	0.000	5.0	0.000	5.0	0.000	5.0	0.000	15.0	0.000
20.0	0.035	10.0	0.000	10.0	0.018	10.0	0.018	10.0	0.000	10.0	0.000	10.0	0.000	10.0	0.000	25.0	0.009
30.0	1.011	15.0	0.053	15.0	0.035	15.0	0.009	15.0	0.009	15.0	0.000	15.0	0.000	15.0	0.000	35.0	0.009
40.0	1.004	20.0	0.070	20.0	0.123	20.0	0.106	20.0	0.176	20.0	0.044	20.0	0.000	20.0	0.000	45.0	0.009
50.0	0.062	25.0	0.097	25.0	1.939	25.0	3.662	25.0	3.857	25.0	1.661	25.0	0.194	25.0	0.009	55.0	0.000
60.0	0.018	30.0	3.040	30.0	8.700	30.0	12.387	30.0	11.146	30.0	0.554	30.0	5.340	30.0	0.141	65.0	0.000
		35.0	5.808	35.0	13.425	35.0	16.416	35.0	16.240	35.0	11.577	35.0	4.190	35.0	0.413		
		40.0	2.290	40.0	8.868	40.0	12.123	40.0	12.026	40.0	7.979	40.0	2.083	40.0	0.106		
		45.0	0.053	45.0	0.405	45.0	0.897	45.0	1.021	45.0	0.396	45.0	0.070	45.0	0.000		
		50.0	0.018	50.0	0.018	50.0	0.018	50.0	0.000	50.0	0.009	50.0	0.000	50.0	0.000		
		55.0	0.018	55.0	0.009	55.0	0.009	55.0	0.000	55.0	0.009	55.0	0.000	55.0	0.000		
		60.0	0.000	60.0	0.009	60.0	0.009	60.0	0.000	60.0	0.000	60.0	0.000	60.0	0.000		
		65.0	0.000	65.0	0.000	65.0	0.000	65.0	0.000	65.0	0.000	65.0	0.000	65.0	0.000		

Experiment No. [illegible]: x = 10 mm, y = 60 mm, Ambient Conc. = 0.097 ppb, Jet Nozzle Conc. = 18.984 ppb

z = 1.5 mm η (mm)	C (ppb)	z = 6.5 mm η (mm)	C (ppb)	z = 11.5 mm η (mm)	C (ppb)	z = 16.5 mm η (mm)	C (ppb)	z = 21.5 mm η (mm)	C (ppb)	z = 26.5 mm η (mm)	C (ppb)	z = 31.5 mm η (mm)	C (ppb)	z = 41.5 mm η (mm)	C (ppb)
0.0	0.000	0.0	0.000	0.0	0.009	0.0	0.009	0.0	0.000	0.0	0.000	0.0	0.000	0.0	0.000
5.0	0.000	5.0	0.000	5.0	0.009	5.0	0.000	5.0	0.000	5.0	0.000	5.0	0.000	5.0	0.000
10.0	0.018	10.0	0.026	10.0	0.053	10.0	0.000	10.0	0.070	10.0	0.070	10.0	0.009	10.0	0.000
15.0	0.035	15.0	0.079	15.0	0.176	15.0	0.255	15.0	0.361	15.0	0.246	15.0	0.062	15.0	0.000
20.0	0.106	20.0	0.282	20.0	0.440	20.0	1.073	20.0	1.507	20.0	1.423	20.0	0.660	20.0	0.026
25.0	0.519	25.0	0.739	25.0	0.994	25.0	1.720	25.0	2.749	25.0	3.166	25.0	0.413	25.0	0.079
30.0	3.207	30.0	3.207	30.0	3.211	30.0	4.126	30.0	4.900	30.0	5.261	30.0	3.425	30.0	0.176
35.0	4.808	35.0	6.317	35.0	8.867	35.0	9.475	35.0	8.771	35.0	6.924	35.0	3.583	35.0	0.132
40.0	4.212	40.0	7.381	40.0	10.284	40.0	11.604	40.0	10.451	40.0	6.581	40.0	2.702	40.0	0.035
45.0	1.705	45.0	2.932	45.0	4.724	45.0	5.428	45.0	4.724	45.0	2.525	45.0	0.092	45.0	0.000
50.0	0.510	50.0	0.475	50.0	0.783	50.0	0.853	50.0	0.862	50.0	0.299	50.0	0.044	50.0	0.000
55.0	0.132	55.0	0.018	55.0	0.018	55.0	0.018	55.0	0.000	55.0	0.000	55.0	0.000	55.0	0.000
60.0	0.079	60.0	0.018	60.0	0.000	60.0	0.000	60.0	0.000	60.0	0.000	60.0	0.000	60.0	0.000
65.0	0.018	65.0	0.000	65.0	0.000	65.0	0.000	65.0	0.000	65.0	0.000	65.0	0.000	65.0	0.000

Velocity Ratio (U0/U) = 6 D/d = 20, d = 12.7 mm

(Concentration readings have been corrected for the ambient value)

Note: Transverse measurements are referenced from the inner boundary of the deflected jet

[illegible] Y = 50 mm, Ambient Conc. = [illegible], Jet Nozzle Conc. = 16.4[illegible] ppb

z = 1.5 mm η (mm)	C (ppb)	z = 11.5 mm η (mm)	C (ppb)	z = 16.5 mm η (mm)	C (ppb)	z = 21.5 mm η (mm)	C (ppb)	z = 26.5 mm η (mm)	C (ppb)	z = 31.5 mm η (mm)	C (ppb)	z = 36.5 mm η (mm)	C (ppb)	z = 41.5 mm η (mm)	C (ppb)	z = 51.5 mm η (mm)	C (ppb)
0.0	[illegible]	0.0	[illegible]	0.0	0.018	0.0	0.018	0.0	0.026	0.0	0.018	0.0	0.018	0.0	0.018	0.0	0.000
10.0	[illegible]	5.0	0.000	5.0	0.044	5.0	0.035	5.0	0.035	5.0	0.053	5.0	0.035	10.0	0.053	10.0	0.009
20.0	0.044	10.0	0.033	10.0	0.000	10.0	0.150	10.0	0.194	10.0	0.150	10.0	0.141	20.0	0.370	20.0	0.070
30.0	0.170	15.0	0.097	15.0	0.194	15.0	0.230	15.0	0.352	15.0	0.422	15.0	0.230	30.0	1.230	30.0	0.317
40.0	0.915	20.0	0.200	20.0	0.519	20.0	0.862	20.0	1.099	20.0	1.015	20.0	0.818	40.0	1.900	40.0	0.334
50.0	4.157	25.0	0.370	25.0	0.897	25.0	1.240	25.0	1.470	25.0	1.409	25.0	1.056	50.0	2.461	50.0	0.300
60.0	3.370	30.0	0.705	30.0	1.400	30.0	2.211	30.0	2.620	30.0	2.655	30.0	2.072	60.0	0.932	60.0	0.035
70.0	0.620	35.0	0.000	35.0	1.507	35.0	2.415	35.0	2.660	35.0	2.832	35.0	2.332	70.0	0.114	70.0	0.000
80.0	0.079	40.0	1.200	40.0	1.730	40.0	2.400	40.0	3.370	40.0	3.767	40.0	3.239	80.0	0.009	80.0	0.000
90.0	0.026	45.0	1.562	45.0	1.800	45.0	2.610	45.0	3.472	45.0	3.944	45.0	3.222	90.0	0.000	90.0	0.000
		50.0	4.830	50.0	4.702	50.0	5.270	50.0	5.534	50.0	5.182	50.0	3.862				
		55.0	5.613	55.0	5.877	55.0	6.220	55.0	5.700	55.0	4.812	55.0	3.583				
		60.0	4.900	60.0	6.061	60.0	5.790	60.0	4.918	60.0	3.422	60.0	1.927				
		65.0	3.500	65.0	3.500	65.0	4.100	65.0	3.141	65.0	2.085	65.0	0.990				
		70.0	0.801	70.0	1.073	70.0	0.977	70.0	0.885	70.0	0.440	70.0	0.167				
		75.0	0.240	75.0	0.290	75.0	0.300	75.0	0.255	75.0	0.114	75.0	0.035				
		80.0	0.018	80.0	0.026	80.0	0.018	80.0	0.026	80.0	0.009	80.0	0.009				
		85.0	0.000	85.0	0.000	85.0	0.000	85.0	0.009	85.0	0.009	85.0	0.000				
		90.0	0.000	90.0	0.000	90.0	0.000	90.0	0.026	90.0	0.018	90.0	0.018				
		95.0	0.018	95.0	0.000	95.0	0.000	95.0	0.000	95.0	0.000	95.0	0.000				

[illegible] x = 20 mm, Y = 95 mm, Ambient Conc. = [illegible], Jet Nozzle Conc. = 17.7[illegible] ppb

z = 1.5 mm η (mm)	C (ppb)	z = 11.5 mm η (mm)	C (ppb)	z = 16.5 mm η (mm)	C (ppb)	z = 21.5 mm η (mm)	C (ppb)	z = 26.5 mm η (mm)	C (ppb)	z = 31.5 mm η (mm)	C (ppb)	z = 41.5 mm η (mm)	C (ppb)	z = 51.5 mm η (mm)	C (ppb)	z = 61.5 mm η (mm)	C (ppb)
0.0	0.000	0.0	0.000	0.0	0.000	0.0	0.000	0.0	0.000	0.0	0.000	0.0	0.000	0.0	0.009	0.0	0.009
10.0	0.000	5.0	0.000	5.0	0.000	5.0	0.009	5.0	0.018	5.0	0.009	5.0	0.000	10.0	0.009	10.0	0.009
20.0	0.026	10.0	0.018	10.0	0.026	10.0	0.026	10.0	0.062	10.0	0.044	10.0	0.026	20.0	0.053	20.0	0.018
30.0	0.070	15.0	0.044	15.0	0.044	15.0	0.079	15.0	0.150	15.0	0.062	15.0	0.044	30.0	0.150	30.0	0.035
40.0	0.132	20.0	0.000	20.0	0.230	20.0	0.255	20.0	0.422	20.0	0.440	20.0	0.246	40.0	0.686	40.0	0.097
50.0	1.377	25.0	0.255	25.0	0.370	25.0	0.686	25.0	1.029	25.0	0.510	25.0	0.405	50.0	1.030	50.0	0.000
60.0	4.500	30.0	0.370	30.0	0.853	30.0	1.205	30.0	1.516	30.0	1.655	30.0	0.889	60.0	0.642	60.0	0.053
70.0	2.800	35.0	0.642	35.0	1.173	35.0	1.924	35.0	2.452	35.0	1.813	35.0	1.284	70.0	0.114	70.0	0.009
80.0	0.700	40.0	0.818	40.0	1.571	40.0	2.350	40.0	2.906	40.0	3.072	40.0	2.127	80.0	0.000	80.0	0.000
90.0	0.141	45.0	0.836	45.0	1.618	45.0	2.306	45.0	2.925	45.0	3.250	45.0	2.647	90.0	0.000	90.0	0.000
		50.0	1.400	50.0	1.760	50.0	2.377	50.0	3.239	50.0	3.906	50.0	3.184				
		55.0	3.800	55.0	2.700	55.0	3.300	55.0	4.170	55.0	4.557	55.0	3.250				
		60.0	5.000	60.0	5.534	60.0	5.622	60.0	5.790	60.0	5.622	60.0	3.239				
		65.0	5.613	65.0	6.229	65.0	6.317	65.0	5.965	65.0	5.437	65.0	2.591				
		70.0	4.918	70.0	5.350	70.0	5.710	70.0	5.182	70.0	3.950	70.0	1.655				
		75.0	2.534	75.0	3.062	75.0	3.062	75.0	2.790	75.0	2.270	75.0	0.617				
		80.0	1.135	80.0	1.223	80.0	1.400	80.0	1.082	80.0	0.757	80.0	0.202				
		85.0	0.220	85.0	0.264	85.0	0.282	85.0	0.230	85.0	0.194	85.0	0.026				
		90.0	0.035	90.0	0.053	90.0	0.035	90.0	0.018	90.0	0.018	90.0	0.009				
		95.0	0.018	95.0	0.009	95.0	0.009	95.0	0.018	95.0	0.009	95.0	0.009				

Velocity Ratio (Uo/U) = 6 D/d = 20, d = 12.7 mm

(Concentration readings have been corrected for the ambient value)

Note: Transverse measurements are referenced from the inner boundary of the deflected jet

Experiment No. B305: x = 45 mm, y = 135 mm, Ambient Conc. = 0.106 ppb, Jet Nozzle Conc. = 17.236 ppb

z = 1.5 mm		z = 11.5 mm		z = 21.5 mm		z = 26.5 mm		z = 31.5 mm		z = 36.5 mm		z = 46.5 mm		z = 56.5 mm		z = 71.5 mm	
η (mm)	C (ppb)	η (mm)	C (ppb)	η (mm)	C (ppb)	η (mm)	C (ppb)	η (mm)	C (ppb)	η (mm)	C (ppb)	η (mm)	C (ppb)	η (mm)	C (ppb)	η (mm)	C (ppb)
0.0	0.000	0.0	0.026	0.0	0.070	0.0	0.044	0.0	0.132	0.0	0.062	0.0	0.106	0.0	0.123	0.0	0.018
10.0	0.044	5.0	0.053	5.0	0.070	5.0	0.123	5.0	0.185	5.0	0.211	5.0	0.132	10.0	1.100	10.0	0.238
20.0	0.106	10.0	0.280	10.0	0.880	10.0	0.933	10.0	1.399	10.0	1.047	10.0	1.249	20.0	1.795	20.0	0.475
30.0	0.194	15.0	0.485	15.0	0.924	15.0	1.267	15.0	1.684	15.0	1.409	15.0	1.517	30.0	2.379	30.0	0.871
40.0	0.520	20.0	0.572	20.0	1.451	20.0	1.674	20.0	2.137	20.0	1.915	20.0	2.045	40.0	2.657	40.0	1.240
50.0	1.813	25.0	0.686	25.0	1.656	25.0	1.934	25.0	2.351	25.0	2.351	25.0	2.295	50.0	2.768	50.0	1.249
60.0	2.619	30.0	0.774	30.0	1.785	30.0	2.174	30.0	2.499	30.0	2.610	30.0	2.657	60.0	2.490	60.0	0.801
70.0	2.674	35.0	0.713	35.0	1.739	35.0	2.101	35.0	2.407	35.0	2.573	35.0	2.740	70.0	1.517	70.0	0.361
80.0	1.390	40.0	0.845	40.0	1.507	40.0	1.952	40.0	2.276	40.0	2.666	40.0	2.990	80.0	0.627	80.0	0.106
90.0	0.651	45.0	1.100	45.0	1.409	45.0	1.851	45.0	2.295	45.0	2.601	45.0	3.046	90.0	0.044	90.0	0.026
		50.0	1.757	50.0	2.257	50.0	2.369	50.0	2.832	50.0	3.110	50.0	3.435				
		55.0	2.407	55.0	2.657	55.0	2.879	55.0	3.213	55.0	3.407	55.0	3.463				
		60.0	3.030	60.0	3.675	60.0	3.842	60.0	4.000	60.0	3.944	60.0	3.574				
		65.0	3.018	65.0	3.658	65.0	3.797	65.0	3.797	65.0	3.797	65.0	3.324				
		70.0	2.925	70.0	3.564	70.0	3.870	70.0	3.885	70.0	3.778	70.0	2.990				
		75.0	2.351	75.0	3.213	75.0	3.129	75.0	3.102	75.0	3.046	75.0	2.295				
		80.0	1.729	80.0	2.230	80.0	2.619	80.0	2.360	80.0	2.360	80.0	1.823				
		85.0	1.211	85.0	1.712	85.0	1.545	85.0	1.573	85.0	1.545	85.0	0.878				
		90.0	0.580	90.0	0.673	90.0	0.812	90.0	0.581	90.0	0.831	90.0	0.457				
		95.0	0.280	95.0	0.433	95.0	0.352	95.0	0.246	95.0	0.378	95.0	0.150				

Experiment No. B306: x = 64 mm, y = 95 mm, Ambient Conc. = 0.123 ppb, Jet Nozzle Conc. = 16.68 ppb

z = 6.5 mm		z = 16.5 mm		z = 26.5 mm		z = 36.5 mm		z = 56.5 mm		z = 86.5 mm	
η (mm)	C (ppb)	η (mm)	C (ppb)	η (mm)	C (ppb)	η (mm)	C (ppb)	η (mm)	C (ppb)	η (mm)	C (ppb)
0.0	0.344	0.0	1.322	0.0	1.767	0.0	1.739	0.0	0.581	0.0	0.000
20.0	0.933	20.0	2.379	20.0	2.085	20.0	2.740	20.0	1.600	20.0	0.009
30.0	1.044	30.0	2.208	30.0	2.573	30.0	2.879	30.0	1.823	30.0	0.018
40.0	1.128	40.0	1.851	40.0	2.601	40.0	3.046	40.0	1.851	40.0	0.009
50.0	2.156	50.0	2.518	50.0	3.018	50.0	3.213	50.0	1.545	50.0	0.000
60.0	2.712	60.0	2.768	60.0	2.990	60.0	2.824	60.0	0.909	60.0	0.000
70.0	2.240	70.0	2.129	70.0	2.268	70.0	1.656	70.0	0.290	70.0	0.000
80.0	1.017	80.0	0.850	80.0	0.655	80.0	0.378	80.0	0.053	80.0	0.000
100.0	0.026	100.0	0.000	100.0	0.000	100.0	0.000	100.0	0.000	100.0	0.000

Velocity Ratio (Uo/U) = 6

D / d = 20, d = 12.7 mm

(Concentration readings have been corrected for the ambient value)

Note: Transverse measurements are referenced from the inner boundary of the deflected jet

Experiment No. B107: x = 166 mm, y = 120 mm, Ambient Conc. = 0.166 ppb, Jet Nozzle Conc. = 16.958 ppb

z = 11.5 mm η (mm)	C (ppb)	z = 21.5 mm η (mm)	C (ppb)	z = 31.5 mm η (mm)	C (ppb)	z = 41.5 mm η (mm)	C (ppb)	z = 51.5 mm η (mm)	C (ppb)	z = 71.5 mm η (mm)	C (ppb)	z = 91.5 mm η (mm)	C (ppb)	z = 121.5 mm η (mm)	C (ppb)
0.0	0.609	0.0	1.451	0.0	2.007	0.0	1.868	0.0	1.785	0.0	0.633	0.0	0.035	0.0	0.000
20.0	1.451	20.0	2.369	20.0	2.563	20.0	2.480	20.0	2.369	20.0	1.201	20.0	0.132	20.0	0.000
30.0	1.701	30.0	2.424	30.0	2.369	30.0	2.369	30.0	2.396	30.0	1.201	30.0	0.097	30.0	0.000
40.0	1.423	40.0	2.007	40.0	2.063	40.0	2.285	40.0	2.313	40.0	1.118	40.0	0.062	40.0	0.000
50.0	1.204	50.0	1.674	50.0	1.896	50.0	2.202	50.0	2.174	50.0	1.034	50.0	0.053	50.0	0.000
60.0	1.590	60.0	1.785	60.0	2.007	60.0	2.230	60.0	1.896	60.0	0.701	60.0	0.035	60.0	0.000
70.0	1.952	70.0	1.896	70.0	1.924	70.0	1.952	70.0	1.368	70.0	0.300	70.0	0.009	70.0	0.000
80.0	1.701	80.0	1.618	80.0	1.368	80.0	1.368	80.0	0.673	80.0	0.097	80.0	0.000	80.0	0.000
100.0	0.720	100.0	1.396	100.0	0.230	100.0	0.229	100.0	0.044	100.0	0.000	100.0	0.000	100.0	0.000

Experiment No. B108: x = 250 mm, y = 150 mm, Ambient Conc. = 0.150 ppb, Jet Nozzle Conc. = 18.984 ppb

z = 11.5 mm η (mm)	C (ppb)	z = 31.5 mm η (mm)	C (ppb)	z = 51.5 mm η (mm)	C (ppb)	z = 61.5 mm η (mm)	C (ppb)	z = 71.5 mm η (mm)	C (ppb)	z = 91.5 mm η (mm)	C (ppb)	z = 111.5 mm η (mm)	C (ppb)	z = 141.5 mm η (mm)	C (ppb)	z = 171.5 mm η (mm)	C (ppb)
0.0	0.000	0.0	0.264	0.0	0.300	0.0	0.290	0.0	0.273	0.0	0.097	0.0	0.009	0.0	0.000	0.0	0.000
30.0	0.000	30.0	1.518	30.0	1.546	30.0	1.510	30.0	1.204	30.0	0.606	30.0	0.150	30.0	0.009	30.0	0.000
50.0	0.176	50.0	1.900	50.0	1.852	50.0	1.704	50.0	1.454	50.0	0.941	50.0	0.246	50.0	0.018	50.0	0.009
60.0	0.255	60.0	1.963	60.0	1.824	60.0	1.649	60.0	1.426	60.0	0.985	60.0	0.282	60.0	0.026	60.0	0.009
70.0	0.282	70.0	1.991	70.0	1.769	70.0	1.649	70.0	1.398	70.0	0.950	70.0	0.299	70.0	0.018	70.0	0.009
80.0	0.422	80.0	1.852	80.0	1.657	80.0	1.482	80.0	1.287	80.0	0.906	80.0	0.230	80.0	0.018	80.0	0.018
90.0	0.605	90.0	1.546	90.0	1.463	90.0	1.343	90.0	1.176	90.0	0.862	90.0	0.220	90.0	0.018	90.0	0.009
100.0	0.924	100.0	1.208	100.0	1.240	100.0	1.287	100.0	1.065	100.0	0.721	100.0	0.167	100.0	0.009	100.0	0.009
110.0	0.994	110.0	1.018	110.0	1.018	110.0	1.009	110.0	0.870	110.0	0.545	110.0	0.106	110.0	0.009	110.0	0.009
130.0	0.977	130.0	0.823	130.0	0.740	130.0	0.676	130.0	0.481	130.0	0.246	130.0	0.018	130.0	0.000	130.0	0.009
150.0	0.774	150.0	0.378	150.0	0.317	150.0	0.194	150.0	0.141	150.0	0.097	150.0	0.000	150.0	0.000	150.0	0.009
180.0	0.220	180.0	0.053	180.0	0.044	180.0	0.009	180.0	0.000	180.0	0.000	180.0	0.000	180.0	0.000	180.0	0.000

Velocity Ratio (Uo/U) = 6 D/d = 20, d = 12.7 mm

(Concentration readings have been corrected for the ambient value)

Note: Transverse measurements are referenced from the inner boundary of the deflected jet

Experiment No. B108: z = 450 mm, y = 140 mm, Ambient Conc. = 0.194 ppb, Jet Nozzle Conc. = 19.182 ppb

z = 1.5 mm η (mm)	C (ppb)	z = 21.5 mm η (mm)	C (ppb)	z = 31.5 mm η (mm)	C (ppb)	z = 41.5 mm η (mm)	C (ppb)	z = 51.5 mm η (mm)	C (ppb)	z = 71.5 mm η (mm)	C (ppb)	z = 91.5 mm η (mm)	C (ppb)	z = 121.5 mm η (mm)	C (ppb)	z = 151.5 mm η (mm)	C (ppb)	z = 191.5 mm η (mm)	C (ppb)
0.0	0.044	0.0	0.167	0.0	0.273	0.0	0.501	0.0	0.457	0.0	0.528	0.0	0.255	0.0	0.062	0.0	0.009	0.0	0.000
30.0	0.100	30.0	0.686	30.0	0.871	30.0	1.169	30.0	1.057	30.0	0.937	30.0	0.713	30.0	0.255	30.0	0.035	30.0	0.000
50.0	0.194	50.0	1.047	50.0	1.196	50.0	1.280	50.0	1.224	50.0	1.021	50.0	0.713	50.0	0.326	50.0	0.070	50.0	0.000
60.0	0.273	60.0	1.100	60.0	1.280	60.0	1.335	60.0	1.280	60.0	1.049	60.0	0.704	60.0	0.326	60.0	0.062	60.0	0.000
70.0	0.334	70.0	1.100	70.0	1.308	70.0	1.419	70.0	1.335	70.0	0.993	70.0	0.686	70.0	0.282	70.0	0.053	70.0	0.009
80.0	0.343	80.0	1.224	80.0	1.335	80.0	1.474	80.0	1.391	80.0	0.965	80.0	0.651	80.0	0.255	80.0	0.053	80.0	0.009
90.0	0.370	90.0	1.196	90.0	1.363	90.0	1.474	90.0	1.447	90.0	0.965	90.0	0.625	90.0	0.229	90.0	0.044	90.0	0.000
100.0	0.396	100.0	1.085	100.0	1.280	100.0	1.391	100.0	1.391	100.0	0.882	100.0	0.563	100.0	0.211	100.0	0.035	100.0	0.000
110.0	0.404	110.0	0.946	110.0	1.196	110.0	1.224	110.0	1.196	110.0	0.798	110.0	0.466	110.0	0.282	110.0	0.026	110.0	0.000
130.0	0.466	130.0	0.686	130.0	0.807	130.0	0.752	130.0	0.835	130.0	0.576	130.0	0.317	130.0	0.097	130.0	0.009	130.0	0.000
150.0	0.590	150.0	0.590	150.0	0.585	150.0	0.474	150.0	0.501	150.0	0.299	150.0	0.132	150.0	0.044	150.0	0.000	150.0	0.000
180.0	0.405	180.0	0.388	180.0	0.299	180.0	0.185	180.0	0.264	180.0	0.079	180.0	0.018	180.0	0.000	180.0	0.000	180.0	0.000

Experiment No. B110: z = 900 mm, y = 230 mm, Ambient Conc. = 0.0[illegible] ppb, Jet Nozzle Conc. = 16.187 ppb

z = 1.5 mm η (mm)	C (ppb)	z = 21.5 mm η (mm)	C (ppb)	z = 41.5 mm η (mm)	C (ppb)	z = 51.5 mm η (mm)	C (ppb)	z = 61.5 mm η (mm)	C (ppb)	z = 71.5 mm η (mm)	C (ppb)	z = 91.5 mm η (mm)	C (ppb)	z = 121.5 mm η (mm)	C (ppb)	z = 151.5 mm η (mm)	C (ppb)	z = 191.5 mm η (mm)	C (ppb)
0.0	0.123	0.0	0.273	0.0	0.370	0.0	0.308	0.0	0.370	0.0	0.370	0.0	0.317	0.0	0.176	0.0	0.035	0.0	0.000
30.0	0.299	30.0	0.440	30.0	0.528	30.0	0.501	30.0	0.475	30.0	0.475	30.0	0.308	30.0	0.229	30.0	0.053	30.0	0.009
50.0	0.264	50.0	0.537	50.0	0.545	50.0	0.537	50.0	0.545	50.0	0.563	50.0	0.422	50.0	0.229	50.0	0.062	50.0	0.009
60.0	0.299	60.0	0.502	60.0	0.589	60.0	0.590	60.0	0.563	60.0	0.598	60.0	0.449	60.0	0.246	60.0	0.079	60.0	0.009
70.0	0.317	70.0	0.607	70.0	0.642	70.0	0.686	70.0	0.651	70.0	0.625	70.0	0.466	70.0	0.246	70.0	0.106	70.0	0.009
80.0	0.343	80.0	0.616	80.0	0.677	80.0	0.721	80.0	0.686	80.0	0.677	80.0	0.493	80.0	0.246	80.0	0.088	80.0	0.009
90.0	0.370	90.0	0.634	90.0	0.704	90.0	0.748	90.0	0.713	90.0	0.686	90.0	0.493	90.0	0.246	90.0	0.070	90.0	0.000
100.0	0.370	100.0	0.642	100.0	0.713	100.0	0.705	100.0	0.748	100.0	0.677	100.0	0.493	100.0	0.246	100.0	0.070	100.0	0.000
110.0	0.388	110.0	0.625	110.0	0.748	110.0	0.748	110.0	0.739	110.0	0.651	110.0	0.493	110.0	0.246	110.0	0.044	110.0	0.000
130.0	0.360	130.0	0.537	130.0	0.713	130.0	0.695	130.0	0.642	130.0	0.563	130.0	0.475	130.0	0.229	130.0	0.035	130.0	0.000
150.0	0.430	150.0	0.405	150.0	0.572	150.0	0.554	150.0	0.484	150.0	0.413	150.0	0.308	150.0	0.202	150.0	0.018	150.0	0.000
180.0	0.388	180.0	0.273	180.0	0.308	180.0	0.343	180.0	0.282	180.0	0.238	180.0	0.211	180.0	0.106	180.0	0.000	180.0	0.000

Velocity Ratio (Uo / U) = 6 D / d = 20, d = 12.7 mm

(Concentration readings have been corrected for the ambient value)

Note: Transverse measurements are referenced from the inner boundary of the deflected jet

Experiment No. B311: x = 1300 mm, y = 230 mm, Ambient Conc. = 0.114 ppb, Jet Nozzle Conc. = 15.923 ppb

z = 1.5 mm η (mm)	C (ppb)	z = 31.5 mm η (mm)	C (ppb)	z = 51.5 mm η (mm)	C (ppb)	z = 61.5 mm η (mm)	C (ppb)	z = 71.5 mm η (mm)	C (ppb)	z = 81.5 mm η (mm)	C (ppb)	z = 101.5 mm η (mm)	C (ppb)	z = 131.5 mm η (mm)	C (ppb)	z = 171.5 mm η (mm)	C (ppb)	z = 211.5 mm η (mm)	C (ppb)
0.0	0.211	0.0	0.290	0.0	0.299	0.0	0.290	0.0	0.308	0.0	0.255	0.0	0.282	0.0	0.141	0.0	0.026	0.0	0.000
30.0	0.273	30.0	0.308	30.0	0.387	30.0	0.352	30.0	0.361	30.0	0.326	30.0	0.282	30.0	0.194	30.0	0.053	30.0	0.000
50.0	0.300	50.0	0.438	50.0	0.449	50.0	0.422	50.0	0.422	50.0	0.405	50.0	0.308	50.0	0.220	50.0	0.062	50.0	0.000
60.0	0.326	60.0	0.449	60.0	0.457	60.0	0.466	60.0	0.457	60.0	0.440	60.0	0.334	60.0	0.229	60.0	0.053	60.0	0.000
70.0	0.343	70.0	0.466	70.0	0.484	70.0	0.510	70.0	0.501	70.0	0.475	70.0	0.343	70.0	0.229	70.0	0.053	70.0	0.000
80.0	0.352	80.0	0.500	80.0	0.510	80.0	0.563	80.0	0.537	80.0	0.484	80.0	0.352	80.0	0.220	80.0	0.053	80.0	0.000
90.0	0.361	90.0	0.528	90.0	0.537	90.0	0.581	90.0	0.563	90.0	0.501	90.0	0.361	90.0	0.220	90.0	0.053	90.0	0.000
100.0	0.387	100.0	0.554	100.0	0.581	100.0	0.572	100.0	0.572	100.0	0.510	100.0	0.361	100.0	0.220	100.0	0.053	100.0	0.000
110.0	0.387	110.0	0.361	110.0	0.563	110.0	0.572	110.0	0.528	110.0	0.484	110.0	0.352	110.0	0.194	110.0	0.044	110.0	0.000
130.0	0.409	130.0	0.334	130.0	0.528	130.0	0.528	130.0	0.493	130.0	0.449	130.0	0.299	130.0	0.176	130.0	0.035	130.0	0.000
150.0	0.413	150.0	0.422	150.0	0.449	150.0	0.405	150.0	0.370	150.0	0.361	150.0	0.238	150.0	0.132	150.0	0.026	150.0	0.000
180.0	0.382	180.0	0.308	180.0	0.308	180.0	0.273	180.0	0.238	180.0	0.211	180.0	0.141	180.0	0.044	180.0	0.000	180.0	0.000

Velocity Ratio (Uo / U) = 6 D / d = 10, d = 12.7 mm

(Concentration readings have been corrected for the ambient value)

Note: Transverse measurements are referenced from the inner boundary of the deflected jet

Experiment No. B301: x = 38 mm, y = 75 mm; C(amb.)=0.282 ppb, C(nozzle)=16.482 ppb

Experiment No. B302: x = 52 mm, y = 85 mm; Ambient Conc. = 0.290 ppb, Jet Nozzle Conc. = 16.124 ppb

Experiment No. B303: x = 95 mm, y = 115 mm. Ambient Conc.= 0.114 ppb, Jet Nozzle Conc=17.236 ppb

B301 z = 1.5 mm η (mm)	C (ppb)	z = 11.5 mm η (mm)	C (ppb)	z = 21.5 mm η (mm)	C (ppb)	B302 z = 1.5 mm η (mm)	C (ppb)	z = 11.5 mm η (mm)	C (ppb)	z = 21.5 mm η (mm)	C (ppb)	z = 31.5 mm η (mm)	C (ppb)	B303 z = 1.5 mm η (mm)	C (ppb)	z = 11.5 mm η (mm)	C (ppb)	z = 21.5 mm η (mm)	C (ppb)	z = 31.5 mm η (mm)	C (ppb)
0.0	0.000	0.0	0.070	0.0	0.211	0.0	0.009	0.0	0.334	0.0	0.818	0.0	0.924	0.0	0.053	0.0	0.449	0.0	1.017	0.0	1.295
20.0	0.007	20.0	1.442	20.0	2.387	20.0	0.150	20.0	1.870	20.0	2.500	20.0	2.509	20.0	0.299	20.0	1.093	20.0	2.490	20.0	2.657
30.0	0.290	30.0	2.220	30.0	2.000	30.0	0.413	30.0	2.367	30.0	2.703	30.0	2.814	30.0	0.493	30.0	1.807	30.0	2.462	30.0	2.657
40.0	0.598	40.0	2.100	40.0	2.603	40.0	0.642	40.0	1.909	40.0	2.509	40.0	2.898	40.0	0.765	40.0	1.832	40.0	2.573	40.0	2.434
50.0	1.000	50.0	2.276	50.0	3.110	50.0	1.517	50.0	2.017	50.0	2.759	50.0	3.299	50.0	1.164	50.0	1.415	50.0	1.934	50.0	2.295
60.0	3.444	60.0	3.646	60.0	4.027	60.0	2.851	60.0	2.962	60.0	3.287	60.0	3.315	60.0	1.004	60.0	1.009	60.0	1.851	60.0	2.351
70.0	3.416	70.0	3.499	70.0	3.300	70.0	2.934	70.0	3.046	70.0	2.953	70.0	2.731	70.0	2.110	70.0	1.943	70.0	2.156	70.0	2.407
80.0	1.899	80.0	1.553	80.0	1.275	80.0	1.909	80.0	1.739	80.0	1.397	80.0	1.035	80.0	1.943	80.0	1.971	80.0	1.934	80.0	1.934
100.0	0.141	100.0	0.009	100.0	0.000	100.0	1.211	100.0	0.000	100.0	0.018	100.0	0.000	100.0	0.006	100.0	0.664	100.0	0.433	100.0	0.322

Velocity Ratio (Uo/U) = 6 D/d = 10, d = 12.7 mm

(Concentration readings have been corrected for the ambient value)

Note: Transverse measurements are referenced from the inner boundary of the deflected jet

Experiment No. B304: x = [illegible] mm; C(amb) = 0.106 ppb, C(nozzle) = 17.236 ppb

z = 11.5 mm η (mm)	C (ppb)	z = 21.5 mm η (mm)	C (ppb)	z = 31.5 mm η (mm)	C (ppb)	z = 41.5 mm η (mm)	C (ppb)
0.0	[illegible]	0.0	[illegible]	0.0	0.124	0.0	0.176
30.0	[illegible]	30.0	[illegible]	30.0	1.137	30.0	1.388
50.0	0.776	50.0	1.400	50.0	1.556	50.0	1.526
60.0	0.940	60.0	1.459	60.0	1.556	60.0	1.526
70.0	[illegible]	70.0	1.509	70.0	1.581	70.0	1.526
80.0	[illegible]	80.0	1.479	80.0	1.556	80.0	1.526
90.0	[illegible]	90.0	[illegible]	90.0	1.470	90.0	1.442
100.0	[illegible]	100.0	1.257	100.0	[illegible]	100.0	1.383
110.0	0.776	110.0	[illegible]	110.0	1.025	110.0	1.081
130.0	[illegible]	130.0	[illegible]	130.0	0.747	130.0	0.720
150.0	[illegible]	150.0	[illegible]	150.0	0.442	150.0	0.398
180.0	[illegible]	180.0	0.185	180.0	0.097	180.0	0.079

Experiment No. B305: x = 530 mm; Ambient Conc. = 0.106 ppb, Jet Nozzle Conc. = 17.236 ppb

z = 21.5 mm η (mm)	C (ppb)	z = 31.5 mm η (mm)	C (ppb)	z = 41.5 mm η (mm)	C (ppb)	z = 51.5 mm η (mm)	C (ppb)
0.0	[illegible]	0.0	[illegible]	0.0	0.376	0.0	[illegible]
30.0	0.721	30.0	[illegible]	30.0	0.985	30.0	0.941
50.0	0.959	50.0	1.126	50.0	1.082	50.0	[illegible]
60.0	1.047	60.0	1.135	60.0	1.100	60.0	[illegible]
70.0	1.073	70.0	1.161	70.0	1.135	70.0	1.144
80.0	[illegible]	80.0	1.179	80.0	[illegible]	80.0	1.161
90.0	[illegible]	90.0	[illegible]	90.0	[illegible]	90.0	1.161
100.0	1.073	100.0	1.170	100.0	1.170	100.0	1.126
110.0	0.933	110.0	[illegible]	110.0	1.073	110.0	[illegible]
130.0	0.730	130.0	0.757	130.0	[illegible]	130.0	[illegible]
150.0	0.563	150.0	0.510	150.0	0.501	150.0	[illegible]
180.0	0.317	180.0	[illegible]	180.0	0.211	180.0	[illegible]

Experiment No. B306: x = 850 mm; Ambt.Conc. = 0.088 ppb, Nozzle Conc. = 15.572 ppb

z = 31.5 mm η (mm)	C (ppb)	z = 41.5 mm η (mm)	C (ppb)	z = 51.5 mm η (mm)	C (ppb)	z = 61.5 mm η (mm)	C (ppb)
0.0	0.317	0.0	[illegible]	0.0	0.387	0.0	0.422
30.0	0.563	30.0	[illegible]	30.0	0.581	30.0	0.554
50.0	0.642	50.0	0.642	50.0	0.642	50.0	[illegible]
60.0	[illegible]	60.0	0.704	60.0	[illegible]	60.0	0.677
70.0	[illegible]	70.0	0.774	70.0	0.739	70.0	0.739
80.0	0.704	80.0	0.748	80.0	0.783	80.0	0.765
90.0	0.739	90.0	[illegible]	90.0	0.774	90.0	0.765
100.0	0.757	100.0	0.827	100.0	0.757	100.0	0.757
110.0	0.739	110.0	[illegible]	110.0	0.721	110.0	[illegible]
130.0	[illegible]	130.0	0.704	130.0	0.581	130.0	0.563
150.0	0.510	150.0	0.404	150.0	0.387	150.0	[illegible]
180.0	[illegible]	180.0	0.264	180.0	[illegible]	180.0	0.176

Velocity Ratio (Uo/U) = 6 D/d = 5, d = 12.7 mm

(Concentration readings have been corrected for the ambient value)

Note: Transverse measurements are referenced from the inner boundary of the deflected jet

Experiment No. B301: x = 3[illegible] mm, y = 7[illegible] mm; C(amb) = [illegible] ppb, C(nozzle) = 16.6[illegible] ppb

z = 1.5 mm η (mm)	C (ppb)	z = 11.5 mm η (mm)	C (ppb)	z = 21.5 mm η (mm)	C (ppb)
0.0	[illegible]	0.0	[illegible]	0.0	[illegible]
20.0	0.170	20.0	2.071	20.0	2.730
30.0	[illegible]	30.0	2.127	30.0	2.877
40.0	2.377	40.0	3.12[illegible]	40.0	4.017
50.0	[illegible]	50.0	[illegible]	50.0	3.015
60.0	[illegible]	60.0	4.007	60.0	4.135
70.0	[illegible]	70.0	[illegible]	70.0	[illegible]
80.0	[illegible]	80.0	[illegible]	80.0	[illegible]
100.0	[illegible]	100.0	[illegible]	100.0	[illegible]

Expt. No. B302: x = 70 mm, y = 75 mm; C(amb) = 0.23[illegible] ppb, C(jet) = 16.5[illegible] ppb

z = 11.5 mm η (mm)	C (ppb)	z = 21.5 mm η (mm)	C (ppb)	z = 31.5 mm η (mm)	C (ppb)
0.0	[illegible]	0.0	1.477	0.0	1.477
20.0	1.783	20.0	[illegible]	20.0	2.704
30.0	1.783	30.0	[illegible]	30.0	[illegible]
40.0	1.533	40.0	[illegible]	40.0	[illegible]
50.0	2.172	50.0	[illegible]	50.0	3.423
60.0	[illegible]	60.0	3.312	60.0	[illegible]
70.0	[illegible]	70.0	[illegible]	70.0	2.812
80.0	[illegible]	80.0	1.783	80.0	1.477
100.0	0.337	100.0	[illegible]	100.0	[illegible]

Expt. No. B303: x = 1100 mm; C(amb) = 0.150 ppb, C(jet) = 17.514 ppb

z = 21.5 mm η (mm)	C (ppb)	z = 31.5 mm η (mm)	C (ppb)	z = 41.5 mm η (mm)	C (ppb)
0.0	[illegible]	0.0	[illegible]	0.0	[illegible]
30.0	[illegible]	30.0	[illegible]	30.0	[illegible]
50.0	1.185	50.0	1.213	50.0	[illegible]
60.0	1.185	60.0	1.185	60.0	[illegible]
70.0	1.185	70.0	[illegible]	70.0	[illegible]
80.0	[illegible]	80.0	[illegible]	80.0	0.981
90.0	1.101	90.0	[illegible]	90.0	[illegible]
100.0	[illegible]	100.0	[illegible]	100.0	[illegible]
110.0	[illegible]	110.0	[illegible]	110.0	[illegible]
130.0	[illegible]	130.0	[illegible]	130.0	[illegible]
150.0	[illegible]	150.0	0.518	150.0	0.453
180.0	[illegible]	180.0	0.323	180.0	[illegible]

Expt. No. B304: x = 1390 mm; C(amb) = 0.132 ppb, C(jet) = 17.514 ppb

z = 21.5 mm η (mm)	C (ppb)	z = 31.5 mm η (mm)	C (ppb)	z = 41.5 mm η (mm)	C (ppb)
0.0	[illegible]	0.0	[illegible]	0.0	[illegible]
30.0	[illegible]	30.0	[illegible]	30.0	[illegible]
50.0	1.230	50.0	1.147	50.0	[illegible]
60.0	[illegible]	60.0	1.119	60.0	[illegible]
70.0	1.175	70.0	1.091	70.0	1.027
80.0	1.147	80.0	[illegible]	80.0	0.999
90.0	[illegible]	90.0	[illegible]	90.0	0.971
100.0	[illegible]	100.0	[illegible]	100.0	0.943
110.0	[illegible]	110.0	[illegible]	110.0	0.832
130.0	[illegible]	130.0	0.730	130.0	[illegible]
150.0	[illegible]	150.0	0.563	150.0	0.526
180.0	[illegible]	180.0	[illegible]	180.0	0.332

Velocity Ratio (Uo / U) = 8 D / d = 20, d = 6.35 mm

(Concentration readings have been corrected for the ambient value)

Note: Transverse measurements are referenced from the inner boundary of the deflected jet

Experiment No. A401: x = 5 mm, y = 21 mm, Ambient Conc. = 0.079 ppb, Jet Nozzle Conc. = 15.660 ppb

z = 1.5 mm		z = 6.5 mm		z = 11.5 mm		z = 16.5 mm		z = 21.5 mm		z = 26.5 mm		z = 31.5 mm	
h (mm)	C (ppb)	h (mm)	C (ppb)	h (mm)	C (ppb)	h (mm)	C (ppb)	h (mm)	C (ppb)	h (mm)	C (ppb)	h (mm)	C (ppb)
0.0	0.009	0.0	0.009	0.0	0.009	0.0	0.009	0.0	0.000	0.0	0.009	0.0	0.000
5.0	0.009	5.0	0.009	5.0	0.009	5.0	0.009	5.0	0.009	5.0	0.009	10.0	0.000
10.0	0.009	10.0	0.009	10.0	0.009	10.0	0.009	10.0	0.000	10.0	0.009	20.0	0.000
15.0	0.009	15.0	0.009	15.0	0.009	15.0	0.009	15.0	0.009	15.0	0.009	30.0	0.009
20.0	0.018	20.0	0.009	20.0	0.026	20.0	0.018	20.0	0.009	20.0	0.018	40.0	0.009
25.0	0.018	25.0	0.009	25.0	0.026	25.0	0.026	25.0	0.018	25.0	0.018	50.0	0.000
30.0	0.114	30.0	0.095	30.0	0.070	30.0	0.053	30.0	0.053	30.0	0.026	60.0	0.000
35.0	0.959	35.0	3.147	35.0	0.194	35.0	0.088	35.0	0.070	35.0	0.035	70.0	0.000
40.0	0.783	40.0	10.654	40.0	1.172	40.0	0.114	40.0	0.062	40.0	0.035	90.0	0.000
45.0	9.932	45.0	13.267	45.0	0.757	45.0	0.106	45.0	0.070	45.0	0.009		
50.0	2.395	50.0	0.369	50.0	0.097	50.0	0.062	50.0	0.018	50.0	0.018		
55.0	0.009	55.0	0.053	55.0	0.044	55.0	0.044	55.0	0.009	55.0	0.009		
60.0	0.009	60.0	0.009	60.0	0.009	60.0	0.009	60.0	0.000	60.0	0.009		
65.0	0.009	65.0	0.000	65.0	0.000	65.0	0.009	65.0	0.000	65.0	0.009		
70.0	0.000	70.0	0.000	70.0	0.000	70.0	0.009	70.0	0.000	70.0	0.000		
75.0	0.009	75.0	0.000	75.0	0.000	75.0	0.000	75.0	0.000	75.0	0.000		
90.0	0.000	90.0	0.000	90.0	0.000	90.0	0.000	90.0	0.000	90.0	0.000		
95.0	0.000	95.0	0.000	95.0	0.000	95.0	0.000	95.0	0.000	95.0	0.000		

Velocity Ratio (U0/U) = 8   D/d = 20, d = 6.35 mm   (Concentration readings have been corrected for the ambient value)

Note: Transverse measurements are referenced from the inner boundary of the deflected jet

[illegible] No. [illegible] X = 27 mm(?), Y = 10.5 mm(?), Ambient Conc. = [illegible] ppb, Jet Nozzle Conc. = 16.187 ppb

z = 1.5 mm η (mm)	C (ppb)	z = 6.5 mm η (mm)	C (ppb)	z = 11.5 mm η (mm)	C (ppb)	z = 16.5 mm η (mm)	C (ppb)	z = 21.5 mm η (mm)	C (ppb)	z = 26.5 mm η (mm)	C (ppb)	z = 31.5 mm η (mm)	C (ppb)	z = 36.5 mm η (mm)	C (ppb)	z = 46.5 mm η (mm)	C (ppb)	z = 56.5 mm η (mm)	C (ppb)
0.0	0.000	0.0	0.000	0.0	0.000	0.0	0.000	0.0	0.000	0.0	0.000	0.0	0.009	0.0	0.000	0.0	0.000	0.0	0.000
10.0	0.000	5.0	0.000	5.0	0.000	5.0	0.000	5.0	0.000	5.0	0.000	10.0	0.018	10.0	0.009	10.0	0.000	10.0	0.000
20.0	0.035	10.0	0.000	10.0	0.000	10.0	0.018	10.0	0.026	10.0	0.026	20.0	0.053	20.0	0.026	20.0	0.009	20.0	0.000
30.0	0.300	15.0	0.000	15.0	0.026	15.0	0.339	15.0	0.035	15.0	0.035	30.0	0.150	30.0	0.044	30.0	0.009	30.0	0.000
40.0	2.015	20.0	0.000	20.0	0.299	20.0	0.282	20.0	0.106	20.0	0.079	40.0	0.132	40.0	0.035	40.0	0.009	40.0	0.000
50.0	2.404	25.0	0.300	25.0	0.800	25.0	0.739	25.0	0.440	25.0	0.176	50.0	0.053	50.0	0.018	50.0	0.000	50.0	0.000
60.0	0.125	30.0	1.320	30.0	2.181	30.0	2.280	30.0	1.282	30.0	0.475	60.0	0.009	60.0	0.000	60.0	0.000	60.0	0.000
70.0	0.000	35.0	1.505	35.0	2.563	35.0	2.730	35.0	2.085	35.0	0.986	70.0	0.009	70.0	0.000	70.0	0.000	70.0	0.000
90.0	0.000	40.0	2.571	40.0	3.516	40.0	3.599	40.0	2.285	40.0	0.600	90.0	0.009	90.0	0.000	90.0	0.000	90.0	0.000
		45.0	3.990	45.0	4.401	45.0	3.870	45.0	2.230	45.0	0.528								
		50.0	3.822	50.0	4.100	50.0	3.210	50.0	1.125	50.0	0.194								
		55.0	1.710	55.0	1.610	55.0	0.951	55.0	0.282	55.0	0.018								
		60.0	0.106	60.0	0.513	60.0	0.062	60.0	0.026	60.0	0.018								
		65.0	0.000	65.0	0.000	65.0	0.000	65.0	0.018	65.0	0.000								
		70.0	0.000	70.0	0.000	70.0	0.000	70.0	0.008	70.0	0.000								
		75.0	0.000	75.0	0.000	75.0	0.000	75.0	0.018	75.0	0.000								
		90.0	0.000	90.0	0.000	90.0	0.000	90.0	0.000	90.0	0.000								
		95.0	0.000	95.0	0.000	95.0	0.000	95.0	0.000	95.0	0.000								

[illegible] No. [illegible] X = 30 mm(?), Y = 20 mm(?), Ambient Conc. = [illegible] ppb, Jet Nozzle Conc. = 15.22[illegible] ppb

z = 1.5 mm η (mm)	C (ppb)	z = 6.5 mm η (mm)	C (ppb)	z = 11.5 mm η (mm)	C (ppb)	z = 16.5 mm η (mm)	C (ppb)	z = 21.5 mm η (mm)	C (ppb)	z = 26.5 mm η (mm)	C (ppb)	z = 31.5 mm η (mm)	C (ppb)	z = 36.5 mm η (mm)	C (ppb)	z = 46.5 mm η (mm)	C (ppb)	z = 56.5 mm η (mm)	C (ppb)
0.0	0.000	0.0	0.000	0.0	0.000	0.0	0.000	0.0	0.009	0.0	0.026	0.0	0.026	0.0	0.026	0.0	0.018	0.0	0.009
10.0	0.000	5.0	0.000	5.0	0.026	5.0	0.062	5.0	0.079	5.0	0.088	10.0	0.764	10.0	0.150	10.0	0.044	10.0	0.026
20.0	0.035	10.0	0.086	10.0	0.088	10.0	0.238	10.0	0.388	10.0	0.352	20.0	1.089	20.0	0.677	20.0	0.088	20.0	0.035
30.0	0.211	15.0	0.097	15.0	0.387	15.0	0.663	15.0	0.765	15.0	0.798	30.0	1.987	30.0	1.320	30.0	0.185	30.0	0.026
40.0	1.300	20.0	0.422	20.0	1.102	20.0	1.737	20.0	1.737	20.0	1.625	40.0	1.987	40.0	1.125	40.0	0.079	40.0	0.026
50.0	1.304	25.0	0.780	25.0	1.636	25.0	1.941	25.0	2.044	25.0	1.988	50.0	1.153	50.0	0.431	50.0	0.035	50.0	0.026
60.0	0.413	30.0	0.836	30.0	1.634	30.0	1.985	30.0	2.265	30.0	2.376	60.0	0.106	60.0	0.035	60.0	0.018	60.0	0.018
70.0	0.033	35.0	0.882	35.0	1.246	35.0	1.747	35.0	2.127	35.0	2.322	70.0	0.018	70.0	0.018	70.0	0.000	70.0	0.009
90.0	0.000	40.0	1.412	40.0	1.881	40.0	2.320	40.0	2.654	40.0	2.571	90.0	0.009	90.0	0.009	90.0	0.000	90.0	0.000
		45.0	1.600	45.0	2.083	45.0	2.470	45.0	2.572	45.0	2.461								
		50.0	1.486	50.0	2.218	50.0	2.348	50.0	2.348	50.0	1.988								
		55.0	0.936	55.0	1.274	55.0	1.663	55.0	1.460	55.0	1.126								
		60.0	0.430	60.0	0.633	60.0	0.500	60.0	0.501	60.0	0.264								
		65.0	0.079	65.0	0.123	65.0	0.150	65.0	0.079	65.0	0.026								
		70.0	0.000	70.0	0.008	70.0	0.000	70.0	0.018	70.0	0.000								
		75.0	0.000	75.0	0.000	75.0	0.000	75.0	0.000	75.0	0.000								
		90.0	0.000	90.0	0.000	90.0	0.000	90.0	0.000	90.0	0.000								
		95.0	0.000	95.0	0.000	95.0	0.009	95.0	0.000	95.0	0.000								

Velocity Ratio (Ub/U) = 8 D/d = 20, d = 6.35 mm (Concentration readings have been corrected for the ambient value)

Note: Transverse measurements are referenced from the inner boundary of the deflected jet

Experiment No. A404: x = 120 mm, y = 107.9 mm, Ambient Conc. = 0.085 ppb, Jet Nozzle Conc. = 16.187 ppb

z = 1.5 mm		z = 6.5 mm		z = 11.5 mm		z = 16.5 mm		z = 21.5 mm		z = 26.5 mm		z = 31.5 mm		z = 36.5 mm		z = 46.5 mm		z = 66.5 mm		z = 91.5 mm	
η (mm)	C (ppb)	η (mm)	C (ppb)	η (mm)	C (ppb)	η (mm)	C (ppb)	η (mm)	C (ppb)	η (mm)	C (ppb)	η (mm)	C (ppb)	η (mm)	C (ppb)	η (mm)	C (ppb)	η (mm)	C (ppb)	η (mm)	C (ppb)
0.0	0.000	0.0	0.000	0.0	0.026	0.0	0.035	0.0	0.114	0.0	0.317	0.0	0.352	0.0	0.545	0.0	0.651	0.0	0.220	0.0	0.000
20.0	0.000	20.0	0.106	5.0	0.000	5.0	0.343	5.0	0.616	5.0	0.897	20.0	1.374	20.0	1.402	20.0	1.249	20.0	0.748	20.0	0.018
30.0	0.044	30.0	0.141	20.0	0.396	20.0	0.387	20.0	0.924	20.0	1.337	30.0	1.457	30.0	1.457	30.0	1.117	30.0	0.845	30.0	0.035
40.0	0.220	40.0	0.176	25.0	0.457	25.0	1.047	25.0	1.320	25.0	1.459	40.0	1.068	40.0	1.040	40.0	0.880	40.0	0.827	40.0	0.044
50.0	0.361	50.0	0.317	30.0	0.449	30.0	0.440	30.0	0.959	30.0	1.337	50.0	0.512	50.0	0.568	50.0	0.686	50.0	0.739	50.0	0.026
60.0	0.308	60.0	0.352	35.0	0.317	35.0	0.766	35.0	0.986	35.0	1.288	60.0	0.484	60.0	0.589	60.0	0.651	60.0	0.528	60.0	0.009
70.0	0.282	70.0	0.308	40.0	0.308	40.0	0.308	40.0	0.537	40.0	0.792	70.0	0.405	70.0	0.466	[illegible]	0.475	70.0	0.299	70.0	0.000
80.0	0.158	80.0	0.211	45.0	0.229	45.0	0.343	45.0	0.466	45.0	0.519	80.0	0.211	80.0	0.255	80.0	0.220	80.0	0.097	80.0	0.000
90.0	0.079	90.0	0.000	50.0	0.290	50.0	0.317	50.0	0.334	50.0	0.405	90.0	0.079	90.0	0.079	90.0	0.062	90.0	0.018	90.0	0.000
				55.0	0.317	55.0	0.334	55.0	0.374	55.0	0.440										
				60.0	0.352	60.0	0.343	60.0	0.378	60.0	0.405										
				65.0	0.290	65.0	0.299	65.0	0.347	65.0	0.378										
				70.0	0.282	70.0	0.264	70.0	0.290	70.0	0.308										
				75.0	0.158	75.0	0.185	75.0	0.220	75.0	0.238										
				80.0	0.158	80.0	0.141	80.0	0.158	80.0	0.167										
				85.0	0.062	85.0	0.062	85.0	0.088	85.0	0.088										
				90.0	0.070	90.0	0.053	90.0	0.053	90.0	0.062										
				95.0	0.000	95.0	0.000	95.0	0.009	95.0	0.026										

Experiment No. A405: x = 300 mm, y = 133 mm, Ambient Conc. = 0.070 ppb, Jet Nozzle Conc. = 17.155 ppb

z = 1.5 mm		z = 11.5 mm		z = 21.5 mm		z = 26.5 mm		z = 31.5 mm		z = 36.5 mm		z = 41.5 mm		z = 46.5 mm		z = 66.5 mm		z = 91.5 mm		z = 121.5 mm	
η (mm)	C (ppb)	η (mm)	C (ppb)	η (mm)	C (ppb)	η (mm)	C (ppb)	η (mm)	C (ppb)	η (mm)	C (ppb)	η (mm)	C (ppb)	η (mm)	C (ppb)	η (mm)	C (ppb)	η (mm)	C (ppb)	η (mm)	C (ppb)
0.0	0.000	0.0	0.000	0.0	0.018	0.0	0.035	0.0	0.026	0.0	0.026	0.0	0.026	0.0	0.035	0.0	0.026	0.0	0.000	0.0	0.000
20.0	0.000	20.0	0.035	20.0	0.088	20.0	0.132	20.0	0.194	20.0	0.229	20.0	0.282	20.0	0.290	20.0	0.246	20.0	0.079	20.0	0.000
40.0	0.044	40.0	0.158	40.0	0.422	40.0	0.545	40.0	0.616	40.0	0.660	40.0	0.677	40.0	0.651	40.0	0.475	40.0	0.229	40.0	0.000
50.0	0.070	50.0	0.273	50.0	0.625	50.0	0.713	50.0	0.765	50.0	0.783	50.0	0.783	50.0	0.748	50.0	0.510	50.0	0.273	50.0	0.018
60.0	0.097	60.C	0.361	60.0	0.739	60.0	0.880	60.0	0.880	60.0	0.915	60.0	0.933	60.0	0.889	60.0	0.501	60.0	0.290	60.0	0.026
70.0	0.106	70.0	0.405	70.0	0.792	70.0	0.897	70.0	0.985	70.0	1.064	70.0	1.082	70.0	1.064	70.0	0.475	70.0	0.273	70.0	0.018
80.0	0.114	80.0	0.300	80.0	0.765	80.0	0.862	80.0	0.977	80.0	1.029	80.0	1.021	80.0	1.021	80.0	0.431	80.0	0.246	80.0	0.018
90.0	0.167	90.0	0.308	90.0	0.616	90.0	0.721	90.0	0.871	90.0	0.818	90.0	0.765	90.0	0.774	90.0	0.352	90.0	0.194	90.0	0.009
100.0	0.211	100.0	0.238	100.0	0.387	100.0	0.440	100.0	0.589	100.0	0.484	100.0	0.475	100.0	0.466	100.0	0.273	100.0	0.141	100.0	0.000
120.0	0.185	120.0	0.176	120.0	0.176	120.0	0.176	120.0	0.220	120.0	0.185	120.0	0.185	120.0	0.185	120.0	0.158	120.0	0.062	120.0	0.000
140.0	0.106	140.0	0.088	140.0	0.070	140.0	0.070	140.0	0.088	140.0	0.062	140.0	0.062	140.0	0.053	140.0	0.035	140.0	0.009	140.0	0.000
170.0	0.018	170.0	0.000	170.0	0.000	170.0	0.000	170.0	0.009	170.0	0.000	170.0	0.000	170.0	0.000	170.0	0.000	170.0	0.000	170.0	0.000

Velocity Ratio (Uo / U) = 8 D / d = 20, d = 6.35 mm (Concentration readings have been corrected for the ambient value)

Note: Transverse measurements are referenced from the inner boundary of the deflected jet

Experiment No. A406: x = 500 mm, y = 147 mm, Ambient Conc. = 0.053 ppb, Jet Nozzle Conc. = 17.792 ppb

z = 1.5 mm η (mm)	C (ppb)	z = 11.5 mm η (mm)	C (ppb)	z = 21.5 mm η (mm)	C (ppb)	z = 26.5 mm η (mm)	C (ppb)	z = 31.5 mm η (mm)	C (ppb)
0.0	0.053	0.0	0.141	0.0	0.246	0.0	0.326	0.0	0.361
20.0	0.097	20.0	0.255	20.0	0.405	20.0	0.475	20.0	0.519
40.0	0.158	40.0	0.343	40.0	0.501	40.0	0.598	40.0	0.686
50.0	0.185	50.0	0.361	50.0	0.510	50.0	0.598	50.0	0.677
60.0	0.185	60.0	0.317	60.0	0.457	60.0	0.519	60.0	0.563
70.0	0.194	70.0	0.273	70.0	0.343	70.0	0.422	70.0	0.422
80.0	0.176	80.0	0.220	80.0	0.246	80.0	0.290	80.0	0.282
90.0	0.141	90.0	0.176	90.0	0.176	90.0	0.202	90.0	0.194
100.0	0.114	100.0	0.123	100.0	0.114	100.0	0.141	100.0	0.132
120.0	0.070	120.0	0.062	120.0	0.053	120.0	0.053	120.0	0.053
140.0	0.026	140.0	0.026	140.0	0.009	140.0	0.018	140.0	0.000
170.0	0.000	170.0	0.000	170.0	0.000	170.0	0.000	170.0	0.000

z = 36.5 mm η (mm)	C (ppb)	z = 41.5 mm η (mm)	C (ppb)	z = 46.5 mm η (mm)	C (ppb)	z = 66.5 mm η (mm)	C (ppb)	z = 91.5 mm η (mm)	C (ppb)	z = 121.5 mm η (mm)	C (ppb)
0.0	0.387	0.0	0.396	0.0	0.387	0.0	0.352	0.0	0.185	0.0	0.062
20.0	0.554	20.0	0.554	20.0	0.501	20.0	0.422	20.0	0.238	20.0	0.079
40.0	0.748	40.0	0.792	40.0	0.792	40.0	0.475	40.0	0.220	40.0	0.079
50.0	0.704	50.0	0.748	50.0	0.739	50.0	0.422	50.0	0.282	50.0	0.070
60.0	0.589	60.0	0.607	60.0	0.501	60.0	0.308	60.0	0.185	60.0	0.053
70.0	0.413	70.0	0.431	70.0	0.405	70.0	0.282	70.0	0.158	70.0	0.044
80.0	0.290	80.0	0.290	80.0	0.264	80.0	0.220	80.0	0.123	80.0	0.035
90.0	0.202	90.0	0.202	90.0	0.176	90.0	0.176	90.0	0.079	90.0	0.026
100.0	0.132	100.0	0.132	100.0	0.123	100.0	0.123	100.0	0.044	100.0	0.009
120.0	0.053	120.0	0.062	120.0	0.044	120.0	0.044	120.0	0.000	120.0	0.000
140.0	0.000	140.0	0.018	140.0	0.000	140.0	0.000	140.0	0.000	140.0	0.000
170.0	0.000	170.0	0.000	170.0	0.000	170.0	0.000	170.0	0.000	170.0	0.000

Experiment No. A407: x = 1000 mm, y = 165.7 mm, Ambient Conc. = 0.062 ppb, Jet Nozzle Conc. = 16.68 ppb

z = 1.5 mm η (mm)	C (ppb)	z = 11.5 mm η (mm)	C (ppb)	z = 21.5 mm η (mm)	C (ppb)	z = 26.5 mm η (mm)	C (ppb)	z = 31.5 mm η (mm)	C (ppb)
0.0	0.062	0.0	0.070	0.0	0.079	0.0	0.106	0.0	0.097
20.0	0.079	20.0	0.114	20.0	0.132	20.0	0.158	20.0	0.176
40.0	0.114	40.0	0.158	40.0	0.202	40.0	0.220	40.0	0.220
50.0	0.132	50.0	0.194	50.0	0.220	50.0	0.255	50.0	0.255
60.0	0.141	60.0	0.202	60.0	0.246	60.0	0.273	60.0	0.273
70.0	0.167	70.0	0.220	70.0	0.273	70.0	0.290	70.0	0.308
80.0	0.176	80.0	0.229	80.0	0.282	80.0	0.317	80.0	0.317
90.0	0.185	90.0	0.238	90.0	0.299	90.0	0.326	90.0	0.326
100.0	0.202	100.0	0.246	100.0	0.299	100.0	0.317	100.0	0.343
120.0	0.220	120.0	0.220	120.0	0.264	120.0	0.282	120.0	0.299
140.0	0.194	140.0	0.211	140.0	0.211	140.0	0.282	140.0	0.211
170.0	0.088	170.0	0.088	170.0	0.079	170.0	0.079	170.0	0.070

z = 36.5 mm η (mm)	C (ppb)	z = 41.5 mm η (mm)	C (ppb)	z = 46.5 mm η (mm)	C (ppb)	z = 66.5 mm η (mm)	C (ppb)	z = 91.5 mm η (mm)	C (ppb)	z = 121.5 mm η (mm)	C (ppb)
0.0	0.106	0.0	0.114	0.0	0.114	0.0	0.114	0.0	0.106	0.0	0.062
20.0	0.176	20.0	0.185	20.0	0.185	20.0	0.176	20.0	0.167	20.0	0.132
40.0	0.238	40.0	0.229	40.0	0.229	40.0	0.229	40.0	0.194	40.0	0.167
50.0	0.264	50.0	0.264	50.0	0.264	50.0	0.246	50.0	0.194	50.0	0.158
60.0	0.290	60.0	0.299	60.0	0.290	60.0	0.255	60.0	0.194	60.0	0.158
70.0	0.326	70.0	0.334	70.0	0.334	70.0	0.308	70.0	0.194	70.0	0.141
80.0	0.343	80.0	0.361	80.0	0.370	80.0	0.334	80.0	0.194	80.0	0.123
90.0	0.361	90.0	0.387	90.0	0.387	90.0	0.343	90.0	0.185	90.0	0.114
100.0	0.361	100.0	0.378	100.0	0.387	100.0	0.317	100.0	0.176	100.0	0.097
120.0	0.317	120.0	0.317	120.0	0.317	120.0	0.229	120.0	0.132	120.0	0.070
140.0	0.211	140.0	0.211	140.0	0.282	140.0	0.132	140.0	0.079	140.0	0.044
170.0	0.088	170.0	0.079	170.0	0.070	170.0	0.044	170.0	0.035	170.0	0.009

Velocity Ratio (Uo / U) = 8 D / d = 20, d = 6.35 mm (Concentration readings have been corrected for the ambient value)

Note: Transverse measurements are referenced from the inner boundary of the deflected jet

Experiment No. A409: x = 4000 mm, y = 203 mm, Ambient Conc. = 0.070 ppb, Jet Nozzle Conc. = 16.124 ppb

z = 1.5 mm		z = 6.5 mm		z = 16.5 mm		z = 26.5 mm		z = 31.5 mm		z = 36.5 mm		z = 46.5 mm		z = 66.5 mm		z = 96.5 mm		z = 121.5 mm	
η (mm)	C (ppb)	η (mm)	C (ppb)	η (mm)	C (ppb)	η (mm)	C (ppb)	η (mm)	C (ppb)	η (mm)	C (ppb)	η (mm)	C (ppb)	η (mm)	C (ppb)	η (mm)	C (ppb)	η (mm)	C (ppb)
0.0	0.123	0.0	0.123	0.0	0.114	0.0	0.114	0.0	0.123	0.0	0.106	0.0	0.123	0.0	0.106	0.0	0.088	0.0	0.088
20.0	0.123	20.0	0.123	20.0	0.114	20.0	0.123	20.0	0.123	20.0	0.114	20.0	0.123	20.0	0.106	20.0	0.097	20.0	0.088
40.0	0.132	40.0	0.132	40.0	0.123	40.0	0.132	40.0	0.123	40.0	0.123	40.0	0.123	40.0	0.106	40.0	0.097	40.0	0.088
50.0	0.132	50.0	0.132	50.0	0.123	50.0	0.132	50.0	0.132	50.0	0.123	50.0	0.123	50.0	0.114	50.0	0.097	50.0	0.079
60.0	0.132	60.0	0.132	60.0	0.123	60.0	0.132	60.0	0.132	60.0	0.123	60.0	0.123	60.0	0.106	60.0	0.088	60.0	0.079
70.0	0.132	70.0	0.132	70.0	0.123	70.0	0.141	70.0	0.132	70.0	0.123	70.0	0.123	70.0	0.106	70.0	0.088	70.0	0.070
80.0	0.132	80.0	0.132	80.0	0.123	80.0	0.141	80.0	0.132	80.0	0.123	80.0	0.123	80.0	0.097	80.0	0.079	80.0	0.070
90.0	0.132	90.0	0.132	90.0	0.123	90.0	0.141	90.0	0.132	90.0	0.123	90.0	0.114	90.0	0.088	90.0	0.079	90.0	0.062
100.0	0.132	100.0	0.132	100.0	0.123	100.0	0.132	100.0	0.123	100.0	0.114	100.0	0.114	100.0	0.088	100.0	0.079	100.0	0.062
120.0	0.123	120.0	0.123	120.0	0.106	120.0	0.123	120.0	0.114	120.0	0.106	120.0	0.097	120.0	0.079	120.0	0.070	120.0	0.053
140.0	0.097	140.0	0.097	140.0	0.088	140.0	0.097	140.0	0.088	140.0	0.088	140.0	0.079	140.0	0.070	140.0	0.062	140.0	0.044
170.0	0.070	170.0	0.062	170.0	0.062	170.0	0.070	170.0	0.062	170.0	0.070	170.0	0.053	170.0	0.053	170.0	0.044	170.0	0.026

Experiment No. A408: x = 1500 mm, y = 177 mm, Ambient Conc. = 0.070 ppb, Jet Nozzle Conc. = 19.182 ppb

z = 1.5 mm		z = 11.5 mm		z = 21.5 mm		z = 26.5 mm		z = 31.5 mm		z = 36.5 mm		z = 41.5 mm		z = 46.5 mm		z = 66.5 mm		z = 91.5 mm		z = 121.5 mm	
η (mm)	C (ppb)	η (mm)	C (ppb)	η (mm)	C (ppb)	η (mm)	C (ppb)	η (mm)	C (ppb)	η (mm)	C (ppb)	η (mm)	C (ppb)	η (mm)	C (ppb)	η (mm)	C (ppb)	η (mm)	C (ppb)	η (mm)	C (ppb)
0.0	0.141	0.0	0.167	0.0	0.185	0.0	0.185	0.0	0.202	0.0	0.211	0.0	0.211	0.0	0.211	0.0	0.202	0.0	0.176	0.0	0.158
20.0	0.167	20.0	0.185	20.0	0.211	20.0	0.211	20.0	0.229	20.0	0.229	20.0	0.238	20.0	0.238	20.0	0.229	20.0	0.176	20.9	0.158
40.0	0.194	40.0	0.202	40.0	0.229	40.0	0.246	40.0	0.264	40.0	0.264	40.0	0.273	40.0	0.282	40.0	0.255	40.0	0.176	40.0	0.141
50.0	0.202	50.0	0.211	50.0	0.246	50.0	0.255	50.0	0.273	50.0	0.273	50.0	0.273	50.0	0.282	50.0	0.255	50.0	0.176	50.0	0.123
60.0	0.202	60.0	0.220	60.0	0.246	60.0	0.255	60.0	0.273	60.0	0.273	60.0	0.273	60.0	0.282	60.0	0.255	60.0	0.167	60.0	0.114
70.0	0.211	70.0	0.220	70.0	0.246	70.0	0.255	70.0	0.273	70.0	0.273	70.0	0.273	70.0	0.273	70.0	0.238	70.0	0.158	70.0	0.097
80.0	0.220	80.0	0.220	80.0	0.238	80.0	0.238	80.0	0.264	80.0	0.264	80.0	0.264	80.0	0.264	80.0	0.211	80.0	0.141	80.0	0.088
90.0	0.220	90.0	0.220	90.0	0.238	90.0	0.229	90.0	0.246	90.0	0.246	90.0	0.238	90.0	0.229	90.0	0.194	90.0	0.123	90.0	0.079
100.0	0.220	100.0	0.211	100.0	0.220	100.0	0.211	100.0	0.211	100.0	0.220	100.0	0.202	100.0	0.211	100.0	0.176	100.0	0.097	100.0	0.070
120.0	0.185	120.0	0.158	120.0	0.167	120.0	0.158	120.0	0.141	120.0	0.158	120.0	0.141	120.0	0.141	120.0	0.106	120.0	0.062	120.0	0.053
140.0	0.097	140.0	0.088	140.0	0.079	140.0	0.079	140.0	0.079	140.0	0.088	140.0	0.070	140.0	0.079	140.0	0.062	140.0	0.026	140.0	0.026
170.0	0.035	170.0	0.035	170.0	0.035	170.0	0.026	170.0	0.026	170.0	0.035	170.0	0.026	170.0	0.026	170.0	0.018	170.0	0.000	170.0	0.000

Velocity Ratio (Uo / U) = 12 D / d = 20, d = 6.35 mm

(Concentration readings have been corrected for the ambient value)

Note: Traverse measurements are referenced from the inner boundary of the deflected jet

[illegible] No. [illegible], x = [illegible] mm, y = 33.5 mm, Ambient Conc. = 0.004 ppb, Jet Nozzle Conc. = 17.514 ppb

z = 1.5 mm η (mm)	C (ppb)	z = 6.5 mm η (mm)	C (ppb)	z = 11.5 mm η (mm)	C (ppb)	z = 16.5 mm η (mm)	C (ppb)	z = 21.5 mm η (mm)	C (ppb)	z = 26.5 mm η (mm)	C (ppb)	z = 31.5 mm η (mm)	C (ppb)
0.0	0.000	0.0	0.000	0.0	0.000	0.0	0.000	0.0	0.000	0.0	0.000	0.0	0.000
10.0	0.000	5.0	0.000	5.0	0.000	5.0	0.000	5.0	0.000	5.0	0.000	10.0	0.000
20.0	0.079	10.0	0.000	10.0	0.000	10.0	0.000	10.0	0.000	10.0	0.000	20.0	0.000
30.0	1.200	15.0	0.000	15.0	0.000	15.0	0.000	15.0	0.000	15.0	0.000	30.0	0.000
40.0	6.006	20.0	0.005	20.0	0.206	20.0	0.000	20.0	0.000	20.0	0.000	40.0	0.000
50.0	0.588	25.0	0.475	25.0	0.202	25.0	0.000	25.0	0.000	25.0	0.000	50.0	0.000
60.0	0.000	30.0	2.900	30.0	1.429	30.0	0.026	30.0	0.009	30.0	0.009	60.0	0.000
70.0	0.000	35.0	5.226	35.0	3.302	35.0	0.132	35.0	0.009	35.0	0.009	70.0	0.000
90.0	0.000	40.0	11.217	40.0	5.322	40.0	0.141	40.0	0.009	40.0	0.009	90.0	0.000
		45.0	9.888	45.0	1.996	45.0	0.018	45.0	0.000	45.0	0.000		
		50.0	0.420	50.0	0.018	50.0	0.000	50.0	0.000	50.0	0.000		
		55.0	0.000	55.0	0.000	55.0	0.000	55.0	0.000	55.0	0.000		
		60.0	0.000	60.0	0.000	60.0	0.000	60.0	0.000	60.0	0.000		
		65.0	0.000	65.0	0.000	65.0	0.000	65.0	0.000	65.0	0.000		
		70.0	0.000	70.0	0.000	70.0	0.000	70.0	0.000	70.0	0.000		
		75.0	0.000	75.0	0.000	75.0	0.000	75.0	0.000	75.0	0.000		
		90.0	0.000	90.0	0.000	90.0	0.000	90.0	0.000	90.0	0.000		
		95.0	0.000	95.0	0.000	95.0	0.000	95.0	0.000	95.0	0.000		

[illegible] No. [illegible], x = 15 mm, y = 76.6 mm, Ambient Conc. = 0.053 ppb, Jet Nozzle Conc. = 17.514 ppb

z = 1.5 mm η (mm)	C (ppb)	z = 6.5 mm η (mm)	C (ppb)	z = 11.5 mm η (mm)	C (ppb)	z = 16.5 mm η (mm)	C (ppb)	z = 21.5 mm η (mm)	C (ppb)	z = 26.5 mm η (mm)	C (ppb)	z = 31.5 mm η (mm)	C (ppb)	z = 36.5 mm η (mm)	C (ppb)	z = 46.5 mm η (mm)	C (ppb)
0.0	[illegible]	0.0	[illegible]	0.0	0.035	0.0	0.053	0.0	0.062	0.0	0.106	0.0	0.044	0.0	0.026	0.0	0.000
10.0	0.070	5.0	0.044	5.0	0.062	5.0	0.088	5.0	0.070	5.0	0.070	10.0	0.326	10.0	0.167	10.0	0.009
20.0	0.206	10.0	0.123	10.0	0.273	10.0	0.475	10.0	0.625	10.0	0.606	20.0	0.977	20.0	0.413	20.0	0.026
30.0	[illegible]	15.0	0.290	15.0	0.633	15.0	1.088	15.0	0.853	15.0	0.660	30.0	1.364	30.0	0.475	30.0	0.053
40.0	3.000	20.0	0.800	20.0	1.500	20.0	1.949	20.0	2.080	20.0	1.865	40.0	0.801	40.0	0.194	40.0	0.202
50.0	3.255	25.0	1.276	25.0	2.005	25.0	2.588	25.0	2.332	25.0	1.859	50.0	0.062	50.0	0.018	50.0	0.000
60.0	1.421	30.0	1.702	30.0	2.609	30.0	3.311	30.0	3.172	30.0	2.580	60.0	0.000	60.0	0.000	60.0	0.000
70.0	0.114	35.0	2.628	35.0	3.508	35.0	3.870	35.0	3.277	35.0	2.388	70.0	0.000	70.0	0.000	70.0	0.000
90.0	0.000	40.0	3.978	40.0	4.117	40.0	4.080	40.0	3.367	40.0	1.977	90.0	0.000	90.0	0.000	90.0	0.000
		45.0	4.008	45.0	4.092	45.0	3.620	45.0	2.582	45.0	1.248						
		50.0	2.977	50.0	2.727	50.0	1.977	50.0	0.976	50.0	0.336						
		55.0	1.432	55.0	1.034	55.0	0.673	55.0	0.247	55.0	0.053						
		60.0	0.457	60.0	0.211	60.0	0.062	60.0	0.018	60.0	0.000						
		65.0	0.079	65.0	0.000	65.0	0.000	65.0	0.000	65.0	0.000						
		70.0	0.000	70.0	0.009	70.0	0.000	70.0	0.000	70.0	0.000						
		75.0	0.000	75.0	0.000	75.0	0.000	75.0	0.000	75.0	0.000						
		90.0	0.000	90.0	0.000	90.0	0.000	90.0	0.000	90.0	0.000						
		95.0	0.000	95.0	0.000	95.0	0.009	95.0	0.000	95.0	0.000						

Velocity Ratio (U0/U) = 12 D/d = 28, d = 6.35 mm

(Concentration readings have been corrected for the ambient value)

Note: Transverse measurements are referenced from the inner boundary of the deflected jet

[illegible] Y = [illegible] mm, Ambient Conc. = [illegible] ppb, Jet Nozzle Conc. = 21.884 ppb

z = 1.5 mm η (mm)	C (ppb)	z = 6.5 mm η (mm)	C (ppb)	z = 11.5 mm η (mm)	C (ppb)	z = 16.5 mm η (mm)	C (ppb)	z = 21.5 mm η (mm)	C (ppb)	z = 26.5 mm η (mm)	C (ppb)
0.0	[illegible]	0.0	[illegible]	0.0	[illegible]	0.0	0.035	0.0	0.053	0.0	0.053
10.0	0.053	5.0	0.035	5.0	0.035	5.0	0.035	5.0	0.079	5.0	0.088
20.0	0.106	10.0	0.053	10.0	0.114	10.0	0.185	10.0	0.352	10.0	0.405
30.0	0.326	15.0	0.097	15.0	0.246	15.0	0.334	15.0	0.537	15.0	0.616
40.0	0.801	20.0	0.264	20.0	0.616	20.0	1.073	20.0	1.405	20.0	1.467
50.0	2.238	25.0	0.440	25.0	1.052	25.0	1.400	25.0	1.821	25.0	1.785
60.0	2.830	30.0	0.941	30.0	1.000	30.0	2.301	30.0	2.663	30.0	2.635
70.0	1.804	35.0	1.061	35.0	1.302	35.0	2.322	35.0	2.800	35.0	2.619
90.0	0.670	40.0	1.301	40.0	2.023	40.0	2.524	40.0	3.004	40.0	3.135
		45.0	1.644	45.0	2.192	45.0	2.711	45.0	3.072	45.0	3.147
		50.0	2.579	50.0	2.941	50.0	3.219	50.0	3.413	50.0	3.247
		55.0	2.704	55.0	2.970	55.0	3.239	55.0	3.128	55.0	2.925
		60.0	2.941	60.0	2.996	60.0	3.052	60.0	2.774	60.0	2.413
		65.0	2.423	65.0	2.275	65.0	2.350	65.0	1.908	65.0	1.704
		70.0	1.551	70.0	1.328	70.0	1.134	70.0	0.828	70.0	0.550
		75.0	0.922	75.0	0.496	75.0	0.459	75.0	0.292	75.0	0.200
		90.0	0.018	90.0	0.000	90.0	0.000	90.0	0.000	90.0	0.000
		95.0	0.000	95.0	0.000	95.0	0.000	95.0	0.000	95.0	0.000

z = 31.5 mm η (mm)	C (ppb)	z = 36.5 mm η (mm)	C (ppb)	z = 46.5 mm η (mm)	C (ppb)	z = 66.5 mm η (mm)	C (ppb)
0.0	[illegible]	0.0	0.053	0.0	0.018	0.0	[illegible]
10.0	0.475	10.0	0.290	10.0	0.114	10.0	0.000
20.0	1.523	20.0	1.056	20.0	0.387	20.0	0.009
30.0	2.496	30.0	1.931	30.0	0.660	30.0	0.009
40.0	2.885	40.0	2.404	40.0	0.748	40.0	0.009
50.0	2.718	50.0	1.987	50.0	0.387	50.0	0.000
60.0	1.634	60.0	0.986	60.0	0.088	60.0	0.000
70.0	0.272	70.0	0.106	70.0	0.009	70.0	0.000
90.0	0.000	90.0	0.000	90.0	0.000	90.0	0.000

[illegible] Y = [illegible] mm, Ambient Conc. = [illegible] ppb, Jet Nozzle Conc. = 21.128 ppb

z = 1.5 mm η (mm)	C (ppb)	z = 6.5 mm η (mm)	C (ppb)	z = 11.5 mm η (mm)	C (ppb)	z = 16.5 mm η (mm)	C (ppb)	z = 21.5 mm η (mm)	C (ppb)	z = 26.5 mm η (mm)	C (ppb)
0.0	[illegible]	0.0	[illegible]	0.0	0.070	0.0	0.141	0.0	0.220	0.0	0.158
10.0	0.044	5.0	0.053	5.0	0.158	5.0	0.413	5.0	0.677	5.0	0.831
20.0	0.106	10.0	0.079	10.0	0.229	10.0	0.493	10.0	0.827	10.0	1.144
30.0	0.220	15.0	0.141	15.0	0.413	15.0	1.086	15.0	1.423	15.0	1.665
40.0	0.739	20.0	0.255	20.0	0.677	20.0	1.236	20.0	1.625	20.0	1.895
50.0	1.584	25.0	0.352	25.0	0.846	25.0	1.479	25.0	1.757	25.0	1.943
60.0	1.987	30.0	0.405	30.0	1.082	30.0	1.514	30.0	1.876	30.0	2.054
70.0	1.025	35.0	0.598	35.0	0.987	35.0	1.312	35.0	1.590	35.0	1.832
90.0	0.406	40.0	0.801	40.0	1.000	40.0	1.375	40.0	1.681	40.0	1.978
		45.0	1.182	45.0	1.340	45.0	1.590	45.0	1.701	45.0	1.915
		50.0	1.514	50.0	1.625	50.0	1.764	50.0	1.951	50.0	2.061
		55.0	1.766	55.0	1.766	55.0	1.757	55.0	1.813	55.0	1.776
		60.0	1.876	60.0	1.848	60.0	1.985	60.0	1.820	60.0	1.811
		65.0	1.710	65.0	1.571	65.0	1.340	65.0	1.340	65.0	1.164
		70.0	1.570	70.0	1.431	70.0	1.347	70.0	1.125	70.0	0.977
		75.0	1.182	75.0	0.932	75.0	0.478	75.0	0.586	75.0	0.317
		90.0	0.387	90.0	0.205	90.0	0.097	90.0	0.079	90.0	0.018
		95.0	0.220	95.0	0.053	95.0	0.009	95.0	0.000	95.0	0.000

z = 31.5 mm η (mm)	C (ppb)	z = 36.5 mm η (mm)	C (ppb)	z = 46.5 mm η (mm)	C (ppb)	z = 66.5 mm η (mm)	C (ppb)
0.0	0.440	0.0	0.510	0.0	0.300	0.0	0.035
10.0	1.394	10.0	1.405	10.0	0.996	10.0	0.132
20.0	2.086	20.0	1.987	20.0	1.497	20.0	0.220
30.0	2.000	30.0	2.126	30.0	1.747	30.0	0.246
40.0	2.000	40.0	2.154	40.0	1.747	40.0	0.282
50.0	2.034	50.0	1.931	50.0	1.338	50.0	0.088
60.0	1.589	60.0	1.431	60.0	0.185	60.0	0.026
70.0	0.671	70.0	0.537	70.0	0.185	70.0	0.000
90.0	0.000	90.0	0.035	90.0	0.000	90.0	0.000

Velocity Ratio (U0 / U) = 12   D / d = 28, d = 6.35 mm   (Concentration readings have been corrected for the ambient value)

Note: Transverse measurements are referenced from the inner boundary of the deflected jet

[illegible] x = 100 mm, y = 158.5 mm, Ambient Conc. = 0.100 ppb, Jet Nozzle Conc. = 18.626 ppb

z = 1.5 mm η (mm)	C (ppb)	z = 11.5 mm η (mm)	C (ppb)	z = 21.5 mm η (mm)	C (ppb)	z = 31.5 mm η (mm)	C (ppb)	z = 36.5 mm η (mm)	C (ppb)
0.0	0.000	0.0	0.388	0.0	1.012	0.0	1.396	0.0	1.387
10.0	0.026	10.0	0.396	10.0	1.145	5.0	1.378	5.0	1.425
20.0	0.123	20.0	0.404	20.0	1.118	10.0	1.479	10.0	1.470
30.0	0.357	30.0	0.422	30.0	0.812	15.0	1.350	15.0	1.314
40.0	0.606	40.0	0.598	40.0	0.756	20.0	1.308	20.0	1.276
50.0	0.924	50.0	0.880	50.0	0.867	25.0	1.044	25.0	1.036
60.0	1.021	60.0	0.924	60.0	0.812	30.0	0.979	30.0	1.053
70.0	0.980	70.0	0.774	70.0	0.580	35.0	0.850	35.0	0.897
90.0	0.537	90.0	0.246	90.0	0.097	40.0	0.885	40.0	0.942
						45.0	0.850	45.0	0.841
						50.0	0.840	50.0	0.831
						55.0	0.786	55.0	0.674
						60.0	0.701	60.0	0.664
						65.0	0.461	65.0	0.424
						70.0	0.413	70.0	0.352
						75.0	0.282	75.0	0.167
						90.0	0.044	90.0	0.066
						95.0	0.018	95.0	0.000

z = 41.5 mm η (mm)	C (ppb)	z = 46.5 mm η (mm)	C (ppb)	z = 51.5 mm η (mm)	C (ppb)	z = 66.5 mm η (mm)	C (ppb)	z = 86.5 mm η (mm)	C (ppb)
0.0	1.331	0.0	1.383	0.0	1.220	0.0	0.757	0.0	0.114
5.0	1.300	5.0	1.300	5.0	1.249	10.0	0.941	10.0	0.167
10.0	1.442	10.0	1.387	10.0	1.331	20.0	0.889	20.0	0.141
15.0	1.300	15.0	1.341	15.0	1.277	30.0	0.748	30.0	0.106
20.0	1.331	20.0	1.276	20.0	1.276	40.0	0.545	40.0	0.062
25.0	1.282	25.0	1.175	25.0	1.138	50.0	0.326	50.0	0.026
30.0	1.100	30.0	1.137	30.0	1.137	60.0	0.167	60.0	0.009
35.0	1.036	35.0	1.036	35.0	0.999	70.0	0.044	70.0	0.000
40.0	0.998	40.0	0.998	40.0	0.970	90.0	0.000	90.0	0.000
45.0	0.924	45.0	0.800	45.0	0.777				
50.0	0.886	50.0	0.885	50.0	0.747				
55.0	0.758	55.0	0.646	55.0	0.554				
60.0	0.664	60.0	0.553	60.0	0.400				
65.0	0.400	65.0	0.343	65.0	0.282				
70.0	0.308	70.0	0.246	70.0	0.185				
75.0	0.150	75.0	0.132	75.0	0.000				
90.0	0.000	90.0	0.000	90.0	0.000				
95.0	0.000	95.0	0.000	95.0	0.000				

[illegible] x = 150 mm, y = 175 mm, Ambient Conc. = 0.063 ppb, Jet Nozzle Conc. = 17.236 ppb

z = 1.5 mm η (mm)	C (ppb)	z = 11.5 mm η (mm)	C (ppb)	z = 21.5 mm η (mm)	C (ppb)	z = 31.5 mm η (mm)	C (ppb)	z = 36.5 mm η (mm)	C (ppb)	z = 41.5 mm η (mm)	C (ppb)
0.0	0.000	0.0	0.000	0.0	0.044	0.0	0.000	0.0	0.079	0.0	0.097
30.0	0.000	30.0	0.150	30.0	0.510	30.0	0.959	30.0	0.985	30.0	1.083
50.0	0.044	50.0	0.300	50.0	0.900	50.0	1.258	50.0	1.240	50.0	1.152
60.0	0.079	60.0	0.370	60.0	0.900	60.0	1.285	60.0	1.179	60.0	1.100
70.0	0.246	70.0	0.282	70.0	0.713	70.0	0.933	70.0	0.994	70.0	0.897
80.0	0.440	80.0	0.317	80.0	0.466	80.0	0.616	80.0	0.686	80.0	0.677
90.0	0.554	90.0	0.431	90.0	0.431	90.0	0.501	90.0	0.554	90.0	0.581
100.0	0.600	100.0	0.528	100.0	0.510	100.0	0.404	100.0	0.510	100.0	0.519
110.0	0.677	110.0	0.554	110.0	0.404	110.0	0.396	110.0	0.422	110.0	0.413
120.0	0.651	120.0	0.528	120.0	0.440	120.0	0.308	120.0	0.299	120.0	0.282
150.0	0.388	150.0	0.194	150.0	0.097	150.0	0.035	150.0	0.044	150.0	0.018
180.0	0.035	180.0	0.018	180.0	0.000	180.0	0.018	180.0	0.000	180.0	0.000

z = 46.5 mm η (mm)	C (ppb)	z = 51.5 mm η (mm)	C (ppb)	z = 66.5 mm η (mm)	C (ppb)	z = 86.5 mm η (mm)	C (ppb)	z = 101.5 mm η (mm)	C (ppb)
0.0	0.132	0.0	0.185	0.0	0.158	0.0	0.035	0.0	0.009
30.0	1.029	30.0	1.083	30.0	0.774	30.0	0.290	30.0	0.053
50.0	1.091	50.0	0.994	50.0	0.792	50.0	0.352	50.0	0.053
60.0	0.994	60.0	0.871	60.0	0.713	60.0	0.317	60.0	0.053
70.0	0.818	70.0	0.739	70.0	0.589	70.0	0.273	70.0	0.035
80.0	0.600	80.0	0.616	80.0	0.404	80.0	0.194	80.0	0.026
90.0	0.554	90.0	0.510	90.0	0.343	90.0	0.106	90.0	0.018
100.0	0.457	100.0	0.396	100.0	0.220	100.0	0.053	100.0	0.009
110.0	0.343	110.0	0.264	110.0	0.114	110.0	0.018	110.0	0.009
120.0	0.229	120.0	0.158	120.0	0.053	120.0	0.026	120.0	0.009
150.0	0.035	150.0	0.035	150.0	0.000	150.0	0.026	150.0	0.009
180.0	0.035	180.0	0.026	180.0	0.026	180.0	0.026	180.0	0.000

Velocity Ratio (U0 / U) = 12   D / d = 28, d = 6.35 mm   (Concentration readings have been corrected for the ambient value)

Note: Transverse measurements are referenced from the inner boundary of the deflected jet

Experiment No. A5[illegible]: x = 500 mm, y = 225 mm, Ambient Conc. = 0.0[illegible] ppb, Jet Nozzle Conc. = 17.792 ppb

z = 1.5 mm		z = 11.5 mm		z = 21.5 mm		z = 31.5 mm		z = 36.5 mm		z = 41.5 mm		z = 46.5 mm		z = 51.5 mm		z = 66.5 mm		z = 91.5 mm		z = 121.5 mm	
η (mm)	C (ppb)	η (mm)	C (ppb)	η (mm)	C (ppb)	η (mm)	C (ppb)	η (mm)	C (ppb)	η (mm)	C (ppb)	η (mm)	C (ppb)	η (mm)	C (ppb)	η (mm)	C (ppb)	η (mm)	C (ppb)	η (mm)	C (ppb)
0.0	0.083	0.0	0.114	0.0	0.176	0.0	0.238	0.0	0.290	0.0	0.308	0.0	0.317	0.0	0.308	0.0	0.290	0.0	0.211	0.0	0.158
30.0	0.106	30.0	0.273	30.0	0.387	30.0	0.431	30.0	0.431	30.0	0.440	30.0	0.422	30.0	0.422	30.0	0.361	30.0	0.220	30.0	0.123
50.0	0.176	50.0	0.361	50.0	0.466	50.0	0.510	50.0	0.537	50.0	0.563	50.0	0.554	50.0	0.598	50.0	0.493	50.0	0.255	50.0	0.088
60.0	0.194	60.0	0.378	60.0	0.493	60.0	0.563	60.0	0.616	60.0	0.651	60.0	0.669	60.0	0.695	60.0	0.581	60.0	0.255	60.0	0.079
70.0	0.202	70.0	0.378	70.0	0.581	70.0	0.607	70.0	0.669	70.0	0.677	70.0	0.713	70.0	0.721	70.0	0.598	70.0	0.255	70.0	0.062
80.0	0.211	80.0	0.369	80.0	0.493	80.0	0.589	80.0	0.642	80.0	0.651	80.0	0.704	80.0	0.686	80.0	0.572	80.0	0.246	80.0	0.053
90.0	0.220	90.0	0.361	90.0	0.484	90.0	0.563	90.0	0.581	90.0	0.589	90.0	0.607	90.0	0.598	90.0	0.484	90.0	0.220	90.0	0.044
100.0	0.264	100.0	0.343	100.0	0.422	100.0	0.493	100.0	0.519	100.0	0.581	100.0	0.581	100.0	0.484	100.0	0.396	100.0	0.176	100.0	0.035
110.0	0.273	110.0	0.308	110.0	0.369	110.0	0.422	110.0	0.413	110.0	0.387	110.0	0.413	110.0	0.387	110.0	0.317	110.0	0.158	110.0	0.026
120.0	0.290	120.0	0.290	120.0	0.317	120.0	0.352	120.0	0.334	120.0	0.308	120.0	0.343	120.0	0.308	120.0	0.255	120.0	0.123	120.0	0.018
150.0	0.229	150.0	0.229	150.0	0.211	150.0	0.211	150.0	0.185	150.0	0.176	150.0	0.176	150.0	0.141	150.0	0.097	150.0	0.026	150.0	0.009
180.0	0.141	180.0	0.158	180.0	0.114	180.0	0.114	180.0	0.088	180.0	0.062	180.0	0.070	180.0	0.053	180.0	0.026	180.0	0.000	180.0	0.000

Experiment No. A5[illegible]: x = 1500 mm, y = [illegible] mm, Ambient Conc. = 0.1[illegible] ppb, Jet Nozzle Conc. = 18.5[illegible] ppb

z = 1.5 mm		z = 11.5 mm		z = 21.5 mm		z = 31.5 mm		z = 36.5 mm		z = 41.5 mm		z = 46.5 mm		z = 51.5 mm		z = 61.5 mm		z = 81.5 mm		z = 111.5 mm	
η (mm)	C (ppb)	η (mm)	C (ppb)	η (mm)	C (ppb)	η (mm)	C (ppb)	η (mm)	C (ppb)	η (mm)	C (ppb)	η (mm)	C (ppb)	η (mm)	C (ppb)	η (mm)	C (ppb)	η (mm)	C (ppb)	η (mm)	C (ppb)
0.0	0.176	0.0	0.194	0.0	0.220	0.0	0.238	0.0	0.264	0.0	0.264	0.0	0.273	0.0	0.282	0.0	0.299	0.0	0.282	0.0	0.194
30.0	0.185	30.0	0.211	30.0	0.246	30.0	0.264	30.0	0.290	30.0	0.317	30.0	0.317	30.0	0.334	30.0	0.334	30.0	0.299	30.0	0.185
50.0	0.202	50.0	0.220	50.0	0.255	50.0	0.264	50.0	0.290	50.0	0.317	50.0	0.317	50.0	0.317	50.0	0.308	50.0	0.273	50.0	0.167
60.0	0.211	60.0	0.229	60.0	0.246	60.0	0.255	60.0	0.255	60.0	0.290	60.0	0.290	60.0	0.290	60.0	0.282	60.0	0.246	60.0	0.150
70.0	0.220	70.0	0.238	70.0	0.238	70.0	0.246	70.0	0.246	70.0	0.264	70.0	0.264	70.0	0.273	70.0	0.255	70.0	0.229	70.0	0.141
80.0	0.220	80.0	0.229	80.0	0.229	80.0	0.229	80.0	0.229	80.0	0.246	80.0	0.246	80.0	0.246	80.0	0.238	80.0	0.202	80.0	0.123
90.0	0.202	90.0	0.211	90.0	0.220	90.0	0.211	90.0	0.211	90.0	0.229	90.0	0.229	90.0	0.211	90.0	0.211	90.0	0.185	90.0	0.106
100.0	0.185	100.0	0.202	100.0	0.211	100.0	0.185	100.0	0.185	100.0	0.211	100.0	0.211	100.0	0.194	100.0	0.185	100.0	0.158	100.0	0.097
110.0	0.158	110.0	0.185	110.0	0.194	110.0	0.167	110.0	0.176	110.0	0.185	110.0	0.176	110.0	0.176	110.0	0.158	110.0	0.141	110.0	0.088
120.0	0.150	120.0	0.176	120.0	0.167	120.0	0.132	120.0	0.150	120.0	0.167	120.0	0.158	120.0	0.150	120.0	0.150	120.0	0.123	120.0	0.070
150.0	0.079	150.0	0.097	150.0	0.088	150.0	0.070	150.0	0.079	150.0	0.088	150.0	0.079	150.0	0.070	150.0	0.070	150.0	0.053	150.0	0.035
180.0	0.035	180.0	0.053	180.0	0.044	180.0	0.026	180.0	0.035	180.0	0.053	180.0	0.035	180.0	0.035	180.0	0.035	180.0	0.026	180.0	0.018

Velocity Ratio (Uo / U) = 12 D / d = 20, d = 12.7 mm

(Concentration readings have been corrected for the ambient value)

Note: Transverse measurements are referenced from the inner boundary of the deflected jet

Experiment No. [illegible]: x = 150 mm, y = 285 mm, Ambient Conc. = 0.158 ppb, Jet Nozzle Conc. = 17.792 ppb

z = 1.5 mm η (mm)	C (ppb)	z = 21.5 mm η (mm)	C (ppb)	z = 41.5 mm η (mm)	C (ppb)	z = 51.5 mm η (mm)	C (ppb)	z = 56.5 mm η (mm)	C (ppb)	z = 61.5 mm η (mm)	C (ppb)	z = 66.5 mm η (mm)	C (ppb)	z = 91.5 mm η (mm)	C (ppb)	z = 121.5 mm η (mm)	C (ppb)
0.0	0.000	0.0	0.132	0.0	0.889	0.0	0.625	0.0	0.309	0.0	0.475	0.0	0.300	0.0	0.369	0.0	0.035
20.0	0.018	20.0	0.528	20.0	1.593	20.0	1.565	20.0	1.417	20.0	1.417	20.0	1.353	20.0	1.158	20.0	0.343
30.0	0.035	30.0	0.704	30.0	1.649	30.0	1.732	30.0	1.695	30.0	1.723	30.0	1.742	30.0	1.436	30.0	0.607
40.0	0.079	40.0	0.660	40.0	1.565	40.0	1.732	40.0	1.779	40.0	1.834	40.0	1.826	40.0	1.548	40.0	0.880
50.0	0.255	50.0	0.581	50.0	1.315	50.0	1.621	50.0	1.695	50.0	1.751	50.0	1.770	50.0	1.631	50.0	1.003
60.0	0.519	60.0	0.495	60.0	1.009	60.0	1.454	60.0	1.529	60.0	1.612	60.0	1.631	60.0	1.603	60.0	1.064
70.0	0.730	70.0	0.510	70.0	0.926	70.0	1.140	70.0	1.334	70.0	1.390	70.0	1.381	70.0	1.575	70.0	1.144
80.0	0.836	80.0	0.704	80.0	0.926	80.0	1.037	80.0	1.167	80.0	1.278	80.0	1.186	80.0	1.492	80.0	1.064
90.0	0.900	90.0	0.853	90.0	0.954	90.0	1.065	90.0	1.084	90.0	1.223	90.0	1.150	90.0	1.436	90.0	1.047
100.0	0.845	100.0	0.906	100.0	0.981	100.0	1.176	100.0	1.112	100.0	1.195	100.0	1.214	100.0	1.381	100.0	0.871
120.0	0.500	120.0	0.713	120.0	0.799	120.0	1.009	120.0	1.084	120.0	1.084	120.0	1.186	120.0	1.158	120.0	0.607
						125.0	0.981	125.0	1.056			125.0	1.103				

Experiment No. [illegible]: x = 250 mm, y = 221.5 mm, Ambient Conc. = 0.150 ppb, Jet Nozzle Conc. = 20.850 ppb

z = 1.5 mm η (mm)	C (ppb)	z = 31.5 mm η (mm)	C (ppb)	z = 61.5 mm η (mm)	C (ppb)	z = 91.5 mm η (mm)	C (ppb)	z = 111.5 mm η (mm)	C (ppb)	z = 131.5 mm η (mm)	C (ppb)	z = 151.5 mm η (mm)	C (ppb)	z = 171.5 mm η (mm)	C (ppb)	z = 191.5 mm η (mm)	C (ppb)	z = 221.5 mm η (mm)	C (ppb)
0.0	0.000	0.0	0.018	0.0	0.290	0.0	0.501	0.0	0.317	0.0	0.220	0.0	0.035	0.0	0.009	0.0	0.009	0.0	0.000
30.0	0.000	30.0	0.220	30.0	1.213	30.0	1.435	30.0	1.176	30.0	0.815	30.0	0.352	30.0	0.150	30.0	0.070	30.0	0.000
50.0	0.018	50.0	0.563	50.0	1.685	50.0	1.574	50.0	1.398	50.0	1.065	50.0	0.598	50.0	0.308	50.0	0.079	50.0	0.018
60.0	0.026	60.0	0.748	60.0	1.796	60.0	1.546	60.0	1.398	60.0	1.120	60.0	0.651	60.0	0.361	60.0	0.097	60.0	0.018
70.0	0.044	70.0	0.880	70.0	1.824	70.0	1.491	70.0	1.315	70.0	1.120	70.0	0.730	70.0	0.378	70.0	0.114	70.0	0.018
80.0	0.114	80.0	0.818	80.0	1.796	80.0	1.435	80.0	1.287	80.0	1.120	80.0	0.845	80.0	0.413	80.0	0.097	80.0	0.009
90.0	0.246	90.0	0.677	90.0	1.713	90.0	1.352	90.0	1.176	90.0	1.065	90.0	0.862	90.0	0.449	90.0	0.106	90.0	0.009
100.0	0.422	100.0	0.440	100.0	1.491	100.0	1.157	100.0	1.148	100.0	0.981	100.0	0.809	100.0	0.334	100.0	0.106	100.0	0.009
110.0	0.528	110.0	0.308	110.0	1.101	110.0	1.018	110.0	1.037	110.0	0.898	110.0	0.783	110.0	0.317	110.0	0.097	110.0	0.009
130.0	0.739	130.0	0.387	130.0	0.684	130.0	0.851	130.0	0.926	130.0	0.815	130.0	0.721	130.0	0.255	130.0	0.062	130.0	0.009
150.0	0.757	150.0	0.495	150.0	0.712	150.0	0.768	150.0	0.676	150.0	0.620	150.0	0.509	150.0	0.141	150.0	0.000	150.0	0.000
180.0	0.500	180.0	0.440	180.0	0.434	180.0	0.490	180.0	0.264	180.0	0.282	180.0	0.246	180.0	0.026	180.0	0.000	180.0	0.000

Velocity Ratio (U_0/U) = 12 D/d = 20, d = 12.7 mm

(Concentration readings have been corrected for the ambient value)

Note: Transverse measurements are referenced from the inner boundary of the deflected jet

Experiment No. [illegible]: x = 450 mm, Ambient Conc. = 0.035 ppb, Jet Nozzle Conc. = 16.958 ppb

z = 1.5 mm η (mm)	C (ppb)	z = 21.5 mm η (mm)	C (ppb)	z = 41.5 mm η (mm)	C (ppb)	z = 61.5 mm η (mm)	C (ppb)	z = 81.5 mm η (mm)	C (ppb)	z = 101.5 mm η (mm)	C (ppb)	z = 131.5 mm η (mm)	C (ppb)	z = 161.5 mm η (mm)	C (ppb)	z = 191.5 mm η (mm)	C (ppb)	z = 221.5 mm η (mm)	C (ppb)	z = 251.5 mm η (mm)	C (ppb)
0.0	0.009	0.0	0.035	0.0	0.282	0.0	0.493	0.0	0.713	0.0	0.660	0.0	0.598	0.0	0.422	0.0	0.211	0.0	0.079	0.0	0.026
30.0	0.018	30.0	0.150	30.0	0.607	30.0	0.871	30.0	0.853	30.0	0.704	30.0	0.589	30.0	0.493	30.0	0.317	30.0	0.106	30.0	0.026
50.0	0.026	50.0	0.246	50.0	0.739	50.0	0.959	50.0	0.933	50.0	0.827	50.0	0.554	50.0	0.501	50.0	0.343	50.0	0.123	50.0	0.035
60.0	[illegible]	60.0	0.273	60.0	0.748	60.0	0.994	60.0	0.994	60.0	0.915	60.0	0.537	60.0	0.449	60.0	0.352	60.0	0.132	60.0	0.026
70.0	0.053	70.0	0.273	70.0	0.730	70.0	1.012	70.0	1.038	70.0	0.994	70.0	0.501	70.0	0.422	70.0	0.343	70.0	0.114	70.0	0.026
80.0	[illegible]	80.0	0.229	80.0	0.721	80.0	0.977	80.0	1.082	80.0	0.977	80.0	0.493	80.0	0.396	80.0	0.317	80.0	0.097	80.0	0.026
90.0	0.123	90.0	0.194	90.0	0.616	90.0	0.933	90.0	1.056	90.0	0.906	90.0	0.466	90.0	0.396	90.0	0.290	90.0	0.106	90.0	0.035
100.0	0.229	100.0	0.150	100.0	0.493	100.0	0.836	100.0	1.029	100.0	0.792	100.0	0.422	100.0	0.396	100.0	0.264	100.0	0.106	100.0	0.026
110.0	0.282	110.0	0.150	110.0	0.396	110.0	0.686	110.0	1.021	110.0	0.598	110.0	0.378	110.0	0.326	110.0	0.246	110.0	0.097	110.0	0.018
130.0	0.352	130.0	0.238	130.0	0.238	130.0	0.431	130.0	0.484	130.0	0.369	130.0	0.273	130.0	0.308	130.0	0.282	130.0	0.070	130.0	0.009
150.0	0.308	150.0	0.299	150.0	0.238	150.0	0.290	150.0	0.308	150.0	0.264	150.0	0.255	150.0	0.238	150.0	0.167	150.0	0.044	150.0	[illegible]
180.0	0.238	180.0	0.282	180.0	0.282	180.0	0.229	180.0	0.246	180.0	0.194	180.0	0.150	180.0	0.123	180.0	0.079	180.0	0.018	180.0	[illegible]

Experiment No. [illegible]: x = 1250 mm, Ambient Conc. = 0.114 ppb, Jet Nozzle Conc. = 16.011 ppb

z = 1.5 mm η (mm)	C (ppb)	z = 21.5 mm η (mm)	C (ppb)	z = 41.5 mm η (mm)	C (ppb)	z = 61.5 mm η (mm)	C (ppb)	z = 81.5 mm η (mm)	C (ppb)	z = 101.5 mm η (mm)	C (ppb)	z = 131.5 mm η (mm)	C (ppb)	z = 161.5 mm η (mm)	C (ppb)	z = 191.5 mm η (mm)	C (ppb)	z = 221.5 mm η (mm)	C (ppb)	z = 251.5 mm η (mm)	C (ppb)
0.0	0.035	0.0	0.150	0.0	0.238	0.0	0.255	0.0	0.308	0.0	0.334	0.0	0.334	0.0	0.246	0.0	0.255	0.0	0.194	0.0	0.185
30.0	0.070	30.0	0.202	30.0	0.290	30.0	0.361	30.0	0.361	30.0	0.405	30.0	0.378	30.0	0.290	30.0	0.282	30.0	0.194	30.0	0.167
50.0	0.097	50.0	0.246	50.0	0.343	50.0	0.369	50.0	0.369	50.0	0.457	50.0	0.413	50.0	0.334	50.0	0.282	50.0	0.220	50.0	0.114
60.0	0.123	60.0	0.273	60.0	0.343	60.0	0.378	60.0	0.405	60.0	0.510	60.0	0.457	60.0	0.343	60.0	0.264	60.0	0.229	60.0	0.114
70.0	0.114	70.0	0.308	70.0	0.361	70.0	0.413	70.0	0.457	70.0	0.528	70.0	0.466	70.0	0.396	70.0	0.282	70.0	0.229	70.0	0.114
80.0	0.123	80.0	0.282	80.0	0.352	80.0	0.431	80.0	0.501	80.0	0.554	80.0	0.493	80.0	0.387	80.0	0.282	80.0	0.220	80.0	0.114
90.0	0.150	90.0	0.246	90.0	0.352	90.0	0.457	90.0	0.554	90.0	0.581	90.0	0.510	90.0	0.413	90.0	0.299	90.0	0.220	90.0	0.114
100.0	0.150	100.0	0.290	100.0	0.369	100.0	0.466	100.0	0.598	100.0	0.607	100.0	0.537	100.0	0.431	100.0	0.290	100.0	0.211	100.0	0.114
110.0	0.150	110.0	0.299	110.0	0.369	110.0	0.484	110.0	0.581	110.0	0.616	110.0	0.501	110.0	0.387	110.0	0.282	110.0	0.194	110.0	0.114
130.0	0.132	130.0	0.290	130.0	0.361	130.0	0.466	130.0	0.563	130.0	0.545	130.0	0.475	130.0	0.396	130.0	0.255	130.0	0.194	130.0	0.079
150.0	0.150	150.0	0.255	150.0	0.352	150.0	0.440	150.0	0.484	150.0	0.440	150.0	0.369	150.0	0.396	150.0	0.229	150.0	0.167	150.0	0.079
180.0	0.167	180.0	0.194	180.0	0.255	180.0	0.326	180.0	0.343	180.0	0.317	180.0	0.264	180.0	0.273	180.0	0.185	180.0	0.132	180.0	0.044

APPENDIX III

Centerline Wall Jet Trajectories for the Momentum Dominated Flow Regimes

(Figures (a) - (u))

Appendix III

Diffusion of Circular Wall Jet in Crossflows

General

The analysis on this section is based on the photographic trajectory data from an experimental study by M. Diebel and N. Rajaratnam which was carried out in the T. Blench hydraulics laboratory, University of Alberta. The results predict both the path and the growth rate of the deflected wall jet and were used to approximate the location of the jet during the dilution investigations.

Diebel's experiments were conducted in the same rectangular channel, 0.91m wide, 0.76 m deep and 36.6 m long, used in the present study. Well-designed nozzles of diameters equal to 6.35 mm and 19.05 mm, located at a distance of about 21 m from the flume entrance were used to generate the wall jet discharges from one side of the flume. Diluted solution of cochineal food color dye used was introduced into the piping system near the jet nozzle by gravity to produce a colored jet. The specific gravity of the dye was 1.020 at a temperature of 16.5 °C and with significant dilution, its density was assumed to approach the freestream water density.

Photographs of the coloured jets with exposure time of a 1/2 to 1 second were taken from above the flume to provide the plan view of the deflected wall jet. Measurements of the jet centerline and its total width B at different locations along the ξ - axis were carried out using a 2 cm x 2 cm grid painted on the bed of the flume at the study section. The mid point between the inner and the outer jet penetration boundaries at each location was taken as the jet centerline. Photographs taken for the side elevation were used to obtain the vertical thickness h of the deflected jet at locations along the axial distance.

Growth of the Deflected Wall Jet

The deflected jet centerline in the work of Diebel was defined by the x and y co-ordinates where x represents the longitudinal distance along the stream and y represents the perpendicular distance to the stream with the origin at the jet nozzle. The axial distance ξ was measured from the nozzle along the centerline of the deflected jet for which the y co - ordinate was written as y_c.

The analysis of the jet trajectory showed no sensitivity to the magnitude of D / d, the ratio of freestream depth to the jet nozzle diameter which was generally in the range of 20-37, in the lateral growth. The present study on deeply submerged jets therefore, would show minimal dependence on the parameter. However the jet growth in the vertical (depth wise) direction would be influenced by the surface effects for relatively low values of D / d.

The Present Investigation

The objectives of the study were to define the flow regimes of the deflected circular wall jet using the photographic data of Diebel and to compare the trajectory relations with those established by Wright (1977). Diebel's data give the co-ordinates of the jet centerline.

The investigation of the flow regimes were carried out by plotting the dimensionless centerline co - ordinates, x / l_m against y_c / l_m and then superimposing the known trajectory solutions for the momentum dominated near and far fields. Based on the trajectory analysis of Wright (1977), the path of a free deflected circular jet in crossflow was fitted by a 1/2 - slope and 1/3 - slope for the MDNF and the MDFF respectively. Diebel's wall jet data are presented graphically in Figures III (a) - (s) for the two jet nozzle diameters used. The plots indicate that most of the data fall on the far field flow regime. The transition point was found to vary in the range of y_c / l_m = 1.0 to 2.0 and approximated the value obtained from the work of Wright (1977) of $y_c / l_m = 1.5$.

The dependence of the proportionality coefficients C_1 and C_2 on the velocity ratio α was also analyzed based on the two slopes for the MDNF and the MDFF respectively. The variation of each of these coefficients against α is presented in Figures III (t) and (u). The coefficients are fitted by the equations:

$$C_1 = 1.11\,\alpha^{0.29} \qquad \text{(III-1)}$$

$$C_2 = 0.98\,\alpha^{0.28} \qquad \text{(III-2)}$$

The results indicate that both these coefficients are not constants but are approximately linear functions of α. The increase of C_1 tends to an asymptotic value of 3, while C_2 approaches a constant value of about 2.5 for α above 20. The results given by the work of Wright showed similar trends but both the coefficients asymptotically approached a constant value of 2 for very high velocity ratios of about $\alpha = 100$. Hodgson (1991) carried out similar analysis for river - like shallow crossflows for α less than 15. The present results from Diebel's data closely approximated Hodgson's results for α less than 10 but about 30 % greater than

Wright's results. The comparisons in the momentum dominated far field regime indicates that the wall jet coefficient C_2 tends to increase faster than values given by the work of Hodgson. These results indicate that the wall jet penetration is greater than that of the corresponding free deflected jet. Low velocity of freestream flow near the bed might be responsible for this difference.

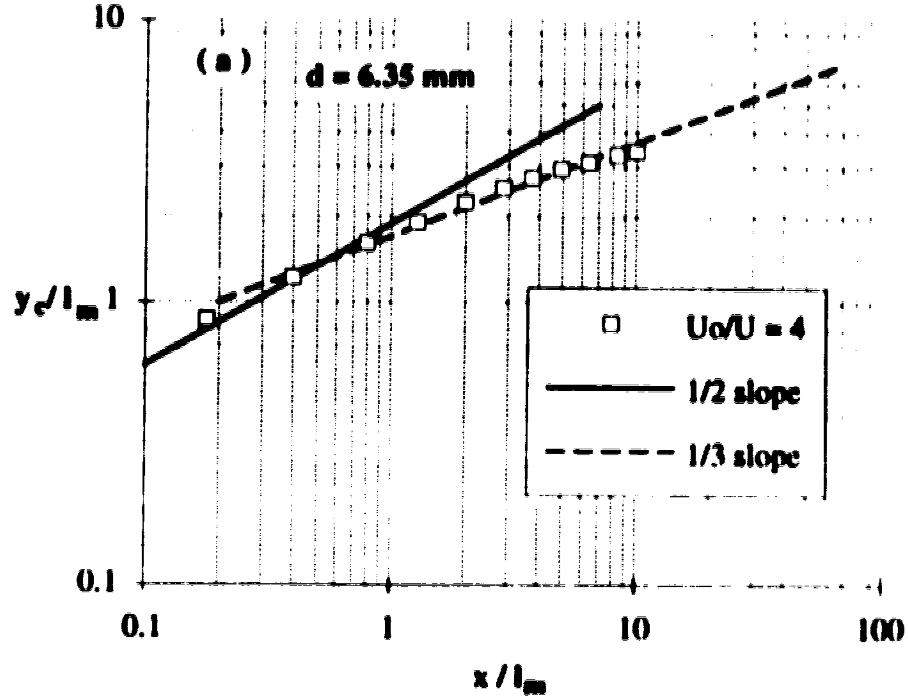

(a)
d = 6.35 mm
Uo/U = 4
1/2 slope
1/3 slope
10
1
0.1
0.1
1
10
100
y_c/l_m
x/l_m

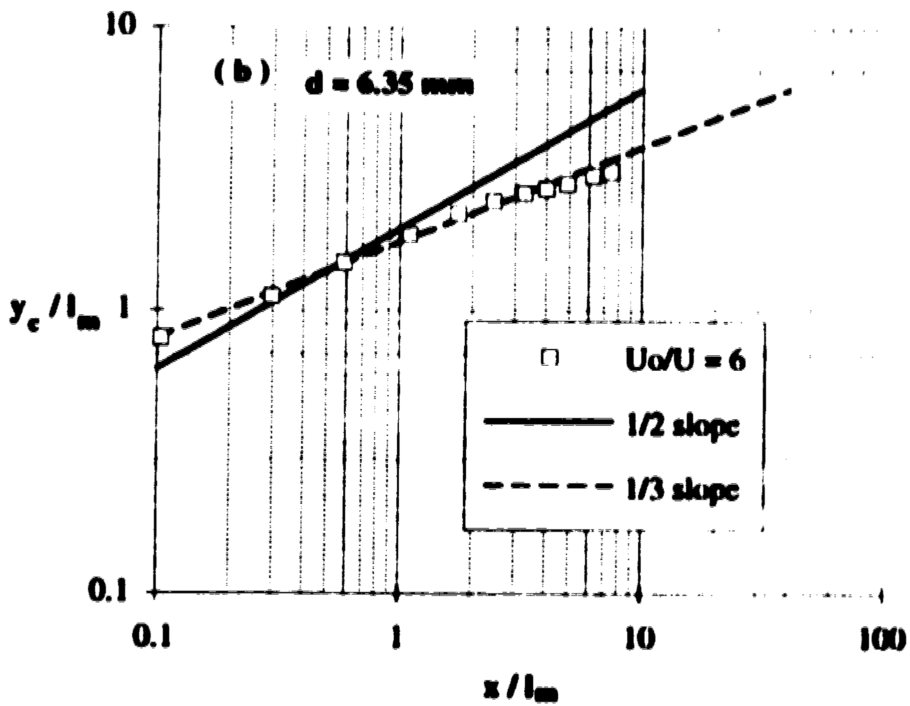

(b)
d = 6.35 mm
Uo/U = 6
1/2 slope
1/3 slope
10
1
0.1
0.1
1
10
100
y_c/l_m
x/l_m

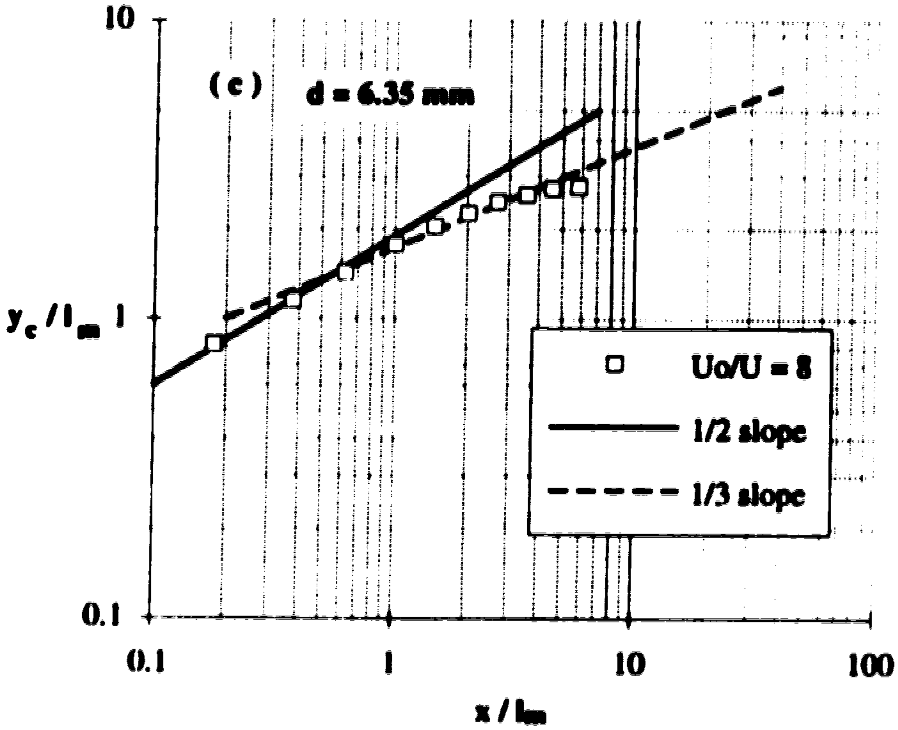
(c)
d = 6.35 mm
y_c / l_m
x / l_m
Uo/U = 8
1/2 slope
1/3 slope
10
1
0.1
0.1
1
10
100

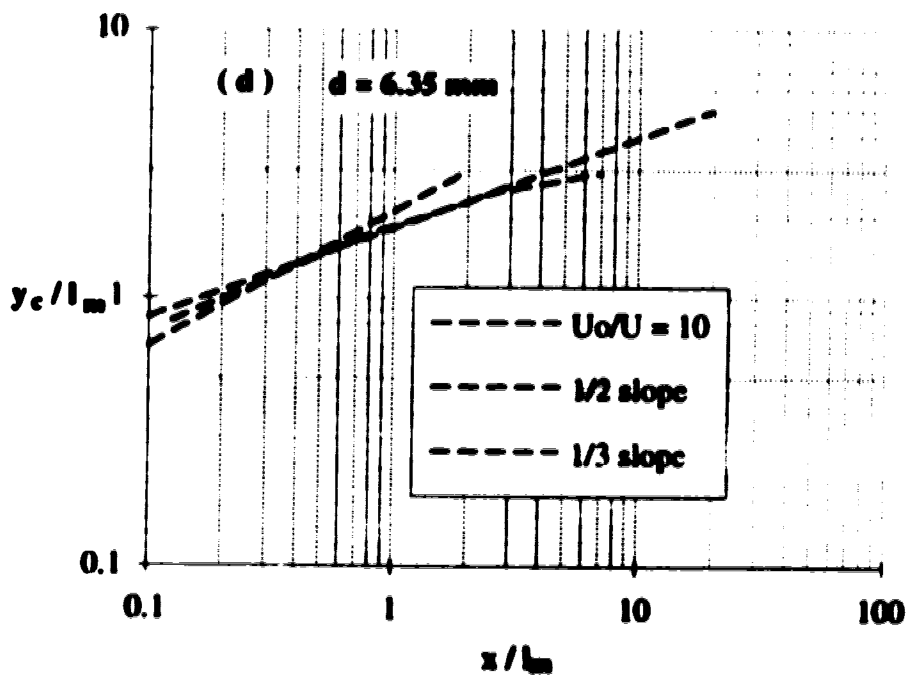
(d)
d = 6.35 mm
y_c / l_m
x / l_m
Uo/U = 10
1/2 slope
1/3 slope
10
1
0.1
0.1
1
10
100

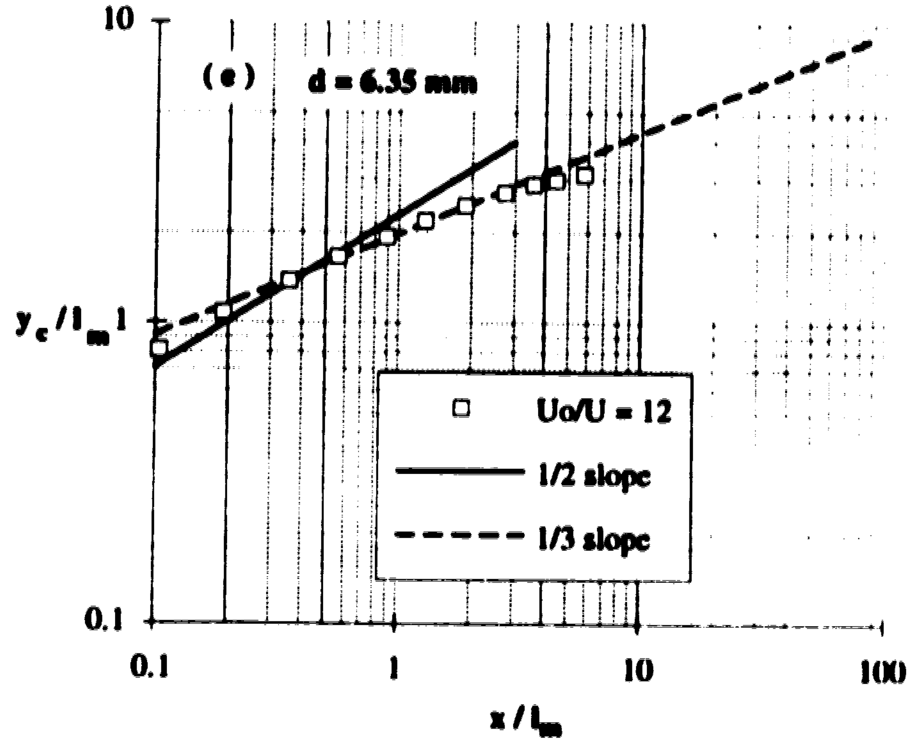
10
(e)
d = 6.35 mm
y_c / l_m 1
Uo/U = 12
1/2 slope
1/3 slope
0.1
0.1
1
10
100
x / l_m

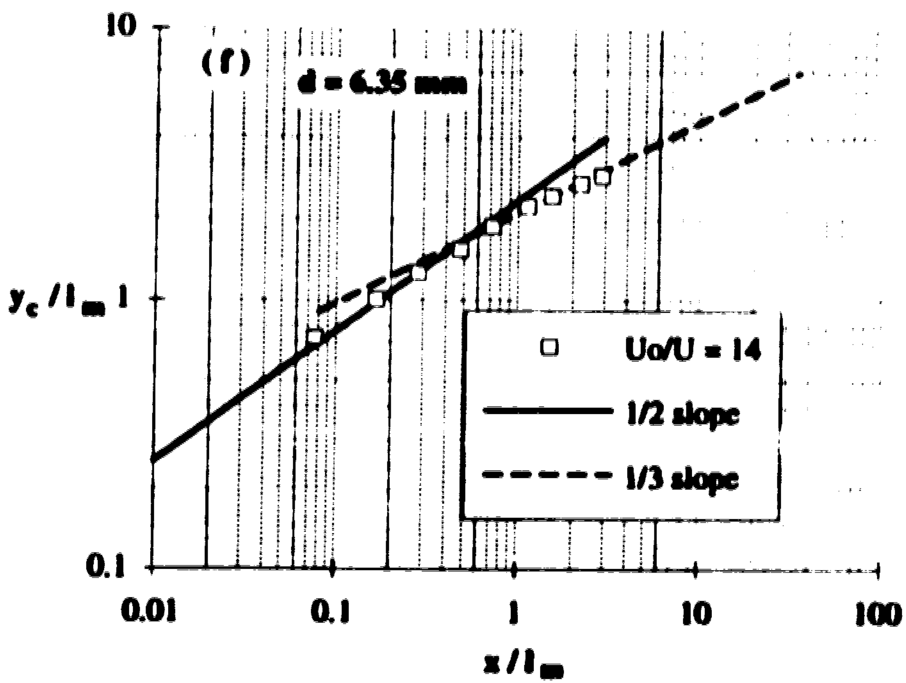
10
(f)
d = 6.35 mm
y_c / l_m 1
Uo/U = 14
1/2 slope
1/3 slope
0.1
0.01
0.1
1
10
100
x / l_m

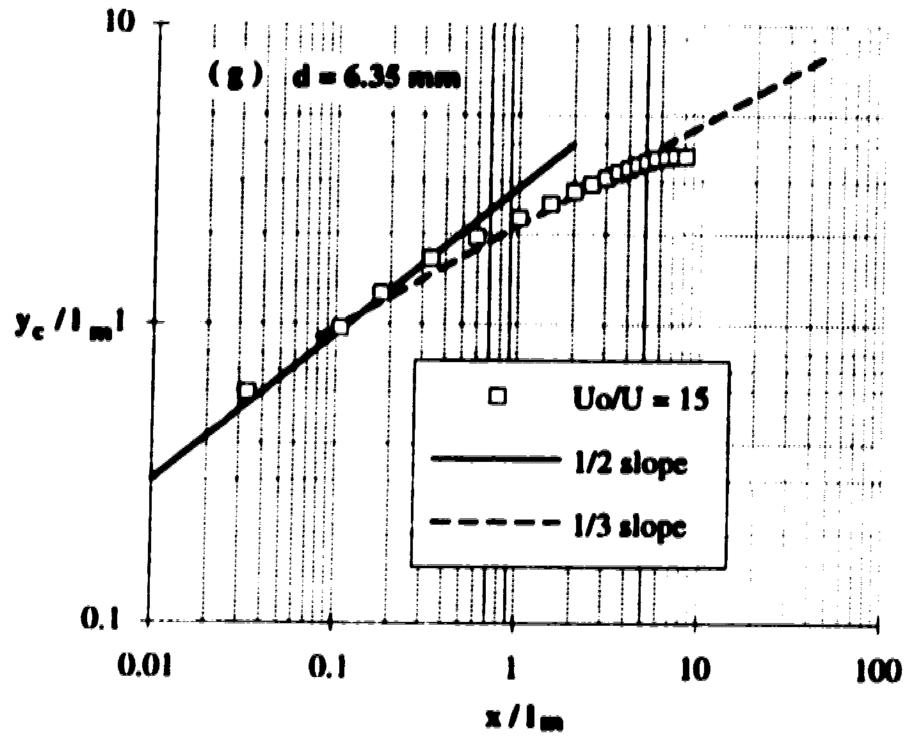
10
(g) d = 6.35 mm
y_c / l_m 1
Uo/U = 15
1/2 slope
1/3 slope
0.1
0.01
0.1
1
10
100
x / l_m

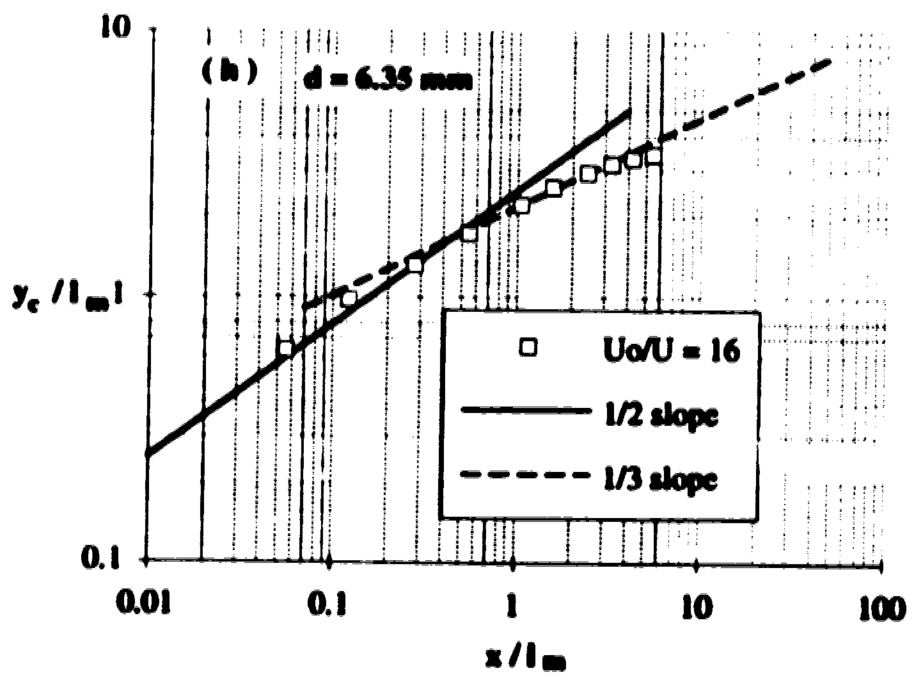
10
(h) d = 6.35 mm
y_c / l_m 1
Uo/U = 16
1/2 slope
1/3 slope
0.1
0.01
0.1
1
10
100
x / l_m

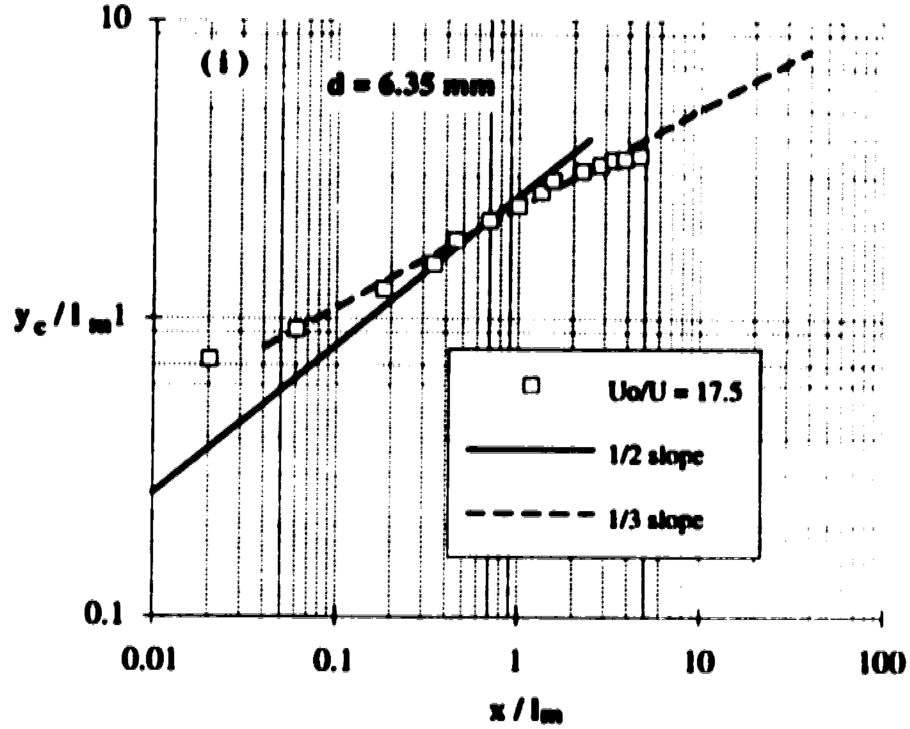
10
(i)
d = 6.35 mm
y_c / l_m 1
Uo/U = 17.5
1/2 slope
1/3 slope
0.1
0.01
0.1
1
10
100
x / l_m

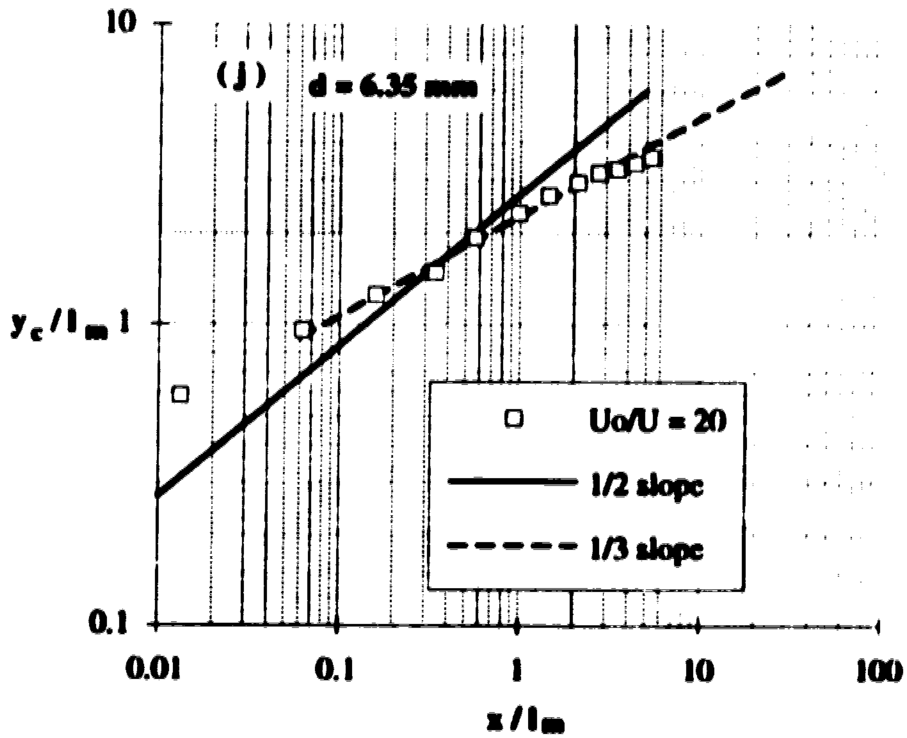
10
(j)
d = 6.35 mm
y_c / l_m 1
Uo/U = 20
1/2 slope
1/3 slope
0.1
0.01
0.1
1
10
100
x / l_m

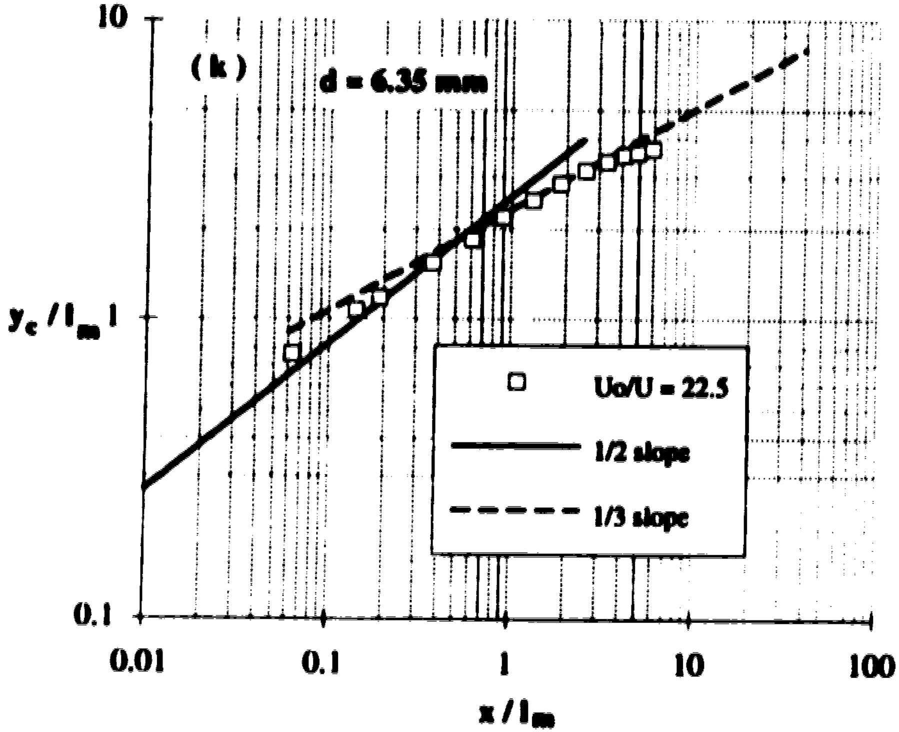
(k)
d = 6.35 mm
Uo/U = 22.5
1/2 slope
1/3 slope
y_c / l_m
x / l_m
10
1
0.1
0.01
0.1
1
10
100

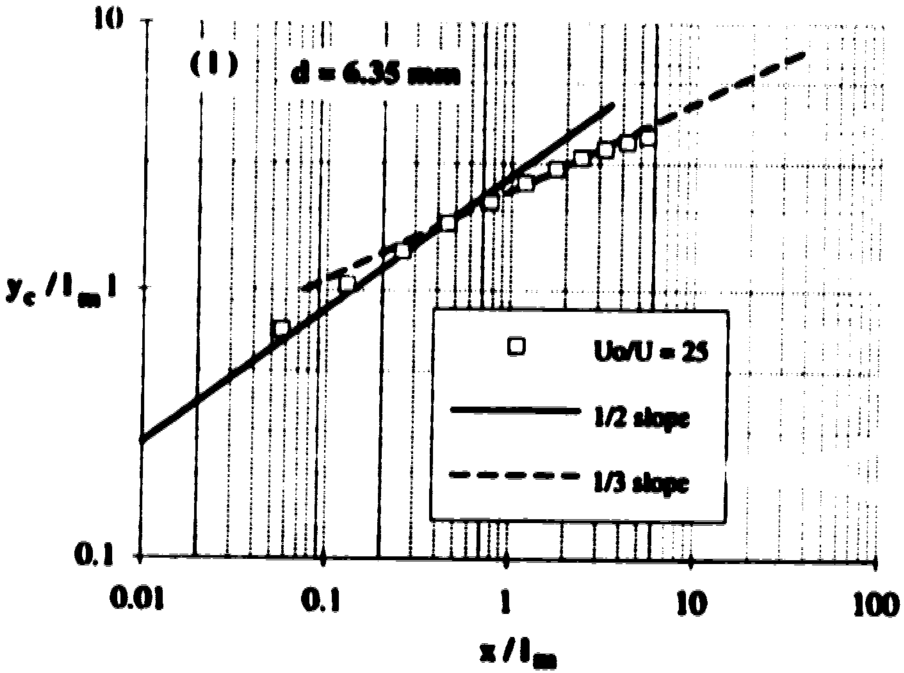
(l)
d = 6.35 mm
Uo/U = 25
1/2 slope
1/3 slope
y_c / l_m
x / l_m
10
1
0.1
0.01
0.1
1
10
100

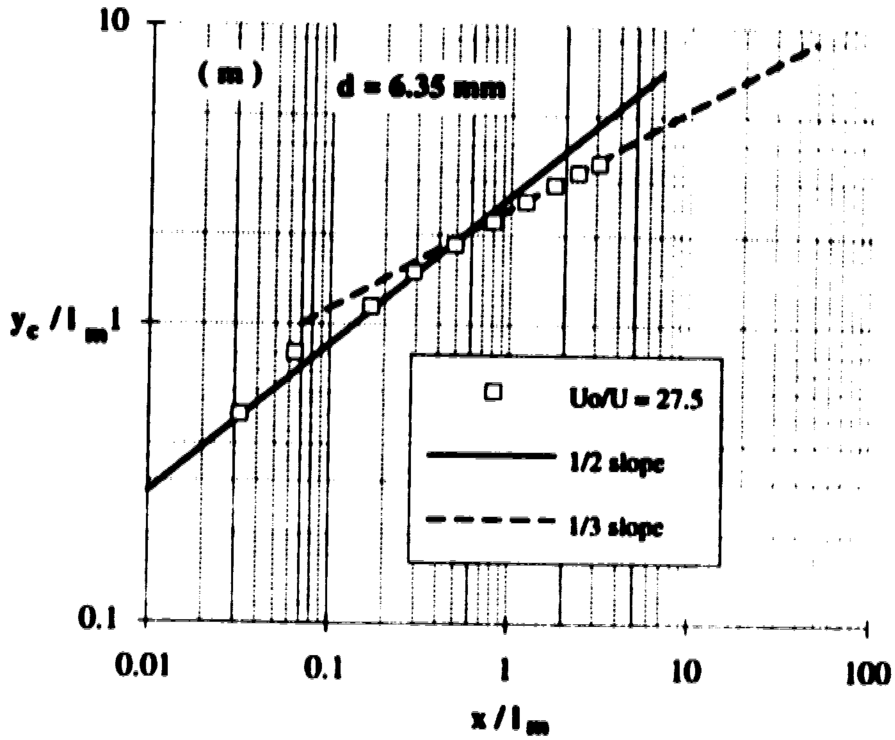

10
(m)
d = 6.35 mm
y_c / l_m
1
0.1
0.01
0.1
1
10
100
x / l_m
Uo/U = 27.5
1/2 slope
1/3 slope

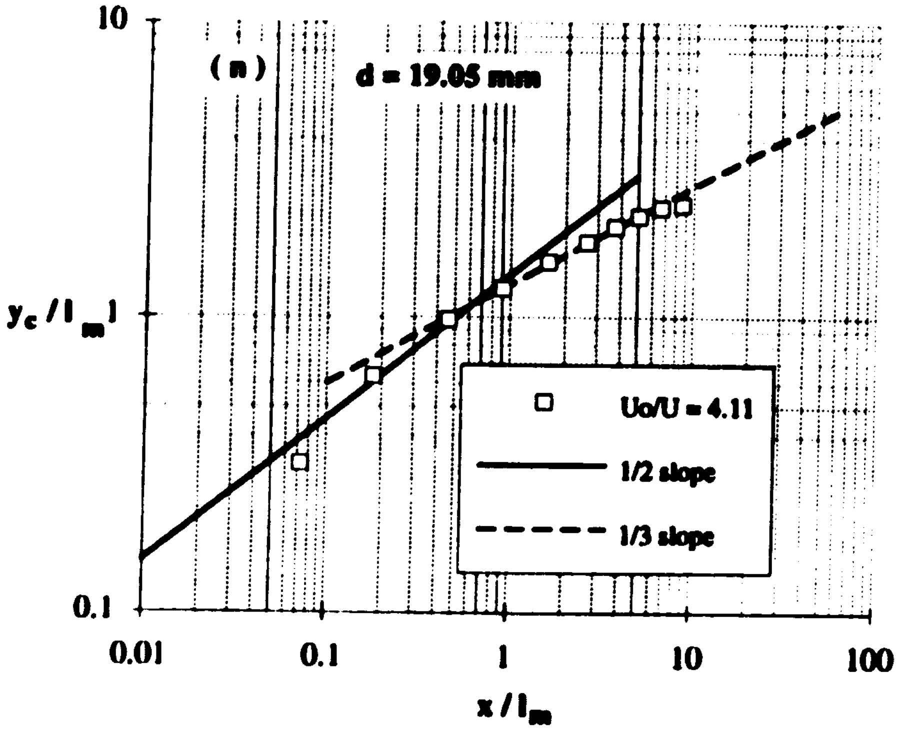
10
(n)
d = 19.05 mm
y_c / l_m 1
Uo/U = 4.11
1/2 slope
1/3 slope
0.1
0.01
0.1
1
10
100
x / l_m

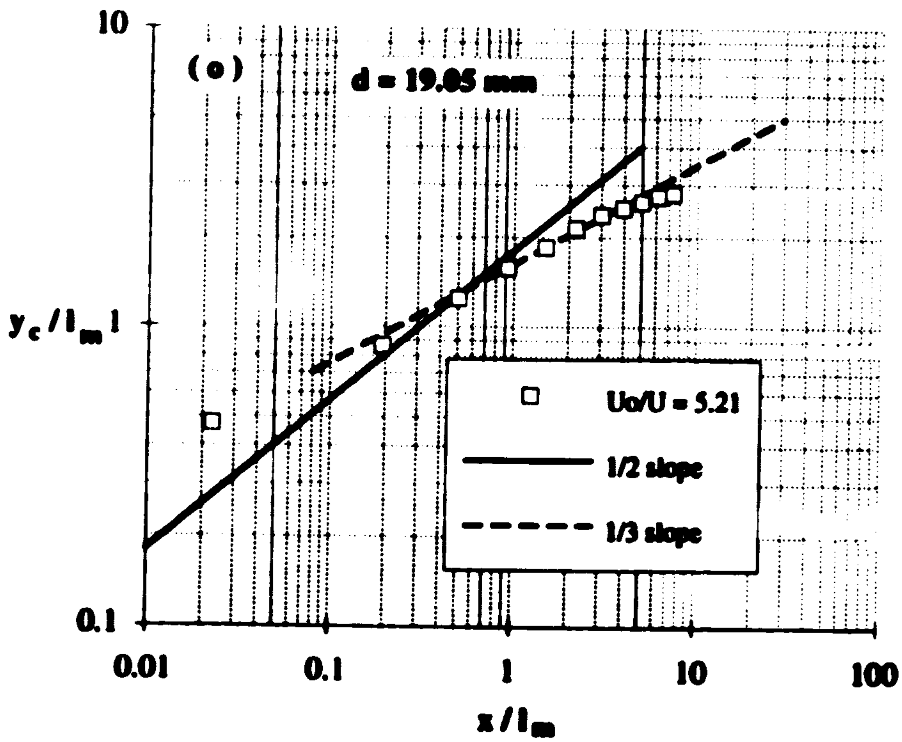
10
(o)
d = 19.05 mm
y_c / l_m 1
Uo/U = 5.21
1/2 slope
1/3 slope
0.1
0.01
0.1
1
10
100
x / l_m

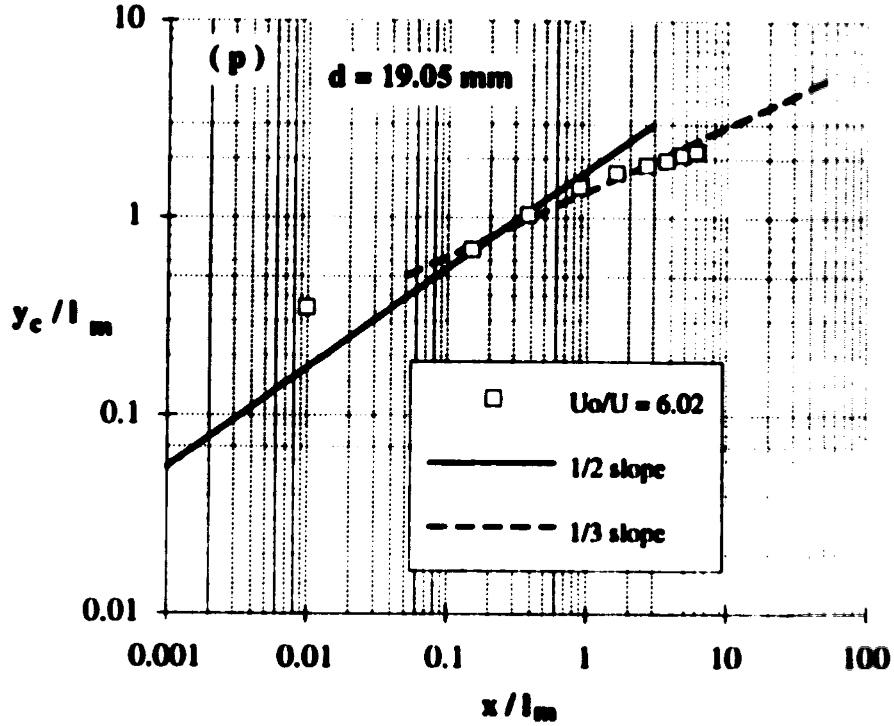
(p)
d = 19.05 mm
Uo/U = 6.02
1/2 slope
1/3 slope
y_c / l_m
x / l_m
10
1
0.1
0.01
0.001
0.01
0.1
1
10
100

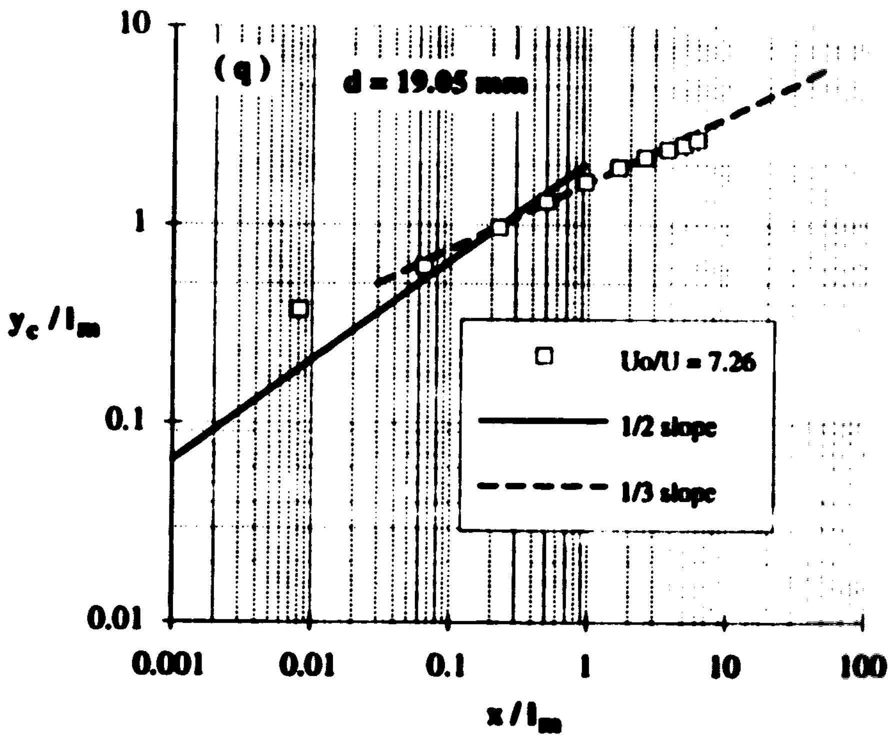
(q)
d = 19.05 mm
Uo/U = 7.26
1/2 slope
1/3 slope
y_c / l_m
x / l_m
10
1
0.1
0.01
0.001
0.01
0.1
1
10
100

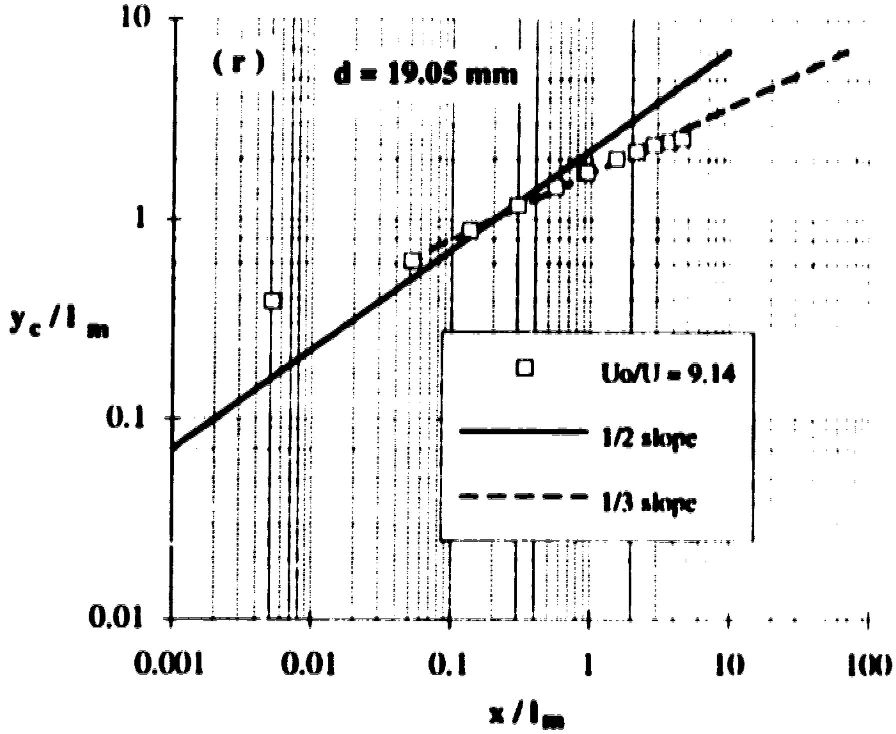
(r)
d = 19.05 mm
Uo/U = 9.14
1/2 slope
1/3 slope
y_c / l_m
x / l_m
10
1
0.1
0.01
0.001
0.01
0.1
1
10
100

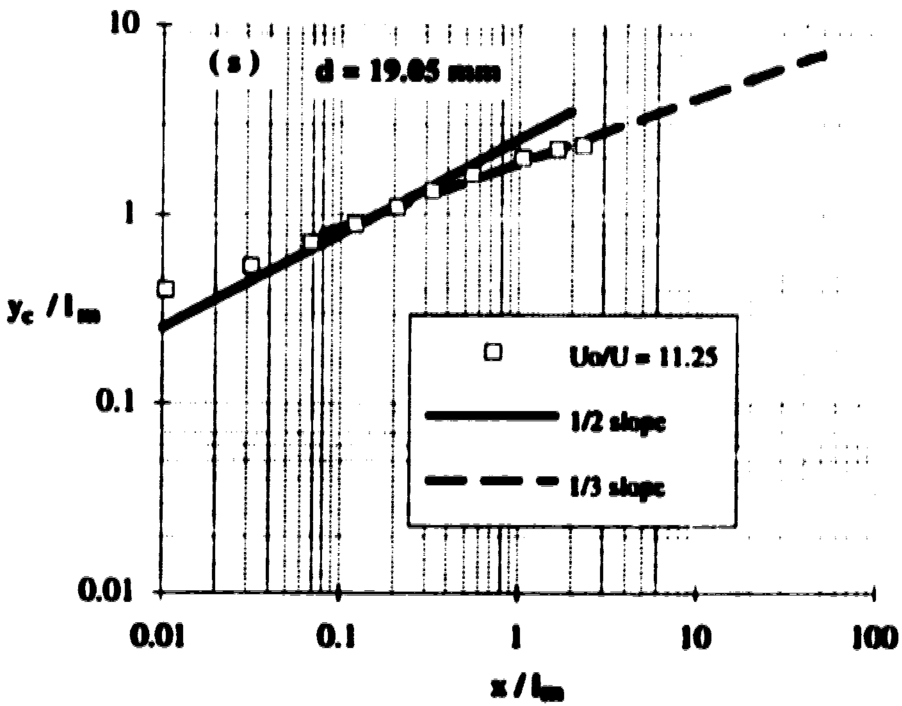
(s)
d = 19.05 mm
Uo/U = 11.25
1/2 slope
1/3 slope
y_c / l_m
x / l_m
10
1
0.1
0.01
0.01
0.1
1
10
100

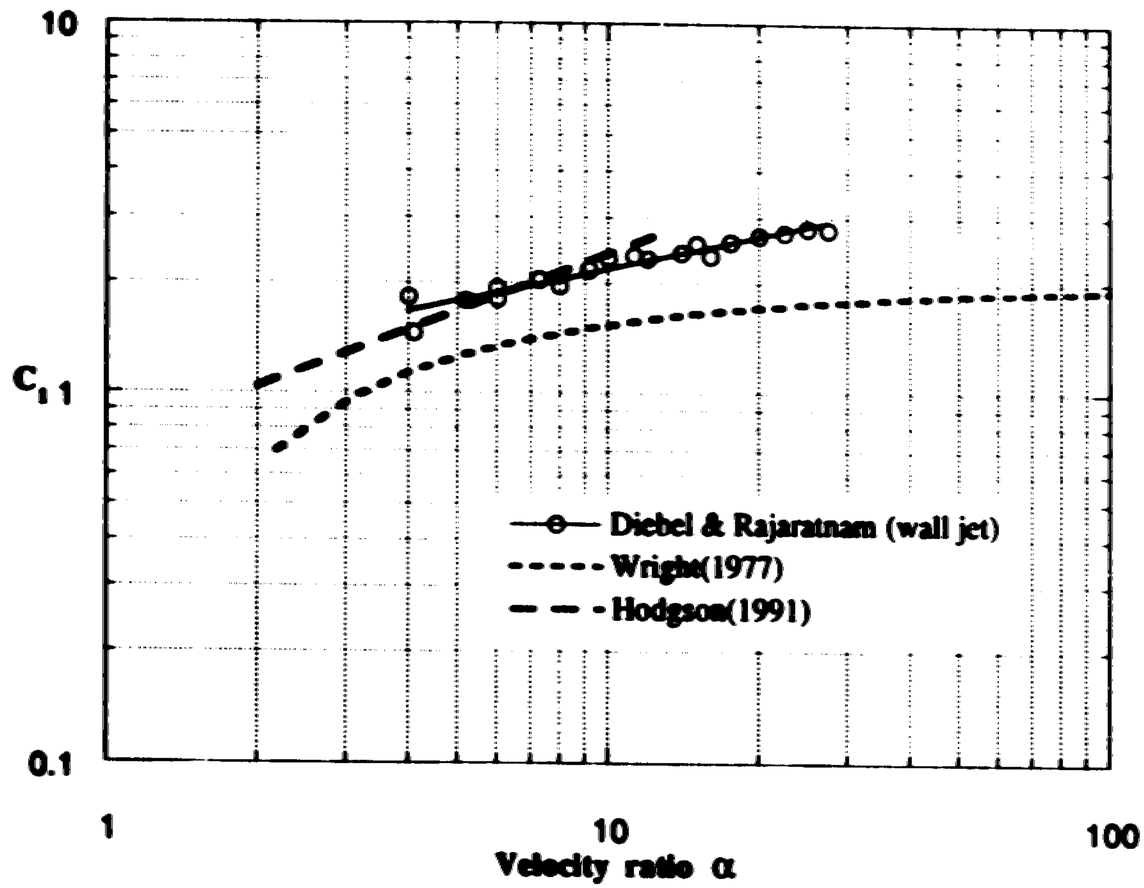

Fig. III (t) Momentum Dominated Near Field Coefficients

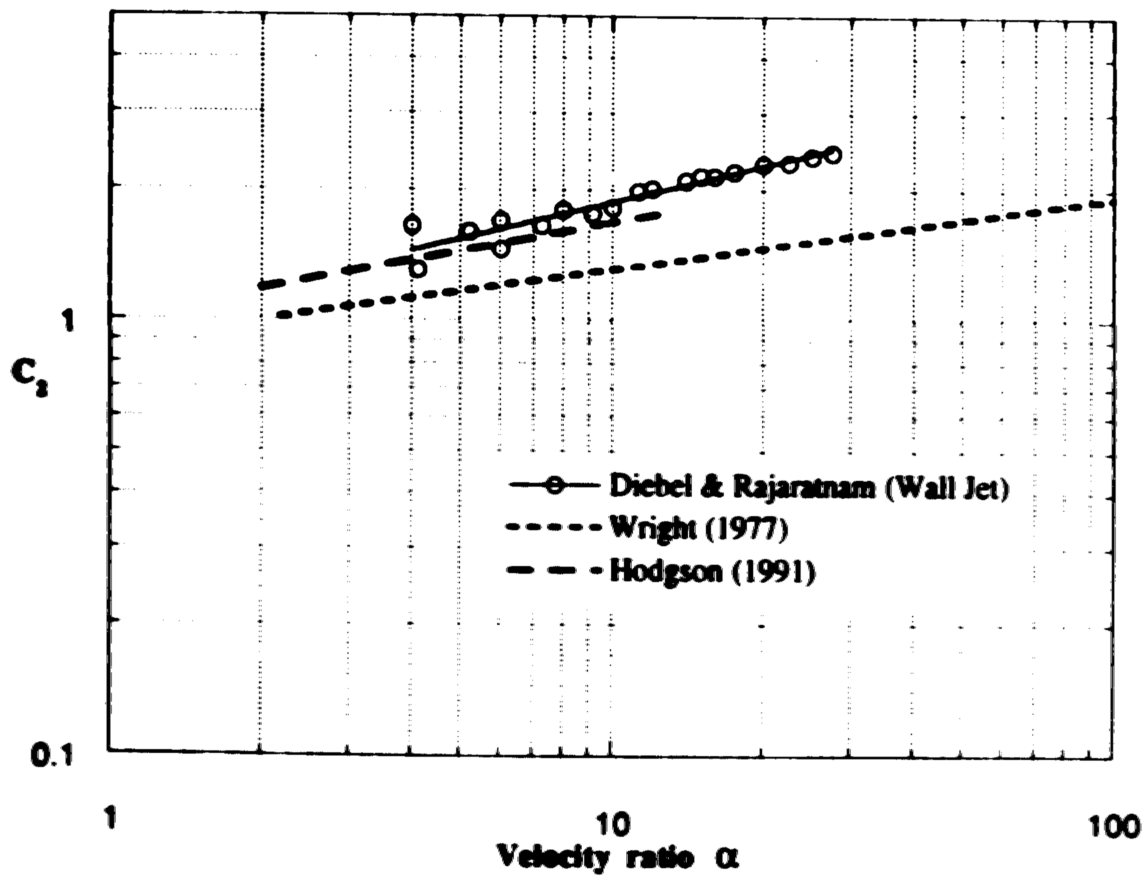

Fig. III (u) Momentum Dominated Far Field Coefficients